REFERENCE ONLY

UNIVERSITY OF LONDON THESIS

Degree PhD Year 2005 Name of Author APPATHURAI S

Investigation of the limiting fibre nonlinearities and their suppression in 40Gbit/s optical transmission systems

V. S. D. Appathurai

A thesis submitted to the University of London for the degree of
Doctor of Philosophy (Ph.D.)

Department of Electronic and Electrical Engineering
University College London
January 2005

ProQuest LLC
789 East Eisenhower Parkway
P.O. Box 1346
Ann Arbor, MI 48106-1346

Abstract

This thesis investigates the fundamental limitations to optical transmission at a bit-rate of 40Gbit/s. The signal distortion due to nonlinear effects, noise and dispersion are analysed and techniques for their suppression through dispersion management and optimum choice of modulation format are demonstrated.

The high launch powers required for overcoming noise from the amplifiers result in an increase in fibre nonlinearities. Transmission at 40Gbit/s favours the RZ modulation format. However, RZ signals were found to be limited by intra-channel cross phase modulation (IXPM) and intra-channel four-wave-mixing (IFWM). These intra-channel nonlinear effects take place as a result of nonlinear interaction between overlapping pulses of the same wavelength channel. Minimising such pulse overlap by controlling the dispersion-induced pulse broadening during propagation in the fibre was investigated by reducing the fibre local dispersion and by pre-compensating the signal at the transmitter. Dispersion compensation using higher-order-mode devices with high nonlinear tolerance was also investigated, enabling transmission over in-line pre-compensated amplifier spans.

In the second part of this thesis, the nonlinear tolerance of the RZ modulation format was increased by use of alternate-polarisation and alternate–phase between adjacent pulses. These techniques were found to improve the transmission performance by approximately 50% and required simple modifications to the transmitter only. These advanced RZ signals were found to be compatible with dispersion management techniques. However, the optimum pre-compensation at the transmitter was found to be dependent on the modulation format and dominant intra-channel effect. A novel modulation format combining alternate-polarisation and phase simultaneously was demonstrated for maximum nonlinear suppression without the use of dispersion management.

Finally, a new experimental technique was demonstrated for the investigation of dispersion tolerance. It was found that the choice of optimum modulation format requires a trade-off between nonlinear tolerance and dispersion tolerance. The results of this work can be applied to optimise the design rules of future optical networks.

Acknowledgements

"If I have seen further... it is by standing upon the shoulder of giants"
Sir Isaac Newton (1642-1727)

I should begin to acknowledge the efforts of those who helped me throughout the course of this work by starting with my supervisor Prof. Polina Bayvel. It is to her, that I owe my venture into the world of fibre optics, a choice I have not regretted since. Her constant guidance, energy and brutal honesty (particularly with regard to the writing of this thesis) were significant to the success of this work, and I am forever grateful for that.

I would also like to thank Dr. Robert Killey for his help with the numerical simulations, and for many discussions on the work presented here. I am eternally indebted to Dr. Michael Düser for his constant encouragement and advice during the writing of this thesis. Dr. Vitaly Mikhailov and Giancarlo Gavioli contributed to this work through experimental advice and assistance in the laboratory, and I sincerely thank them for doing so.

I am deeply grateful to Nortel Networks in Harlow (Essex) for funding a Ph.D studentship covering a significant part of this work. In particular, I thank Drs. Takis Hadjifotiou, Julian Fells and Peter Kean for their invaluable knowledge and guidance of this work in highlighting the necessity of researching commercially attractive solutions to the challenges of 40Gbit/s optical transmission.

I also acknowledge the generous awards of the Overseas Research Scholarship (ORS) and the Ian Karten Charitable Trust.

I am truly fortunate to have friends and colleagues of the Optical Networks Group, and the Ultrafast Photonics Group, who created a pleasant atmosphere in the office, and also organised numerous sports and cultural outings. I apologise for subjecting them to my 'dry' humour, but it was necessary to cope with the wet days in London.

Finally, I would like to thank my parents for the numerous sacrifices they endured that I might have the very best in life. *Deo Gracias.*

Table of Contents

List of figures

Chapter 1 Introduction

The recent growth in data communication has increased the need for high capacity transmission links, and over the last decade optical fibre communication systems have emerged as the dominant technology capable of satisfying these demands. At present the highest single channel bit-rate in commercial systems operates at 10Gbit/s, and the required Tbit/s link capacities are achieved through wavelength division multiplexing (WDM) [KEI'99]. Higher bit-rates are being researched at present as they allow the required link capacity to be achieved with fewer number of WDM channels. Indeed for a four-fold increase in bit-rate, a cost reduction of ~40% can be expected through the reduced number of transceivers required and their maintenance costs [WIN'03, MIK'04]. Increasing the bit-rate also leads to a higher spectral efficiency in WDM transmission systems, resulting in a more efficient use of optical amplifier bandwidths. However, as the bit-rate increases, the system becomes increasingly sensitive to the fundamental limitations of optical transmission such as chromatic dispersion, nonlinear effects and noise. For example, at a single channel bit rate of 40Gbit/s the signal is 16 times more sensitive to dispersion than at 10Gbit/s, and it requires at least 6dB higher signal-to-noise-ratio (SNR) at the receiver for the equivalent bit-error-rate (BER) [KAM'01]. Counteracting this requires an increase in signal launch power which increases the nonlinear signal distortion in the fibre, as described later in this thesis. Furthermore, recent research has found that at 40Gbit/s, the nonlinear distortion occurs not only between WDM channels, but also affects single channel transmission [ESS'99]. This increase in single channel nonlinear distortion arises due to nonlinear interaction between overlapping pulses of the same wavelength channel, caused by dispersion-induced pulse broadening, and is known as intra-channel nonlinear distortion. Therefore, increasing the bit-rate to 40Gbit/s leads to new challenges in managing the link's dispersion profile, as not only is the tolerance to uncompensated dispersion decreased, but the system's nonlinear behaviour is also related to the dispersion profile [PIN'04].

Fig. 1.1 highlights the significant sources of penalty in optical transmission and related areas of research aimed at overcoming them. The most common source of penalty which limits system performance is noise from the amplifiers [WAL'91]. Reducing the overall loss of signal power and low noise amplifiers are the main

Chapter 1 Introduction

The recent growth in data communication has increased the need for high capacity transmission links, and over the last decade optical fibre communication systems have emerged as the dominant technology capable of satisfying these demands. At present the highest single channel bit-rate in commercial systems operates at 10Gbit/s, and the required Tbit/s link capacities are achieved through wavelength division multiplexing (WDM) [KEI'99]. Higher bit-rates are being researched at present as they allow the required link capacity to be achieved with fewer number of WDM channels. Indeed for a four-fold increase in bit-rate, a cost reduction of ~40% can be expected through the reduced number of transceivers required and their maintenance costs [WIN'03, MIK'04]. Increasing the bit-rate also leads to a higher spectral efficiency in WDM transmission systems, resulting in a more efficient use of optical amplifier bandwidths. However, as the bit-rate increases, the system becomes increasingly sensitive to the fundamental limitations of optical transmission such as chromatic dispersion, nonlinear effects and noise. For example, at a single channel bit rate of 40Gbit/s the signal is 16 times more sensitive to dispersion than at 10Gbit/s, and it requires at least 6dB higher signal-to-noise-ratio (SNR) at the receiver for the equivalent bit-error-rate (BER) [KAM'01]. Counteracting this requires an increase in signal launch power which increases the nonlinear signal distortion in the fibre, as described later in this thesis. Furthermore, recent research has found that at 40Gbit/s, the nonlinear distortion occurs not only between WDM channels, but also affects single channel transmission [ESS'99]. This increase in single channel nonlinear distortion arises due to nonlinear interaction between overlapping pulses of the same wavelength channel, caused by dispersion-induced pulse broadening, and is known as intra-channel nonlinear distortion. Therefore, increasing the bit-rate to 40Gbit/s leads to new challenges in managing the link's dispersion profile, as not only is the tolerance to uncompensated dispersion decreased, but the system's nonlinear behaviour is also related to the dispersion profile [PIN'04].

Fig. 1.1 highlights the significant sources of penalty in optical transmission and related areas of research aimed at overcoming them. The most common source of penalty which limits system performance is noise from the amplifiers [WAL'91]. Reducing the overall loss of signal power and low noise amplifiers are the main

techniques aimed at minimising penalties due to noise. Such techniques were dominant even at low bit-rates, but the technology involved in achieving these aims has improved with the increase in bit-rate. One such advancement was the introduction of Raman amplifiers which introduce low noise to the transmission system [MOR'00, ISL'02]. In Raman amplified systems the transmission fibre acts as the gain media requiring very high optical pump powers to be used. At present there are concerns about using Raman amplifiers in commercial systems [DIA'02], hence, this work does not investigate noise limitations in Raman amplified systems, and focuses instead on erbium-doped fibre amplifier (EDFA) systems.

Dispersion limitations, unlike noise have become more dominant with the increase in bit-rate. Dispersion compensation, hardly required at low bit-rates has not only become a necessity at 40Gbit/s transmission, but also requires a high level of accuracy owing to the quadratic increase in sensitivity. While it is possible to decrease the dispersion limitations by operating at wavelengths close to the zero dispersion such as in dispersion shifted fibre (DSF) with $D=0ps/(nm.km)$, this is not a viable option in WDM transmission as it leads to FWM which distorts the signals [MAR'91, TKA'95]. As such more targeted research on dispersion tolerances and compensation devices is required, and is topic of discussion in this thesis. In fact, the intra-channel nonlinear effects which are most related to the increase in bit-rate to 40Gbit/s has been due to the inter-dependence of dispersion and nonlinear interaction [SHA'98, MAM'99]. These intra-channel nonlinear effects are most significant in the presence of dispersion-induced pulse overlap, and have, therefore, led to the investigation of dispersion managed fibre links for their mitigation. Hence, the advent of 40Gbit/s transmission has led to a merging of the fundamental limitations, with each effect related to the other. *Fig. 1.1* illustrates this fact, where advancements in dispersion tailoring have implications on the nonlinear behaviour. Similar behaviour is also seen when considering various modulation formats for improving the overall transmission performance. For example, intra-channel nonlinear interaction occurs in the presence of dispersion-induced pulse overlap, but as the dispersion of various modulation pulse formats is related to their inherent spectral properties, they lead to different levels of nonlinear distortion.

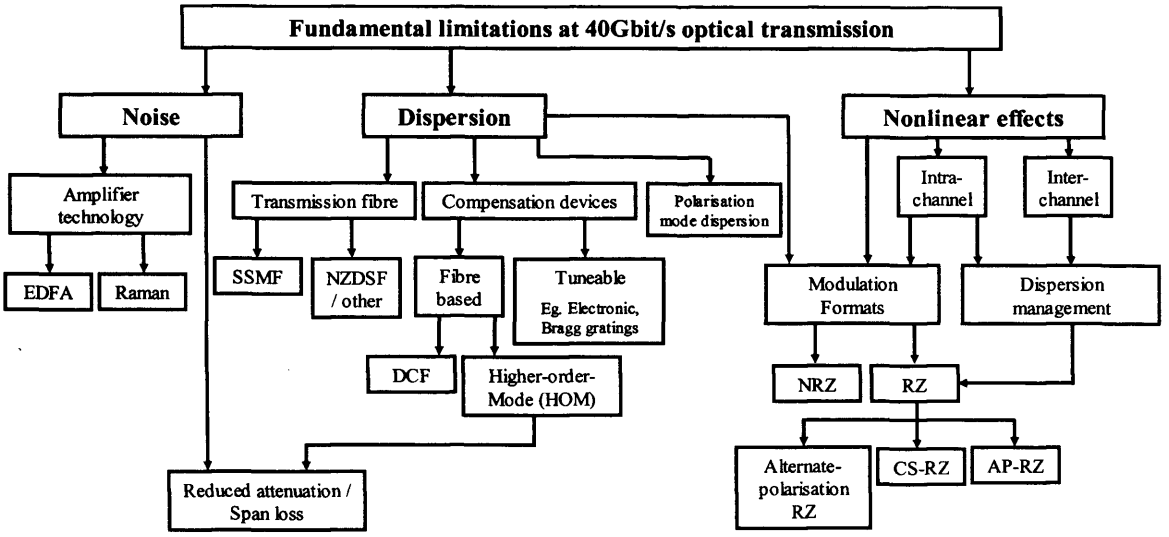

Fig. 1.1 *Overview of 40Gbit/s research illustrating fundamental limitations and related techniques for their suppression (shaded regions indicate areas not covered in this work)*

Table 1.1 summarises the current trend in optical communications research and gives the recent results for transmission experiments, indicating the movement towards higher bit-rates and longer distances. One of the key limitations in increasing the channel bit-rate is the speed of electronic components. Hence, most work on high-speed transmission has been achieved optically, in particular through optical-time-division multiplexing (OTDM). To date, single channel bit-rates as high as 1280Gbit/s [NAK'00], total fibre capacity over 10Tbit/s [FUK'01] and bandwidth-distance product of 41Pbit/s.km [CAI'03], have been demonstrated. These are impressive results and indicate the vast potential for high-speed optical transmission, satisfying all commercial requirements. This might lead to the conclusion that the challenges at 40Gbit/s are easily solved. However, these experiments were performed with careful optimisation of fibre type and dispersion map, using complex modulation formats, with little or no tolerance to most experimental parameters, making the system very expensive in practice. This is not acceptable in the commercial implementation of systems, as a trade-off exists between optimum performance and cost.

Author	Channel Bit-rate (Gbit/s)	Number of channels	Distance (km)	Signal format	Fibre type	Bandwidth x Distance ~(Pbit/s.km)
[TAN'02]	10	1001	120	NRZ	PDF,RDF	29
[MOL'03]	10	109	18,000	Dispersion Managed RZ	NZDSF	20
[CAI'03]	10	373	11,000	RZ-DPSK	PDF	41
[FUK'01]	40	273	117	RZ	PSCF	1
[GRO'02]	42.7	128	1280	CS-RZ	SSMF	7
[CHA'03]	42.7	157	1700	PSBT	SSMF	11
[RAS'03]	40	40	10,000	CSRZ-DPSK	UltraWave™	16
[GNA'04]	42.7	6	200	Alternate-polarisation RZ-DPSK	SSMF	0.05
[CHA'04]	42.7	149	6120	DPSK	UltraWave™	39
[MIK'01]	160	6	400	RZ	NZDSF	0.3
[RAY'00]	320	1	200	RZ	NZDSF	0.06
[MAR'04]	640	1	160	DPSK	SLA-fibre	0.1
[NAK'00]	1280	1	70	Chirped RZ	DF-DDF	0.01

Table 1.1 *Bit-rate-distance products for recent record single- and multi-channel experimental demonstrations*

The largest proportion of the overall cost in the implementation of a fibre optic system is the deployment of the transmission fibre. In *Table 1.1* it can be seen that a majority of the 40Gbit/s work was based on transmission over novel fibre types specifically designed for operation at this bit-rate. However, as the majority of deployed fibre is either dark (un-used) or under-utilised (operating at low bit-rates), the technology drive at present is significantly based on upgrading existing systems for 40Gbit/s operation [KAH'04]. SSMF is the most commonly deployed fibre type [KOG'00], but its fibre local dispersion $D=17ps/(nm.km)$ is significantly high and may limit the transmission performance due to intra-channel nonlinear distortion. Whilst dispersion compensation generally applies in the linear transmission regime, it can nevertheless, be exploited in the suppression of the nonlinear distortion [BER'96b], where the *dispersion compensation* is managed throughout the entire link based on pulse broadening and power. The intricate interplay between dispersion and its interaction with nonlinearities, generally referred to as *dispersion management*, is part of the

research carried out and described in this thesis. In particular, this thesis focused on understanding the dominant nonlinearities and optimising 40Gbit/s transmission over SSMF, and dispersion management techniques which decrease the impact of the fibre local dispersion, by pre-compensating the signal at the transmitter to decrease the intra-channel nonlinear distortions are studied [GOV'98, ESS'99, KIL'00].

While transmission in SSMF may be a cheaper option commercially, other fibre types and relevant dispersion management schemes were also considered in this work, exploring the potential improvement in system performance. However, improvements in transmission performance over new fibre types require justification against the increase in cost of deploying them. This thesis discusses the use of non-zero dispersion shifted fibre (NZDSF) as an alternative transmission fibre to SSMF as it has a dispersion parameter *D=4ps/(nm.km)* which is significantly less than that of SSMF. This decreases the pulse broadening during transmission, which is attractive in suppressing intra-channel nonlinear distortion as mentioned previously, and also eases the constraints on dispersion compensation. Dispersion compensation of NZDSF was achieved here using a higher-order-mode dispersion-management-device (HOM-DMD). The HOM-DMD consists of a short length of fibre with large effective area enabling the device to operate linearly and also consists of low loss. This is potentially more advantageous compared to that of the highly nonlinear and lossy dispersion compensating fibre (DCF) used for the compensation of SSMF. The dispersion slope compensation required for simultaneous broadband compensation over the C-band was also investigated using the HOM-DMD, eliminating the need for dispersion trimming on a per channel basis.

Dispersion sensitive distortions are linear and in most cases can be minimised with appropriate dispersion compensation at the receiver. However, the nonlinear distortions which occur in fibre optic systems are not so easily suppressed and require careful optimisation of channel powers and power budgets and appropriate dispersion management [TUR'03]. Hence, a systematic investigation of the launch power range for maximum transmission distance was carried out in this work, to study the transmission over SSMF and NZDSF transmission links. These investigations were also carried for the choice of modulation format in the system which affects the transmission behaviour in the presence of fibre nonlinearities [GNA'04b]. The

variation in nonlinear behaviour for the different modulation formats may occur for reasons such as, decreased pulse overlap for similar values of dispersion, or reduced efficiency in the nonlinear interaction for similar pulse overlap. The work in this thesis initially looked at these effects for 40Gbit/s transmission using the most common non-return-to-zero (NRZ) and return-to-zero (RZ) modulation formats. Variants of the RZ modulation format were also investigated, based on alternate-polarisation [SUZ'98] and alternate-phase [OHH'01] between adjacent pulses for suppressing intra-channel nonlinear distortion. A novel modulation format, based on the simultaneous implementation of alternate-polarisation and alternate-phase is proposed and investigated for enhanced suppression of intra-channel nonlinear distortion. The impact of modulation format with optimised dispersion management is also discussed, and a new technique for the study of in-line residual dispersion tolerance is described.

Ultra long-haul transmission distances (greater than 1000km) at 40Gbit/s have been demonstrated with remarkable performance *(Table 1.1)*. However, it is not possible to understand from such, highly optimised, demonstrations the dominant sources of penalty affecting the transmission performance. Indeed, it is unclear if acceptable transmission performance is achievable in less complex systems over metro and long-haul distances. Thus, the final goal of this work is a simplified description of intra-channel nonlinear effects, enabling the prediction of this and other penalties such as noise and dispersion occurring at 40Gbit/s, for transmission over deployed 10Gbit/s systems. The suppression of these penalties is also investigated based on simple techniques enabling non-complex upgradeability of existing systems.

Overview of the thesis

The theory of optical fibre propagation needed for the work in this thesis, is described in Chapter 2. The first section discusses the linear dispersive effects and dispersion compensation. Nonlinear behaviour due to the change in refractive index with signal intensity is then presented. The different properties of the NRZ and RZ modulation formats are described. The intra-channel four-wave-mixing (IFWM) and intra-channel cross-phase-modulation (IXPM) affecting single channel transmission through nonlinear interaction between overlapping pulses operating at 40Gbit/s are described next. These effects are analysed by use of the perturbation analysis and are compared with numerical simulations carried out using the split-step Fourier method to solve the nonlinear Schrödinger equation. The noise due to amplifier spontaneous emission in erbium-doped-fibre-amplifiers and its impact on transmission performance is then described. Finally, parameters for quantifying system performance, such as eye-opening penalty, Q-factor and bit-error-rate (BER) are explained, along with a technique for investigating system limitations due to signal launch power.

An overview of existing research on 40Gbit/s optical transmission is given in chapter 3. This includes previous investigations on the comparison of modulation formats and their nonlinear tolerance. The literature survey also presents work on dispersion compensation and optimisation of transmission performance using dispersion management. This highlights the aspects of 40Gbit/s transmission which require further investigation, and formed the basis of the work described in this thesis in the following chapters.

Chapter 4 begins with an explanation of the experimental set-up and numerical simulator which was used in these investigations. The first results compare transmission performance of NRZ and RZ over SSMF, with detailed investigation of intra-channel nonlinear distortion. The transmission performance of these two modulation formats are then compared for transmission over NZDSF links compensated by HOM-DMD. New amplifier span designs are presented to take advantage of the linear behaviour of the HOM-DMD. Finally, dispersion management techniques through pre-compensation are investigated for suppressing intra-channel

nonlinear distortion. Numerical simulations are verified experimentally for all cases of transmission over SSMF and NZDSF fibre links.

Advance modulation formats based on RZ are investigated in chapter 5 to understand and improve nonlinear tolerances. Experimental investigation of alternate-polarisation RZ and alternate-phase RZ (AP-RZ) is presented. A detailed investigation of the optimum peak-to-peak phase modulation of AP-RZ is also described for maximum suppression of the intra-channel nonlinear effects individually and for good overall system performance. Dispersion management is then investigated for the different modulation formats, as it was important to determine if the optimum dispersion map is independent of modulation format. A new modulation format combining alternate-polarisation RZ and AP-RZ is proposed and investigated. It is shown to lead to good suppression of intra-channel nonlinear distortion without the need for dispersion management. Dispersion tolerance for RZ and AP-RZ modulation formats are discussed for linear and nonlinear transmission over SSMF in chapter 6. A novel experimental technique for this, making use of the dispersion slope in fibre is also discussed.

Finally, chapter 7 provides a summary of the work done during the course of this research. Possible areas for further research are identified.

Original contributions

The following original contributions to the field of 40Gbit/s optical transmission were made in the course of this research:

- First experimental power-dependent analysis of intra-channel nonlinear distortion as a function of transmission distance which isolates signal distortion due to nonlinear and noise effects separately, enabling the quantification of various suppression techniques [MIK'02, KIL'02]
- Detailed investigation of HOM-DMD with in-line pre-compensated amplifier spans, exploiting the high nonlinear tolerance of the HOM-DMD [MIK'02, KIL'02].
- Quantification of inter-channel nonlinear distortion in 40Gbit/s RZ transmission as a function transmission distance over NZDSF [MIK'02b, KIL'02]
- Demonstration of simultaneous broadband dispersion compensation of WDM channels using the HOM-DMD without dispersion trimming on a per-channel basis at the receiver [KIL'02]
- Detailed experimental investigation of dispersion management through pre-compensation at the transmitter, and the importance of the modulation format in its optimisation [APP'03, APP'04b]
- Detailed investigation of the AP-RZ modulation format, identifying a peak-to-peak phase modulation of π radians as the optimum [APP'04b]
- Proposal of a new modulation format with simultaneous implementation of alternate-polarisation and alternate-phase for maximum suppression of intra-channel nonlinear distortion [APP'04]
- First experimental investigation of in-line residual dispersion for RZ and AP-RZ modulation format using a single span recirculating fibre loop, identifying the required trade-off between nonlinear tolerance and dispersion tolerance [APP'04c]

Publications and conference presentations

1. **S. Appathurai**, V. Mikhailov, R. I. Killey and P. Bayvel "Investigation of nonlinear and in-line residual dispersion tolerance of RZ/AP-RZ modulation formats at 40Gbit/s", Proc. 30th European Conference on Optical Communication (ECOC'2004), Stockholm, Sweden, Sept 2004, paper Mo4.5.4.

2. **S. Appathurai**, V. Mikhailov, R. I. Killey and P. Bayvel "Effective suppression of intra-channel nonlinear distortion in 40Gbit/s transmission over standard single mode fibre using alternate-phase RZ and alternate-polarisation", IEE Electronics Letters, Vol. 40, No. 14, 2004, pp 897-898.

3. **S. Appathurai**, V. Mikhailov, R. I. Killey and P. Bayvel "Investigation of the optimum alternate-phase RZ modulation format and its effectiveness in the suppression of intra-channel nonlinear distortion in 40Gbit/s transmission over standard single mode fiber", IEEE Journal of Selected Topics in Quantum Electronics, Vol. 10, No. 2, 2004, pp 239-249.

4. **S. Appathurai**, V. Mikhailov, R. I. Killey and P. Bayvel "Suppression of intra-channel nonlinear distortion in 40Gbit/s transmission over standard single mode fibre using alternate-phase RZ and alternate-polarisation", Proc. Optical Fiber Communications Conference (OFC'2004), Feb 22-27, Los Angeles, California, paper ThE5, 2004.

5. **S. Appathurai**, V. Mikhailov, R. I. Killey and P. Bayvel "Suppression of intra-channel nonlinear distortion in 40Gbit/s transmission over standard single mode fibre using alternate phase RZ and optimised pre-compensation", Proc. 29th European Conference on Optical Communication (ECOC'2003), Rimini, Italy, Sept 2003, paper Tu3.6.5.

6. V. Mikhailov, R. I. Killey, **S. Appathurai** and P. Bayvel "Investigation of intra-channel nonlinear distortion in 40Gbit/s transmission over standard fibre", Fibre and Integrated Optics, Vol. 22, No. 3, June 2003, pp 189-195.

7. R. I. Killey, V. Mikhailov, **S. Appathurai**, and P. Bayvel "Investigation of nonlinear distortion in 40Gb/s transmission with higher order mode fiber dispersion compensators", IEEE Journal of Lightwave Technology, Vol. 20, No.12, 2002, pp 2282-2289.

8. V. Mikhailov, **S. Appathurai**, R. I. Killey and P. Bayvel "Wideband 40Gbit/s WDM transmission under higher-order-mode fiber dispersion management", in Proc. Lasers and Electro Optics Society Conference (LEOS 2002) Nov. 10-14, Glasgow, United Kingdom, 2002, paper MI4.

9. V. Mikhailov, **S. Appathurai**, R. I. Killey and P. Bayvel "Investigation of intra-channel nonlinear distortion in 40Gbit/s transmission over non-zero dispersion shifted fibre", Proc. 28th European Conference on Optical Communication (ECOC 2002), Copenhagen, Denmark, 2002, paper 8.1.6.

10. V. Mikhailov, R. I. Killey, **S. Appathurai** and P. Bayvel "Investigation of intra-channel nonlinear distortion in 40Gbit/s transmission over standard fibre", Proc. 27th European Conference on Optical Communication (ECOC 2001), Amsterdam, Netherlands, 2001, paper Mo.L.3.3.

11. R. I. Killey, **S. Appathurai**, H. J. Thiele and P. Bayvel "Nonlinear signal distortion with 10- and 40-Gbit/s channel rates", Proc. London Communications Symposium (LCS), University College London, September14-15, 2000, pp 7-11.

Chapter 2 Theory

This chapter describes the physical processes which take place during the propagation of an optical signal in fibre. These processes can be divided into linear and nonlinear processes. The description of intra-channel nonlinear effects namely, intra-channel four-wave-mixing (IFWM) and intra-channel cross-phase-modulation (IXPM) are focused on, as they form the main subject of investigation in this thesis. The two most common types of modulation formats are also described, and their behaviour at high bit rates are explained. The impact of noise due to the presence of optical amplifiers is also explained along with techniques for theoretically and numerically quantifying the signal performance such as Q-factor and bit-error-rate measurements, which are used in the experiments to characterise the system performance. While no new results are presented in this theory, it supplements the discussion of the results described in chapters 4-6.

2.1 The propagation of optical signals in fibre using the nonlinear Schrödinger equation (NLSE)

Optical signals in fibre undergo signal distortion owing to many characteristics of the fibre and the nature of the signal transmitted. These characteristics are described by equation (2.1), and is known as the nonlinear Schrödinger equation (NLSE), where *A(z,t)* is a vector characterising the field of an optical signal [AGR'01]. There are 3 main sources of signal distortion, namely, attenuation and dispersion which are linear effects and appear on the left hand side of equation (2.1), and nonlinear effects which appear on the right hand side.

$$\frac{\partial A}{\partial z}+\beta_1\frac{\partial A}{\partial t}+\frac{i}{2}\beta_2\frac{\partial^2 A}{\partial t^2}+\frac{\alpha}{2}A=i\gamma\,|A|^2\,A \qquad (2.1)$$

α denotes the attenuation of the signal, while β_1 characterises the propagation delay, and β_2 the group velocity dispersion (GVD). The nonlinear coefficient is represented by γ. These parameters are explained in more detail in the following sections.

2.2 Attenuation of the signal in fibre

In general the power of the signal launched into an optical fibre decreases exponentially with the distance travelled in the fibre due to absorption of the signal by fibre molecules and scattering of the signal due fluctuations in the fibre density during the manufacturing process. The overall fibre loss is described by the following equation [AGR'01]:

$$P_L = P_O \exp(-\alpha L) \qquad (2.2)$$

where P_L = Power at transmission distance L

P_O =Power launched at the input of a fibre of length L

α = Attenuation constant also referred to as the fibre loss (often given in dB/km).

Signal attenuation is compensated periodically by use of optical amplifiers to achieve long transmission distances. Unfortunately, amplifiers introduce noise, and while it is desirable to keep the total number of amplifiers in a transmission link to a minimum, the long amplifier spacings required to do so increase the rate of noise accumulation. The signal-to-noise ratio (SNR) is used to measure the quality of the signal, and a detailed description is given in section 2.8.1. The SNR can be improved by increasing the signal launch power, however, this leads to an increase in nonlinear distortion of the signal. This thesis studies the optimisation of the signal launch power as a trade-off between noise and nonlinear limitations, and details of this technique can be found in section 2.8.5.

2.3 Dispersion and pulse broadening

Chromatic dispersion arises due to the frequency dependence of the refractive index of the fibre $n(\omega_s)$. The signal, which is an electromagnetic wave, interacts with the bound electrons of the dielectric medium to bring about this effect. Hence, a short optical pulse, which is made up of many frequency components (ω_s), undergoes pulse broadening as each frequency component travels at different a speed, given by

$c/n(\omega_s)$. The effects of fibre dispersion are governed by the mode propagation constant β which can be expanded in a Taylor series about the centre or carrier frequency ω of the signal, to give the following equation [AGR'01]:

$$\beta(\omega) = \beta_0 + \beta_1(\omega) + \frac{1}{2}\beta_2(\omega^2) + \frac{1}{6}\beta_3(\omega^3) + ... \qquad (2.3)$$

the parameter $\beta_1 = 1/v_g$ where $v_g=c/n_g$ is the group velocity and β_2 is its derivative with respect to the optical frequency as follows:

$$\beta_2 = -\frac{1}{v_g^2}\frac{dv_g}{d\omega} = -\frac{\lambda}{c}\frac{d^2n(\lambda)}{d\lambda^2} \qquad (2.4)$$

The parameter β_2 is defined as the group velocity dispersion (GVD) as it represents the variation of the group velocity with frequency. Equation (2.4) is a second order derivative and therefore indicates turning points of v_g, i.e wavelengths at which β_2 is zero. For standard single mode fibre (SSMF), β_2 is zero at wavelength of 1.3μm. However, there is dispersion due to the third order dispersion term β_3 which appears in equation (2.2), even when β_2 is zero. This can distort short pulses at high bit-rates, and is considered in more detail in the description of dispersion compensators in section 2.3.2, where dispersion caused by the dispersion slope $D'=dD/d\lambda$ must be taken into account. D is known as the dispersion parameter. The dispersion parameter D is more commonly used in place of β_2 and is defined as

$$D = \frac{d\beta_1}{d\lambda} = -\frac{2\pi c}{\lambda^2}\beta_2 \approx \frac{\lambda}{c}\frac{d^2n(\lambda)}{d\lambda^2} \qquad (2.5)$$

The dispersion of the fibre can be varied by selecting appropriate fibre design parameters such the core radius a, the core-cladding index difference Δn and the index profile. The second derivative of $n(\lambda)$ from equation (2.5) indicates that the dispersion can be zero at the wavelengths corresponding to the turning points. As such, different fibre types such as SSMF $(D = 17ps/(nm.km)$ @ $1.55\mu m)$ where $\lambda_0=1.3\mu m$, non-zero dispersion shifted fibre (NZDSF) $(D = 4ps/(nm.km)$ @ $1.55\mu m)$, where $\lambda_0=1.52\mu m$ can be appropriately manufactured for the desired fibre dispersion. Indeed, dispersion

compensating fibres with $D<0$ also exist, and are used in transmission links to ensure an overall dispersion close to zero, thereby minimising inter-symbol-interference (ISI) caused by pulse broadening in the presence of dispersion. Fibre types with positive dispersion ($D>0$) are sometimes referred to as anomalous, and fibres with negative dispersion ($D<0$), normal [AGR'01].

The NLSE for the case when $\alpha = 0$ and $\gamma = 0$ describes only the dispersive effects in a frame of reference moving at the group velocity $v_g = 1/\beta_1$ of the pulse.

$$i\frac{dA(z,t)}{dz} = \frac{\beta_2}{2}\frac{d^2A(z,t)}{dT^2} \tag{2.6}$$

This equation is solved by using the Fourier transform method to give the solution of an ordinary differential equation

$$i\frac{dA(z,\omega)}{dz} = -\frac{\beta_2}{2}\omega^2 A(z,\omega) \tag{2.7}$$

$$A(z,\omega) = A(0,\omega)\exp\left(\frac{1}{2}i\beta_2\omega^2 z\right) \tag{2.8}$$

From equations (2.7) and (2.8), it can be seen that the GVD changes the phase of each spectral component within the pulse but does not affect the pulse spectrum even though it modifies the shape of the pulse. This equation is used in the numerical simulator for the description of dispersion $\hat{D}$, as described section in 2.9. This solution can then be substituted in the general solution of the NLSE for dispersive effects only, to give

$$A(z,T) = \frac{1}{2\pi}\int_{-\infty}^{\infty} A(0,\omega)\exp\left(\frac{1}{2}i\beta_2\omega^2 z - i\omega T\right)d\omega \tag{2.9}$$

Considering the dispersion of a Gaussian pulse, described as follows:

$$A(0,t) = \exp\left(-\frac{T^2}{2T_0^2}\right) \tag{2.10}$$

where, T_0 represents the half width at the level of *1/e* of the pulse peak power, and is related to the full width at half maximum (FWHM) as $T_{FHWM}=1.665T_0$, shows that the amplitude at any point *z*, along the fibre is given as

$$A(z,T) = \frac{T_0}{(T_0^2 - i\beta_2 z)^{1/2}} \exp\left(-\frac{T^2}{2(T_0^2 - i\beta_2 z)}\right) \tag{2.11a}$$

$$A(z,T) = |A(z,T)|\exp[i\phi(z,T))] \tag{2.11b}$$

These equations highlight the two distinct characteristics of propagation which can be seen. The first being that the pulse maintains its shape but its width increases with *z* as

$$T_1(z) = T_0(0)\sqrt{1+\left(\frac{z}{L_D}\right)^2} \tag{2.12a}$$

$$L_D = \frac{T_0^2}{|\beta_2|} \tag{2.12b}$$

Where L_D is known as the dispersion length over which dispersive effects are important for pulse evolution, and decreases with increasing frequency (quadratically). The work described in this thesis predominantly investigated 40Gbit/s transmission and pulsewidth of 11.25ps (FWHM) over SSMF with $D=17ps/(nm.km)$. For these parameters, the dispersion length $L_D=2km$. *Fig. 2.1* shows the dispersion-induced pulse broadening for 11.25ps pulse at dispersion lengths of $2L_D$ and $4L_D$ for transmission over SSMF using the numerical simulator described in section 2.9. However, for a pulsewidth of 25ps the dispersion length increases to 10.4km, which is typical for the NRZ modulation format (see section 2.5). It should be noted that even

when the dispersion length is short, the nonlinear interaction (section 2.4) can remain significant and should not be ignored at distances longer than the dispersion length. Equation (2.11a) also shows the chirp, defined as the rate of change of the carrier frequency, which in this case is due to GVD and varies linearly across the pulse. The chirp can also vary in a nonlinear fashion, such as that seen in the presence of SPM described in section 2.4.2.

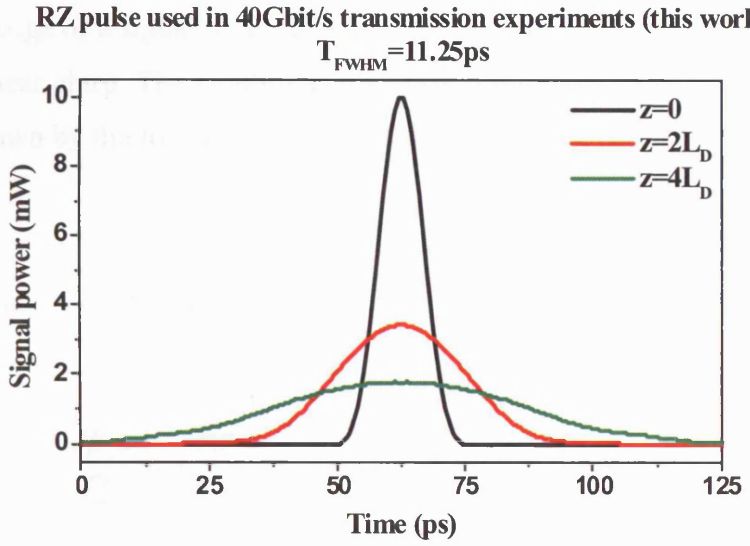

Fig. 2.1 *Dispersion-induced pulse broadening of a Gaussian pulse for transmission in SSMF with D=17ps/(nm.km). L_D = 2km*

It is clear from equation (2.12a) and (2.12b) that an unchirped pulse undergoes dispersion broadening regardless of the sign of β_2. Hence, a pulse will broaden by an equal amount governed by β_2 in both normal and anomalous fibre types for a given length of L_D. However, if the initial pulse is linearly chirped this does not hold and the pulse evolution differs for normal and anomalous dispersion regimes (section 2.3.1). While the dispersion-induced pulse broadening is a linear effect, it plays a significant role at bit rates of 40Gbit/s and higher where the pulses broaden out rapidly, creating the necessary condition for intra-channel nonlinear effects as described in detail in section 2.6 and 2.7. Furthermore, pulse broadening also leads to ISI making the system susceptible to any uncompensated dispersion (see chapter 6). The dispersion property of the fibre is therefore significant in the overall transmission performance, and is investigated in more detail in chapter 4.

2.3.1 Chirped pulses and dispersion-induced broadening

A linearly chirped Gaussian pulse is described mathematically as follows:

$$A(0,T) = \exp\left(-\frac{(1+iC)}{2}\frac{T^2}{T_0^2}\right) \tag{2.13}$$

The chirp is the measure of the instantaneous frequency variation between the leading and trailing edge of a signal pulse. C is the chirp parameter and in this case represents the initial linear chirp. The amplitude and pulse broadening factor of the pulse at any point z is shown by the following equations using equation (2.11a) [AGR'01]:

$$A(z,T) = \frac{T_0}{[T_0^2 - i\beta_2 z(1+iC)]^{1/2}}\exp\left(-\frac{(1+iC)T^2}{2[T_0^2 - i\beta_2(1+iC)z]}\right) \tag{2.14}$$

$$\frac{T_1(z)}{T_0(0)} = \sqrt{\left(1+\frac{C\beta_2 z}{T_0^2}\right)^2 + \left(\frac{\beta_2 z}{T_0^2}\right)^2} \tag{2.15}$$

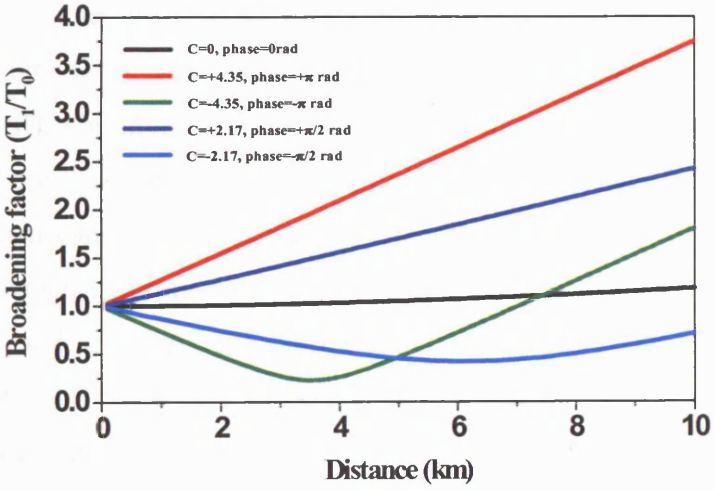

Fig. 2.2 *Broadening factor for a chirped Gaussian pulse for increasing propagation distance over SSMF with β_2=21.7ps/(nm^2.km). The chirp of ±4.35 and ±2.17 corresponds to a phase variation of ±π and ±π/2, respectively. This is similar to that present in the π-AP-RZ and π/2-AP-RZ modulation formats described in chapter 5*

In the case of π-alternate-phase RZ (AP-RZ) described in chapter 5, the chirp induced is ±4.35 between adjacent pulses. *Fig. 2.2* shows the pulse broadening due to chirp for transmission over SSMF. Equation (2.15) differs from equations (2.11a) and (2.12b), for the unchirped pulse in that the broadening is dependent on the relative signs of β_2 and C. While the pulse may broaden monotonically with z if $\beta_2 C>0$, it initially narrows and then begins to broaden when $\beta_2 C<0$. This pulse narrowing occurs because the dispersion induces chirp which is opposite to the initial chirp leading to a minimum pulse width when the two chirps (due to dispersion and inherent in π-AP-RZ) cancel each other. Beyond this stage, however, the dispersion-induced chirp begins to dominate for increasing propagation distances leading to constant pulse broadening. Another property of chirped pulses is that it leads to an increase in spectral width by a factor of $(1+C)^{1/2}$. This behaviour of chirp in the presence of dispersion is significant in the pulse evolution of the alternate-phase RZ modulation format discussed in chapters 5 and 6.

2.3.2 Dispersion compensation

Pulse broadening is undesirable as it interferes with the pulse detection process if the pulse spreads outside its allocated bit slot, and this effect is known as inter-symbol-interference (ISI). Counteracting ISI by signal transmission at the zero-dispersion wavelength where pulse broadening is kept to a minimum is not a practical option as only one channel can be used at this wavelength in a WDM system. Furthermore, nonlinear effects such as four-wave-mixing (described later), occur when the GVD is relatively low and the walk-off (section 2.4.3) between WDM channels is also minimised leading to an increase in penalty (also see IFWM described in section 2.6). Hence, dispersion management techniques employ systems with low GVD over the entire transmission link to reduce ISI, while the local dispersion of each fibre section is maintained as high as possible to minimise the nonlinear effects.

In its most basic form dispersion compensation employs two types of fibre with opposite values of β_2 between each amplifier span to give a low average dispersion. For example 60km of SSMF with β_2 =-21.7ps/(nm^2.km), is compensated by 12km of

DCF with β_2 =108.5ps/(nm^2.km), giving an average dispersion of zero. In practice, this is not easily achieved owing to the different lengths of amplifier spacings in the transmission link as the dispersion compensators are typically of fixed lengths [YOK'03].

In general, the dispersion slope corresponds to the change in the dispersion parameter D, with wavelength λ, and like D varies with fibre type. Therefore, incomplete dispersion compensation also arises if β_3 (which also quantifies the dispersion slope as described in equation (2.3) and from the derivative of equation (2.6)) of the transmission fibre and dispersion compensator are not matched, in which case total dispersion compensation is achieved for a single wavelength only, leading to varying amounts of undesirable residual dispersion at other wavelengths. There has been progress in developing dispersion compensators capable of broadband dispersion compensation, where β_3 is also compensated for, and is still under research [KNU'02]. As such dispersion slope compensation has gained significance, particularly with the increase in operating bit-rate. Chapter 4 investigates the dispersion slope compensation of a higher-order-mode dispersion management device (described next) for simultaneous compensation of 10 WDM channels at 40Gbit/s, eliminating the need for dispersion trimming on a channel-by-channel basis [XIE'00]. However, while uncompensated dispersion slope is generally undesirable, it is made use of in a novel experimental technique (described in chapter 6), for investigating dispersion tolerances.

The most common fibre optic links use SSMF compensated by DCF. DCF typically has higher loss and is also highly nonlinear owing to its design, as it incorporates a single mode of transmission (as in SSMF) but has a relatively small core diameter as illustrated in *Fig. 2.3*, thereby enabling signal propagation in a medium of refractive index capable of reversing the dispersive properties of SSMF. This thesis predominantly investigates amplifier spans consisting of 60km SSMF compensated by 12km of DCF. The transmission link is described in greater detail in section 4.2.

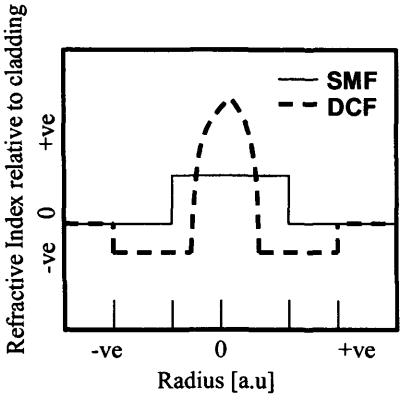

Fig. 2.3 *Refractive index profile of SSMF and DCF*

Compensating fibre types which support higher-order-modes are being researched as they are capable of loss similar to that of SSMF whilst also incorporating large negative dispersion, and hence require shorter fibre lengths. Furthermore, it is possible to compensate dispersion over a broad bandwidth with these higher-order-mode based devices by compensating simultaneously for β_2 and β_3 for a particular fibre type [GNA'00, TUR'01].

One such higher-order-mode (HOM) dispersion compensator which was investigated in this work, is the HOM-dispersion management device (HOM-DMD) developed by LaserComm Inc. It required mode converters at the input ($LP_{01} \rightarrow LP_{02}$) and at the output ($LP_{02} \rightarrow LP_{01}$), where LP denotes linearly polarised mode. It was made up of approximately 750m of HOM fibre, designed to support the LP_{02} mode and was designed to compensate 75km of NZDSF *(Fig. 2.4)*. The selected LP_{02} mode was used because of its dispersive properties and circular symmetry [GNA'00]. This principle allowed the use of a shorter length of fibre and larger core diameter compared to standard DCF, with much lower nonlinearity and loss. These features were used in the design of novel dispersion maps described in chapter 4, enabling high launch powers into the HOM-DMD and new span designs. Typical properties of various transmission fibres and dispersion compensation elements can be found in Appendix 1.

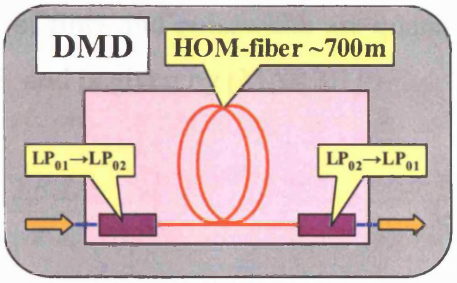

Fig. 2.4 *Schematic diagram of LaserComm Inc., higher-order-mode dispersion management device (HOM-DMD)*

2.3.3 Description of typical dispersion maps

In practice, fibre optic links consist of many amplifier spans, where each amplifier span consists of the transmission fibre and dispersion compensation. Hence, for identical amplifier spans (as in the case of recirculating fibre loop experiments) the dispersion map is cumulative. *Fig. 2.5* shows a schematic diagram of a typical fibre optic link, and also describes the effects of residual dispersion.

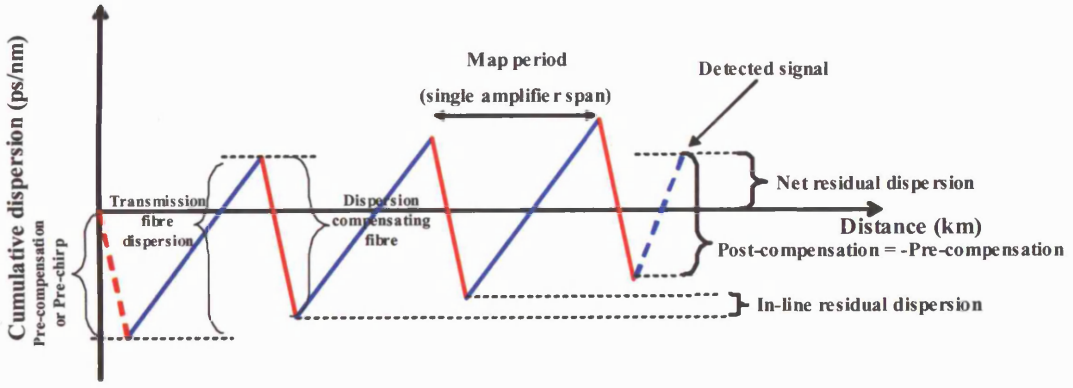

Fig. 2.5 *Typical dispersion map of a transmission fibre link. Further compensation at the receiver is required to cancel the net residual dispersion*

The compensation length of fibre and pulsewidth are quantified by the dimensionless dispersion map strength S, and is given by [MAR'01]:

$$S = \frac{2\beta_2 L}{\tau^2} \qquad (2.16)$$

where L is the length, β_2 is the dispersion of the fibre and τ is the FWHM pulsewidth at the start of the transmission fibre. The dispersion map in this case is assumed to be a two-step profile made up with fibres with normal and anomalous dispersion and of equal length L [HIR'02]. While dispersive effects are linear, the dispersion map is critical in the presence of fibre nonlinearities and, hence, very different behaviour can be observed at different map strengths [ABL'00]. The impact of map strength on transmission performance is described in chapter 4.

2.4 Fibre nonlinearities

There are two types of nonlinear distortion which occur in the optical fibre. The first is known as the Kerr nonlinearities, which occurs due to the third order susceptibility ($\chi^{(3)}$) of the fibre. Self-phase modulation (SPM), cross-phase modulation (XPM) and four-wave-mixing (FWM) are examples of these effects and are described below. These nonlinear effects can take place between adjacent WDM channels, and at high bit rates between pulses of the same wavelength channel and are then known as intra-channel effects. The second type of nonlinear distortion occurs due to the stimulated inelastic scattering between the electrical field and phonon modes in the fibre, such as stimulated Brillouin scattering (SBS) and stimulated Raman scattering (SRS). The work described in this thesis is based on the Kerr nonlinearities and are therefore described in detail in the following section.

2.4.1 Kerr nonlinearities

When the signal power launched into a fibre and transmission distances are increased the nonlinear effects become more significant. The optical medium has a nonlinear response to the incoming electric field E as shown in equation (2.1).

$$P = \chi^{(3)}\varepsilon_0 \vdots E(r,t).E(r,t).E(r,t) \qquad (2.17)$$

Where P = Induced polarisation

$\chi^{(3)}$ = Third order susceptibility

ε_0 = Permittivity of vacuum

$E(r,t)$ = Electric field

The effects of the linear susceptibility $\chi^{(1)}$ are included through the refractive index n and the attenuation coefficient α, while $\chi^{(2)}$ is responsible for second harmonic generation and sum frequency generation. $\chi^{(2)}$ is nonzero only in media that lack inversion symmetry at the molecular level, but, as silica is a symmetric molecule second order nonlinear effects are not observed in optical fibres. $\chi^{(3)}$ causes the generation of four-wave-mixing and nonlinear refraction.

Nonlinear refraction is the intensity dependence of the refractive index. It is represented by the following equation:

$$n = n_0(\omega) + n_2|A|^2 \qquad (2.18)$$

Where $n(\omega)$ is the linear part and $|A|^2$ is the optical intensity inside the fibre.

$$n_2 = \frac{3}{8n(\omega)}\chi^{(3)} \qquad (2.19)$$

Fibre nonlinear effects can be separated into those which arise during the transmission of a single wavelength channel (intra-channel) and in multi-channel transmission (inter-channel), as described in the introduction in chapter 1.

2.4.2 Self-Phase Modulation (SPM)

This refers to the self induced phase shift experienced by single wavelength optical field during its propagation in an optical fibre. The phase change due to intensity can be described as follows:

$$\phi_{NL} = \hat{N} = \left(n_0 + n_2|A(z,t)|^2\right)k_0 L \qquad (2.20)$$

where n_0 is refractive index, n_2 is the intensity-dependant refractive index, $k_0=2\pi/\lambda$ and is known as the propagation constant, and L is the length of the fibre. Equation (2.20) describes the nonlinear propagation $\hat{N}$, in the numerical simulator as described in equation (2.78) in section 2.9.

The definition of pulse evolution due to the induced phase caused by SPM can be derived in a similar fashion to that of GVD. By assuming $\beta_2 = 0$ in the NLSE it is possible to show that the phase shift due to SPM is:

$$\phi_{NL}(L,T) = |A(0,T)|^2\left(L_{eff}/L_{NL}\right) \qquad (2.21)$$

Nonlinear effects are dependent on the signal power, and the effective length L_{eff} defines the length of fibre over which nonlinear effects cannot be ignored. L_{eff} and L_{NL} are defined as follows:

$$L_{eff} = \frac{\left[1 - e^{-\alpha L}\right]}{\alpha} \tag{2.22}$$

$$L_{NL} = \frac{1}{\gamma P_0} \tag{2.23}$$

$$\gamma = \frac{k_0 n_2}{\lambda} = \frac{n_2 \omega_0}{c A_{eff}} \tag{2.24}$$

A_{eff} and ω_0 in equation (2.24) represents the effective area of the fibre and zero dispersion frequency respectively. It is clear from equation (2.20) that a maximum phase shift occurs at the centre of the pulse where the pulse power is at a maximum (P_0), and this phase shift is defined as

$$\phi_{\max} = \frac{L_{eff}}{L_{NL}} = \gamma P_0 L_{eff} \tag{2.25}$$

with L_{eff} and L_{NL} constant.

The resultant spectral broadening is a dominant characteristic of SPM. It is explained by the fact that the varying phase implies that the instantaneous optical frequency differs across the pulse from the centre with:

$$\delta\omega(T) = -\frac{\partial \phi_{NL}}{\partial T} \tag{2.26}$$

The time-dependence of $\delta\omega$ also manifests itself as chirp (C) in equation (2.14), however, in this instance it increases with propagating distance. The variation of nonlinear phase and the induced frequency chirp increase for steeper leading and trailing edges of the pulse. The resultant chirp is red-shifted at the leading edge and blue-shifted at the trailing edge. *Fig. 2.6* illustrates the variation in chirp between a

Gaussian pulse *(m=1)* and super-Gaussian pulse *(m=3)*, where *m* indicates the rise and fall time of the pulse edges and is described mathematically as follows:

$$A(0,T) = \exp\left(-\frac{(1+iC)}{2}\left(\frac{T}{T_0}\right)^{2m}\right) \tag{2.27}$$

These values are comparable to the RZ and NRZ modulation format used in the experiments described in chapters 4-6.

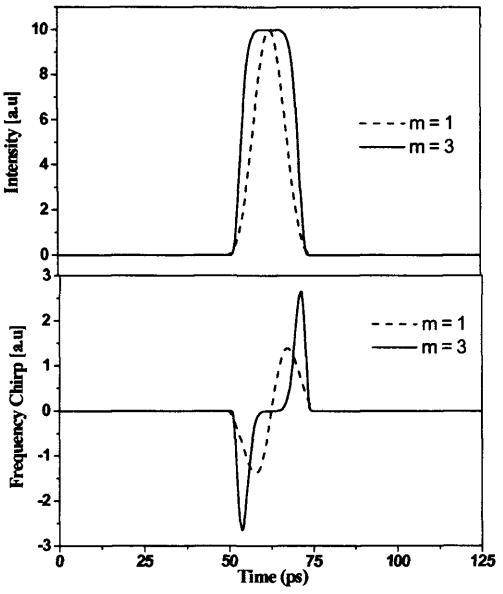

Fig 2.6 *SPM-induced chirp due to intensity variation in the time domain chirp occurs only at the pulse edges. Leading edge is (red shifted) trailing edge (blue-shifted)*

The SPM-induced chirp alone does not introduce any transmission penalty when detected using intensity-modulation direct-detection (IM-DD), used in the experimental investigations of chapters 4-6, as such receivers only detect the intensity of the waveform and all phase information is lost. However, as discussed in section 2.3 which described fibre dispersion, the effect of pulse broadening occurs due to the different velocities of the spectral components and this effect is enhanced in the presence of the new spectral components generated by the SPM chirp.

In section 2.3.1 it was shown how a chirped pulse can be compressed whenever the dispersion parameter β_2 and the chirp C happen to have opposite signs so that $\beta_2 C$ is negative. As SPM-induced chirp is positive, while β_2 for transmission fibre (eg. SSMF, NZDSF) is negative, the condition such that SPM-induced chirp is exactly equal and opposite to the dispersion parameter β_2 can be achieved. Under this condition, the SPM chirp cancels out the dispersion-induced pulse broadening resulting in the undistorted propagation of the signal, without the need for any dispersion compensation. This type of transmission is known as soliton transmission. However, as soliton transmission is sensitive to fluctuations in signal power and dispersion it was considered unsuitable for WDM transmission with periodic amplification, where the fibre dispersion varies with wavelength.

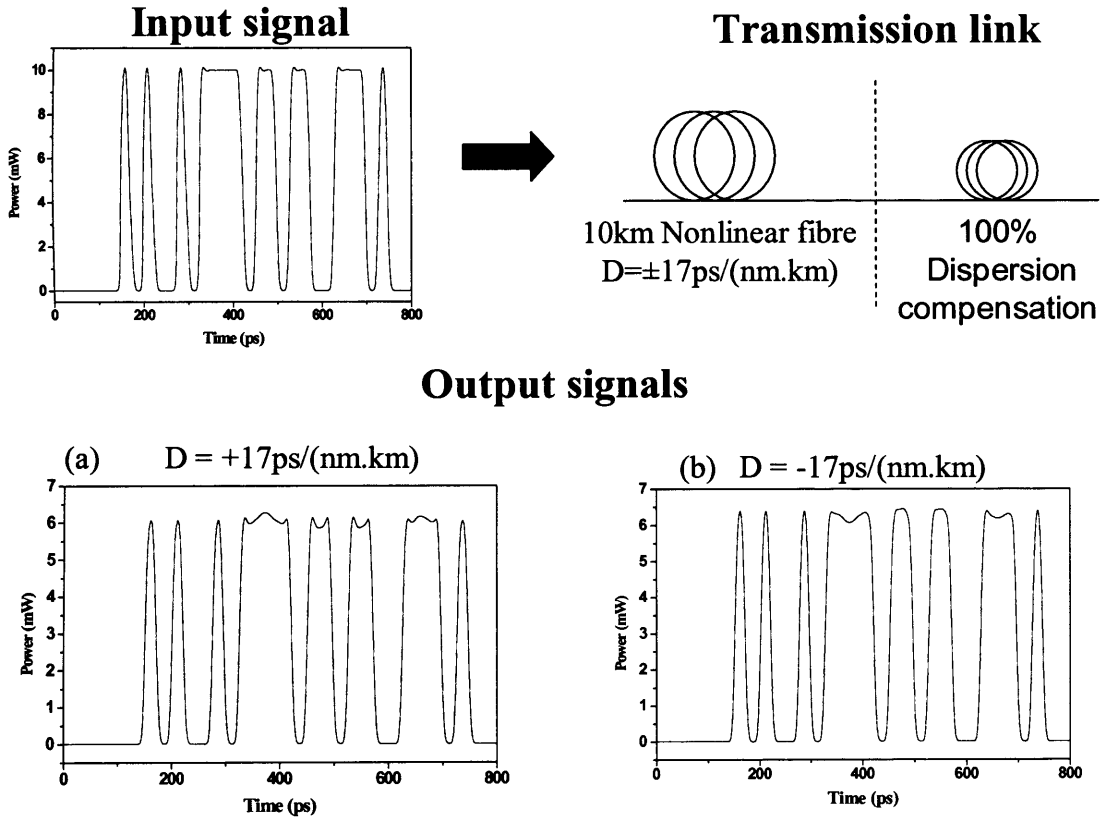

Fig. 2.7 *Illustration of SPM distortion due to PM-IM for (a) D>0 and (b) D<0. The dispersion compensator is linear and exactly compensates for the nonlinear fibre*

Fig. 2.7 shows the conversion of phase modulation to intensity modulation (PM-IM) in the presence of dispersion, where the different arrival times of the spectral components lead to pulse distortion for transmission over a perfectly compensated fibre link. The sign of the dispersion parameter leads to variations in the intensity modulation and is useful in identifying the presence of SPM by the analysis of eye diagrams. These effects were observed in the study of dispersion tolerances in chapter 6, where SPM was observed to enhance the dispersion tolerance for nonlinear propagation, while phase modulation led to intensity modulation during linear propagation.

2.4.3 Cross-Phase Modulation (XPM) and walk-off

XPM is caused by the nonlinear phase shift of an optical field induced by an optical field co-propagating at a different wavelength. Hence, this is known as an inter-channel nonlinear effect and occurs in WDM transmission, unlike SPM which is present even in the propagation of a single channel only. When two co-polarised optical fields at frequencies ω_1 and ω_2, propagate simultaneously inside the fibre, the nonlinear phase shift for the field at ω_1, is given by the equation [AGR'01]:

$$\phi_{NL} = \left(n_0 + n_2 \left(\left| A_{\lambda_1}(z,t) \right|^2 + 2 \left| A_{\lambda_2}(z,t) \right|^2 \right) \right) k_0 L \qquad (2.28)$$

The first term in equation (2.28) is due to SPM and the second is due to XPM and like in the case of SPM, signal distortion occurs due to PM-IM conversion in the presence of fibre dispersion. However, unlike SPM, XPM can be cancelled by a physical process known as walk-off.

Walk off occurs due to overlapping pulses at different wavelengths propagating at different speeds inside the fibre because of the group velocity mismatch [MAR'94]. During this process, the induced XPM between two optical pulses at different wavelengths ceases to occur, as the faster moving pulse has completely walked through the slower moving pulse, undoing the induced XPM created when the pulses were partially overlapped.

For pulses of width T_0 the walk-off length is defined by the following relation:

$$L_W = \frac{T_0}{|d_{12}|} \qquad (2.29a)$$

and the walk off parameter d_{12} is defined as follows:

$$d_{12} = v_g^{-1}(\lambda_1) - v_g^{-1}(\lambda_2) \qquad (2.29b)$$

In equation (2.29b), v_g is the group velocity of a particular wavelength. Hence, it can be seen that walk-off can be increased by increasing the channel spacing between the interacting channels or by increasing the dispersion of the nonlinear fibre. Equation (2.29a) shows that the walk-off length decreases with decreasing pulsewidth and increasing fibre local dispersion. Therefore, narrow pulsewidths and high fibre local dispersion are desirable in the suppression of XPM. However, as described previously narrow pulsewidths are more sensitive to fibre dispersion leading to rapid pulse broadening (section 2.2), leading to a trade-off in the optimal pulsewidth and fibre type.

While it is clear that SPM occurs in single channel transmission and XPM in multi-channel transmission, it was important to investigate which of these effects dominate the overall signal distortion, particularly for transmission at 40Gbit/s where the walk-off is a factor of 16 higher compared to that seen at 10Gbit/s. As the walk-off decreases with pulsewidth, section 2.5 discusses the impact of SPM and XPM for the NRZ and RZ modulation format. For example, for a channel spacing of 0.8nm (as investigated in chapter 4) the walk-off length, L_W, for the NRZ modulation format is 1.85km, and decreases to 0.82km for the RZ modulation format for transmission over SSMF. The low fibre local dispersion in NZDSF, however, increases the walk-off length to 7.81km (NRZ) and 3.51km (RZ). As the shorter walk-off lengths are more desirable it can be seen that RZ transmission over SSMF is most desirable for the suppression of XPM [THI'00]. Further, experimental and numerical investigations of these effects are also carried out in chapter 4.

2.4.4 Four-wave-mixing (FWM)

As mentioned in section 2.4.1, the third order susceptibility causes nonlinear refraction (discussed in the previous sections) and four-wave-mixing. Like XPM, FWM is an inter-channel nonlinear effect, and is described from the basic equation describing nonlinear equations as described in equation (2.17). Considering optical fields with carrier frequencies ω_1, ω_2 ω_3 and ω_4 co-propagating simultaneously along the x-axis inside the fibre, equation (2.17) can be represented as:

$$P = \hat{x}\frac{1}{2}\left[P_1 e^{i(k_1 z-\omega_1 t)} + P_2 e^{i(k_2 z-\omega_2 t)} + P_3 e^{i(k_3 z-\omega_3 t)} + P_4 e^{i(k_4 z-\omega_4 t)}\right] \tag{2.30}$$

Where $k_i=n_i\omega_i/c$ is the wave-vector or propagation constant. The nonlinear behaviour of ω_4, can therefore be described by the following equation by substituting equation (2.20) in equation (2.30), and is similar for the optical frequencies at ω_1, ω_2 and ω_3:

$$P_4 = \frac{3\varepsilon_0}{4}\chi^{(3)}_{xxxx}\Big\{\Big[\underbrace{|E_4|^2}_{SPM} + \underbrace{2\left(|E_1|^2+|E_2|^2+|E_3|^2\right)}_{XPM}\Big]E_4 + \underbrace{2E_1E_2E_3e^{i[(k_1+k_2+k_3-k_4)z-(\omega_1+\omega_2+\omega_3-\omega_4)t]}}_{FWM} + \underbrace{2E_1E_2E_3^* e^{i[(k_1-k_2-k_3-k_4)z-(\omega_1+\omega_2-\omega_3-\omega_4)t]}}_{FWM} + \underbrace{\ldots}_{FWM}\Big\} \tag{2.31}$$

The FWM terms in the above equation generate new frequency components, which may coincide with the existing signal frequencies and appear as inter-channel cross-talk. Signal distortion in the signal channels occur even if these new frequency components lay outside the existing signal frequencies because of the loss in channel power. However, FWM requires the interacting frequencies to be phase matched which occurs when the wave vectors are matched such that $\Delta k=0$. In practice, this is not easily achieved, and the achievable FWM terms commonly occur under the following conditions:

$$\Delta k = k_3 + k_4 - k_1 - k_2 = 0 \tag{2.32a}$$

$$\omega_3 + \omega_4 = \omega_1 + \omega_2 \tag{2.32b}$$

The FWM process can be viewed as a scattering process in which two photons of energies $h\omega_1$ and $h\omega_2$ create new photons of energies $h\omega_3$ and $h\omega_4$. The phase matching condition then stems from the requirement for the conservation of energy, making the above conditions most feasible.

The FWM can be minimised through the use of high local dispersion. The amount of FWM generated for a given phase mismatch $\Delta\beta=\beta_1+\beta_2+\beta_3-\beta_4$, between the propagation constant β_4, of the optical signal at frequency ω_4 is given by the following FWM efficiency η_{FWM}:

$$\eta_{FWM}(\Delta\beta)=\frac{\alpha^2}{\alpha^2+(\Delta\beta)^2}\left(1+\frac{4e^{-\alpha L}\sin^2\left(\frac{\Delta\beta L}{2}\right)}{\left(1-e^{-\alpha L}\right)^2}\right) \qquad (2.33)$$

with $\eta_{FWM}=1$, when $\Delta\beta=0$. The presence of fibre dispersion reduces the phase matching condition. This feature makes the transmission over dispersion shifted fibre (DSF) undesirable [MAR'91. TKA'95]. In the work described in this thesis, FWM between WDM wavelength channels does not exist due to the non-zero dispersion of the transmission fibre investigated. However, this process is present in between pulses of the same wavelength channel and is described in more detail in section 2.6.

2.5 Standard modulation formats

Non-return-to-zero (NRZ): This is the most widely employed modulation format at present. This is largely due to historic reasons where digital signals were coded electronically as on-off-keying (OOK) which required simpler device technologies. Furthermore, when digital systems were first implemented for optical transmission over fibre, the signal was modulated by varying the pump current of laser diodes to vary the output power. As varying the laser current cannot be achieved at high-speeds, the NRZ format was favoured owing to the reduced bandwidth requirements. This can be seen in the reduced spectral bandwidth of an NRZ signal *(Fig. 2.7)*. Simple direct-detection at the receiver, where the received power is measured on a photo-detector, can be used for the intensity-modulated (IM) NRZ data.

Return-to-zero (RZ): The advantage of this modulation format is that every single representation of a logical 'one' is identical in shape and, hence, affected in a similar manner by dispersion and nonlinearities. Furthermore, it enables optical time division multiplexing (OTDM) which is useful for increasing the bit rate within the same wavelength channel. The modulation bandwidth of RZ is greater than that of NRZ *(Fig. 2.7)*, leading to a decrease in spectral efficiency. However, a channel spacing of 100GHz (0.8nm), as used in commercial 10Gbit/s systems is wide enough for both NRZ and RZ operation at 40Gbit/s with no added penalty. The RZ intensity-modulated format is also detected at the receiver using photo-detector.

Fig. 2.7 illustrates the difference between the NRZ and RZ modulation format in the time and frequency domains, for identical 32-bit pseudo-random-bit-sequence (PRBS). The two formats in the figure are unchirped and similar to the pulsewidths and shapes used in the experiments described in chapters 4-6. The NRZ format is generated by simulation using 6^{th} order Bessel filtered rectangular pulses, while the RZ format is generated using Gaussian pulses with a pulsewidth of 11.25ps (FWHM). More details of the transmitter parameters can be found in section 2.9.

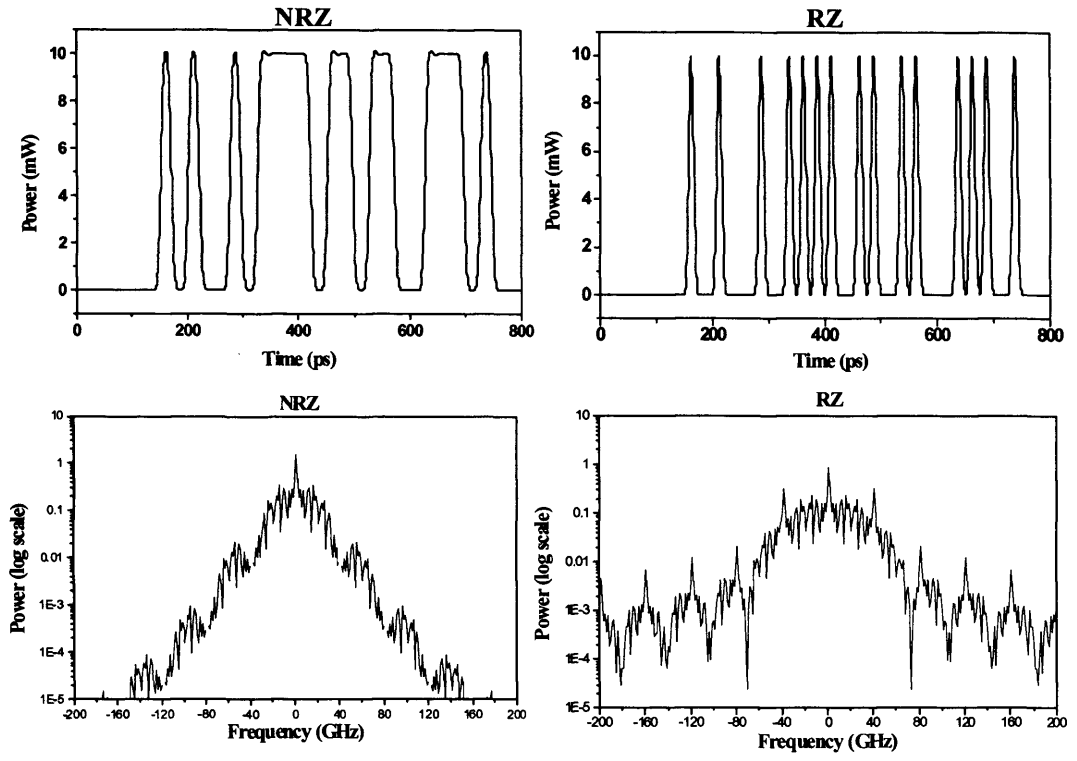

Fig. 2.7 *Signal encoded with the identical 32 bit pseudo random bit sequence, at a bit-rate of 40Gbit/s.* ***Left:*** *NRZ,* ***Right:*** *RZ format* T_{FWHM}*=11.25ps*

2.5.1 Comparison of NRZ and RZ modulation formats in the presence of dispersion and nonlinear effects

The first comparison of NRZ and RZ, the two most common modulation formats employed in systems with intensity-modulated direct-detection (IM-DD), were performed by Personick in 1973 in order to understand which modulation format had the superior receiver sensitivity [PER'73]. It was shown that the optimal input pulse for an IM-DD optical communication system is an impulse. Hence, for receivers with *p-i-n* photodiodes an improvement of 2dB in sensitivity can be obtained for RZ compared to NRZ, and a duty cycle of 50% was sufficient to achieve the majority of this improvement. The reason for this is that the RZ pulse energy is concentrated in a shorter time interval, providing a larger eye opening for the same filter bandwidth or the possibility of enhanced noise rejection for the same inter-symbol-interference (ISI).

Chromatic dispersion causes a delay between the spectral components of the signal. The lower the duty cycle ρ, the larger the modulation bandwidth, resulting in the signal being more susceptible to dispersion. The dispersion length L_D at which the penalty is not negligible, for a bit rate R, is represented for the RZ modulation format as follows [FOR'97]:

$$L_D = \frac{c}{\lambda^2}\frac{\rho}{R^2 D} \qquad (2.34)$$

This differs from equation (2.12) where the dispersion is proportional to T_0^2 (or ρ^2), but it does not reflect system penalties for the RZ format, where the pulse duration is reduced by a factor ρ, while the bit duration remains constant.

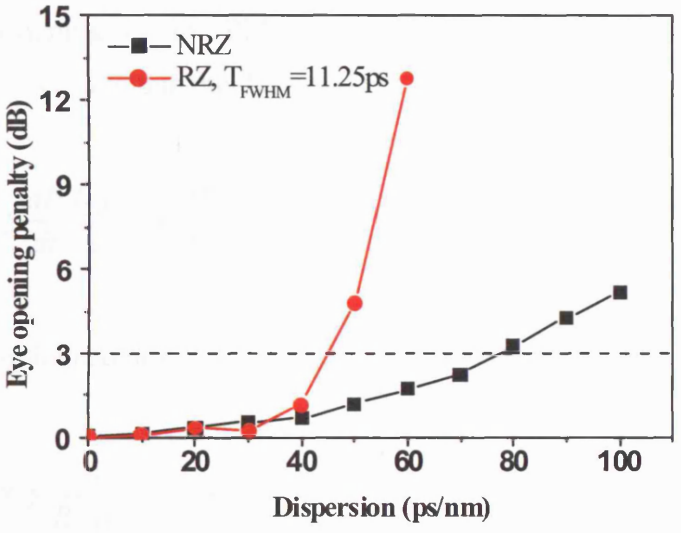

Fig. 2.8 *Eye opening penalty at 40Gbit/s for NRZ and RZ modulation formats. The low duty cycle of the RZ modulation increases dispersion penalty*

Fig. 2.8 plots the eye opening penalty (described in 2.7.3) as a function of dispersion for initially unchirped NRZ and RZ transmission at 40Gbit/s. The results show reduced dispersion tolerance for the RZ modulation (ρ=0.45), compared to NRZ (ρ=1) as expected according to equation (2.34).

The walk-off distance defined as the distance over which two pulses (ρ=1 (NRZ), ρ=0.45 (RZ)) in adjacent channels, which are initially overlapped, to completely separate is [FOR'97]:

$$L_W = \frac{c}{\lambda^2}\frac{\rho}{R^2 D\Delta f} \tag{2.35}$$

where Δf is the channel spacing. Equations (2.34) and (2.35) can be re-arranged to give

$$L_D = \frac{\Delta f}{R}.L_W \tag{2.36}$$

The spectral broadening due to SPM described by equations (2.25) and (2.26) can be modified as follows to include the duty cycle ρ:

$$\Delta B = \gamma \frac{dP}{dt}\frac{L_{eff}}{\rho} \propto \gamma \frac{P}{\rho T}\frac{L_{eff}}{\rho} \tag{2.37}$$

and the SPM length becomes:

$$L_{SPM} \propto \gamma \frac{1}{R\Delta B.D} = \frac{\rho^2}{\gamma P L_{eff} R^2 D} \tag{2.38}$$

It can therefore be seen that the SPM distortion decreases rapidly with decreasing pulse duty cycle (as rapid pulse broadening decreases the pulse peak power), and therefore impacts on the choice of modulation format (NRZ/RZ).

For XPM the spectral broadening is given as:

$$\Delta B = 2\gamma \frac{dP}{dt}\frac{\varepsilon L_W}{\rho} = 2\gamma \frac{1}{\rho \in \rho T}\frac{P}{\lambda^2}\frac{c}{D\Delta f}\frac{\varepsilon \rho T}{} \tag{2.39}$$

where *dP/dt* is the time derivative of the power in the interfering pulse and $\varepsilon \rho T$ is the rise time of the pulse edge. This is the worst case of a two-channel interaction as it represents an incomplete pulse collision where the interfering pulse has passed through only partially through the affected signal pulse. The characteristic length for XPM is hence given as:

$$L_{XPM} \propto \gamma \frac{1}{R\Delta B.D} \propto \frac{\Delta f}{R} \frac{\rho}{2\gamma P} \tag{2.40}$$

Unlike for SPM, the XPM decreases proportionally with the duty cycle. The weaker dependence results from the reduced duty cycle leading to a reduction in the interacting length.

It can be seen from the theory described in this section, that the pulsewidth plays a significant role on strength of the SPM and XPM interaction during signal propagation. In general, as these distortions decrease with pulsewidth, it maybe concluded that optimum transmission performance is obtained for signals with the narrowest possible pulsewidth. However, as spectral broadening is inversely proportional to the pulsewidth, the use of narrow pulses can lead to linear cross-talk between WDM channels, and mitigating this effect can lead to reduced spectral efficiency. Furthermore, as shown in *Fig. 2.8*, narrowing the pulsewidth makes the signal less tolerant to dispersion, which leads to two significant disadvantages. Firstly, the signal becomes less tolerant to dispersion, and secondly this dispersion-induced pulse overlap leads to further nonlinear interaction between overlapping pulses of the same wavelength channel known as intra-channel nonlinear distortions (described in the next section). Hence, the choice of modulation format, in particular the pulsewidth (or duty cycle) was investigated in chapter 4. The impact of the properties of the transmission fibre was significant in this investigation, and based on this study, further techniques for optimising the modulation format were investigated in chapter 5.

2.6 Intra-channel nonlinear interaction

As described in section 2.4.2, the nonlinear interaction occurring during the propagation of a single wavelength channel is SPM, which is present even for the propagation of a single isolated pulse. Nonlinear signal distortion may also take place between pulses of different wavelength channels, which affect WDM systems such XPM (section 2.4.3) and FWM (section 2.4.4). However, as dispersion-induced pulse overlap increased with bit-rate, such multi-wavelength channel nonlinear interactions were found to take place between overlapping pulses of the same wavelength channel. This differs from SPM, which also occurs for single wavelength propagation, where at least two pulses are required for this physical mechanism to take place. These intra-channel effects were first reported in [JAC'92], but was identified as a possible source of signal limitation in 40Gbit/s optical transmission by [ESS'99, MAM'99].

2.6.1 Intra-channel four-wave-mixing (IFWM)

A significant source of nonlinear distortion occurring between highly dispersed pulses within a given wavelength channel is the intra-channel four-wave-mixing. The nonlinear interaction leads to the growth of 'ghost' or shadow pulses in the 'zero' bit slots and amplitude jitter in the 'ones'. This takes place as a result of four-wave-mixing (section 2.4.4) interaction between different spectral components of overlapping pulses, and the dispersed pulses experience a small portion of their field shifted by a discrete frequency value [SHA'98]. Hence, when such pulses are dispersion compensated, the induced frequency shift appears in adjacent bit slots as signal distortion when observed in the time domain, and is illustrated schematically in *Fig. 2.9.*

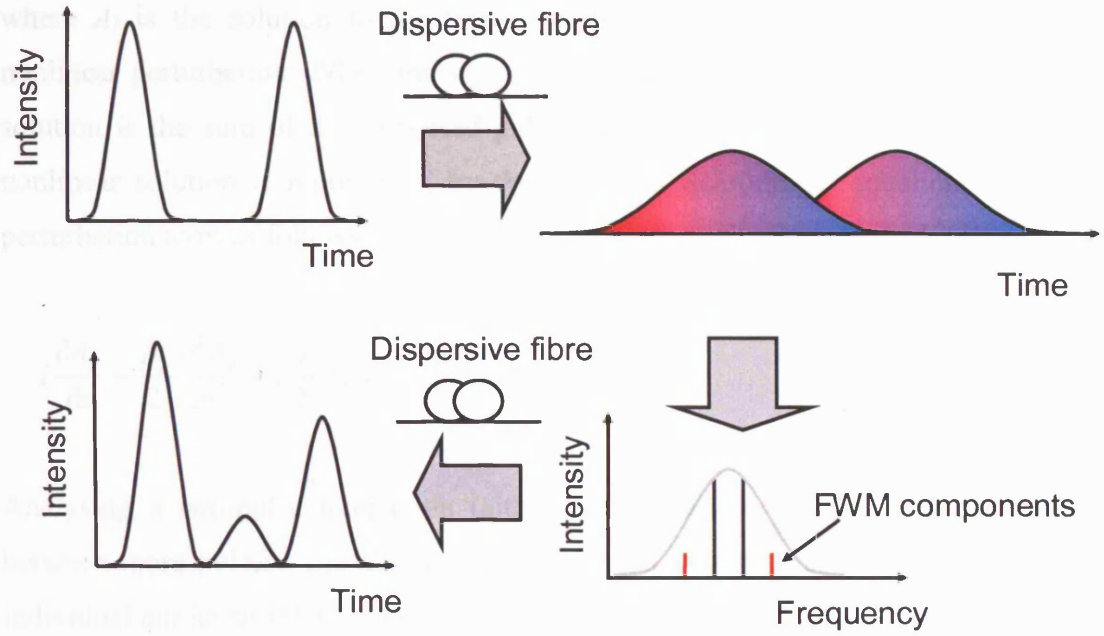

Fig. 2.9 ***Schematic description of IFWM:*** *A '101' pattern undergoes dispersion-induced pulse broadening. The frequency components between overlapping pulses beat and generate new frequency components. The new frequency components appear as a shadow or 'ghost' pulse in the '0' bit slot, while the resulting loss of spectral power in '1' bit slot appears as amplitude jitter.*

Unlike split-step-Fourier simulations (described in section 2.9), which numerically solves the NLSE, the perturbation approach is useful to analyse the physical mechanisms which take place during the propagation of an optical signal in fibre individually [MEC'00, JOH'01]. Furthermore, as the perturbation approach is a semi-analytical investigation, it is quicker than that of split-step-Fourier simulations [TUR'99b]. In this instance, the IFWM is investigated using the small-field perturbation analysis, and is described as follows.

For a dispersion managed system where the nonlinearity is a small perturbation the total signal amplitude is written as:

$$A(z,t) = A_l(z,t) + A_p(z,t) \qquad (2.41)$$

where A_l is the solution to the linear Schrödinger equation *(γ=0)* and A_p is the nonlinear perturbation. When the signal is a sequence of Gaussian pulses the linear solution is the sum of the dispersed pulses with no interaction between them. The nonlinear solution is represented by the nonlinear Schrödinger equation, using the perturbation term as follows:

$$i\frac{\partial A_p}{\partial z} - \frac{\beta_2}{2}\frac{\partial^2 A_p}{\partial t^2} + i\frac{\alpha}{2}A_p + \gamma|A_l|^2 A_l = 0 \tag{2.42}$$

Analysing a two-pulse interaction (although this can be extended for interactions between more pulses), the above equation can be re-written as follows to show the individual nonlinear interactions [JOH'01].

$$i\frac{\partial A_p}{\partial z} - \frac{\beta_2}{2}\frac{\partial^2 A_p}{\partial t^2} + i\frac{\alpha}{2}A_p = -\gamma\left[\underbrace{|A_1|^2 A_1 + |A_2|^2 A_2}_{SPM} + \underbrace{2|A_1|^2 A_2 + 2|A_2|^2 A_1}_{IXPM} + \underbrace{A_1^2 A_2^* + A_2^2 A_1^*}_{IFWM}\right] \tag{2.43}$$

Equation 2.43, describes the SPM, IXPM and IFWM as indicated. Hence, for investigating the IFWM only, the terms $A_1^2 A_2^*$ and $A_2^2 A_1^*$ can be considered separately. The effect of the dispersion is to broaden the pulses, such that neighbouring pulses overlap and interact through the fibre nonlinearity. Assuming that each amplifier span in a transmission link has an identical configuration, with exact linear dispersion compensation, the perturbation analysis yields the following expression for the amplitude of the ghost pulse at the output of the N-span link [KIL'02]:

$$A_p = 2i\gamma N\int_0^L \Im^{-1}\left[\Im\left(A_1^2 A_2^*\right)\exp\left(\frac{i}{2}\beta_2\omega^2\right)\exp\left(-\frac{\alpha}{2}\right)\right]dz \tag{2.44}$$

where $\Im$ indicates the Fourier transform. The factor of two appears when considering the $A_2^2 A_1^*$ interaction from equation (2.43).

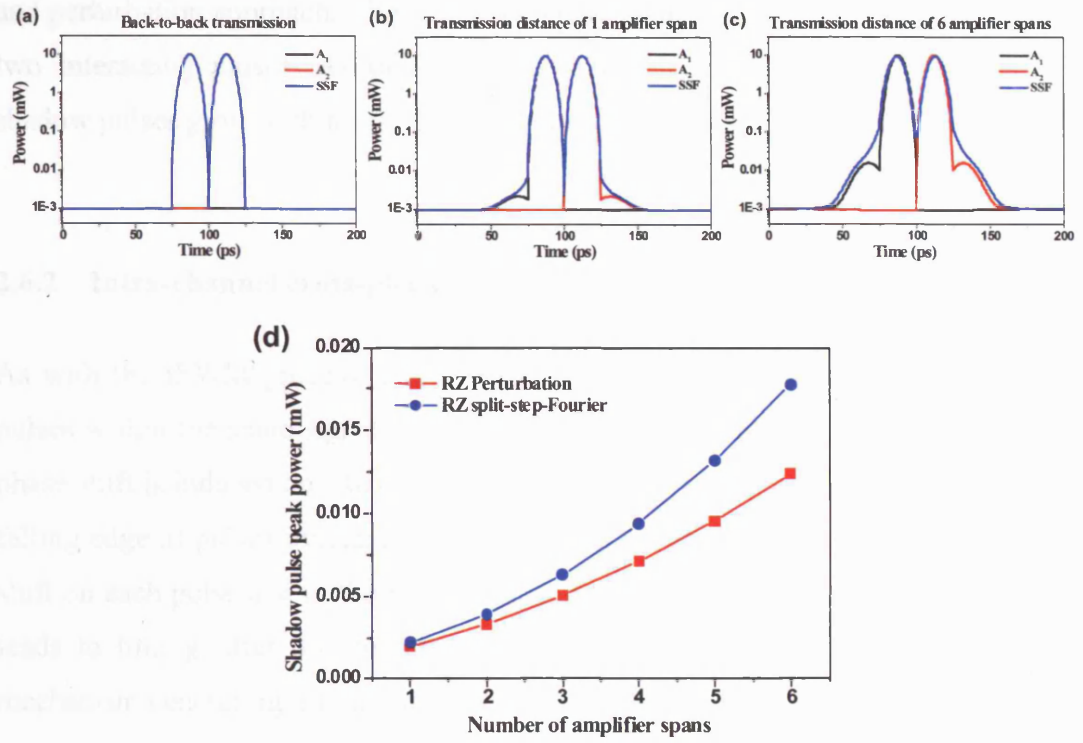

Fig. 2.10 ***Top:*** *40Gbit/s signal waveform of two pulses A_1 and A_2 in the 4^{th} and 5^{th} bit-slot after transmission over (a) back-to-back (b) 60km (c) 360km SSMF, with 10mW pulse peak power at the output of line amplifiers, showing the generated shadow pulses at in the 3^{rd} and 6^{th} bit-slot.* ***Bottom:*** *Growth of shadow pulse power for comparison of perturbation theory with results using split-step-Fourier (SSF) analysis.*

A two-pulse interaction was calculated using the perturbation analysis and is compared with results obtained by split-step-Fourier numerical simulations (described in section 2.9). The resultant evolution of the two pulses is then plotted in *Fig. 2.10(a)-(c)* for back-to-back transmission, and transmission over 1 and 6 amplifier spans in the time domain. Each amplifier span consisted of 60km of SSMF perfectly compensated by 12km of DCF (see appendix 1 for parameters) and the pulse peak power was 10mW. The results shown in *Fig. 2.10* investigate the emergence of 'ghost' or shadow pulses due to IFWM. It should be noted that the ISI is higher in the case of the split-step-Fourier analysis, as the perturbation approach treats the propagation of the two pulses separately. However, when analysing IFWM effects only, from in *Fig. 2.10(a)-(c)*, there is good agreement between the split-step-Fourier

and perturbation approach, where shadow pulses appear as pedestals either side of the two interacting pulses. As this process, is repeated in every amplifier span, the shadow pulses grow with transmission distance, as calculated in *Fig. 2.10(d).*

2.6.2 Intra-channel cross-phase-modulation (IXPM)

As with the IFWM process, IXPM also takes place in the presence of overlapping pulses within the same signal in dispersion managed transmission. Here, a nonlinear phase shift is induced on adjacent pulses due to the varying intensity in the rising and falling edge of pulses overlapping in time. This induced phase generates a frequency shift on each pulse due to the random pulse pattern of 'zeroes' and 'ones', and hence leads to timing jitter due to the dispersion of the transmission fibre. The IXPM mechanism generating timing jitter is illustrated in *Fig. 2.11.*

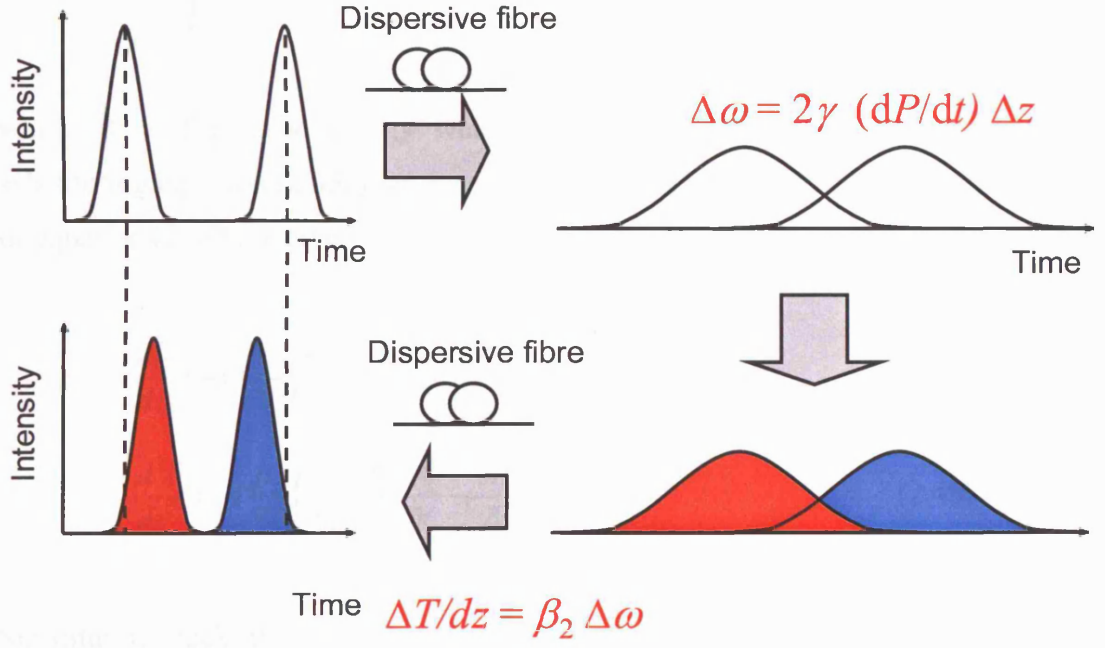

Fig. 2.11 ***Schematic description of IXPM:*** *A '101' pattern undergoes dispersion-induced pulse broadening. The overlapping pulses generate a phase shift on each other. This phase shift is converted to timing jitter when the signal is dispersion compensated.*

The nonlinear phase shift is induced by pulses within the same wavelength channel. However, it is similar in behaviour to XPM between two WDM channels as the pulses are highly chirped due to dispersion and start to overlap in time. From equation (2.43), it is possible to investigate the IXPM effects only by considering the following equations for interaction between two pulses A_1 and A_2 [AGR'01]:

$$i\frac{\partial A_1}{\partial z} = \frac{\beta_2}{2}\frac{\partial^2 A_1}{\partial t^2} - \gamma\left(|A_1|^2 + 2|A_2|^2\right)A_1 - i\frac{\alpha}{2}A_1 \tag{2.45a}$$

$$i\frac{\partial A_2}{\partial z} = \frac{\beta_2}{2}\frac{\partial^2 A_2}{\partial t^2} - \gamma\left(|A_2|^2 + 2|A_1|^2\right)A_2 - i\frac{\alpha}{2}A_2 \tag{2.45b}$$

The mean temporal position of A_1 is defined as [JOH'02b]:

$$\bar{t} = \frac{\int_{-\infty}^{\infty} t|A_1|^2 dt}{\int_{-\infty}^{\infty}|A_1|^2 dt} = \frac{1}{W}\int_{-\infty}^{\infty} t|A_1|^2 dt \tag{2.46}$$

where W is the pulse energy which is conserved throughout transmission. By substituting equation (2.45a) for the z derivative of A_1, the first and second derivatives of equation (2.46) are given as follows.

$$\frac{d\bar{t}}{dz} = -i\frac{\beta_2}{2W}\int_{-\infty}^{\infty}\left(A_1\frac{\partial A_1^*}{\partial t} - \frac{\partial A_1}{\partial t}A_1^*\right)dt \tag{2.47}$$

$$\frac{d^2\bar{t}}{dz^2} = -i\frac{\beta_2}{W}\int_{-\infty}^{\infty}\left(\frac{\partial A_1}{\partial z}\frac{\partial A_1^*}{\partial t} - \frac{\partial A_1}{\partial t}\frac{\partial A_1^*}{\partial z}\right)dt \tag{2.48}$$

Substituting back the second derivative of A_2 from equation (2.45b), simplifies equation (2.48) to give

$$\frac{d^2\bar{t}}{dz^2} = -i\frac{2\gamma\beta_2}{W}\int_{-\infty}^{\infty}|A_1|^2\frac{\partial}{\partial t}|A_2|^2 dt \tag{2.49}$$

By substituting $\Delta T = 2\tilde{t}$ (separation between A_1 and A_2) and $W = \sqrt{\pi}\tau_0 T_0^2$, the pulse separation for two Gaussian pulses (equation 2.10), is related to the pulsewidth and the bit period, and described by the following equation [MAR'01]:

$$\frac{d^2\Delta T}{dz^2} = 2\sqrt{\frac{2}{\pi}}\beta_2 \frac{\gamma W}{\Delta T^2} \frac{\exp\left(-\frac{\Delta T^2}{2\tau_0^2}\right)}{\left(\frac{\tau_0}{\Delta T}\right)^3} \tag{2.50}$$

The induced frequency shift ΔF, which is the mean frequency of the leading pulse minus the mean frequency of the trailing pulse, is related to the pulse separation as follows:

$$\frac{d\Delta T}{dz} = -2\pi\beta_2 \Delta F \tag{2.51}$$

The dimensionless function $F(\tau_0/\Delta T)$ describes the strength of the XPM induced interaction of the pulses and is a measure of the pulse overlap, where

$$F(x) = \frac{\exp\left(\frac{1}{2x^2}\right)}{x^3} \tag{2.52}$$

Equations (2.50)-(2.52) can then be combined to give the induced frequency shift in equation (2.53), as seen in *Fig. 2.12.*

$$\frac{d\Delta F}{dz} = -\frac{1}{\pi}\sqrt{\frac{1}{\pi}}\frac{\gamma W}{\Delta T^2} F\left(\frac{\tau_0}{\Delta T}\right) \tag{2.53}$$

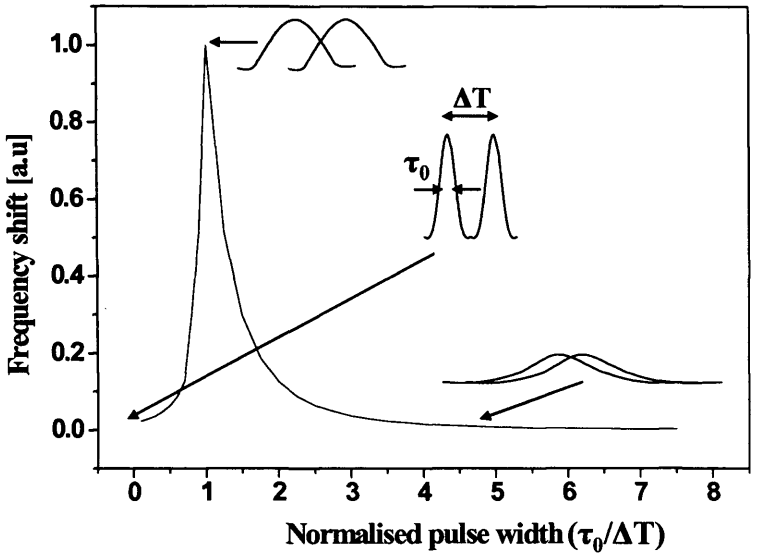

Fig. 2.12 *XPM induced frequency shift as a function of the pulsewidth normalised to the pulse separation [MAM'99]*

It is clear from *Fig. 2.12* that the interaction is strongest when $\tau_0/\Delta T \approx 1$ when the pulses begin to overlap and the pulse derivative is still high. The weak interactions which occur at instances other than $\tau_0/\Delta T \approx 1$ are due to pulse broadening decreasing the pulse derivative at $\tau_0/\Delta T << 1$ and the sign of the derivative changing as the region of overlap increases at $\tau_0/\Delta T >> 1$, leading to a minimal net IXPM effect. It is a feature that is exploited in the transmission of dispersion managed solitons [SMI'97].

2.7 Alternate-polarisation for the suppression of IXPM and IFWM

Sections 2.4.3 and 2.4.4 discussed nonlinear interactions between channels at different frequencies which produce XPM and FWM respectively. However, these coupling effects can also take place between channels of the same frequency but with different polarisation. The magnitude of the optical field components that propagate with orthogonal polarisation between each other is governed by the third order susceptibility $\chi^{(3)}$ (equation (2.17)) and can be written as [AGR'01]:

$$p_x = \frac{3\varepsilon_0}{4}\chi^{(3)}\left[\left(|E_x|^2 + \frac{2}{3}|E_y|^2\right)E_x + \frac{1}{3}\left(E_x^* E_y\right)E_y\right] \quad (2.54a)$$

$$p_y = \frac{3\varepsilon_0}{4}\chi^{(3)}\left[\left(|E_y|^2 + \frac{2}{3}|E_x|^2\right)E_y + \frac{1}{3}\left(E_y^* E_x\right)E_x\right] \quad (2.54b)$$

The nonlinear effects due to the different refractive indices are

$$\Delta n_x = n_2\left(|E_x|^2 + \frac{2}{3}|E_y|^2\right) \quad (2.55a) \qquad \Delta n_y = n_2\left(|E_y|^2 + \frac{2}{3}|E_x|^2\right) \quad (2.55b)$$

These expressions are similar to the nonlinear phase shift due to SPM and XPM, and in fact quantify exactly that for the particular axis of polarisation. They show that the nonlinear phase shift due to the perpendicular axis of polarisation is only 2/3 and not 2 as for co-polarised signals described in section 2.4.3.

Rewriting (P_x,P_y) according to the NLSE, equation (2.1) gives

$$\frac{\partial A_x}{\partial z} + \beta_{1x}\frac{\partial A_x}{\partial t} + \frac{i\beta_2}{2}\frac{\partial^2 A_x}{\partial t^2} + \frac{\alpha}{2}A_x = i\gamma\left(|A_x|^2 + \frac{2}{3}|A_y|^2\right)A_x + \frac{i\gamma}{3}A_x^* A_y^2 e^{-2i\Delta\beta z} \quad (2.56a)$$

$$\frac{\partial A_y}{\partial z} + \beta_{1y}\frac{\partial A_y}{\partial t} + \frac{i\beta_2}{2}\frac{\partial^2 A_y}{\partial t^2} + \frac{\alpha}{2}A_y = i\gamma\left(|A_y|^2 + \frac{2}{3}|A_x|^2\right)A_y + \frac{i\gamma}{3}A_y^* A_x^2 e^{2i\Delta\beta z} \quad (2.56b)$$

with the last term describing the coherent coupling between the polarisation states leading to degenerate four-wave-mixing. If, however, the fibre length $L>>L_B$ where $L_B=\lambda/B_m$ (B_m is the modal birefringence and is typically around 1cm) the sign of the

coherent coupling term changes from positive to negative many times during propagation and hence averages out, leading to zero four-wave-mixing. This reduced IXPM and IFWM interaction between orthogonal pulses was therefore investigated in the alternate-polarisation RZ modulation format in chapter 5, giving improved nonlinear tolerance compared to that of standard RZ. The use of alternate-polarisation is also applicable for suppressing nonlinear interaction between WDM channels, and also helps improve the overall spectral efficiency by reducing cross-talk between closely spaced channels [ZHU'02, FRI'02b].

2.8 Characterisation of system performance

2.8.1 Signal degradation due to erbium doped fibre amplifiers

Fibre optic transmission systems are limited by dispersion and nonlinear effects as discussed, as well as the loss due to attenuation in the fibre. Previously long haul transmission systems employed regenerators in the electronic domain to overcome the loss [GNA'85]. However, in the mid 1980s erbium doped fibre amplifiers (EDFA) were developed and proved to be a commercially viable alternative for amplification in the optical domain. EDFAs amplify incident light through stimulated emission where gain is provided when the amplifier is pumped to obtain population inversion in the doped fibre [DES'94]. However, like all amplifiers it introduces noise and hence its quantification is an important parameter to a system's performance. In the case of EDFAs noise is generated due to spontaneous emission, and decreases the electrical signal-to-noise-ratio (SNR) measured at the output of the optical amplifier. This occurs due to the finite lifetime of excited carriers in the amplifier, which spontaneously undergo de-excitation, thereby emitting photons which are incoherent with respect to the incoming signal. These spontaneously generated photons then multiply in the amplification process and appear as noise added to the amplified signal [DES'94].

The SNR degradation due to amplification is defined as the noise figure:

$$F_n = \frac{SNR_{in}}{SNR_{out}} \tag{2.57}$$

The SNR mentioned above, refers to the electrical power when an optical signal is converted to electric current using a photo-detector. For an ideal photo-detector limited by shot noise only, the input SNR is given by the following equation in terms of the average photocurrent $I=RP_{in}$, the responsivity of the ideal photo-detector $R=q/hv$ and the shot noise $\sigma_s^2 = 2q(RP_{in})\Delta f$, where Δf is the detector bandwidth, q is the electron charge and v is the optical frequency.

$$SNR_e^{in} = \frac{I^2}{\sigma_s^2} = \frac{(RP_{in})^2}{2q(RP_{in})\Delta f} = \frac{P_{in}}{2hv\Delta f_e} \tag{2.58}$$

The spontaneous emission noise is

$$S_{sp}(v) = (G-1)n_{sp}hv \tag{2.59}$$

n_{sp} is the spontaneous emission or population inversion factor and is defined as $n_{sp} = \frac{N_2}{N_2 - N_1}$ with N_1 and N_2 being the atomic densities in the two energy states.

The spontaneous emission distorts the signal in the optical domain and remains when the signal is converted to the electrical domain by way of a photo-detector. The resultant photocurrent due to noise is then given by:

$$\sigma^2 = 2q(RGP_{in})\Delta f_e + 4(RGP_{in})(RS_{sp})\Delta f_e \tag{2.60}$$

The first term in the above equation is due to shot noise which can be neglected when $G>>1$, while the second term is due to beating between the signal and the spontaneous emission, and Δf_e is the electrical bandwidth. The SNR at the output of the amplifier can, hence, be defined using $I=RGP_{in}$ where G is the gain of the amplifier as follows:

$$SNR_e^{out} = \frac{(RGP_{in})^2}{\sigma^2} \approx \frac{GP_{in}}{4S_{sp}\Delta f_e} \qquad (2.61)$$

Substituting the expressions for SNR_e^{in} and SNR_e^{out} in the definition of the noise figure gives:

$$F_n = \frac{2n_{sp}(G-1)}{G} \approx 2n_{sp} \qquad (2.62)$$

Equation (2.62) shows that even for an ideal amplifier when $n_{sp}=1$ the SNR is degraded by a factor of 2 (3dB). The EDFAs used in the experiments and simulations described within this thesis had a noise figure of 4.5dB.

Substituting S_{sp} in SNR_e^{out} in (2.61) gives:

$$SNR_e^{out} = \frac{GP_{in}}{4(G-1)n_{sp}h\nu\Delta f_e} \qquad (2.63)$$

Most of the experiments performed in the course of this work and described in this thesis, were performed using a recirculating loop test-bed. Therefore, to avoid transients between loop cycles, the amplifier gain was set to exactly compensate the loss of the loop components, which was typically between 20dB and 25dB. Hence as G is significantly greater than 1, equation (2.63) can be re-written as:

$$SNR_e^{out} = \frac{P_{in}}{4n_{sp}h\nu\Delta f_e} \qquad (2.64)$$

When the ASE is relatively small compared to the input signal power, it can be assumed that for a cascaded series of identical amplifiers where the gain exactly compensates the amplifier span loss (as in the recirculating loop test-bed) the signal power at the end of the cascaded series is equal to the power at the input of the first amplifier [BEC'99]. Therefore, each amplifier generates an equal amount of ASE and

the ASE propagates along with the signal to the end of the amplifier chain. Hence the ASE at the end of the amplifier series is a linear addition of the ASE generated by each amplifier in the series. For such an amplifier chain equation (2.64) can be modified to give:

$$SNR_{out}^{N} = \frac{P_{in}^{N}}{4n_{sp}h\nu\Delta f_e.NF_nL} \tag{2.65}$$

where L is the loss of a single amplifier span. For a signal with an equal probability of 'ones' and 'zeroes' and considering signal-ASE noise is present for the 'ones' only (2.65) becomes:

$$SNR_{out}^{N} = \frac{P_{in}^{N}}{2n_{sp}h\nu\Delta f_e.NF_nL} \tag{2.66}$$

where $P_{in}{}^{N}$ is the average optical power.

The calculation of the optical SNR (OSNR) is similar to that of the electrical SNR, with the electrical bandwidth Δf_e, replaced by the optical bandwidth $\Delta f_{optical}$.

$$OSNR^{N} = \frac{P_{in}^{N}}{2n_{sp}h\nu\Delta f_{optical}.NF_nL} \tag{2.67}$$

Equation (2.67) can be written in the logarithmic form for λ=1550nm measured on an optical spectrum analyser with bandwidth 0.4nm (50GHz) corresponding the minimum optical filter bandwidth for a 40Gbit/s receiver, as follows:

$$OSNR^{NdB} = 52 + P_{in}^{NdB} - F_n^{NdB} - L^{dB} - 10\log N \tag{2.68}$$

The above equation can be modified according to the optical bandwidth, which is directly dependent on the channel bit rate. For example, for optical transmission at 10Gbit/s $\Delta f_{optical}$ corresponds to a 0.1nm bandwidth (12.5GHz) and equation (2.67) is written logarithmically as follows:

$$OSNR^{NdB} = 58 + P_{in}^{NdB} - F_n^{NdB} - L^{dB} - 10\log N \qquad (2.69)$$

By comparing equations (2.68) and (2.69), it can be seen that sensitivity to SNR required for 40Gbit/s transmission is 6dB higher compared to that of 10Gbit/s transmission.

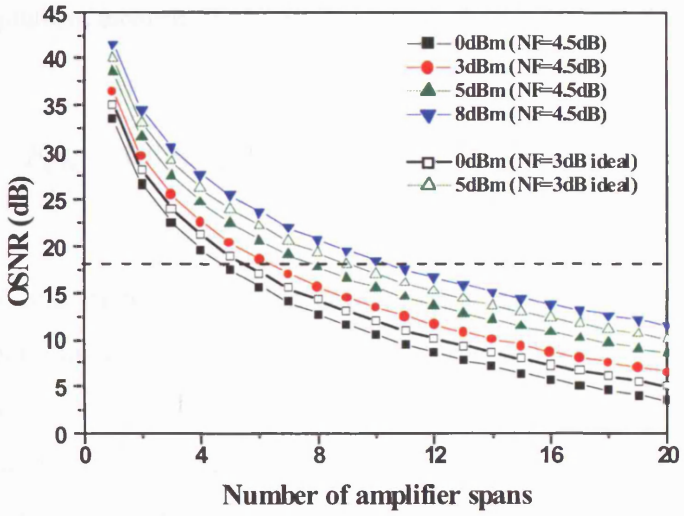

Fig. 2.13 *OSNR evolution with transmission distance for an amplifier span with 20dB loss at signal launch powers of 0dBm, 3dBm, 5dBm and 8dBm and noise figure of 4.5dB and 3dB (ideal).*

The calculated OSNR for an increasing number of amplifier spans, using equation (2.65), is plotted in *Fig. 2.13,* where each amplifier span had a loss of 20dB compensated for by an EDFA with noise figure 4.5dB. These values correspond to those of the experimental set-up used throughout the thesis described in detail in section 4.2, and are typical of other transmission experiments. The dotted line indicates the minimum OSNR requirement (17.8dB) for an ideal receiver operating at 40Gbit/s. *Fig. 2.13* indicates that increasing the optical launch power increases the maximum achievable transmission distance. However, in practical systems it is not possible to arbitrarily increase the launch power, because of amplifier saturation and fibre nonlinearities.

The experimental amplifier spans described in chapters 4 and 5, consisted of the transmission fibre followed by the dispersion compensation, where the dispersion compensator was included in the span loss, as described schematically in *Fig. 2.14(a).* This leads to a reduction of the OSNR, as described in equation (2.67). However, traditionally dispersion compensators are placed between the pumps of the EDFA [KAM'01], leading to the span loss being equal to the loss encountered in the transmission fibre, as shown in *Fig. 2.14(b),* and used in the experiments described in chapter 6. In such systems, the noise figure of the amplifiers is modified according to the following equation, assuming identical properties in every amplifier.

$$F_{n,DC} = 10\log F_n\left(1+\frac{\alpha_{DC}P_{in}^{amp}}{P_{DC}}\right) \qquad (2.70)$$

where α_{DC} is the loss of the dispersion compensator and P_{DC} is optical power at the input of the dispersion compensator. P_{in}^{amp} is the optical power into the first amplifier in the series. However, in such systems as the loss of the compensator is not included as part of the span loss, provided the loss of the compensator is significantly less than that of the transmission fibre in the amplifier span, an overall improvement in the OSNR can be expected as calculated from equation (2.67). The calculated OSNR of the SSMF amplifier span used in the experimental investigation described in chapters 4-6, with the dispersion compensator of 6dB loss (12km DCF) placed between two EDFA stages as described in *Fig. 2.14(b)*, is plotted in *Fig. 2.15*. This configuration shows an improvement of over 5dB in the noise tolerance, compared to the configuration with the compensator placed within the amplifier span. This was confirmed experimentally in chapter 6.

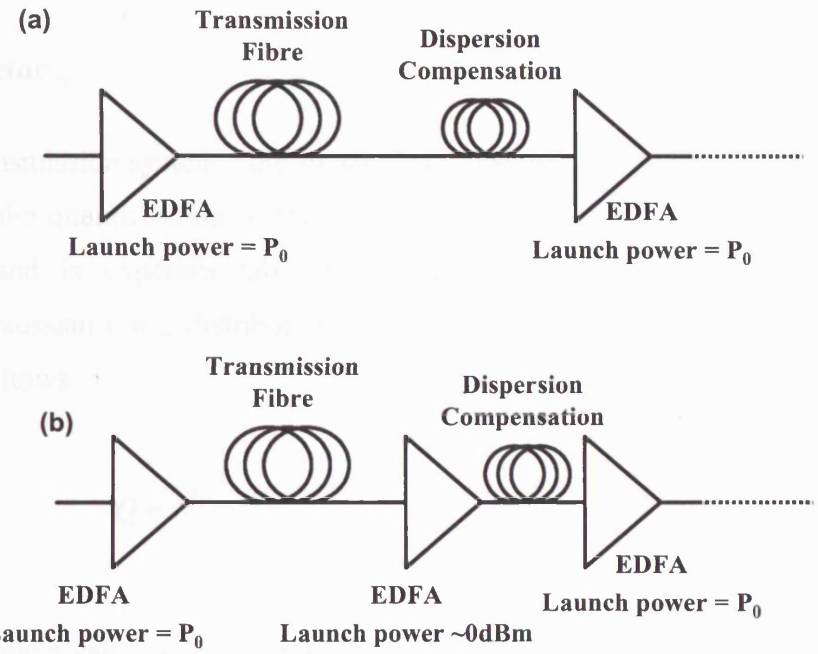

Fig. 2.14 Schematic description of (a): in-line dispersion compensation (b): Dispersion compensation within amplifier stage.

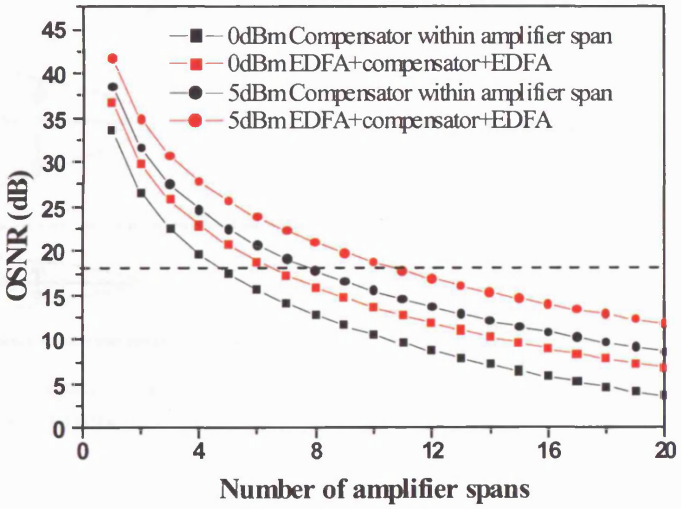

Fig. 2.15 Comparison of OSNR evolution with distance for (squares): an amplifier span with in-line dispersion compensation (fig. 2.8a) (circles): dispersion compensation within the amplifier block (fig. 2.8b), at optical launch power of 0dBm and +5dBm. The transmission fibre and dispersion compensator consisted of 14dB and 6dB loss respectively.

2.8.2 Q-factor

In digital transmission systems, the signal quality can be defined by the Q-factor. This is based on the quantification of the signal distortion in the 'zero' and 'one' levels separately, and is experimentally measured in electrical parameters [BER'93]. Assuming Gaussian noise distributions for both 'zeroes' and 'ones', the Q-factor is defined as follows:

$$Q = \frac{|\mu_1 - \mu_0|}{\sigma_1 + \sigma_0} \qquad (2.71)$$

$\mu_{1,0}$ are the mean value of the marks/spaces rail in volts or amperes and $\sigma_{1,0}$ are the standard deviations of the detected voltage or current of the bits received when plotted as a voltage histogram, as shown in *Fig 2.16* for a 40Gbit/s NRZ signal.

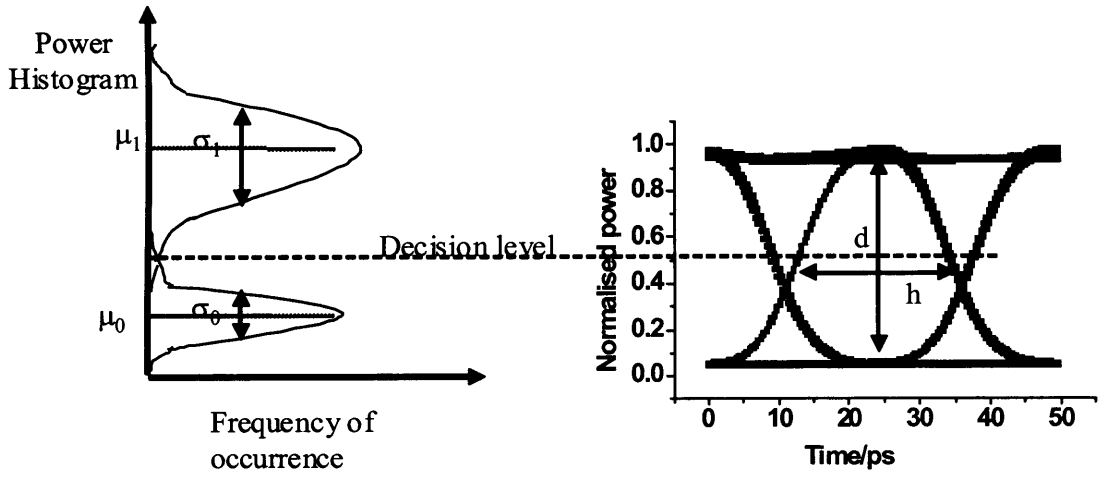

Fig. 2.16 *Technique for measuring $\mu_{1,0}$ and $\sigma_{1,0}$ for calculating the Q factor d=Vertical eye-opening, h=horizontal eye-opening*

For a noise limited signal with extinction ratio r, the OSNR is related to the Q-factor according to the following equation [AGR'01]:

$$OSNR = \frac{Q}{\Delta f}\frac{Q^2 \Delta f_e}{\Delta f_{optical}}\frac{1+r}{\left(1-\sqrt{r}\right)^2} \qquad (2.72)$$

It should be noted however, that the OSNR in this equation can be affected by the noise limiting detection, the modulation format, the nature of the signal distortion (eg. timing or amplitude jitter) and the receiver design. Furthermore, while nonlinear distortions will also affect the accuracy of this relationship, it is useful in estimating the theoretical optimum transmission performance of a system with the described parameters.

2.8.3 Eye opening penalty

The distortion of the signal can also be measured by the eye opening penalty, and is commonly used to compare transmission performance in simulation results, as described in [PEC'03] and [HOD'02]. Eye opening penalty is useful for quick qualitative analysis, hence, it is commonly used in numerical simulations. It should be noted however, that good eye opening penalty does not necessarily correspond to error-free transmission, and hence, should be treated with care in quantitative experimental measurements.

The eye opening penalty is determined by the height of the highest rectangle with width 20% of the bit-slot fitted inside the eye-opening as shown in Fig. 2.17 and is defined as follows, where P_{ave} in the above equation is the average pulse power [KAM'01]:

$$EyeOpeningPenalty(dB) = -10\log\left(\frac{P_R}{2P_{ave}}\right) \qquad (2.73)$$

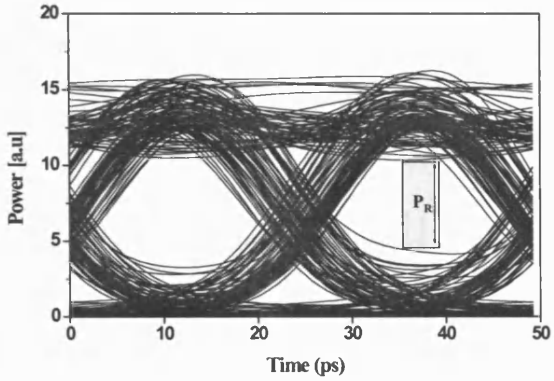

Fig. 2.17 *Calculation of eye opening penalty. Note: Width of rectangle is 20% of bit slot to include effect of clock jitter on decision sampling point*

2.8.4 Bit Error Rate (BER)

The BER is calculated by measuring the number of errors detected at the receiver for a given transmitted signal. While the Q-factor is usually estimated experimentally using a digital sampling oscilloscope to obtain a power histogram down the centre of the eye, by recording the voltage level of every bit transmitted like that in *Fig 2.16*, this technique does not give a good correlation between the measurement of Q and BER. This is because the variation seen around each rail represents a mix of pattern effects such as inter-symbol-interference (ISI) and noise. Hence, the calculation of the Q for the experimental results were done according to a technique proposed in [BER'93] which is briefly described.

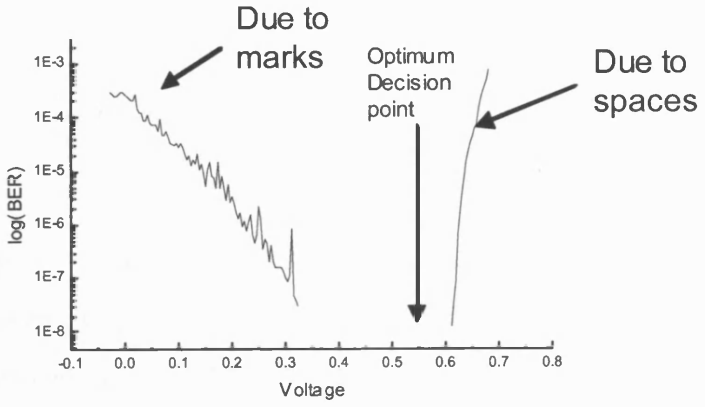

Fig. 2.18 *Typical result for BER vs decision threshold*

The BER is calculated for the varying voltage decision level D, using the following equation.

$$BER(D) = \frac{1}{2}\left\{erfc\left(\frac{|\mu_1 - D|}{\sigma_1}\right) + erfc\left(\frac{|\mu_0 - D|}{\sigma_0}\right)\right\} \tag{2.74}$$

The data are then separated into two sets where the BER is dominated by the marks rail and spaces rail as shown in Fig. 2.18. The point of separation being the value of D where error-free performance is achieved. Each of these data sets is then fitted to an ideal curve which assumes Gaussian noise statistics. It should be noted however, that in the presence of nonlinear distortion, the probability density functions of the 'zeroes' and 'ones' deviates from pure Gaussian statistics. While this affects the predicted optimum decision level threshold the ultimate corresponding BER varies by less than 0.1 dB [HUM'91, CHA'97], validating the use of Gaussian statistics in this case. These two data sets are then passed through an inverse error function given as follows [BER'93]:

$$\left\{\log\left(\frac{1}{2}erfc(.)\right)\right\}^{-1}(x) \approx 1.192 - 0.6681x - 0.0162x^2 \tag{2.75}$$

and x is *log(BER)*.

erfc(x) is a form of the complementary error function defined as:

$$erfc(x) = \frac{1}{\sqrt{2\pi}}\int_x^{\infty} e^{-\frac{x^2}{2}}dx \tag{2.76}$$

A linear regression is then performed with the decision levels and the equivalent $\sigma_{1,0}$ and $\mu_{1,0}$, are given by the slope and intercept of the linear regression. These values at the optimum decision point, which is the cross point of the two Gaussian probability density functions are then used to calculate the BER using equation (2.76). This is then correlated to the Q-factor by the following equation.

$$BER = \frac{1}{2} erfc\left(\frac{Q}{\sqrt{2}}\right) \tag{2.77}$$

In general, BER of 10^{-9} is considered to be error-free and indicates the measurement of a single bit in error for a total of 10^{10} sampled bits, in order to measure a minimum of 10 errors. The Q-factor can be quoted in decibels using the conversion $10\log(Q^2)$, and a BER of 10^{-9} corresponds to a Q of 6 or 15.56dB. This relationship between BER and Q-factor is useful in the comparison of numerical simulations and experimentally measured results. It is clear that in order to measure a BER of 10^{-9} numerically would require a minimum simulation of 10^{10} bits, which is significantly time consuming. As such, the numerical simulations described in this thesis, quantify system performance using the Q as described in section 2.7.2, and use a pattern length of 2^9 bits which was shown to be sufficient for accurate modelling of 40Gbit/s transmission [HOD'02b].

2.8.5 Quantification of system tolerance due to cumulative signal distortion using signal launch power

Signal distortions due to noise, nonlinear effects and residual dispersion accumulate with the number of amplifier spans in the transmission link (distance). In the event of achieving error-free transmission, it is not possible to identify the system margin for achieving it and the dominant source of signal distortion. Therefore for example, if nonlinear effects were the main source of signal distortion, an increase in signal launch power would lead to errors, but, a decrease in signal launch power would not, as this would decrease the nonlinear distortion. Hence, even when error-free transmission is obtained it is possible that the system parameters are not optimal. In this work, system performance is investigated as a function of transmission distance for increasing signal launch power and residual dispersion.

Varying the signal launch power is a useful way to understand the limitations due to linear effects such as noise at low powers, and nonlinear effects such as SPM, IXPM and IFWM at high powers for a single channel transmission. In the experimental work described in this thesis, these limits were explored by initially decreasing the signal

launch power until a BER of 10^{-9} is achieved to give the linear or noise limit. Increasing the signal launch power until the BER again reaches 10^{-9} indicates the nonlinear limit. This procedure is repeated as the number of amplifier spans is increased until the maximum transmission distance is achieved, indicating the optimum power. This technique of obtaining the linear (noise) and nonlinear limit is illustrated in *Fig. 2.19*. The figure shows that the noise and nonlinear effects accumulate, as the linear limit increases with transmission distance while the nonlinear limit decreases with transmission distance. These limits converge at the maximum transmission distance at the optimum signal launch power.

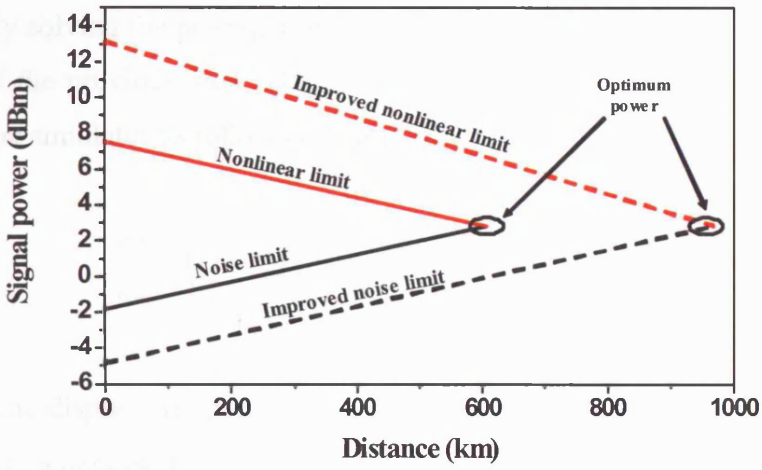

Fig. 2.19 *Schematic illustration of noise and nonlinear limit as a function of transmission distance. The maximum transmission distance is achieved when the two limits converge. Dotted lines indicate the typical behaviour due to suppression of noise and nonlinear effects*

Presenting the transmission performance as a function of signal launch power is attractive in identifying the effectiveness of techniques specifically targeted at suppressing the noise or nonlinear distortion. In such cases the noise limit would be decreased and the nonlinear limit increased, leading to an increase in transmission distance as indicated by the dotted lines in *Fig. 2.19*.

2.9 Numerical simulation techniques and system modelling

To enable a comparison of experimental results with those predicted by theory, numerical simulations were used in this work. The simulator is a useful tool for the analysis of signal propagation, as it provides flexibility in the investigation of the different causes of signal distortion both individually and collectively. Simulation of the optical transmission in fibre is primarily based on solving the NLSE, described in equation (2.1). The simulations described in this thesis used the split-step Fourier algorithm [HAR'73], to calculate the solution to the NLSE. The propagating distance is calculated as a series of small step sizes h, and the fibre propagation is simulated by approximately solving the propagation equation in each step, starting from the field at the output of the previous step. The NLSE is simplified as a first order differential equation in the simulator as follows [AGR'01]:

$$\frac{\partial A}{\partial z} = \left(\hat{D} + \hat{N}\right)A \qquad (2.78)$$

where $\hat{D}$ is the dispersion operator and $\hat{N}$ is the nonlinear operator for propagation $z \rightarrow z+h$. This separates the linear and nonlinear effects and each operation is performed individually within each step h. The first step has the GVD effects acting according to equation (2.8) (presented in section 2.3) and also simulates the attenuation (equation (2.2)), with the nonlinear effects taken as zero. The second step simulates the nonlinearities using equation (2.20) (section 2.4), while the dispersion effects and attenuation are assumed to be zero. The nonlinear phase shift is calculated in the time domain, while the frequency dependent phase shift due to GVD is calculated in the frequency domain. Hence, a fast Fourier transform (FFT) is carried out at each step, dominating the overall simulation time. The step size is chosen such that the nonlinear phase shift over each step is small enough, to ensure good accuracy. The choice of step sizes is a topic for some discussions, see for example [FRA'99, RAS'00, SIN'03]. All simulations described in this thesis used a step size of 100m and were in good agreement with results obtained experimentally.

In order that numerical simulations be comparable with results obtained experimentally, it is important that fixed system parameters such as the fibre properties (dispersion, nonlinear coefficient), amplifier noise figure etc. are modelled with close likeness to the experimental set-up. Other parameters such as signal launch power and so on which are optimised during the experiment, were selected and inserted in the model so that the dominant effects under investigation were more easily identifiable in the analysis. The selection of such tuneable parameters was made such that, while the experimental results could be validated against those obtained by simulation, they do not measure identical quantities. For example, while experimental investigations carried out during the course of this work were predominantly based on optimising the signal launch power according to BER measurements, numerical simulations were carried out to calculate Q-factors at fixed signal launch powers. Therefore, as BER and Q-factor measurements give correlated results (equation 2.77), the experimental measurements enabled the quantification of signal launch power margins, while numerical simulations quantified the signal distortion in the 'ones' and 'zeroes' which help in identifying the dominant source of distortion.

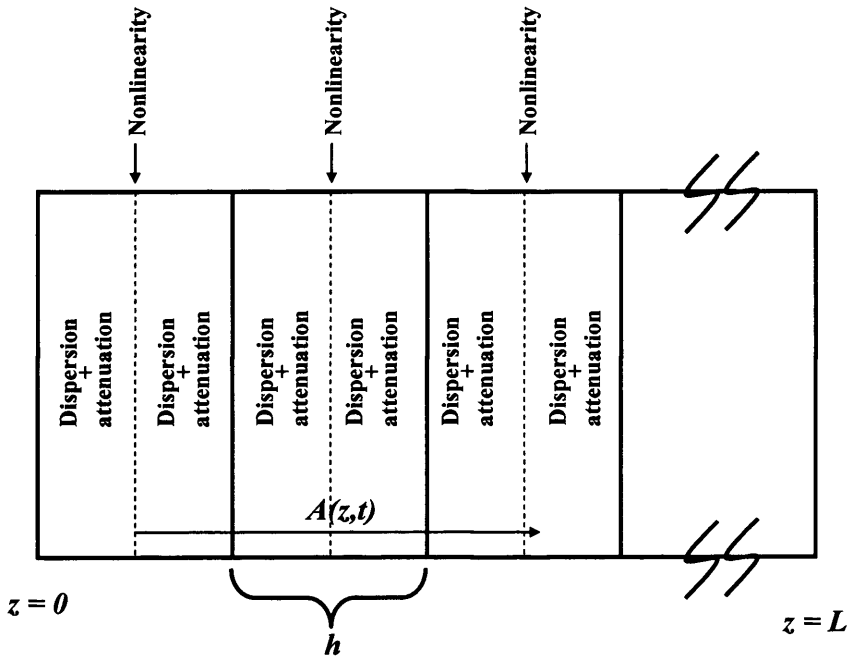

Fig. 2.20 *Schematic illustration of the split-step Fourier method used for numerical simulations, where h is the step size over which dispersion and nonlinearity are considered to act independently*

2.9.1 Transmitter model

The pulsewidth and extinction ratio used in the numerical model were obtained experimentally, as measured using an autocorrelator. The extinction ratio of the NRZ and RZ modulation format used in the experimental work of this thesis was approximately 16dB and 30dB respectively, with RZ pulses consisting of 11.25ps pulsewidth (FWHM). NRZ signals were generated in the numerical model by filtering rectangular pulses using a 6^{th} order Bessel Filter with 32GHz bandwidth [HUI'04]. The experimental RZ pulse shape was fitted with both Gaussian and sech-shaped approximations and found to have no significant difference according to chi-square distributions. Hence, all RZ simulations in this work assumed Gaussian pulse shapes, as it was more easily compatible with the theory. Simulations at bit-rates below 40Gbit/s were carried out for pattern lengths of 32 bits (2^5) with good accuracy. However, owing to the pattern dependent intra-channel nonlinear effects, the simulation of 40Gbit/s transmission required a minimum of 512 bits (2^9) [SHA'01, HOD'02b, SHA'04]. The signal pattern was generated using the 'seed' and 'rand' functions in Matlab to a pseudo-random-bit-sequence (PRBS), which was identical in every simulation (apart from WDM simulations, where the interfering channels consisted of different PRBS).

2.9.2 Receiver model

While transmitter parameters such as pulsewidth and shape remained largely unchanged during the course of this work, despite the use of OTDM and ETDM systems (described in chapter 4), the receiver design varied significantly from a 10Gbit/s system with optical de-multiplexing, through to an erbium p-i-n pre-amp receiver with direct detection at 40Gbit/s. As mentioned in section 2.8.2, the receiver design can affect the correlation between OSNR and Q-factor. Hence, Q-factor calculation were carried out on the received optical signal (a technique not feasible experimentally), filtered by a flat-top filter with 75GHz (0.6nm) 3dB-bandwidth and a 20dB-bandwidth of 100GHz. This filter specification was typical of commercially available arrayed waveguide gratings (AWGs). The non-ideal behaviour of the

receiver due to limiting filter bandwidth and noise was then quantified as a fixed penalty in each experimental set-up.

To study the relative impact of IXPM and IFWM in the overall nonlinear distortion, the timing jitter and standard deviation of power in the 'zero' bit slots were calculated from the received optical signal. The IXPM was calculated as the average timing jitter at the full width at half maximum of the jitter in the leading and trailing edges of every pulse, while the standard deviation of the power in the 'zero' bit slots was calculated by recording the power at the mid point of every 'zero' bit to give a measure of the IFWM. It should be noted that it is not possible to calculate the timing jitter when the Q-factor is significantly lower than 15.56dB and the signal distortion is severe, as the leading and trailing edges become indistinguishable due to inter-symbol-interference.

2.9.3 Transmission link

The transmission fibre was simulated according to experimental parameters [*Appendix 1*]. The HOM-DMD however, was simulated as a linear device. This was justified as the length of fibre within the device was approximately 700m, which was significantly lower than the nonlinear length (equation (2.23)). A further 2dB loss was included within each amplifier span to incorporate losses due to AOMs in the experimental recirculating loop. The EDFAs within the recirculating loop had a noise figure of 4.5dB as obtained from the relevant data-sheets.

2.10 Summary

This chapter described the theory governing the propagation of optical signals in fibre. This was divided into linear effects encompassing dispersion and noise, and nonlinear effects due to the intensity dependence of the refractive index. The properties of the two most commonly used modulation formats (NRZ and RZ) were discussed. At high bit rate transmission, intra-channel nonlinear effects such as IXPM and IFWM take place as a result of nonlinear interaction between overlapping pulses caused by dispersion-induced pulse broadening. The intra-channel nonlinear interactions lead to timing jitter, amplitude jitter and the growth of shadow pulses in the 'zero' bit slots. Chapters 4 and 5 describe the experimental investigation of the complex nature these nonlinear effects and techniques for their suppression using different modulation formats, fibre types and dispersion maps, based on the optical system parameters defined in this chapter.

In this work, different parameters are used to characterise the transmission quality. The optical signal-to-noise-ratio (OSNR) is a measure of the signal quality in the presence of ASE noise. The transmission performance is closely dependent on the modulation format and the signal distortion can be described by the eye opening penalty. A more detailed assessment of the signal quality is given by the Q-factor, which measures the signal distortion of the 'ones' and 'zeroes' individually. The Q-factor measurements are used in numerical simulations and predict the maximum achievable transmission distance for comparison with experimental results. The transmission performance is measured experimentally using the bit-error-rate (BER). Error-free transmission distance is achieved for $BER<10^{-9}$ and corresponds to a Q-factor of 6, enabling the experimental results to be easily compared with those obtained by numerical simulation. A technique for measuring the noise and nonlinear limitations as a function of signal launch power was also described. This technique also enables the distortion suppression methods to be quantified, giving a simplified description of the complex processes which take place, and an indication of which improvements might be expected by optimising the system design.

Chapter 3 Literature Review

In this chapter the existing literature describing the fundamentals of 40Gbit/s optical transmission is reviewed. The motivation and challenges for transmission at this bit-rate are surveyed, and initial work on its optimisation is discussed. The work carried out during the course of this research, is then placed in context with those carried out previous to, or in parallel with, this work.

3.1 Motivation and challenges for 40Gbit/s optical transmission

When 10Gbit/s systems were deployed commercially towards the end of 1996, investigation of 40Gbit/s transmission began as the next generation of high capacity systems [HAD'96]. At the time, intensity modulated direct detection formats were the most commonly used modulation formats in fibre optic communication systems with the non-return-to-zero (NRZ) modulation the preferred format. This was due to the simpler device technology required for generating the NRZ format in early systems [KAZ'96, GOW'93]. Return-to-zero (RZ) pulses had also been investigated for soliton propagation, where the pulse shape was maintained throughout transmission [HAS'73]. This technique was implemented experimentally by transmitting the signal over dispersion shifted fibre (DSF) with dispersion close to zero [KAW'95], or by soliton transmission which counteracts dispersion effects with SPM [MOL'96, FUR'01]. Neither of these solutions are favoured in the commercial deployment of optical systems, as DSF is not suitable for WDM transmission (see chapter 2), and counteracting dispersion with SPM leads to low tolerance to fluctuations in dispersion and also requires high signal launch powers. However, when 40Gbit/s systems were first investigated [IWA'92], the absence of high-speed electronic multiplexers and de-multiplexers, led to the renewed interest in the RZ modulation format, as it enabled the generation of 40Gbit/s signals through optical-time-division-multiplexing (OTDM) with 10Gbit/s electronics [LEE'96, GUY'96], as used in early 40Gbit/s experiments.

As the volume of research on 40Gbit/s transmission began to increase, it soon became evident that for cost-efficient implementation of such systems, they must operate over SSMF, the most commonly deployed fibre [KOG'00, KAH'04]. As soliton

transmission cannot be easily achieved over SSMF, most work was focused on the NRZ modulation format, as this technology was well understood through previous implementation of lower bit-rate transmission, as well as the RZ modulation format owing to the ease of generation without the need for high-speed electronics [IWA'92, LEE'96, GUY'96]. The first comparison of the NRZ and RZ modulation format at 40Gbit/s was performed by numerical simulation for transmission over SSMF and showed that superior transmission performance is obtained using the RZ modulation format [BRE'96]. This is mainly due to the improved tolerance to fibre nonlinearity of the RZ modulation format, as RZ signals are strongly broadened under dispersion which decreases the pulse peak power, thereby lessening the influence of SPM on the signal [BRE'96]. Furthermore, RZ format gives rise to a 2dB improvement in the receiver sensitivity [FOR'97], as described in section 2.5. These advantages led the research community to investigate the RZ format as a serious alternative to the traditional NRZ in the implementation of 40Gbit/s systems. The first experimental investigation of NRZ and RZ transmission at 40Gbit/s was demonstrated in [LUD'99] comparing single channel transmission, where it was shown that the receiver sensitivity was improved by greater than 3dB for RZ signals compared to NRZ signals of the same average power when transmitted over 218km of SSMF. This confirmed the results obtained through numerical simulations in [BRE'96], although the improvement in receiver sensitivity consisted of the improvements due to the nonlinear tolerance as well as the inherent improvement in receiver sensitivity of the RZ format, giving no quantification of the nonlinear behaviour in each case. As no work existed for the study of isolating and quantifying nonlinear distortion from noise limitation and receiver sensitivity for NRZ and RZ modulation formats, it was investigated during the course of this work and is addressed in chapter 4.

3.2 Intra-channel nonlinear effects

The nonlinear effect affecting a single wavelength channel NRZ signal during propagation is caused by SPM (as described in section 2.4.2), and it was found to be suppressed when using RZ modulation formats [BRE'96, BRE'97]. However, for RZ signals the dispersion-induced pulse broadening of the RZ format causes pulses within the same wavelength channel to overlap and interact through fibre nonlinearity,

giving rise to intra-channel nonlinear distortion [SHA'98, MAM'99, ESS'99]. Indeed, though SPM is more dominant in NRZ transmission [BRE'96], RZ transmission was more significantly affected by such intra-channel nonlinear effects. One reason for this is due to the higher dispersion-induced pulse overlap in RZ signals owing to the larger modulation bandwidth [HAY'99]. However, as dispersion-induced pulse broadening affects both NRZ and RZ formats, the degree of pulse overlap required further investigation. This effect is described in chapter 4, by analysing the physical property of a string of 'ones' in NRZ and RZ signals [KIL'02].

The first of these intra-channel effects was demonstrated by Shake *et al*, where the FWM process between two 4ps pulses in a 100Gbit/s OTDM signal was observed when pulses overlapped during transmission [SHA'98]. Mamyshev *et al*, were the first to give theoretical explanation for nonlinear distortion caused by pulse overlapping [MAM'99]. Indeed, it was described in [MAM'99] and chapter 2, that when pulse overlap is partial, cross-phase-modulation between pulses takes place (IXPM). In such cases, the partial pulse overlap would induces a phase shift on the adjacent pulses which manifests itself as timing jitter in the presence of dispersion. Furthermore, as pulse broadening increases, the IFWM effect takes place as identified in [SHA'98], leading to amplitude jitter and shadow pulses in the 'zero' bit slots. The emergence of shadow or 'ghost' pulses in zero bit slots due to IFWM, and signal degradation resulting from timing jitter caused by IXPM was demonstrated experimentally in [ESS'99]. This experimental demonstration required signal launch powers as high as +15dBm. Therefore, while intra-channel nonlinear effects had been discovered as a source of signal degradation, it was still unclear how serious these effects were in limiting the achievement of error free transmission. Hence, quantifying the nonlinear signal distortion at signal launch powers typical in WDM applications, where a single EDFA is used to simultaneously amplify many wavelength channels (thereby significantly reducing the signal launch power of individual channels) formed part of the work described in this thesis. This also included studies on optimising the signal launch power for reducing intra-channel nonlinear distortion.

As intra-channel nonlinear effects were identified as a possible source of severe signal degradation, techniques for their mitigation soon began to be widely researched. The

most common, yet effective technique for achieving this was to reduce the nonlinear interaction between pulses by controlling the dispersion-induced pulse overlap, through dispersion management. Another technique was based on optimising the modulation format, in order to obtain improvements in intra-channel nonlinear tolerance. The suppression of intra-channel nonlinear distortions by tailoring the dispersion in a fibre link is discussed in more details in section 3.2.1 and 3.2.2, while a discussion on optimisation of the modulation format is described in section 3.3

3.2.1 Fibre local dispersion and related nonlinear behaviour

From the theory of intra-channel nonlinear effects, it is clear that minimising dispersion-induced pulse broadening during transmission minimises these effects, as the pulse overlap is decreased. Hence, SSMF was not considered to be the optimal fibre type for 40Gbit/s owing to its high local dispersion [BER'99, BIG'99]. However, reducing the fibre dispersion by employing fibre with zero chromatic dispersion as in DSF, is not a viable option either, as the combination of ASE noise with four-wave-mixing leads to severe distortion of the signal by creating new frequency components [MAR'91, TKA'95]. Furthermore, these new frequency components broaden the optical spectra and result in loss of signal power when fed through in-line filters, further decreasing the OSNR. In the theory related to WDM transmission, the walk-off parameter is directly proportional to chromatic dispersion of the transmission fibre [THI'00], further emphasising the importance of dispersion. Therefore, around 1999, research groups started to investigate alternative fibre types such as NZDSF with dispersion in the region of ~4ps/(nm.km), which reduced the pulse overlap compared to SSMF during transmission, while still avoiding the disadvantages associated with fibres such as DSF with ~0ps/(nm,km) dispersion [BER'99, BIG'99].

A more comprehensive study of intra-channel nonlinear distortion was described in [ESS'99] for 40Gbit/s RZ transmission showing superior transmission performance using TrueWave^{TM} fibre (TWF) which has similar properties to NZDSF compared to transmission in SSMF. In [KON'01] the optimum fibre dispersion was shown by numerical simulations to be dependent on the product DB^2 of the dispersion D and bit-rate B [KON'01]. Using this fibre characterisation technique the optimum fibre for

40Gbit/s transmission was found to be NZDSF. An 8x40Gbit/s experimental WDM transmission over large effective area NZDSF was demonstrated, showing a launch power greater than +7dBm could be tolerated for a transmission distance of 640km, indicating good nonlinear tolerance [MUR'00b]. It was claimed in [TSU'00], that NZDSF holds a distinct advantage over other fibre types due its large effective area being able to support higher input powers giving greater nonlinear tolerance. Even so, the overall advantages NZDSF (or similar fibre) compared to that of SSMF in the implementation of 40Gbit/s were not conclusive, particularly regarding the interactions between dispersion and nonlinear effects, as discovered in [BRE'98]. The experimental investigation of a single channel 40Gbit/s RZ transmission in [BRE'98] revealed that post-compensation reduces the nonlinear distortion in a 150km transmission link of SSMF or TWF, with SSMF tolerating 4dB higher signal launch powers compared to TWF. Likewise, while NZDSF is becoming increasing popular for good suppression of nonlinear effects for 40Gbit/s transmission, much research is still carried out on maximising the transmission performance in SSMF. This is because SSMF is the most widely deployed fibre and maximising its usage to incorporate 40Gbit/s systems provides significant cost benefits. As such, a more detailed investigation comparing and contrasting SSMF and NZDSF transmission fibre was required, and was undertaken in the course this work, and is described in chapter 4. This work focused on investigating the NRZ and RZ modulation format for transmission over metro and long-haul distances, where acceptable transmission performance could be achieved using simple cost-efficient techniques [KIL'02].

Dispersion compensation: At the start of this work, dispersion compensation was mostly achieved by use of DCF. However, the small cross section of the fibre (section 2.3.2, equation (2.24)) leads to higher nonlinearity [BOS'95], splice losses and bending losses [VEN'94], and fibre bending was also found to affect the dispersion in DCF [CHE'98]. These effects make the use of DCF less attractive, particularly for 40Gbit/s operation where tolerances to nonlinear distortion, noise and dispersion are significantly reduced. Furthermore, commercially installed DCF is not always slope compensated and as such only one WDM channel is fully compensated during transmission [IZA'92]. However, while improvements in the fibre have led to the design of slope-compensated DCF, the dispersion slope is -0.15ps/(nm^2.km) which is still not optimal for broadband compensation of SSMF, NZDSF and TWF which

consist of a dispersion slope ~0.07-0.08 ps/(nm^2.km) [BRE'98, KNU'02]. This leads to the non-central WDM channels requiring additional dispersion trimming at the receiver. Tuneable dispersion compensators where dispersion can be tuned on a per channel basis have been demonstrated to overcome such penalties but require significant hardware resources for large wavelength channel counts [XIE'00].

As the high nonlinearity and loss of DCF is related to the ratio between the refractive index n_2, and the effective area A_{eff} of the fibre [BOS'95, BOS'96, GRU'96], a method of eliminating these effects was proposed by employing higher-order-mode (HOM) fibre [TUR'01]. The advantage of this fibre type is based on increasing A_{eff}, which increases the nonlinear threshold power, as demonstrated using Raman amplification in [RAM'02]. In such fibre, the signal propagates in the LP_{02} mode which is highly dispersive, hence, a given amount of dispersion can be achieved with a much shorter section of HOM fibre [POO'94, MUR'00, TUR'01]. Furthermore, the design of dispersion slope compensation is more accurately achieved with HOM fibre, and is hence, suitable for simultaneous broadband dispersion compensation at bit-rates of 40Gbit/s [GNA'00, TUR'01]. However, slope compensation does vary for different fibre types and, hence, slope compensation is not always optimal even when employing HOM compensation fibre. The use of HOM compensators for 40Gbit/s transmission is not a very well researched topic, particularly in systems employing EDFA amplification. To address this, work was carried out on the properties of HOM compensators for EDFA systems in chapter 4, where the improved nonlinear tolerance of the HOM compensator was investigated in new amplifier span designs for improved nonlinear tolerance [KIL'02]. These amplifier span designs were subsequently demonstrated in [BIS'04], further emphasising the benefits of HOM compensators and their inherent nonlinear tolerance. The dispersion slope compensation of the HOM compensator was also investigated experimentally for the first time in chapter 4, for simultaneous broadband compensation of 75km NZDSF over the C-band [KIL'02].

3.2.2 Suppression of intra-channel nonlinear distortion by dispersion management

Reducing the intra-channel nonlinear interaction by selection of the optimum fibre type is advantageous, but requires significant improvement in transmission performance to justify the increase in cost associated with deploying the new fibre. It is interesting to note even though both SSMF [BRE'98] and NZDSF [MUR'00b, TSU'00] are proposed as optimum for 40Gbit/s transmission, the authors commonly conclude the nonlinear coefficient (dependant on the effective area of the fibre – equation (2.24)) is more significant in terms of the fundamental limitations to the transmission performance, when compared to the dispersion sensitivity which is more reliably controlled through dispersion management.

Dispersion management was first proposed in [CHR'93] to reduce nonlinear interaction between signal and noise in both single and WDM systems at 10Gbit/s. However, it has gained in significance with the emergence of 40Gbit/s, where dispersion management is used in the transmission of dispersion managed RZ (sometimes referred to as dispersion managed solitons) [SMI'97, GOV'98], and in the suppression of intra-channel nonlinear effects [BRE'97b, TUR'99]. Dispersion managed RZ transmission is based on using a periodic dispersion map where the average GVD is low in each period but consists of relatively large local dispersion [SMI'97]. This differs from standard solitons as its amplitude and width varies periodically within each amplifier span. The periodic length of the dispersion management is an important topic of investigation [GOV'98, TUR'99], as the intra-channel nonlinear interaction is controlled by appropriate dispersion maps, as timing jitter is dominant when pulses overlap partially and amplitude jitter is dominant in large map strengths where pulses significantly overlap each other [HIR'02]. Dispersion management through pre-compensation, where part of the dispersion is compensated at the transmitter before launching into the transmission link is the most common use of dispersion management [GOV'98, ESS'99, KIL'00], as it enables the dispersion map to be altered with changes being made only at the transmitter and receiver. This is advantageous, as it enables the upgrade of existing fibre links without the need for deployment of new fibre.

Pre-compensation is achieved by placing an amount of normal dispersive fibre (negative dispersion) before launching the signal into the transmission fibre anomalous dispersion (positive dispersion). This leads to the launch of pre-broadened pulses (by normal dispersion) which gradually compresses as it propagates along the (anomalous) transmission fibre until the initial pulsewidth reached, after which the pulses begin to broaden again under the anomalous dispersion of the transmission fibre. Hence, as the total pulse overlap during the propagation of the signal in the nonlinear transmission fibre is minimised, intra-channel nonlinear interaction between the pulses is also minimised. As the pulse overlap determines the strength of the intra-channel nonlinear distortion, it was shown by [HAR'99], that launching pre-broadened pulses into the transmission fibre led to an improvement in the transmission of the RZ signal. Owing to the fixed lengths of fibre employed in this experimental demonstration, the potential for improving the transmission performance was shown in [HAR'99] by re-ordering the launch position of the signal into a recirculating loop test-bed consisting of two stages of anomalous fibre and a single stage of normal fibre whilst ensuring a total residual dispersion close to zero. The improvement in transmission performance by launching pre-broadened pulses by dispersion management was also confirmed by simulation and theoretical analysis of IXPM [MEC'00b, MAR'01, ABL'01] and for IFWM [INO'00, KUM'02]. However, while the technique for the launch of pre-broadened pulses was known to suppress intra-channel nonlinear effects, the optimum pre-compensation at the transmitter was derived by Killey *et al* giving an analytical equation for its calculation depending on the length and dispersion parameter of the transmission fibre (SSMF) in the amplifier span [KIL'00]. Much work on dispersion management was based on numerical simulation, owing to the difficulty of constructing variable dispersion maps experimentally, and prior to the work described in this thesis, there was no experimental demonstration of this technique. (The first experimental investigation of this technique is described in Chapter 4). In addition, it was unclear whether this design rule holds for modulation formats other than RZ. Both these issues are addressed in this work in chapters 4 and 5, where experimental verification of this technique and its application for advanced modulation formats are described.

The large dispersion-induced pulse broadening of the RZ format has also been exploited to generate the regime of 'pseudo linear' transmission, another technique of dispersion management. This technique was demonstrated in [PAR'00], where a high

launch power of the RZ format was used, and all dispersion compensation was performed at the end of the transmission link, thereby enabling an increase in the amplifier span length to 120km (SSMF). This is significantly larger than standard amplifier span lengths which are in the region of 50-80km, and despite the increase in span length no significant increase in OSNR penalty is incurred. This also reduces the cost of requiring many dispersion compensation sites over the link. While placing the entire dispersion compensation at the receiver end of the transmission link is advantageous as mentioned, it is usable only in point-to-point links. Lumped compensation makes the system incompatible with the aim of flexible and dynamic optical networks, where add-drop points exist at different distances within any given point-to-point transmission link. Furthermore, the significant pulse overlap can lead to increased levels of IFWM when amplified in successive spans with no dispersion compensation. Hence, in-line compensation still remains the preferred choice of dispersion management, and 'pseudo-linear' transmission is not investigated in this work for this reason. Instead, this work focuses on the role of dispersion on intra-channel nonlinear effects in transmission links with dispersion compensation in every amplifier span. This was carried out for transmission over SSMF and NZDSF fibres with largely different fibre local dispersion, and also for dispersion management by use of pre-compensation at the transmitter for transmission links with these types of fibre.

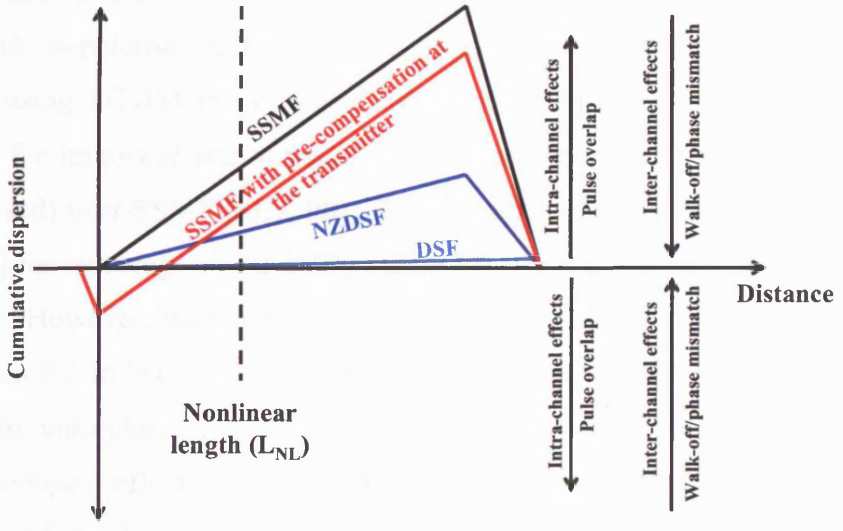

Fig. 3.1 *Schematic illustration of the suppression of nonlinear distortion by dispersion management for a single amplifier span, where the choice of transmission fibre or pre-compensation at the transmitter minimises the pulse overlap within the nonlinear length*

3.3 Advanced modulation formats

As described in the previous sections, fibre dispersion must be managed rather than eliminated in order to obtain simultaneous suppression of inter- and intra-channel nonlinear effects. Thus, even in optimised dispersion maps, the presence of fibre dispersion leads to pulse overlap creating the necessary conditions for intra-channel nonlinear effects to take place, albeit significantly less than is the case with no dispersion management. Thus, the so called advanced modulation formats (i.e formats which are more complex than those of RZ/NRZ), which are more tolerant to intra-channel nonlinear effects in the presence of the unavoidable dispersion-induced pulse overlap are of interest and are discussed in chapter 5. The modulation formats investigated in this work are based on intensity modulated RZ pulses, as they are easily compatible with existing systems, with changes required only at the transmitter. In order to exploit this advantage, however, the required 40Gbit/s transmission should be achieved over SSMF. As such, this work investigates the advanced modulation formats for transmission solely over SSMF.

3.3.1 Alternate-polarisation RZ

It was shown in [DeA'96] that adjacent pulses with orthogonal states of polarisation show weaker interaction compared to those with the same state of polarisation (parallel or co-polarised pulses). Alternate-polarisation RZ was first investigated at 40Gbit/s using OTDM transmission with adjacent tributary channels orthogonally polarised for improved transmission performance compared to that of standard RZ (co-polarised) over SSMF [SUZ'98]. This technique had been demonstrated earlier in [EVA'92] for reducing optical multiplexing penalty at 2.5Gbit/s for two-fold increase in bit-rate. However, the improved transmission performance obtained for alternate-polarisation RZ in [SUZ'98] was attributed to the weaker ISI at the receiver, and no analysis of intra-channel nonlinear effects were given. The suppression of intra-channel nonlinear effects using alternate-polarisation was subsequently investigated in [MOR'99, MAT'99]. However, these nonlinear studies of alternate-polarisation RZ were performed for transmission over DSF with dispersion ~0.13ps/(nm.km) and no research or definitive studies existed on the influence of IXPM and IFWM for transmission over SSMF when they are at their strongest, until the time of this work

[MIK'01b]. Other publications on the use of alternate-polarisation have focused on increasing spectral efficiency [HIN'01], and a novel technique for its generation using polarisation beam splitters and phase modulation [HOD'03, XIE'04]. Alternate-polarisation RZ also lends itself to various demultiplexing techniques based on channel polarisation, which are described in [HAY'01, HIN'01]. However, these techniques were not investigated in this work. Instead alternate-polarisation RZ transmission over SSMF explored in chapter 5 uses standard IM-DD techniques, and focused on characterising the nonlinear distortion. This allowed the improvement in transmission performance to be solely quantified by the suppression of intra-channel nonlinear effects [MIK'01b]. Furthermore, the behaviour of alternate-polarisation RZ in the presence of dispersion management is also discussed in chapter 5. Alternate polarisation can also be used in combination with other advanced modulation formats as described in section 3.3.3.

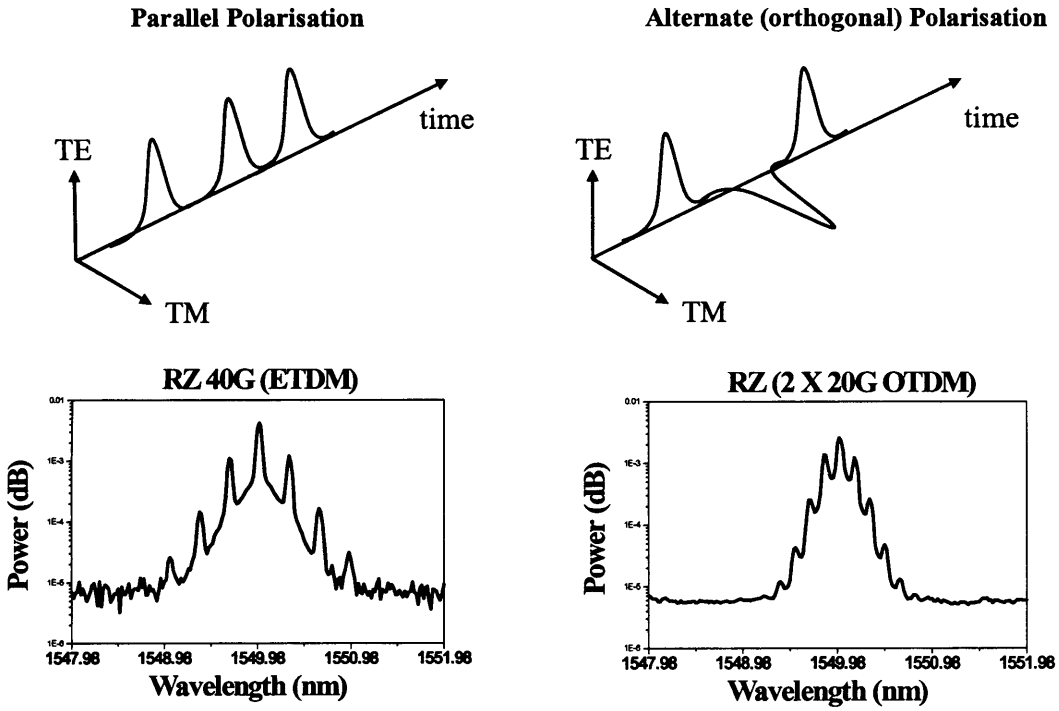

Fig. 3.2 *Schematic illustration of alternate-polarisation RZ with orthogonal polarisation between adjacent bits. The figure also shows the difference in signal spectra between ETDM (parallel polarisation) and OTDM (used for polarisation bit interleaving in this work)*

3.3.2 Alternate-phase RZ

As 40Gbit/s transmission is highly dispersion sensitive, carrier suppressed RZ (CS-RZ) was proposed as a highly dispersion tolerant modulation format with a modulation bandwidth half that of standard RZ [MIY'98]. The CS-RZ format exhibits a step phase change of 0 and π between adjacent bits. This phase change is inherent to the generation technique using a Mach-Zehnder modulator, where the modulator was biased at the turning point of the quadrature transmission window and driven by a clock signal at half the bit-rate, leading to alternate pulses being phase shifted by π radians (rad) relative to the phase of the transmission window [MIY'98]. Other techniques using planar lightwave circuits have also been demonstrated for generating CS-RZ with variable pulsewidth [MOR'02], although the implementation of this technique is cumbersome and has not been demonstrated since. The peak-to-peak phase modulation of π rad has the added benefit of increasing dispersion tolerance through minimisation of ISI [PEN'97]. Furthermore, an alternate phase of π rad is potentially more tolerant to pre-filtering as described in [AGA'03]. The nonlinear tolerance of CS-RZ was subsequently investigated, demonstrating 8x40Gbit/s WDM transmission over 360km of SSMF with a signal launch power of +11dBm/channel [MIY'99]. However, in 2001 Ohhira *et al* proposed an alternative modulation format to CS-RZ (with step or square wave phase change between adjacent pulses), with sinusoidally varying phase and showed that this led to 2dB greater tolerance to nonlinear distortion [OHH'01, SEK'03]. Owing to the sinusoidal phase-variation adjacent pulses are oppositely chirped and hence the format called alternate-chirp RZ. This modulation format has now become better known in the literature as alternate-phase RZ (AP-RZ). (Indeed, the use of alternate-phase has also been proposed for improving NRZ transmission in [HOD'02] with minor improvement transmission performance). While AP-RZ requires an additional phase modulator at the transmitter, the pulsewidth is variable unlike in the case of CS-RZ where a duty cycle of 67% is required to obtain good extinction ratio through the operation of the Mach-Zehnder modulator used to generate it [HIR'03]. Owing to its similarity to CS-RZ but with potentially higher nonlinear tolerance, AP-RZ prompted further investigation as a suitable modulation format for 40Gbit/s transmission (Chapter 5). Much work exists on CS-RZ transmission as a superior modulation format compared to RZ, with respect

to its dispersion tolerance [PEC'03] and high spectral efficiency [MOR'02b]. Hence, in this work the investigation of CS-RZ is more focused on its nonlinear behaviour, with particular emphasis on its comparison with AP-RZ, as discussed in chapters 5 and 6.

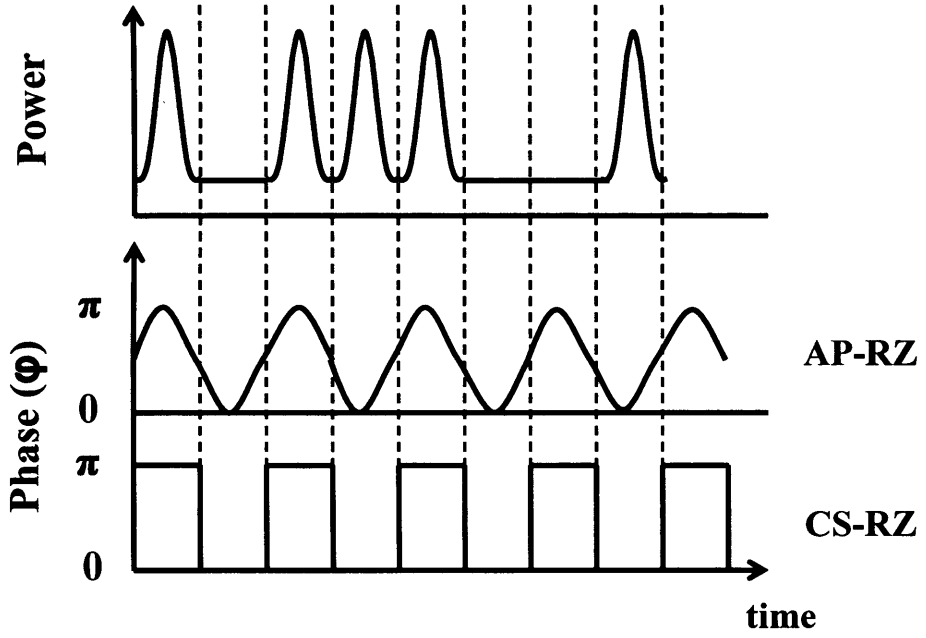

Fig. 3.3 *Schematic illustration of alternate-phase RZ (AP-RZ) and carrier-suppressed RZ (CS-RZ), where the sinusoidal phase variation chirps the pulses in AP-RZ. Note: This illustration assumes identical pulsewidths for both AP-RZ and CS-RZ, however, in general the duty cycle is 67% for CS-RZ modulated signals for Mach-Zehnder generation*

In recent work on the nonlinear behaviour of AP-RZ, it was found by perturbation analysis and numerical simulation, that optimum suppression of IFWM-induced shadow pulses was achieved for an alternating peak-to-peak phase modulation of $\pi/2$ rad between adjacent pulses [JOH'02]. Further numerical simulations based on this work showed that overall optimum transmission performance is obtained for a peak-to-peak phase modulation of $\pi/2$ rad for transmission over SSMF [FOR'02]. These results suggest IFWM as the source dominant nonlinear distortion. However, the results in [FOR'02] also show identical behaviour for RZ and CS-RZ, in disagreement

with the experimental demonstration of CS-RZ [MIY'99], and AP-RZ with peak-to-peak phase modulation of π radians [OHH'01]. Furthermore, experimental investigation of AP-RZ was demonstrated in [GIL'03], and it was noted that not all IFWM processes are efficiently suppressed with a total phase shift of $\pi/2$ rad. These conflicting results raised unanswered questions on the optimum peak-to-peak phase modulation of the AP-RZ modulation format for the overall improvement in system performance. The impact of varying the amount of peak-to-peak phase modulation was thus a subject of this work and is discussed in chapter 5, comparing $\pi/2$ and π rad, variously explored as optimal [APP'04b] (Note: the optimum phase modulation was also discussed for alternate-phase NRZ in [HOD'02]). This study of the optimum phase modulation in AP-RZ requires understanding of the evolution of the differently phase-modulated pulses, as determined by the dominant nonlinearity. The effect of pre-filtering the signal at the transmitter is also taken into account, as it is important in spectrally efficient WDM systems. Finally, investigations combining of AP-RZ with pre-compensation are described [APP'03].

It has also been shown that IFWM can be suppressed using phase modulation at $1/4^{th}$ the bit-rate with peak-to-peak phase modulation of π rad [MAR'02]. Phase modulation was also shown to suppress IFWM by alternating the phase between 'ones' only, with a value of π rad [CHE'02, LIU'02, KAN'03]. This is also known as alternate-mark-inversion (AMI). However, while this requires additional electronic logic circuits in addition to the phase modulator at the transmitter, leading to an increase in complexity and cost, the improvement in transmission performance compared to that of AP-RZ is less than 0.5dB, and therefore not investigated in this work.

Table 3.1 compares the advantages and disadvantages of the most commonly used modulation formats for 40Gbit/s transmission. The time and spectral domain illustrations of these formats can be found in [BIG'04], although it should be noted that [BIG'04] uses square-wave phase modulation with peak-to-peak phase modulation of $\pi/2$ radians, for the general description of AP-RZ instead of the more commonly used sine-wave phase modulation. Furthermore, no differentiation is made between π-AP-RZ and $\pi/2$-AP-RZ.

Modulation Format	Advantages at 40Gbit/s	Disadvantages at 40Gbit/s	References
NRZ	• Narrow modulation bandwidth • Single modulator stage • Mature technology • Dispersion tolerant	• Susceptible to nonlinear effects such as SPM, and XPM	[BRE'96] [LUD'99] [KIL'02]
RZ	• 2dB improvement in receiver sensitivity over NRZ • Nonlinear tolerant • Good compatibility with OTDM operation	• Large modulation bandwidth • Susceptible to intra-channel effects such as IXPM and IFWM • Requires two modulators at Tx • Reduced dispersion tolerance	[HAD'96] [FOR'97] [LUD'99] [KIL'02] [ALL'99] [HAR'99] [ESS'99]
Alternate-polarisation RZ	• Improved tolerance to IXPM • Compatible with polarisation based demultiplexing schemes	• Requires 3 modulators at Tx or 2 modulators and polarisation division multiplexing stage	[EVA'92] [SUZ'98] [MAT'99] [MOR'99] [MIK'01b] [HAY'01]
CS-RZ	• Narrow spectrum • Dispersion tolerant	• Fixed duty cycle of 67% based on standard generation using Mach-Zehnder modulators	[MIY'98] [MIY'99]
AP-RZ	• Good suppression of intra-channel nonlinear effects • Tuneable pulsewidth	• Requires 3 modulators at Tx • Reduced spectral efficiency • Reduced dispersion tolerance due to chirped pulses	[OHH'01] [JOH'02] [FOR'02] [APP'03] [APP'04b] [APP'04c]
DPSK	• 3dB OSNR improvement (with balanced receiver) • Constant envelope modulation decreases SPM, XPM	• Interferometric detection required • Requires DPSK receiver for optical channel monitoring in optical line system • Channel spacing limited to 100GHz	[YON'96] [RHE'00] [RHO'00] [MIY'00] [GNA'02] [MIY'02] [HOS'02]

Table 3.1 Comparison of the modulation formats used in the transmission of 40Gbit/s signals, with their relative advantages and disadvantages

3.3.3 Combination of alternate-polarisation and alternate-phase RZ

As alternate-polarisation RZ and modulation formats such as AP-RZ, have been shown to be effective in suppressing intra-channel nonlinear distortions, combining these two schemes into a single format was an attractive solution for creating a modulation format with maximum nonlinear tolerance. The combination of the advanced modulation format with pre-compensation described in chapter 5, made it possible to understand the dominant nonlinearity for varying values of dispersion-induced pulse overlap. This led to the proposal and demonstration of a novel modulation format with simple simultaneous implementation of the alternate-polarisation RZ and AP-RZ modulation format described in chapter 5 [APP'04]. It was shown experimentally, for the first time, that combining these two techniques is effective in suppressing the intra-channel nonlinear distortions at 40Gbit/s in SSMF, showing an improvement in nonlinear tolerance with respect to standard RZ without requiring any dispersion management. Indeed, the combination of polarisation and phase modulation has previously been proposed at a bit-rate of 5Gbit/s in [BER'96] for the suppression of polarisation hole burning and the improvement of the EOP, and also in [FUJ'03] for improved spectral efficiency and operation in networks without clock synchronisation. However, around the same time the work described in [APP'04] was carried out, a similar technique combining CS-RZ with alternate-polarisation was investigated in a Raman amplified SSMF link [XIE'04], and showed similar improvements in nonlinear tolerance. This technique has since been extended to other phase modulated formats such as differential-phase-shift-keying (DPSK) with alternate-polarisation [KAN'04, GNA'04].

3.3.4 Differential-Phase-Shift-Key (DPSK)

DPSK was initially proposed for optical transmission at a bit-rate of 10Gbit/s [ELR'91, YON'96] in order to obtain higher sensitivities in IM-DD receivers, as described in [LIV'96]. However, with the increase in research on 40Gbit/s transmission, an intensity-modulated DPSK (IM-DPSK) format was proposed in [MIY'00] with potentially higher tolerance to fibre nonlinear effects and improved

receiver sensitivity. In general for DPSK signals, a CW laser source is phase modulated by a differentially encoded NRZ signal. Differential encoding is typically achieved by use of a one-bit-delay feedback loop along with an exclusive-OR (XOR) logic gate. This modulation causes the transition from a logical '0' to '1' to be represented by a π phase change in the optical carrier. However, this phase-change which is caused by the modulation, chirps the signal and is affected by SPM-GVD in the transmission fibre leading to poor nonlinear tolerance. Hence, in IM-DPSK, the signal is re-modulated by an intensity modulator driven by a clock signal synchronised with the data signal to suppress such signal distortion. This intensity modulation attenuates the optical intensity at the bit transition, and therefore, significantly reduces the frequency chirping caused by SPM. The resultant IM-DPSK signal is similar to RZ signals, where the data is encoded on the optical phase of each RZ pulse [HOS'02]. The generation of RZ pulses can also be achieved in a similar manner to that of CS-RZ [MIY'98], to further improve spectral efficiency and nonlinear tolerance [MIY'02].

The detection of such signals requires a delayed detector based on Mach-Zehnder interferometer at the receiver to convert phase modulation into intensity modulation for conventional direct-detection (IM-DD). In such interferometric structures, the signal is split into two arms, one of which is delayed by a single bit-period (25ps for 40Gbit/s transmission) and then interfered with each other such that if there is no phase difference there is constructive interference giving a logical '1' and destructive interference to give a '0' in the presence of a π phase difference.

As described in *Table 1.1.* DPSK formats have been significant in achieving ultra-long transmission distances with total capacity in the PBit/s range. However, owing to the increase in complexity at the transmitter and receiver DPSK modulation formats were not studied in this work, which mainly focused on the simplest, and thus, cost-efficient implementation of 40Gbit/s systems over metro and long-haul transmission.

3.4 Other technique for suppression of intra-channel nonlinear effects

Other techniques for suppressing intra-channel nonlinear distortion have also been investigated. Statistical studies of pattern dependent intra-channel nonlinear effects were carried out in [SHA'01,SHA'04], and it was shown that the density of 'ones' dramatically affects the quality of transmission. Hence, data encoding by inserting additional 'zero' bits (bit-stuffing) [SHA'03] and by data-dependent phase modulation [ALI'02]. While, these techniques are effective, they require an additional bandwidth overhead for their implementation, as data processing is required at both the transmitter and receiver. Indeed, similar techniques have been used for forward-error-correction (FEC), which improve the system margin by approximately 5dB in noise limited systems. It has also been shown that IFWM can be suppressed for unequally spaced pulses [KUM'01], similar to the technique of unequally spaced WDM channels to suppress FWM [FOR'94]. However, this technique is not favoured as a commercially viable option, as it is not compatible with standard clock recovery techniques and cannot be included in time-division-multiplexed applications. Inter-pulse interactions were also shown to be minimised in the presence of distributed amplification [MEC'01]. Distributed amplification can be achieved experimentally by Raman amplification [MOR'00, ISL'02], which enables the design of transmission links which are symmetrical about a mid-point in terms of dispersion and power, cancelling nonlinear interactions at the end of the transmission link. However, despite the significant improvement in transmission performance *(see Table 1.1)*, Raman amplifiers have not yet been deployed in commercial systems. This is because Raman amplification is somewhat inefficient as it requires the use of high power laser pumps (~1W) to obtain the gain required for optical communication systems. Further, disadvantages such as multi-path interference [FLU'01], pump noise transfer to the signal [YAN'01], and spectral tilt of the noise figure [KAD'02] are also associated with Raman amplification, and is therefore beyond the scope of this work, and noise limitations are investigated for EDFA systems only.

3.5 Dispersion tolerance

Along with a detailed investigation of the nonlinear distortion in 40Gbit/s transmission it is important to investigate the other sources of signal degradation. Deployed fibre links suffer from incomplete dispersion compensation owing to the variable amplifier span lengths and fixed step sizes of the dispersion compensation modules. For this reason, in dispersion managed links which are used in the suppression of intra-channel nonlinear effects (section 3.2.2), uncompensated dispersion can arise due to non optimal values of dispersion in the pre-compensation at the transmitter, post-compensation at the receiver and in the in-line compensation. The research described in [FRI'00, FRI'02, PEC'03] investigate dispersion tolerances for the pre/post-compensation at the transmitter/receiver and the in-line dispersion separately and are claimed to be essential in system design. Although in general, the total cumulated dispersion from the pre-compensation, post-compensation and in-line compensation also referred to as residual dispersion, is a more useful parameter. It is, however, important to distinguish between dispersion tolerances for linear (at low signal launch powers) and nonlinear (at high signal launch powers) transmission, as it is of particularly importance for transmission at 40Gbit/s, owing to the strong interdependence between dispersion and nonlinear interaction between adjacent pulses. The work reported in [FRI'00], investigated these effects for comparison of the NRZ and RZ modulation formats, showing NRZ to be most dispersion tolerant, while RZ with short duty cycle the least tolerant to dispersion. However, the induced nonlinear distortion showed opposite behaviour to that seen for dispersion tolerance, with NRZ least tolerant nonlinear distortion and RZ with short duty cycle the most tolerant.

Advanced modulation formats can significantly improve these tolerances, and ultimately lead to less complex fibre link design [MIK'04]. Results of a comprehensive study involving 1,000,000 numerical simulations of dispersion tolerance for various modulation formats were reported in [PEC'03]. This work was carried out for investigation of 40Gbit/s transmission over 1500km of TeraLight^{TM} fibre *(D=8ps/(nm.km)*. The authors reported that CS-RZ was most tolerant to residual dispersion, although no physical explanation for this was given. Furthermore, at the

time of the work described in this thesis [APP'04c], very little experimental investigation of residual dispersion tolerances existed for transmission at 40Gbit/s. Furthermore, most experimental demonstrations of dispersion tolerances were carried out using tuneable compensators at the receiver, and there were no reports on varying the in-line residual dispersion in every amplifier span. *Table 3.2* shows the maximum tolerable uncompensated dispersion for various modulation formats, as taken from published literature, with the maximum dispersion tolerance taken at an EOP of 3dB.

The existing work on dispersion tolerances were mostly carried out by use of numerical simulations. However, as numerical simulations do not perform BER measurements, but quantify the transmission limit using the EOP, they may lead to erroneous conclusions, as for certain modulation formats an EOP greater than 3dB may still enable a BER<10^{-9} to be achieved. The experimental investigation of dispersion tolerances is therefore more informative, as it incorporates BER measurements. An experimental investigation of the dispersion tolerances of different modulation formats were therefore carried out for the first time during the course of this work, and is described in chapter 6 [APP'04c]. The work described in chapter 6 investigates 40Gbit/s transmission for both linear and nonlinear transmission over SSMF experimentally, as SSMF remains the most commercially viable option for 40Gbit/s transmission. A new experimental technique, based entirely on fibre elements was demonstrated to achieve this. Investigation of the dispersion tolerance of the AP-RZ modulation format is also described for the first time in chapter 6, highlighting its advantages and disadvantages.

Modulation Format	Dispersion tolerance (ps/nm)	Remarks	References
NRZ	70	Experimental Back-to-Back BER measurement, with tuneable dispersion compensator at the Receiver	[BIS'03]
NRZ	70	Extrapolation from 10Gbit/s measurements	[HAG'98]
NRZ	65 (back-to-back) 30 (1500km)	Total residual dispersion calculated by simulation of cumulative pre/post-compensation and in-line residual dispersion	[PEC'03]
RZ	40	Indicates decreasing dispersion tolerance with decreasing pulsewidth (duty cycle)	[HAG'98]
RZ	50 (back-to-back) 32 (1500km)	Signal launch power 0dBm (linear propagation)	[PEC'03]
RZ	40	Residual dispersion over 4 spans (320km SSMF)	[HOD'02b]
RZ	50	Experimental BER measurement at a distance of 240km, with tuneable dispersion compensator at the Receiver	[SUZ'98]
RZ	±60 (0dBm) ±45 (+5dBm)	Experimentally measured (BER), for varying in-line residual dispersion in step sizes of 5ps/nm in the region of ±15ps/nm	[APP'04c]
Alternate-polarisation RZ	70	• Improved tolerance attributed to the suppression of ISI by alternate-polarisation between adjacent bits (240km)	[SUZ'98]
CS-RZ	72	Dispersion tolerance varies with extinction ratio (back-to-back)	[CHO'01]
CS-RZ	70	Dispersion tolerance decreases with increase in signal launch power (320km)	[HOD'02b]
CS-RZ	48 (back-to-back) 45 (1500km)	Maximum dispersion tolerance given as a percentage (12%) of total dispersion within each amplifier span	[PEC'03]
AP-RZ	-45→+30 (0dBm) ±30 (+5dBm)	PM-IM conversion decreases dispersion tolerance due to chirp and uncompensated dispersion (480km)	[APP'04c]
DPSK	56 (back-to-back) 40 (1500km)	RZ-DPSK dispersion tolerance was 45ps/nm (back-to-back)	[PEC'03]

Table 3.2 Comparison of the dispersion tolerances of various modulation formats for transmission at a bit-rate of 40Gbit/s

3.6 Summary

The review of the literature exploring 40Gbit/s transmission discussed in this chapter highlights the challenges to be overcome when upgrading from 10Gbit/s systems. These include tighter restrictions due to nonlinear effects, noise and dispersion. While these challenges existed even at lower bit rate transmission, the intra-channel nonlinear effects begin to be significant at 40Gbit/s and higher bit-rates are relatively new and required further investigation. It is shown in the following chapters that it is possible to design and implement hybrid systems based on the advantages of particular fibre type, dispersion management scheme and modulation format for successful 40Gbit/s operation. The results of this research will provide network operators with the ability to selectively install and operate 40Gbit/s channels where traffic loads demand them or use existing technology upgradeable for cost-effective implementation. The transmission distances of interest in this thesis are of lengths based on European core networks, also known as long-haul transmission. It is common for deployed systems to possess an error-free margin of 5dB. This work does not incorporate this margin, however, the required system margins for commercial applications can be obtained at the achieved distances with the use of forward-error-correction (FEC).

Chapter 4 Dispersion managed fibre links

4.1 Introduction

As described in previous chapters, optical signals become increasingly susceptible to dispersion, noise and nonlinear effects as the transmission bit-rate is increased to 40Gbit/s. In chapter 2, it was described how intra-channel nonlinear distortion arises in the presence of dispersion-induced pulse overlap, and how fibre dispersion plays a key role in this effect. From the literature survey in chapter 3 it is evident that clear cost benefits exist in retaining SSMF, the most commonly deployed fibre type when upgrading to 40Gbit/s transmission. The work described in this chapter, therefore, initially investigates 40Gbit/s transmission over SSMF in order to gain an understanding of the maximum achievable transmission distance and relevant system parameters. The results of this initial experiment provide a basic understanding of system performance, and enable the verification and comparison of the experimental recirculating loop measurements with that obtained using the split-step-Fourier numerical simulations.

Transmission experiments and numerical simulations were then carried out in order to investigate the potential improvement in transmission performance when NZDSF was used instead of SSMF. Results focusing on the intra-channel nonlinear interactions in NZDSF were obtained and compared with that for transmission over SSMF, giving a good understanding of the trade-off required between cost benefits gained from using already installed SSMF against the performance benefits of using NZDSF. The NZDSF link described in this chapter investigates new designs of amplifier spans based on a HOM-DMD for dispersion compensation. WDM transmission is also carried out and compared with single channel transmission results to identify the dominant source of nonlinear distortion. The use of the HOM-DMD as a broadband dispersion compensation device is also demonstrated for simultaneous dispersion compensation of 10 WDM channels over the C-band.

Finally, the chapter investigates the suppression of intra-channel nonlinear distortion by controlling the pulse overlap when launched into the transmission fibre. This is achieved by pre-dispersion compensating the signal at the transmitter. The technique

is investigated with systematic analytical, numerical and experimental investigation, and is explored for transmission over both SSMF and NZDSF.

4.2 Experimental set-up of 40Gbit/s optical transmission systems

4.2.1 Transmitter

NRZ signal generator: A 40Gbit/s NRZ signal was generated using a 40Gbit/s pulse pattern generator (PPG) as shown in *Fig. 4.1*. The electrical signal from a 40Gbit/s PPG was used to drive a single electro-absorption modulator (EAM) which modulated the constant wavelength (CW) signal from the external cavity laser (ECL), with side-mode suppression of greater than 60dB. The resultant 2^{31}-1 PRBS 40Gbit/s NRZ optical signal had an extinction ratio of 16dB, and is typical for systems employing EAMs [MIK'03]. This value of the extinction ratio was also used in the numerical simulations used for comparison with results obtained experimentally.

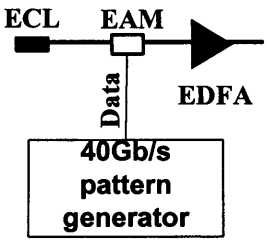

Fig. 4.1 40Gbit/s NRZ transmitter

RZ signal generator: The RZ signal generation was performed experimentally both by use of optical-time-division-multiplexing (OTDM) and by electrical-time-division-multiplexing (ETDM). At the start of this work ETDM multiplexers operating at 40Gbit/s were not easily available, and thus the experimental work was performed using OTDM. The use of OTDM is advantageous as it does not require electronic components operating at 40GHz, but at the lower sub rate of 10GHz [MIK'03].

Optical time division multiplexer (OTDM): An external cavity laser (ECL) was employed and the output of this laser was modulated by an electro-absorption-modulator (EAM) encoding a 2^{31}-1 10GBit/s NRZ pseudo-random-bit-sequence. The

resultant NRZ signal was fed into two cascaded EAMs, driven by a combination of the base clock signal at 10GHz and 20GHz which converted the NRZ signal into a 10Gbit/s RZ signal with narrow pulses of width varying from 10.5-14ps (FWHM). See for example [MOO'95, ELL'97]. OTDM was achieved by splitting the 10Gbit/s RZ signal via a 3dB coupler and introducing a delay in one arm. This interleaver process was repeated twice to obtain a 40Gbit/s signal. The two delays in each interleaver consisted of 30m and 15m of dispersion shifted fibre to de-correlate the bits, and a variable optical delay for accurate bit interleaving with no active components. The interleaver also included polarisation controllers which controlled relative polarisation between adjacent pulses, allowing both parallel and orthogonal polarisation states to be investigated (eg. Alternate-polarisation RZ in chapter 5).

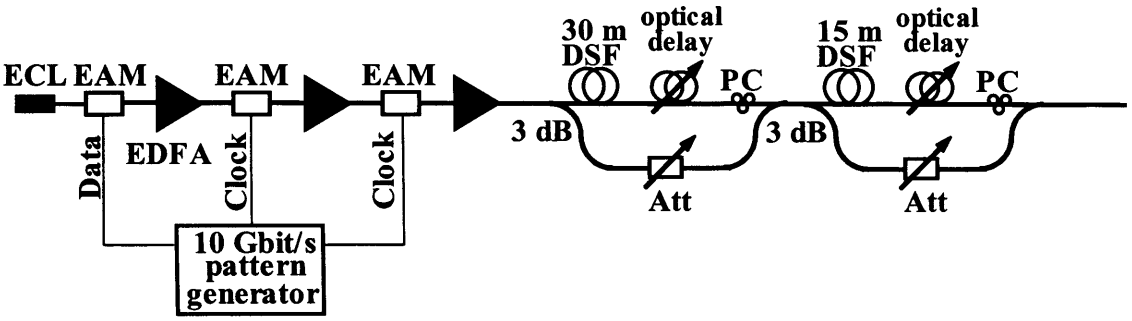

Fig. 4.2(a) 40Gbit/s OTDM transmitter

Electrical time division multiplexer (ETDM): This system required one less EAM for the generation of the RZ signal compared to that of the OTDM set-up. The system is identical to that generating the 40Gbit/s NRZ signal, but with the resultant NRZ signal fed into a second EAM driven by a 40GHz clock signal also obtained from the pattern generator, resulting in a RZ signal of pulsewidth 11.25ps (FWHM) as measured on an autocorrelator *(Fig. 4.2(b))*. The extinction ratio of the RZ signal was approximately 30dB for both ETDM and OTDM 40Gbit/s signals, also measured using an autocorrelator.

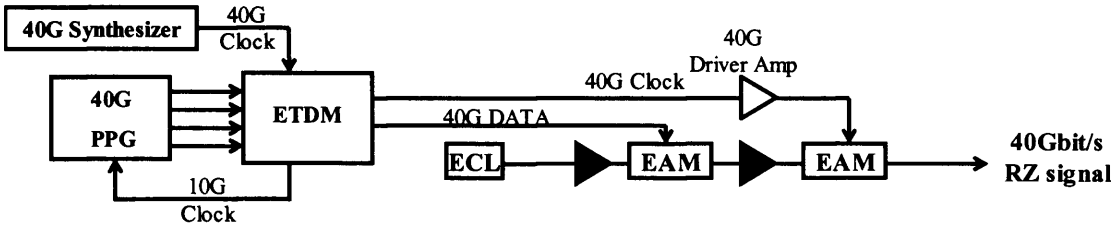

Fig. 4.2(b) 40Gbit/s ETDM transmitter

4.2.2 Transmission set-up using a recirculating fibre loop

The transmission experiments were carried out in a recirculating fibre loop to simulate long transmission distances with a single amplifier span. This provided great flexibility when reconfiguring dispersion maps and allowed the measurement variation of distance dependent nonlinear impairments. In general, recirculating loop measurements use identical components to that used in straight line experiments, but with significantly reduced quantity. The only additional components required in a recirculating loop compared to that not required for straight line transmission are 2 acousto-optic-modulators (AOMs) which behave as optical switches, and an optical coupler, while all test and measurement equipment should be capable of performing measurements under external gating, as the measurement time is not continuous (burst mode operation) like in standard measurements.

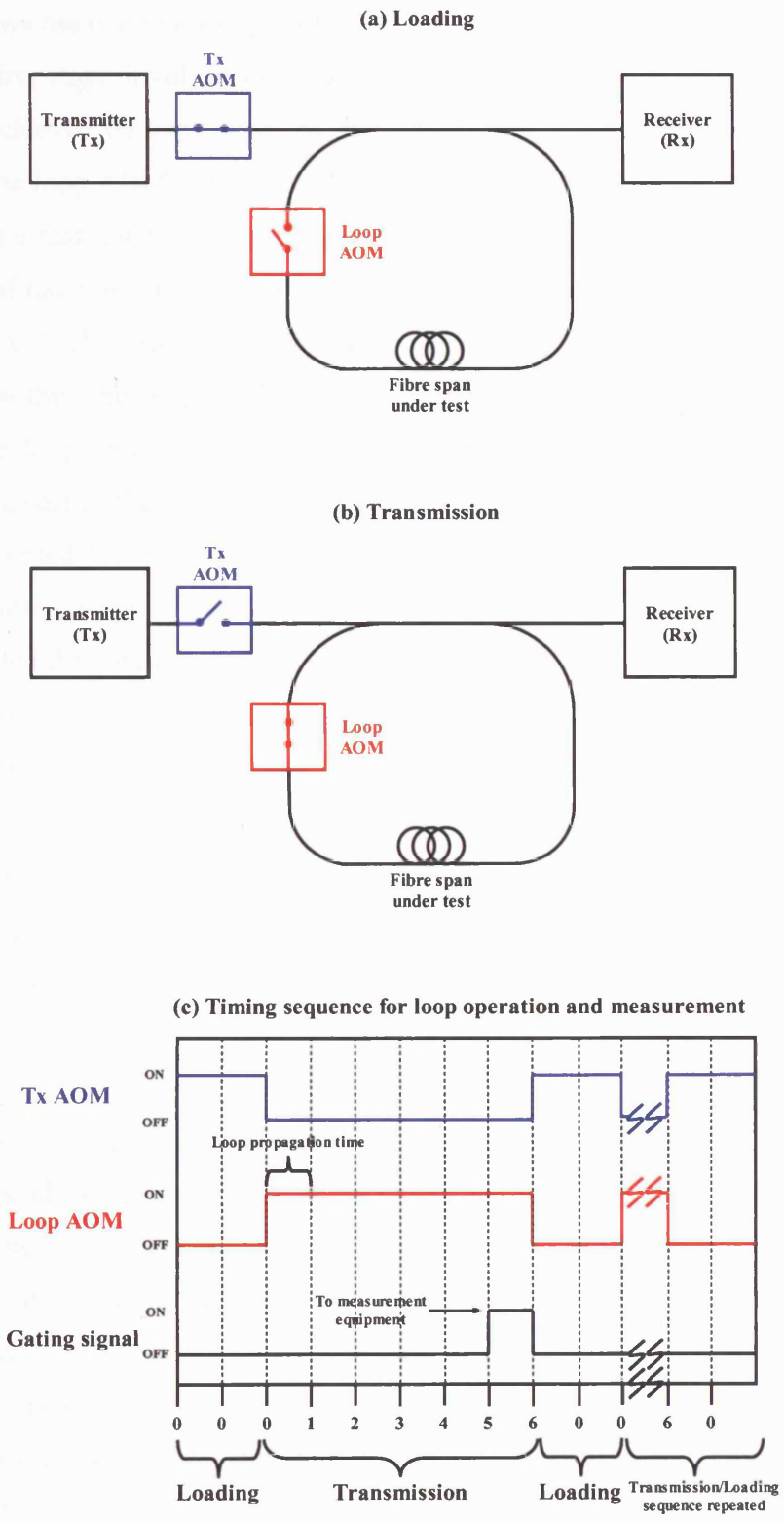

Fig. 4.3 *Principle of operation of the recirculating fibre loop: (a) Loading stage (b) Transmission stage (c) Timing diagram illustrating AOM and gating sequence for transmission over 6 recirculations.*

Fig. 4.3 shows the two main stages of operation for transmission using a recirculating loop. The first stage involves the loading of the signal into the loop. This loading process is achieved by switching 'on' the Tx AOM to the transmit mode and at the same time the loop AOM is switched 'off' *(Fig. 4.3(a))*. This takes place for a period of time longer than the time of propagation for a single recirculation within the loop. At the end of loading stage, the loop is filled with the signal under test. In the second stage, the Tx AOM and loop AOM are inverted enabling the signal under test to recirculate within the loop while the signal from the transmitter is blocked from entering the loop, and is known as the transmission stage *(Fig. 4.3(b))*. During transmission, part of the signal is continuously coupled out of the loop. However, this can be accounted for as part of the loop loss and is compensated for by the loop EDFA. Finally, a trigger pulse is sent to the measurement equipment after the signal has propagated through the required number of recirculations. This trigger pulse is of time equal to or shorter than the time of propagation for a single recirculation. These stages are then repeated over a long period of time in order to collect sufficient data for the measurement process. The timing diagram of the switching and measurement stages are synchronised by a delay generator with multiple programmable outputs, and an example of this timing diagram for transmission over 6 spans is shown in *Fig. 4.3(c)*. A more detailed description of recirculating loop operation can be found in [MIK'03].

In these experiments, the recirculating fibre loop was used to investigate and quantify distance dependent effects, such as the accumulated nonlinear phase shift, dispersion and noise. The loop EDFA output *(Fig 4.4)* was always saturated and had a gain equal to the total loss within the loop span. This ensured that the signal power launched into the amplifier span remained constant for an infinite number of recirculations. To investigate signal degradation due to intra-channel nonlinear distortion, it was important to vary the signal power without varying the noise figure of the loop EDFA. This was achieved by combining 5 CW WDM channels with the 40Gbit/s channel at the input of the loop. The signal power (and SNR) was varied by changing the coupling ratio between 40Gbit/s channel and CW channels maintaining the pump currents of the loop EDFA and therefore, maintaining its gain, output power and noise figure constant. At the loop output the signal channel was filtered using one port of a flat-top arrayed-waveguide-grating (AWG, with a 0.6nm 3dB-bandwidth), detected

and measured using a bit-error-rate-test-set (BERT). Furthermore, as the length of the loop was relatively short, the polarisation of the signal into the loop was adjusted using a fibre polarisation controller to give the minimum bit-error-rate (BER) for all measurements. The average power within the loop was constantly monitored and found to vary by less than ±0.1 dB during the measurement gating time for all recirculations. Detailed diagrams of the different experimental set-ups related to each set of experiments are given in the relevant sections.

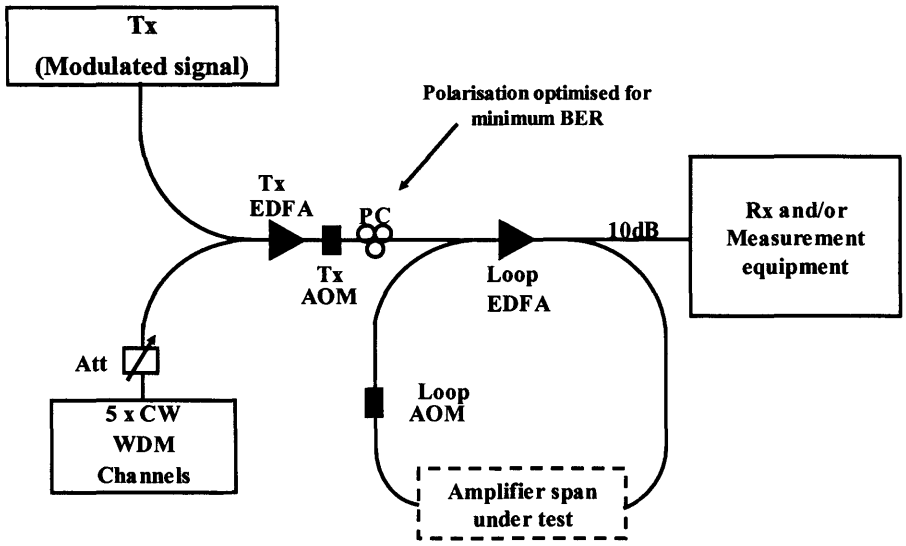

Fig. 4.4 *Schematic diagram of recirculating loop, where the signal launch power into the loop was varied by changing the coupling ratio between the modulated signal and the 5 CW WDM channels. This is achieved by varying the power of the 5 CW WDM channels using a tuneable attenuator*

4.2.3 Transmission fibre and dispersion compensation

In the course of this work, the propagation of optical signals was investigated for different transmission fibre types and compensation modules. These included standard single mode fibre (SSMF) and dispersion compensating fibre (DCF) as well as large-effective-area non-zero dispersion shifted fibre (NZDSF) and higher-order-mode compensators was investigated. SSMF as the most commonly deployed fibre was investigated first, in a single amplifier span placed within the recirculating loop. The SSMF had an attenuation coefficient α=0.21dB/km and had a dispersion parameter D=17ps/(nm.km) @1550 nm, with an effective area A_{eff} = 55μm^2 and n_2=2.3x10^{-20}

m^2/W (Corning data-sheet SMF-28). Experimental and theoretical analysis was performed for a link consisting of 60km of SSMF dispersion compensated by a slope compensating DCF module (Lucent DK-60). The lengths were chosen such that the total loss within the amplifier span was approximately 20dB and capable of being compensated for by the gain of the EDFA. The DCF module consisted of approximately 12km of fibre with D=-85ps/(nm.km) and attenuation coefficient α=0.5dB/km with $A_{eff} = 19\mu m^2$ and $n_2=2.66x10^{-20}$ m^2/W (Lucent DK-60).

NZDSF was also investigated as the dispersion parameter D=4ps/(nm.km) @1550 nm reduces the pulse overlap compared to that seen in SSMF, thereby reducing the intra-channel nonlinear effects. The NZDSF link was compensated by a LaserComm higher-order-mode dispersion management device (HOM-DMD) which was capable of compensating 75km of NZDSF. The DMD had a loss of approximately 4dB, and with $A_{eff} = 70\mu m^2$ and length ~700m which provides a distinct advantage over DCF as the overall nonlinearities are significantly reduced due to the combination of reduced interacting length and increase in effective area, enabling the device to behave in a linear manner. The dispersion versus wavelength was measured for the two links and the results are shown in *Fig. 4.5*, measured using an Agilent HP 86037C chromatic dispersion analyser test-set.

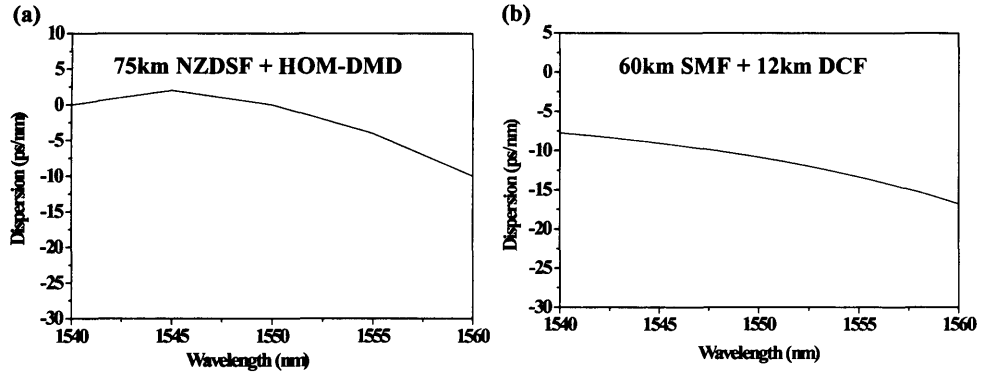

Fig. 4.5 *Measured dispersion (a) NZDSF amplifier span (b) SMF amplifier span*

The SSMF amplifier was under-compensated by -8ps/nm, while the NZDSF amplifier span was over-compensated by 1.5ps/nm at 1550nm. However, during the course of the experiments the residual dispersion was compensated at the receiver in order to achieve approximately 0ps/nm residual dispersion for all distances.

4.2.4 Receiver & clock recovery

Bit-Error-Rate (BER) measurements were performed both at 10Gbit/s and at 40Gbit/s. Initial measurements were performed at 10Gbit/s, where the 40Gbit/s signal was optically demultiplexed down to 10Gbit/s and BER measurements were performed at the receiver at 10Gbit/s. The optical demultiplexing was performed by using two cascaded EAMs providing a narrow switching window capable of selecting one of the four 10Gbit/s tributaries in both the RZ and NRZ transmission, as shown in *Fig. 4.6.* EAM1 was driven by the recovered 10GHz clock signal only, while EAM2 was driven by a combination of the 10GHz and 20GHz recovered clock signal. While providing a switching window of extinction ratio greater than 40dB this 2-stage demultiplexer was also useful in the power management especially when demultiplexing RZ signals as it allowed a higher average power at the input of EAM2 while the peak power was still safe for EAM operation [MIK'03]. As BER measurements in this scheme can be performed for a single 10Gbit/s tributary only, during the course of these measurements it was necessary to measure all 4 tributaries of the 40Gbit/s signal separately.

Clock recovery was initially performed at 10Gbit/s by transmitting a 10Gbit/s NRZ signal on an auxiliary optical channel at a non-interfering wavelength to the 40Gbit/s signal channels. The results were comparable, however, when a clock recovery unit based on phase locked loop technology (on loan from Nortel Research Laboratories, Harlow, Essex) was used to recover the clock directly from the incoming 40Gbit/s signal.

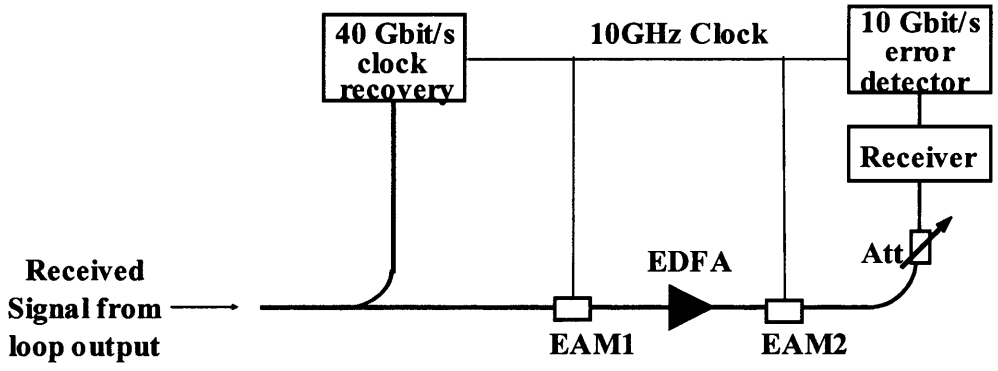

Fig. 4.6 OTDM demultiplexer and receiver set-up

Subsequently BER measurements were performed directly at 40Gbit/s as described in *Fig. 4.7.* The signal detected on the broadband photo-detector (bandwidth>45GHz) was maintained at a constant power of +3dBm, which was sufficient for electrical de-multiplexing (Anritsu MP1804A de-multiplexer) and BER measurements using the BERT (Ando AP9951).

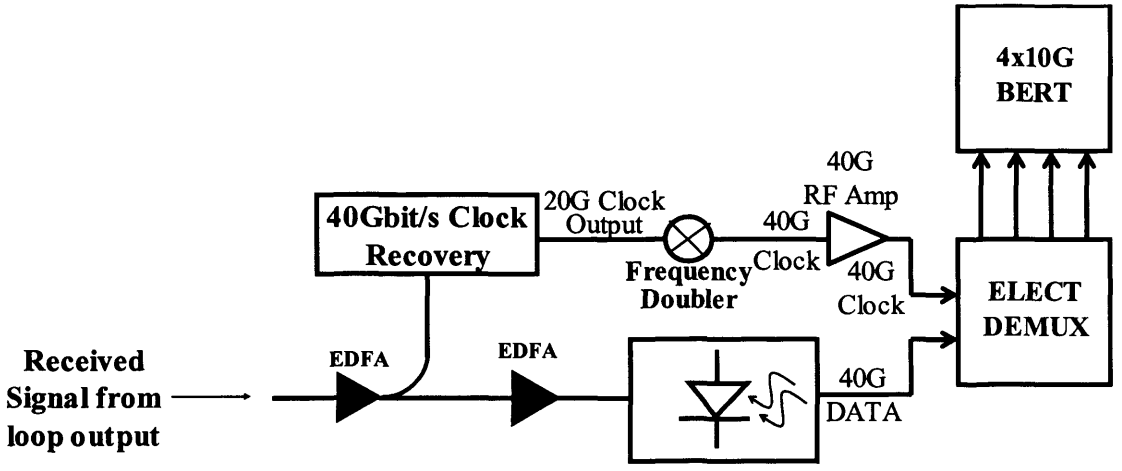

Fig 4.7 Electrical demultiplexer and receiver set-up

4.2.5 Noise and OSNR characterisation

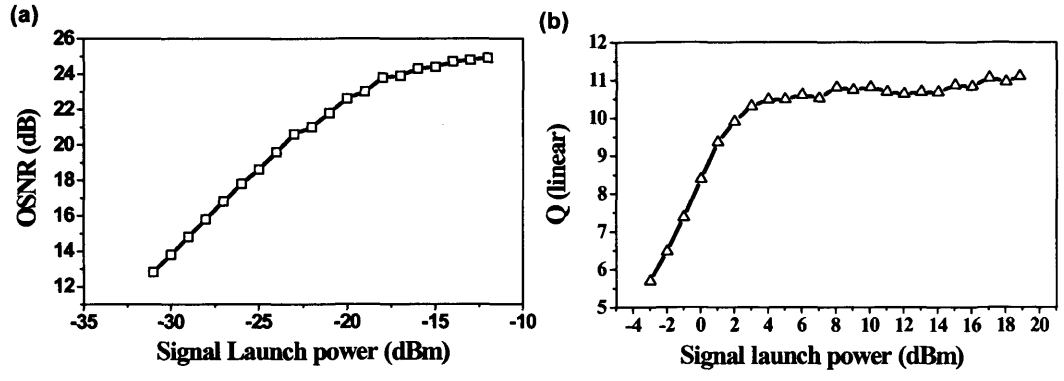

Fig. 4.8 *(a) Experimentally measured OSNR using an OSA with 1nm resolution bandwidth as a function of signal launch power for OTDM 40Gbit/s RZ signal (b) Back-to-back Q-factor measurements as a function of signal launch power measured on the OTDM de-multiplexer/receiver*

System characterisation was performed for the OTDM transmitter and OTDM demultiplexer/receiver. The OSNR of the signal launched into the loop was measured as a function of the signal launch power on an optical spectrum analyser (OSA) with a resolution of 0.5nm. The launch power was varied as described in section 4.2.4. The results shown in *Fig. 4.8(a)* indicate that the OSNR saturates at a value of approximately ~25dB, at signal launch power of -15dBm. *Fig. 4.8(b)* shows the measured Q-factor at the output of the loop for back-to-back transmission. It can be seen that a Q-factor>6 (15.56dB) is achieved at a signal launch power of –3dBm and saturating at approximately 11 (20.82dB) for signal launch powers greater than +4dBm. This behaviour indicates constant OSNR and noise distortion in the receiver set-up as the receiver erbium pre-amplifier becomes saturated.

4.3 Transmission over standard single mode fibre (SSMF)

4.3.1 Simulated transmission of NRZ and RZ signals over SSMF

40Gbit/s transmission was initially investigated by numerical simulation of the NRZ and RZ modulation format over SSMF, in order to compare the transmission performance of the two modulation formats and also to obtain parameters for the experimental investigation. The simulated transmission system is shown in Fig. 4.9. The NRZ and RZ modulation formats were simulated as described in section 2.9, with a PRBS of 2^9 bits. The transmission link consisted of 60km of SSMF post-compensated by 12km DCF giving 100% dispersion compensation. The amplifier noise figure was 4.5. The resultant Q-factor was calculated at the receiver, as a function of transmission distance, according to the technique described in section 2.8.4.

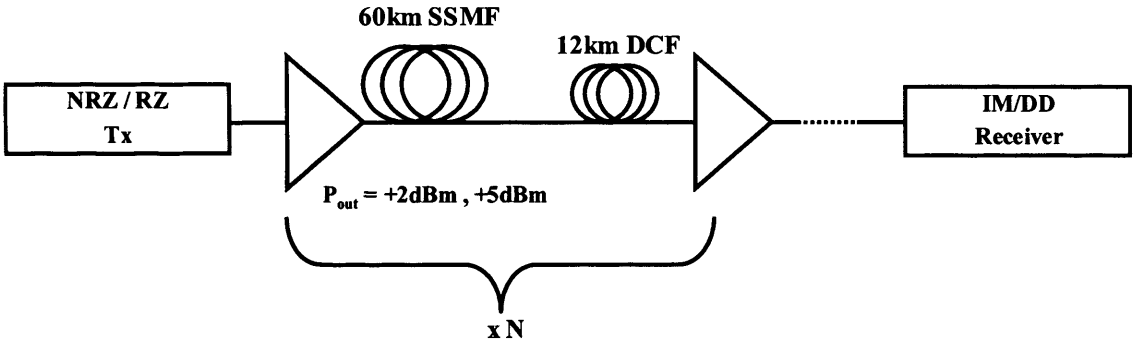

Fig. 4.9 *Schematic diagram of transmission system for NRZ and RZ transmission over 60km SSMF post-compensated by 12km of DCF. The amplifier noise figure was 4.5 and the average signal launch power was +2dBm and +5dBm for both modulation formats*

The graphs in *Fig 4.10* show the calculated Q factor for increasing transmission distance. It can be seen that the simulations predict a transmission distance of 300km for NRZ transmission and 480km for RZ transmission +2dBm (average power). RZ signals correspond to a 3dB lower average power compared to NRZ signals for the same peak power due to the shorter duty cycle. This is consistent with the theory described in section 2.5, and leads to a decrease in the nonlinear distortion thereby

increasing the transmission distance. It should be noted, however, that the comparison of NRZ and RZ modulation formats were intentionally carried out for identical dispersion maps and link lengths with 100% dispersion compensation, which is preferred for RZ signals, while NRZ signals are optimised in the presence of under-compensation, as mentioned in chapter 3. This was in order to identify *(compare)* the impact of dominant nonlinearities, rather than optimise transmission for each particular case (which can be achieved through dispersion management, choice of optimum power and other techniques, which must be separately optimised for each individual link).

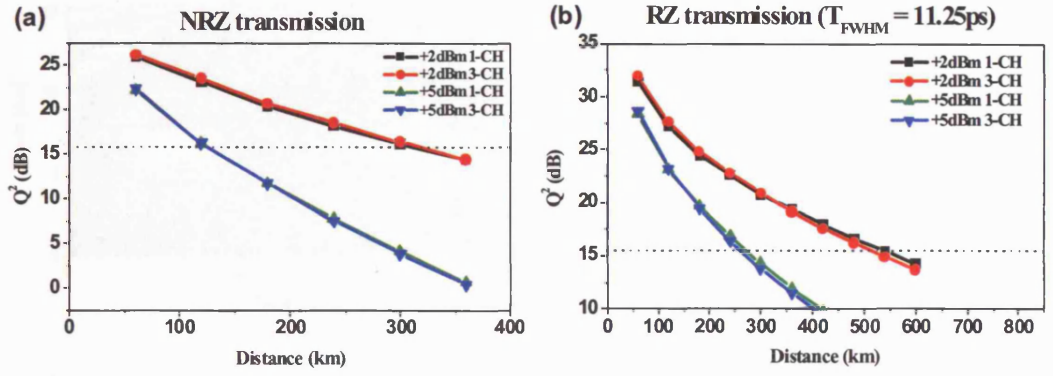

Fig. 4.10 ***(a):*** *NRZ,* ***(b):*** *RZ, transmission over SSMF. Dotted line indicates a Q factor of 6 which corresponds to error-free transmission (BER<10^{-9}). A wavelength spacing of 0.8nm (100GHz) was used in the simulation of the 3-channel WDM transmission*

The main advantage of the RZ modulation format over NRZ is due to the fact that a single RZ pulse undergoes severe pulse broadening due to the high dispersion in the SSMF. Hence, the pulse peak power is decreased after only a few kilometres (~ 4km) of transmission. The reduced pulse peak power combined with pulse broadening lessens the influence of SPM, and allows for higher launch powers of the RZ signal into the fibre. The NRZ modulation format is more severely affected by SPM compared to the RZ modulation format *(Fig. 4.11)*, hence the decrease in transmission distance for similar launch powers. The pulse distortion can be seen in the calculated eye diagrams for both NRZ and RZ signals in *Fig. 4.11.* While the RZ modulation format is less affected by SPM [ESS'99, MIK'99], signal distortion is caused by the

intra-channel nonlinear effects such as IXPM and IFWM. Indeed, the IXPM-induced timing jitter, and the amplitude jitter and emergence of shadow pulses caused by IFWM can be seen in the RZ modulation format eye diagrams *(Fig. 4.11(b))*. This is because the nearest spacing of pulses for NRZ signal occurs in a 10101... bit sequence where adjacent pulses are 50ps apart *(Fig 4.12)*. For RZ pulses however, the nearest spacing between adjacent pulses occurs at only 25ps in a 1111... bit sequence. Hence, the pulse overlap is more significant for RZ transmission, leading to higher intra-channel nonlinear distortion.

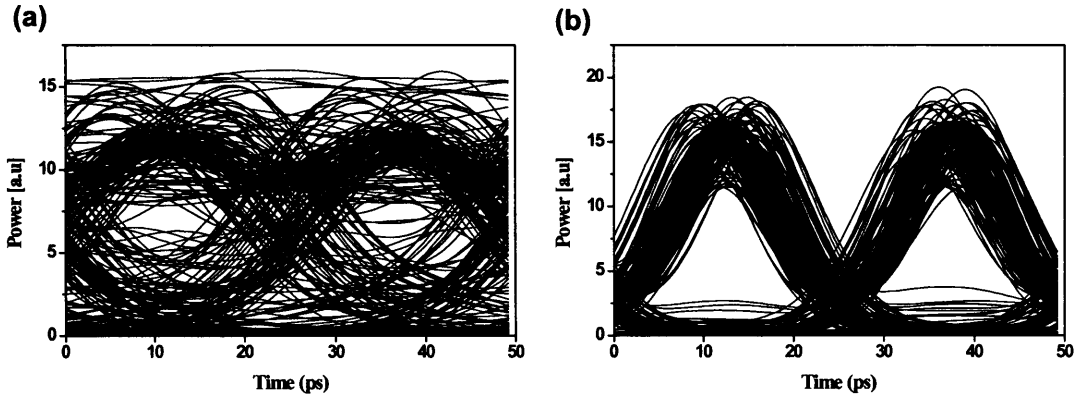

Fig. 4.11 *Simulation of 40Gbit/s signal transmitted over 240km (a) NRZ (b) RZ at a signal launch power of +5dBm. Note: the link consisted of 100% dispersion compensation with no further optimisation of the dispersion at the receiver*

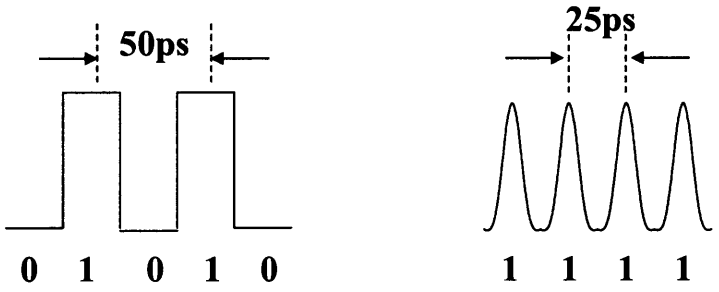

Fig. 4.12 *Adjacent pulses in the NRZ format are 50ps apart and only 25ps apart in the RZ format*

Although SPM is significant in the NRZ modulation when comparing the 3-channel WDM transmission the effect of XPM is minimal for both NRZ and RZ, which yield almost similar values of the Q-factor as that of the single channel transmission. The

reduced XPM effect, particularly for the NRZ transmission is explained by the high bit-rate of transmission, as the inter-channel XPM effect decreases with increasing bit-rate due to an increase in walk-off as described in [THI'00]. In the case of the RZ transmission, in addition to the walk-off, the rapid pulse broadening leads to a reduction in the induced phase shift, as the slopes of the leading and trailing edges decrease rapidly, together with the pulse peak power. It can thus be explained, that for high bit-rate transmission such as at 40Gbit/s (and higher), the limiting nonlinear distortion occurs for the single channel transmission, where SPM is the limiting nonlinear distortion for the NRZ modulation format and IXPM and IFWM are the sources of the limiting nonlinear distortion in the RZ modulation format.

4.3.2 Experimental investigation of NRZ and RZ signals over SSMF

The results obtained by numerical simulations were then compared with those from the experiments. *Fig 4.13* shows the recirculating fibre loop experimental set-up used for investigating the transmission of NRZ and RZ modulation formats over SSMF. The details of the transmission link are given in section 4.2.3.

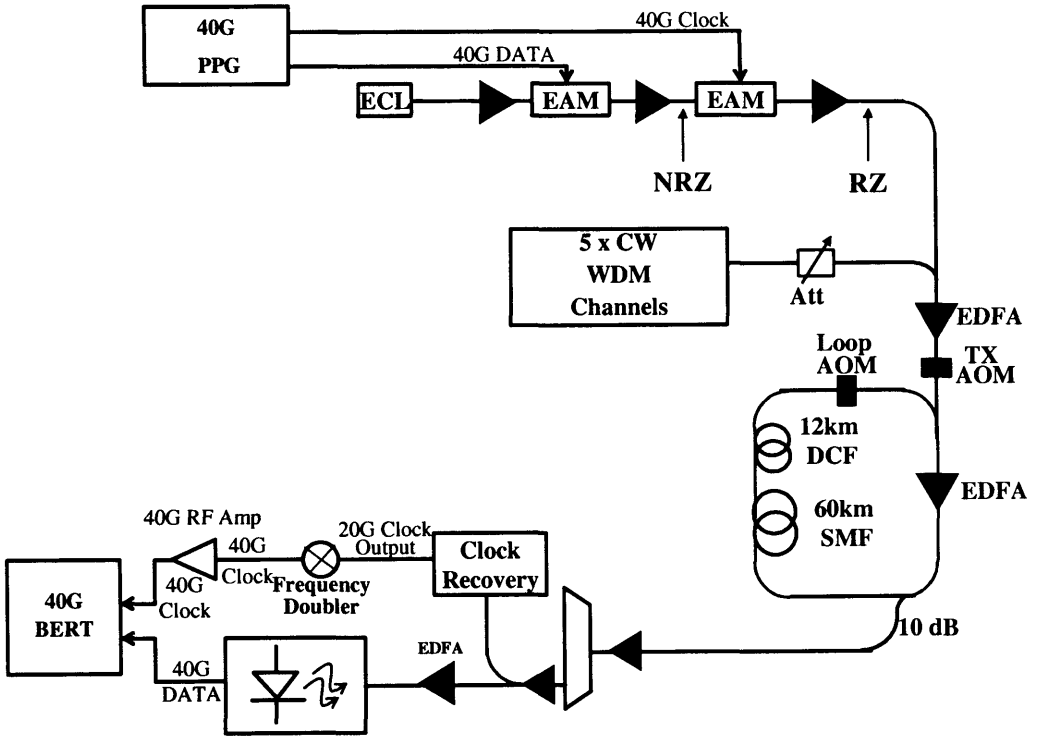

Fig. 4.13 *40Gbit/s transmission of NRZ and RZ modulation formats in a recirculating fibre loop experimental set-up. The amplifier span consisted of 60km SSMF compensated by 12km of DCF.*

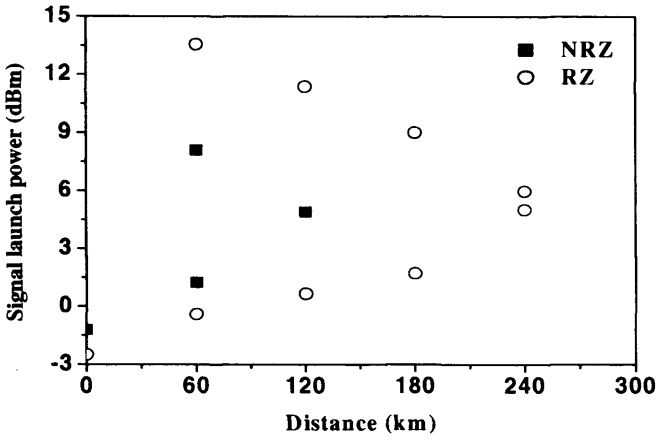

Fig. 4.14 *Launch power range for BER<10^{-9} for transmission over SSMF using NRZ (squares) and RZ (circles) modulation formats*

As described in section 2.8, the maximum and minimum launch powers at a given distance at which a BER<10^{-9} was achieved are plotted in *Fig. 4.14*, giving a good understanding of the nonlinear and noise limitations for each modulation format. The results show that the maximum transmission distance was limited to 120km for NRZ modulation, but increased to 240km when RZ modulation was used at a signal launch power of approximately +5dBm. However, longer transmission distances were achieved by decreasing the signal launch power in the numerical simulations, which was not possible in the experimental investigation. This was because in the numerical simulations, the transmission performance was quantified using an ideal receiver with bandwidth approximately 75GHz (see section 2.9), while the experimental investigation is subject to additional ASE noise from the receiver EDFAs, and the limited bandwidth (~45GHz) of the photo-detector. Taking this penalty into account experimental results are in good agreement with those obtained by numerical simulation, which shows similar achievable transmission distances at a signal launch power of +5dBm in section 4.3.1.

Having validated the numerical simulator against experimental investigation, the following work was focused on whether the power margin between the nonlinear and linear limits at which error-free transmission is achieved could be increased. This is investigated in the following section for transmission over NZDSF, a type of fibre designed for improved nonlinear tolerance at 40Gbit/s.

4.4 Transmission over non-zero dispersion shifted fibre (NZDSF)

The results described in the previous section showed that 40Gbit/s transmission over SSMF reduces the inter-channel nonlinear effects due to the high local dispersion and bit-rate. However, the high local dispersion leads to rapid pulse broadening and gives rise to intra-channel nonlinear distortion between overlapping pulses within the same wavelength channel, and was found to be one of the dominant sources of penalty for RZ transmission at 40Gbit/s. One way to minimise the pulse overlap is to reduce the local dispersion of the transmission fibre. Dispersion-shifted-fibres with 0ps/(nm.km) local dispersion are not suitable for minimising pulse overlap, as it reduces the inter-channel XPM walk-off, and also increases the FWM as described in chapter 3. Hence, NZDSF, with values of fibre local dispersion significantly lower than that of SSMF were investigated [ESS'99, KAM'01, MUR'00b]. In addition to the reduced fibre local dispersion, NZDSF was also developed with large effective areas at the core of the fibre to further reduce nonlinear behaviour [LIU'95, TSU'00]. These benefits are further investigated in this work, where the NZDSF had a fibre local dispersion D = *4ps/(nm.km)* and consisted of a large effective area of approximately 70μm^2 (also see appendix 1).

The NZDSF transmission link investigated in these experiments employed a higher-order-mode dispersion compensator, also known as a dispersion management device (HOM-DMD) [POO'94, GNA'00]. The HOM-DMD was capable of dispersion and dispersion slope compensation of 75km of NZDSF. Such dispersion compensators allow a higher signal launch power into it, as the fibre effective area is much larger than that of DCF (by a factor of ~4-5). As described in section 2.3.2 and 2.4.2, this feature enables the fibre to be designed with large negative dispersion. Hence, shorter lengths of fibre are required for dispersion compensation leading to a lower overall loss in the amplifier span. In commercial systems compensated by conventional DCF, the DCF is usually placed between amplifier stages to reduce the span loss or at the end of the span to minimise nonlinear distortion (see section 2.7). However, as the effective area of the HOM-DMD is comparable to that of the large effective area NZDSF, it was possible to investigate pre-compensated amplifier spans where the

dispersion compensator was placed directly at the output of the amplifier in the amplifier span *(Fig 4.15)*.

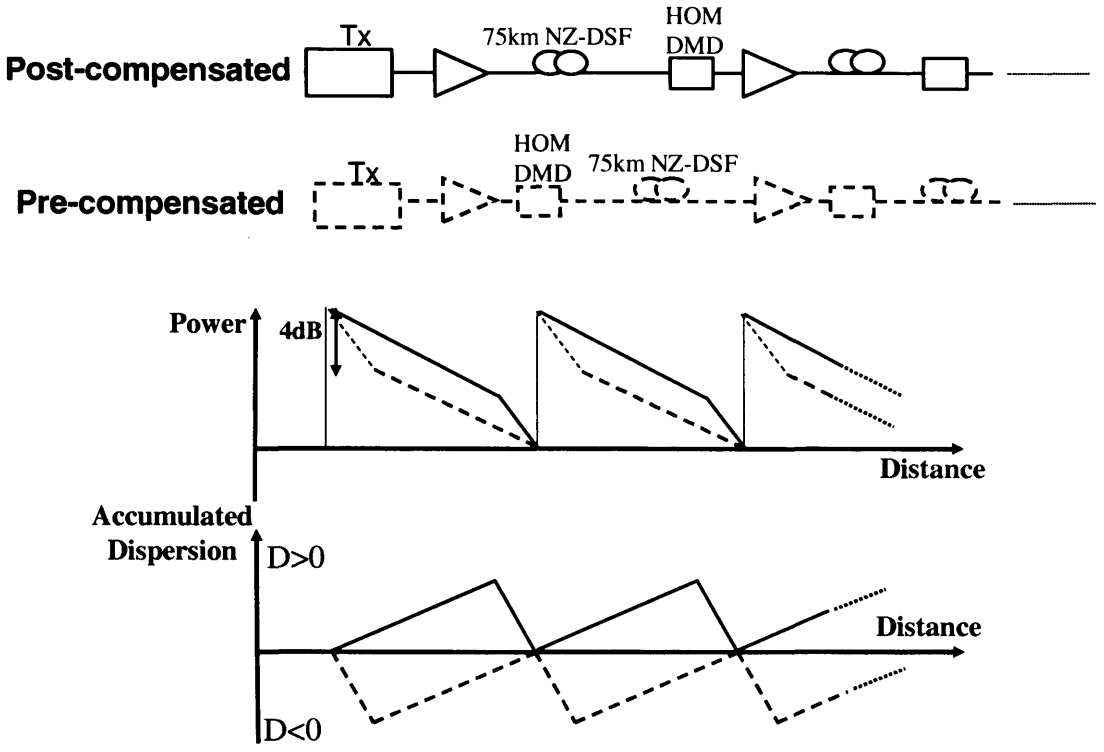

Fig. 4.15 *Dispersion map and power profile for transmission in NZDSF compensated by a HOM-DMD for in-line post- and pre-compensated amplifier spans.*

The amplifier spans illustrated in *Fig. 4.15* were investigated for optimum transmission performance, in terms of nonlinear and noise limitations. It should be noted that placing the HOM-DMD at the output of the EDFA in every span (in-line pre-compensation) is unique, and is not deployable with conventional DCF owing to the high nonlinear coefficient and loss in DCF.

4.4.1 NRZ transmission over NZDSF

In section 4.3 it was found that NRZ modulation format was limited by SPM for transmission over SSMF and, therefore, considered unsuitable for 40Gbit/s transmission. However, as NZDSF consists of a large effective area, the SPM distortion will be reduced. Furthermore, for in-line pre-compensated amplifier spans the attenuation in the HOM-DMD will reduce the nonlinear behaviour in the NZDSF further decreasing the SPM. It was, therefore, important to investigate the transmission performance of the NRZ modulation format over the NZDSF amplifier spans described in *Fig. 4.15*.

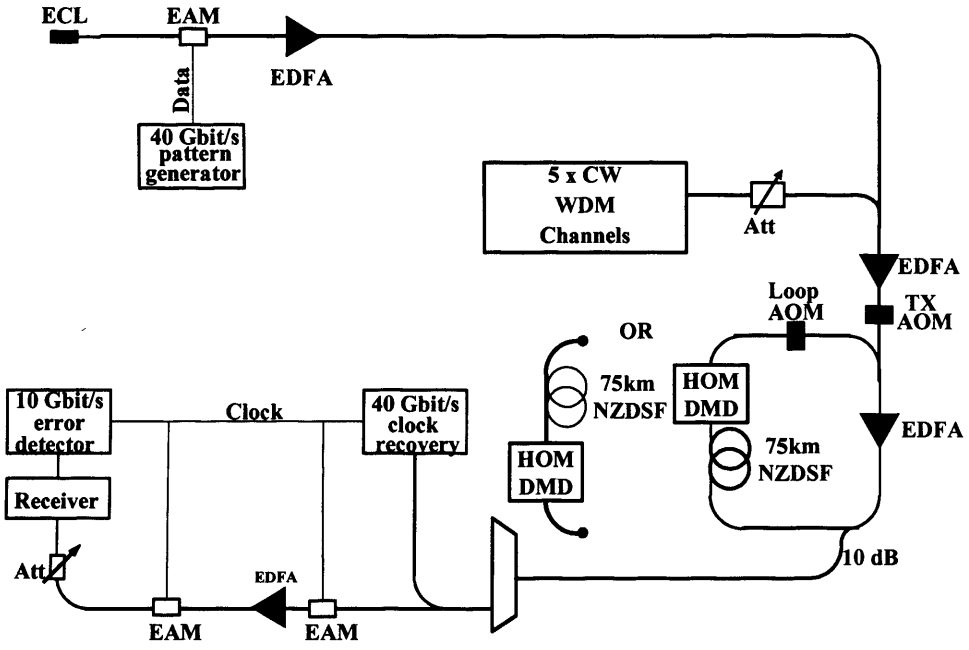

Fig. 4.16 *40Gbit/s ETDM transmission in experiments with NZDSF and HOM-DMD amplifier spans*

The experimental set-up for the investigation of the NRZ modulation format in a transmission link consisting of in-line pre- and post-compensated amplifier spans is shown in *Fig. 4.16*. The NRZ signal was generated using a 40Gbit/s PPG, but as BER measurements were performed at 10Gbit/s, it was necessary to de-multiplex the incoming 40Gbit/s down to 10Gbit/s at the receiver. This was achieved using the optical de-multiplexer, as described in section 4.2.4 *(Fig. 4.6)*.

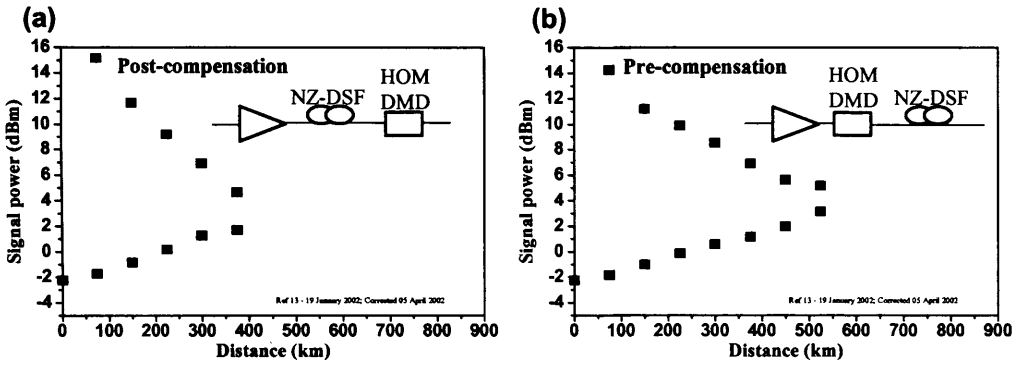

Fig. 4.17 *Launch power range for BER<10^{-9} for NRZ transmission over NZDSF with in-line (a) post-compensated (b) pre-compensated amplifier spans*

The maximum and minimum launch powers at which a BER<10^{-9} was achieved for a given transmission distance were measured as described in section 2.8.5, and are shown in *Fig. 4.17*. It can be seen that a maximum achievable transmission distance of 375km for in-line post-compensated amplifier spans and 525km for in-line pre-compensated amplifier spans can be obtained. This is a 40% improvement in transmission distance for in-line pre-compensated amplifier spans, and leads to two main conclusions. Firstly, a transmission distance of over 500km, shows that NRZ transmission can be used for metro and long-haul transmission at 40Gbit/s. Secondly, the longer transmission distance of 525km was achieved using the in-line pre-compensated amplifier spans, a dispersion scheme not practical with DCF because of the small effective area and higher nonlinearities associated with such fibre types. The superior transmission performance obtained when using in-line pre-compensated amplifier spans is explained by the reduced nonlinear interaction in the NZDSF, where the signal power is decreased by the attenuation in the HOM-DMD (which behaves virtually linearly), compared to that in post-compensated amplifier spans. This method of launching high powered signals into the HOM-DMD has also been used to increase the OSNR and extend the transmission distance in a 40Gbit/s transmission link [RAM'01]. The eye diagrams show characteristic distortion due to SPM such as pulse broadening and amplitude distortion, which are the limiting impairments in this case *(Fig 4.18)*. Therefore, the placement of the DMD directly at the output of the amplifier resulted in the signal power attenuated by 4dB (the loss of

the device) prior to propagation in the nonlinear NZDSF, as was the case for the post-compensated scheme, thereby leading to less SPM and a longer transmission distance. Analysis of the BER limitation showed that both compensation schemes had similar minimum launch powers for which BER<10^{-9} was achieved. This indicated that the linear propagation was not affected by the dispersion compensation scheme, and the noise contribution was similar for both in-line pre- and post-compensated amplifier spans.

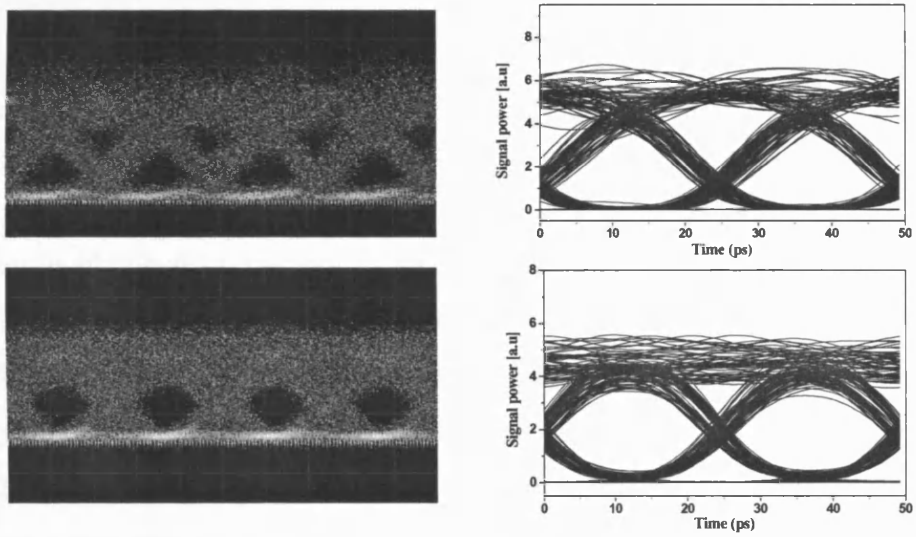

Fig. 4.18 *Experimental and simulated eye diagram for an average launch power of +4.5dBm at distance 375km. Top: pre-compensated, Bottom: post-compensated*

The experimental results obtained were then compared to that obtained by numerical simulation in order to further validate the results. The numerical simulations calculated the Q-factor as a function of the transmission distance *(Fig. 4.19)*. The transmission link consisted of amplifier spans with 75km NZDSF (parameters given in Appendix 1), 100% compensated by the HOM-DMD. As mentioned earlier, the HOM-DMD behaves linearly at high power owing to its large effective area and length of less than 1km, and was thus described in the simulator as a linear device. The simulations investigated transmission for in-line post- and pre-compensated amplifier spans, and the results are plotted in *Fig. 4.19*.

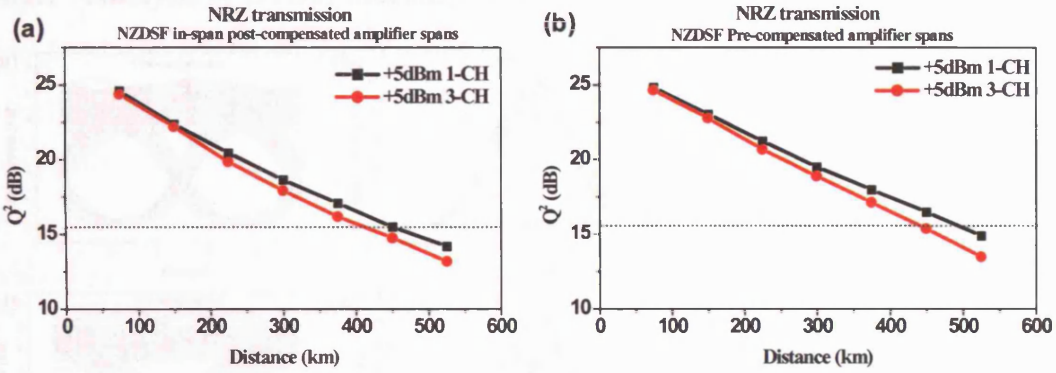

Fig. 4.19 *Calculated Q-factors for NRZ transmission over NZDSF link with* ***(a):*** *in-line post-compensated* ***(b):*** *in-line pre-compensated amplifier spans by numerical simulation. A wavelength spacing of 0.8nm (100GHz) was used in the simulation of the 3-channel WDM transmission*

The results obtained by numerical simulation of the NRZ transmission over NZDSF amplifier spans are plotted in *Fig. 4.19*, and show a maximum transmission distance of 450km for both in-line post- and pre-compensated amplifier spans. However, the calculated Q-factor was approximately 1dB higher for in-line pre-compensated amplifier spans. This was similar to that obtained experimentally, although, the maximum transmission distances achieved were 375km and 525km for in-line post- and pre-compensated amplifier spans respectively. As the signal distortion of the simulated signal is similar to that of the experimental results as seen in the comparative eye diagrams of *Fig 4.18*, this discrepancy was attributed to the fact that the experimental system which employed optical de-multiplexing at the receiver performed 2-R regeneration (re-shaped and re-amplified) on the received signal. The OTDM de-multiplexer was not included in the numerical simulations, where Q factor calculations were performed on the received 40Gbit/s optical signal. Analysis of the eye-diagrams in *Fig. 4.18* suggests the in-line pre-compensated scheme, leads to a received signal shape more suited to 2-R regeneration, hence, the discrepancy between transmission distances obtained experimentally and by numerical simulation. This regeneration effect in the OTDM de-multiplexer required further investigation and is discussed in the next section.

4.4.1.1 Analysis of OTDM demultiplexer

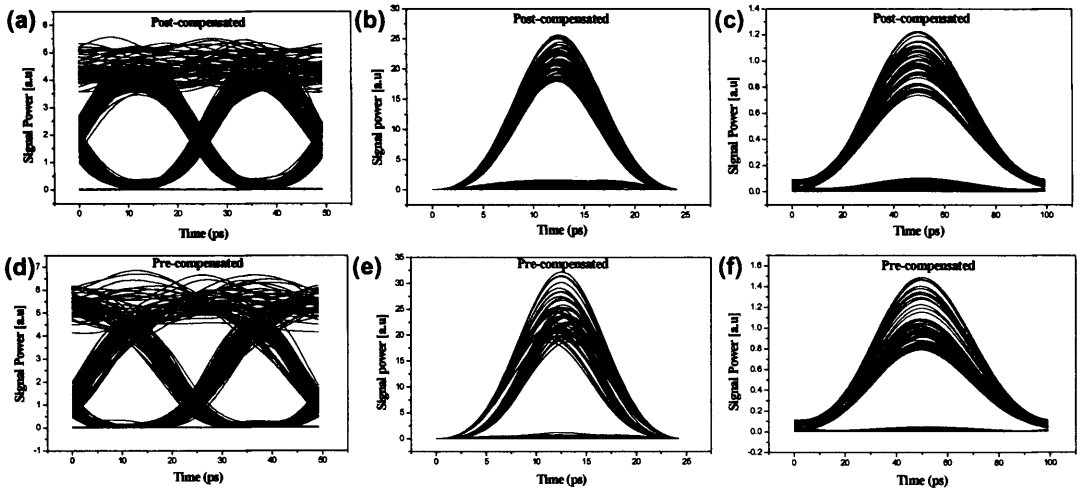

Fig 4.20 *NRZ transmission in NZDSF link* ***Top:*** *post-compensated,* ***Bottom:*** *pre-compensated* ***Left:*** *After 450km transmission* ***Centre:*** *transmitted signal (450km) optically demultiplexed* ***Right:*** *Optically demultiplexed signal after 8GHz electrically filtering (10Gbit/s receiver)*

The eye diagrams obtained by numerical simulation of the NRZ modulation format in a transmission link consisting of in-line post- and pre-compensated amplifier spans are shown in *Fig 4.20.* The regenerative effect of the optical demultiplexer can be explained by analysis of the optical eye after optical de-multiplexing and the eye-detected on the 10Gbit/s receiver. When optical demultiplexing is employed, the NRZ signal is converted to RZ by the switching window of the de-multiplexer. As the switching window occurs periodically, synchronised to the recovered clock, the timing jitter of the signal that lies outside the switching window of the demultiplexer is suppressed, and the signal re-amplified by the EDFAs in the optical de-multiplexer set-up (see *Fig. 4.6*). These two effects induced by the optical demultiplexer can be analysed as re-shaping and re-amplification to give 2-R regeneration. The resultant signal out of the optical demultiplexer is a 10Gbit/s signal with a pulse width defined by the switching window. In the case of the experiments and simulations this was fixed at 11.5ps *(Fig 4.20(b),(d))*. The demultiplexed signal was then fed into the 10Gbit/s receiver which consists of an 8GHz electrical filter, typical in 10Gbit/s receivers for NRZ IM-DD. This filtering caused the pulse to broaden over the 100ps bit-slot available for a 10Gbit/s signal *(Fig 4.20(c),(f))* and also eliminated any high-frequency noise components.

The simulated eye diagrams in *Fig 4.20(a),(d),* show the received NRZ signal at a transmission distance of 450km before optical-time-division-demultiplexing. The cross point between adjacent pulses in the eye diagram is lower for transmission in the pre-compensated scheme *(Fig 4.20(d))*. This similarity to an RZ signal leads to reduced ISI between adjacent bit slots, thus making the signal better suited to optical-time-division-demultiplexing. This is clearly visible in the demultiplexed eye-diagram of the in-line post-compensated amplifier spans *(Fig 4.20(b)),* where there is significantly more power visible in the 'zero' level compared to that of the in-line pre-compensated case *(Fig 4.20(e))*. This remains even after the 8GHz electrical filtering in the 10Gbit/s receiver. This demultiplexer and receiver behaviour, along with the than 1dB margin for error-free transmission (Q=15.56dB at 450km in *Fig.4.19*), explains the reduction in maximum transmission distance by one amplifier span, as obtained experimentally.

The steeper rising and falling edges of the pulses, present in in-line pre-compensation lead to the timing jitter conversion to amplitude jitter when switched by the optical-time-division-demultiplexer [WAN'01,HOL'02]. However, the presence of the 8GHz electrical filter in the 10Gbit/s receiver caused the power to be dispersed about the 100ps bit-slot and minimises the amplitude jitter about the centre of the eye *(Fig 4.20(d),(f))* thereby resulting in an improved BER/Q factor. This was seen experimentally by the increase in transmission distance by one extra span.

4.4.2 NRZ WDM transmission over NZDSF

The WDM transmission over NZDSF differs from the transmission in SSMF as the XPM penalty is 1dB higher (as shown in *Fig 4.10* and *Fig 4.19*). In the presence of inter-channel nonlinearities, the high dispersion of the SSMF gives rise to a higher walk-off *($d=D.\Delta\lambda$),* dependent on the dispersion parameter D and channel spacing $\Delta\lambda$. The channel spacing $\Delta\lambda$ is constant (0.8nm, 100GHz) for transmission in both fibre types and indicates a time-dependant channel alignment owing to the different group velocities of each channel. This, in turn, leads to the interfering channels inducing both positive and negative chirp on the detected signal channel, averaging out the

nonlinear interaction between the channels. In the case of NZDSF the induced XPM is higher than that in SSMF as the walk-off is lower because of the lower dispersion D in the fibre. However, as the inter-channel nonlinear penalty is less than 2dB, inter-channel nonlinear effects can be ignored in the design of such transmission systems, where the single channel effects dominate the signal distortion.

4.4.3 RZ transmission over NZDSF

While SPM was still clearly the limiting nonlinear distortion for NRZ signal it was shown that it can be mitigated by in-line dispersion and power management using NZDSF and HOM-DMD compensated amplifier spans. The reduced fibre dispersion and in-line dispersion management of NZDSF amplifier spans was, therefore, investigated for the suppression of intra-channel nonlinear effects which were found to limit the propagation of RZ signals over SSMF. The experimental set-up shown in *Fig. 4.21* was similar to that shown in *Fig 4.13* with the ETDM NRZ transmitter replaced by the RZ OTDM transmitter in order to investigate the in-line post- and pre-compensated amplifier spans of the NZDSF link for RZ transmission.

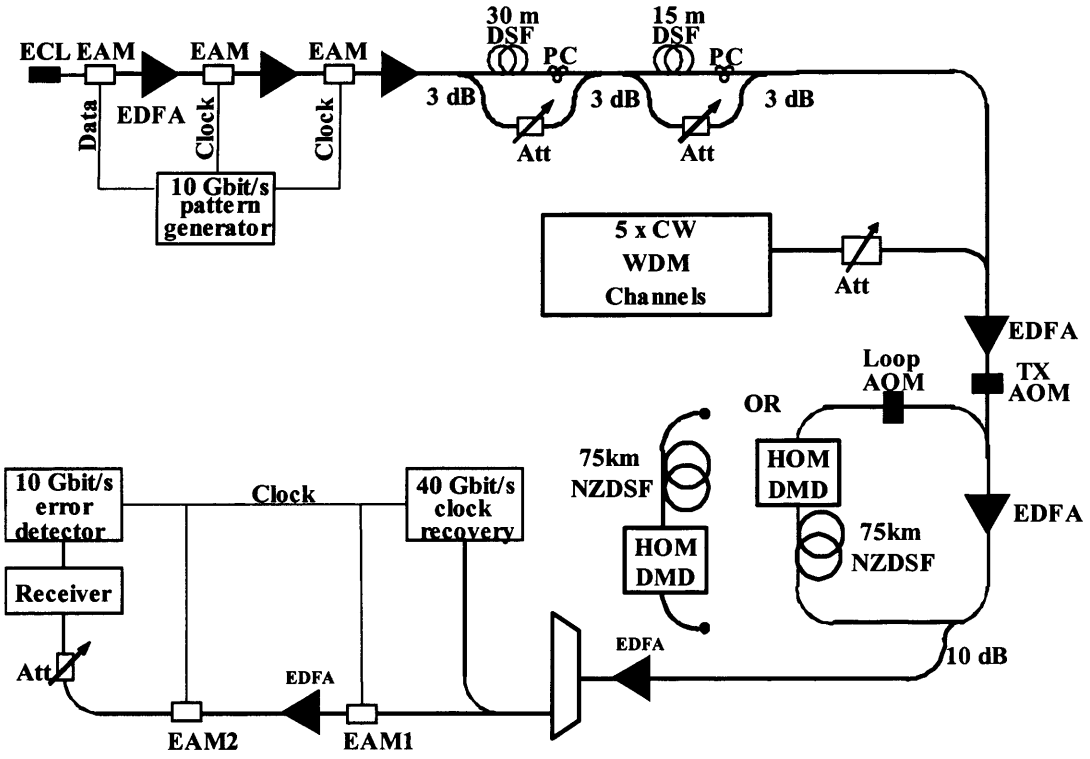

Fig 4.21 *40Gbit/s RZ OTDM transmission over NZDSF compensated by a HOM-DMD*

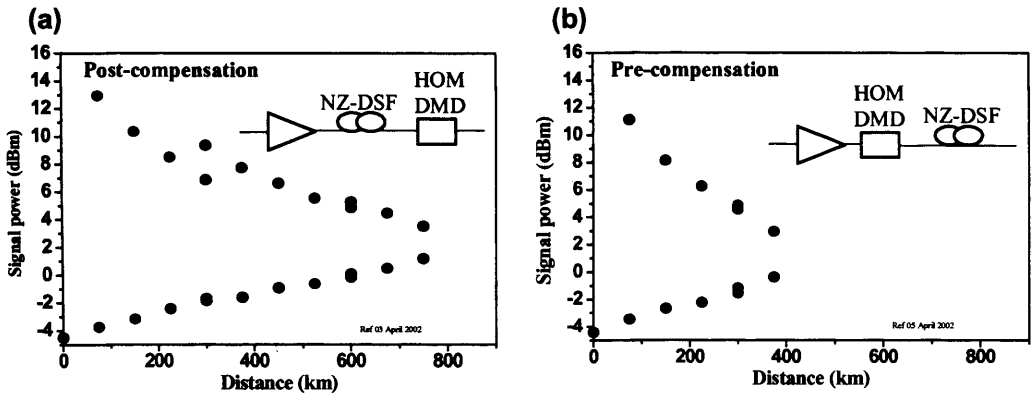

Fig. 4.22 *Launch power range for BER<10^{-9} for RZ transmission over NZDSF in a (a) post-compensated (b) pre-compensated link*

As before, the signal launch power was varied at increasing transmission distances whilst a BER<10^{-9} was still achievable, and the results of RZ transmission over in-line post- and pre-compensated amplifier spans are shown in *Fig. 4.22*. From *Fig 4.22* it is clearly seen that, unlike for NRZ signals the maximum transmission distance was achieved for in-line post-compensated amplifier spans. As the same optical demultiplexing process was employed for both RZ and NRZ transmission, the receiver penalties were similar for both cases. However, the noise limited values are 2dB lower than that for NRZ transmission, as a result of the higher peak power of the RZ pulses for a given average signal power. This is in good agreement with the theory in section 2.5.1. The two data points for power limits at four and eight spans are the result of the addition of 10ps/nm and 20ps/nm dispersion compensation at the receiver respectively, to compensate for the -1.4ps/nm residual dispersion of each span. This was not required in the NRZ investigation owing to the dispersion-tolerant nature of NRZ [PEC'03]. Whilst the linear limit is similar for both the pre- and post-compensated schemes, the nonlinear limit was approximately 2dB lower for the in-line pre-compensated case. The slope of the nonlinear limit indicates the penalty in dBs due to nonlinear distortions per kilometre. As the pre-compensated scheme exhibited a steeper slope of 0.03dB/km compared to a slope of 0.01dB/km for the post-compensated scheme in the nonlinear limit, the results clearly show the strong enhancement of intra-channel nonlinear interactions in the pre-compensated amplifier span. The maximum achievable distance at BER<10^{-9}, was only 375km, compared to

750km for the post-compensated scheme. This is because for propagation in in-line pre-compensated amplifier spans the pulse width at the output of the HOM-DMD, launched into the NZDSF given by equation (2.12a) in the theory, shows that a single pulse was broadened to nearly 90ps FWHM. This resulted in a pulse overlap of over 6 adjacent bit slots. Such pulse overlap increased the nonlinear interaction between adjacent bits leading amplitude jitter and IFWM shadow pulses, which are clearly visible in eye diagrams obtained from the numerical simulations *(Fig 4.23)*. This confirmed that even when the signal power is 4dB lower when launched into the NZDSF, the pulse overlap caused by the dispersed pulses at the output of the DMD lead to much stronger intra-channel nonlinear interaction, making in-line pre-compensation unsuitable for RZ transmission.

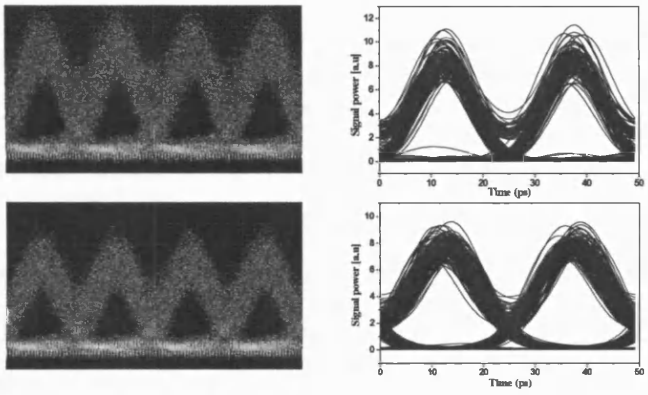

Fig 4.23 *Experimental and simulated eye diagram for an average launch power of +5dBm at distance 375km. Top: pre-compensated, Bottom: post-compensated*

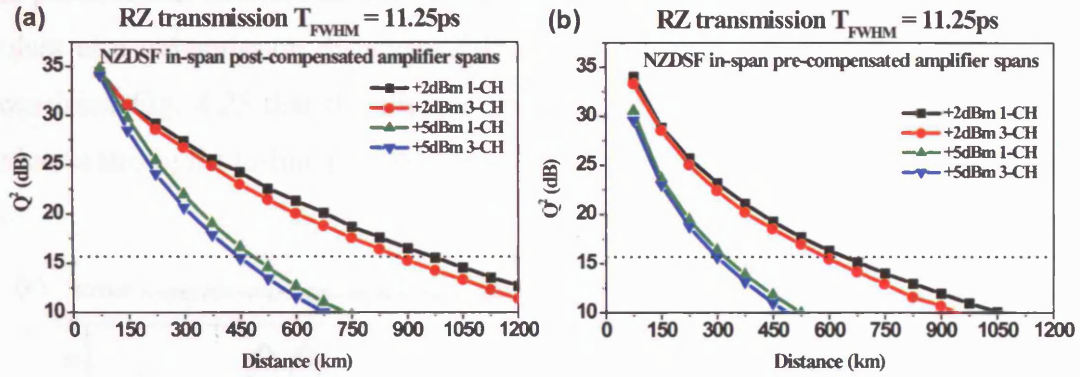

Fig. 4.24 *Calculated Q-factors for RZ transmission over NZDSF link with* ***(a):*** *in-line post-compensated* ***(b):*** *in-line pre-compensated amplifier spans by numerical simulation. Channel spacing of 100GHz (0.8nm) was used in the 3-channel WDM transmission*

The numerical simulation results in *Fig 4.24,* shows the Q-factor as a function of the transmission distance, for RZ transmission over NZDSF employing pre- and post-compensated amplifier spans, as described previously. The experimental results in *Fig 4.22* show good agreement with those obtained by simulation, where the maximum transmission distance was also achieved for transmission over post-compensated amplifier spans. The Q-factor results at signal launch power of +2dBm shows reduced Q-factor degradation with increasing transmission distance in the post-compensated transmission, compared to that seen for pre-compensated transmission. This effect can be explained by the linear and nonlinear nature of the HOM-DMD and transmission fibre respectively. For post-compensated transmission, the pulses disperse more slowly than in the case of pre-compensated transmission, thereby decreasing the intra-channel nonlinear interactions. In the pre-compensated transmission, the pulses disperse rapidly and overlap, hence the IFWM nonlinear distortion dominates when the signal propagates through the nonlinear NZDSF.

To confirm that nonlinear distortion is dominated by IFWM in in-line pre-compensated amplifier spans, the nonlinearity was analysed using the perturbation analysis and split-step-Fourier (SSF) numerical simulations, described in section 2.6.1. *Fig. 4.25* plots the signal distortion for two consecutive pulses A_1 and A_2 using

the perturbation analysis as well as the split-step-Fourier simulation for the same two pulses at a transmission distance of 450km at a launch power of +5dBm. It can be seen from *Fig. 4.25* that the shadow pulses emerging in the 3rd and 6th bit-slots are twice as strong for in-line pre-compensation compared to in-line post-compensation.

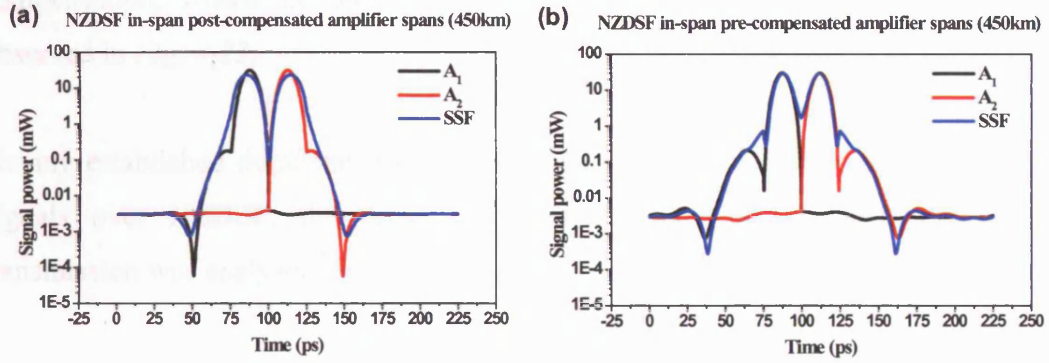

Fig. 4.25 *40Gbit/s signal waveform of two pulses A_1 and A_2 in the 4th and 5th bit-slot after transmission over 450km NZDSF using (a) in-line post-compensated (b) in-line pre-compensated amplifier spans at a launch power of +5dBm at the output of line amplifiers, showing the generated shadow pulses at in the 3rd and 6th bit-slot.*

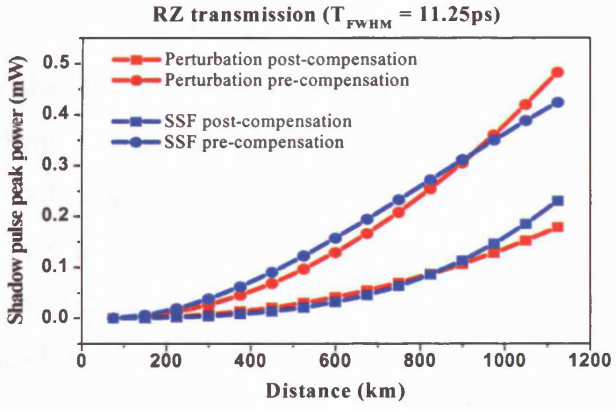

Fig. 4.26 *Growth of shadow pulse power for transmission over NZDSF with in-line post- and pre- compensated amplifier spans for comparison of perturbation theory with results using split-step-Fourier (SSF) analysis at a signal launch power of +5dBm*

Fig. 4.26 shows the shadow pulse powers as a function of transmission distance for a signal launch power of +5dBm. Although the loss of the HOM-DMD reduces the signal launch power into the nonlinear NZDSF, the power of the shadow pulses reaches 0.4mW for in-line pre-compensation, compared with only 0.2mW with in-line post-compensation. The effect of IFWM was negligible in the case of in-line post-compensation, where the main distorting effect is timing jitter due to IXPM as observed in *Fig. 4.23*.

Having established dominant nonlinear effect for single channel transmission of RZ signals over NZDSF, the impact of inter-channel signal distortion in WDM transmission was analysed next.

4.4.4 3-channel WDM transmission of RZ modulated signals over NZDSF

From the previous experiments it is clear that optimum transmission performance is achieved using the RZ modulation format over the NZDSF link with in-line post-compensated amplifier spans. As most commercial systems employ WDM transmission to further increase the overall transmission capacity, it was important to study the inter-channel signal distortion of the RZ modulation format over the same link.

The effect of inter-channel nonlinear distortion was first investigated by numerical simulation for 3-channel WDM transmission with channel spacing of 100GHz at launch powers of +2dBm and +5dBm average power (see *Fig. 4.24*). *Fig.4.24* plots the calculated Q-factor as a function of transmission distance and it can be seen that the penalty due to WDM transmission over the optimum in-line post-compensated link was approximately 1dB higher than that for transmission over SSMF. This was due to the lower local dispersion of the NZDSF reducing the walk-off effect thereby increasing the XPM effect. In the case of in-line pre-compensated amplifier spans, the high dispersion of the HOM-DMD at the beginning of the span leads to a reduction in the peak power and slope of the leading and trailing edges, hence decreasing the XPM. Even though the original pulse shape is achieved towards the end of the amplifier span, the signal attenuation ensures the XPM is minimal in this case.

The experimental set-up shown in *Fig. 4.27* was used to investigate a 3-channel WDM transmission system over NZDSF. The 3 channels were co-polarised. Channels 1 and 3 were decorrelated from channel 2 with ~30m of DSF. Hence, while the adjacent signal channels were decorrelated, channels 1 and 3 were correlated in time and induced the maximum nonlinear phase shift on channel 2, the detected signal. The measured system degradation is thus, highly conservative, justifying the minimum 3-channel transmission for investigation of the inter-channel signal distortion.

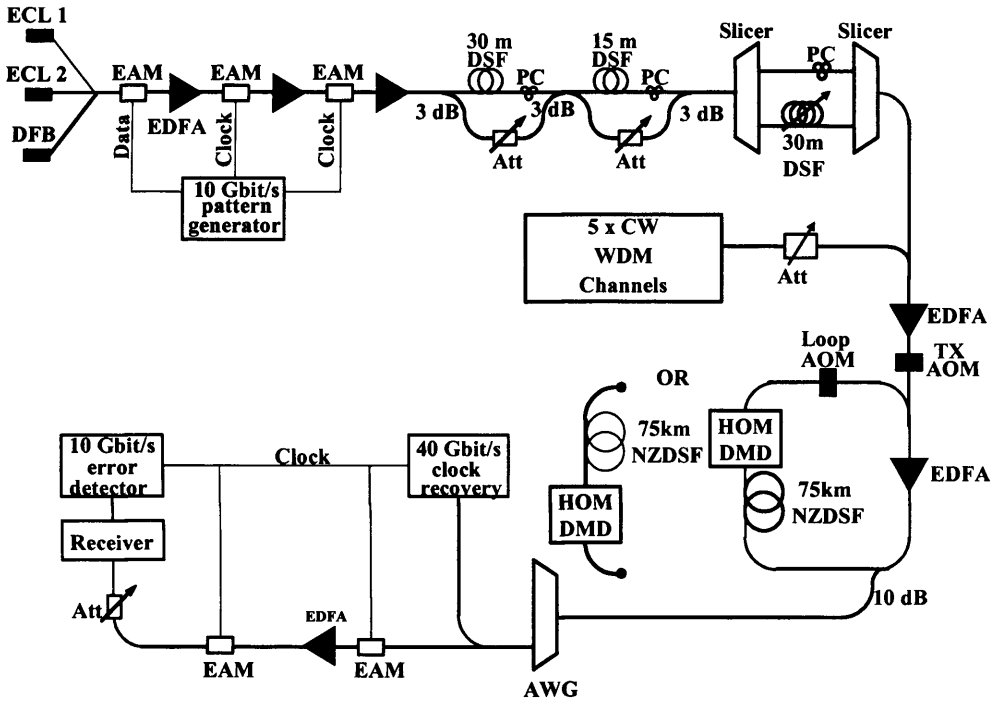

Fig. 4.27 *3-channel WDM transmission with 100GHz channel spacing for transmission over NZDSF link*

Fig. 4.28(a) shows the experimentally obtained channel power margins required to achieve BER<10^{-9} for transmission distances up to 750km for single and 3-channel transmission, with in-line post-compensated amplifier spans. At transmission distances up to 150km, the difference in the maximum signal launch power was less than 0.6dB between single and 3-channel transmission, indicating the linear crosstalk between the channels was insignificant. This confirmed that despite the broad spectrum of the RZ modulation format, 100GHz channel spacing between WDM channels is still achievable, with no additional penalty in spectral efficiency or in-complete de-multiplexing in the AWG. However, the effect of nonlinear interactions

between pulses in the neighbouring WDM channels resulted in a reduction of the maximum launch power at longer distances, giving a reduction in the launch power range from 5.5dB for a single (-0.2 to +5.3dBm) to 2.2dB for 3-channels (+1 to 3.2dBm) after 600km. This indicated the penalty due to inter-channel nonlinear effects accumulates and becomes significant with increasing transmission distances over 225km. This nonlinear behaviour was also observed in the results obtained by numerical simulation in *Fig. 4.24*.

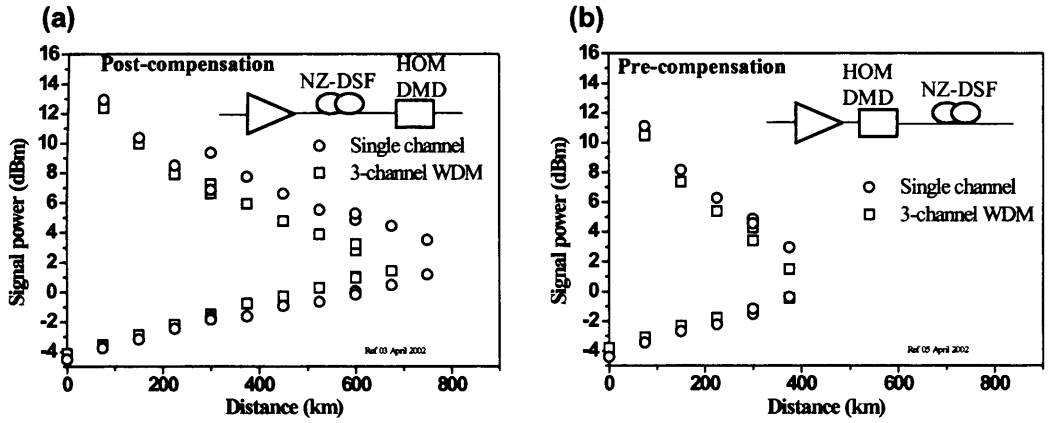

Fig. 4.28 *Launch power range for BER<10^{-9} for 3-channel WDM RZ transmission over NZDSF in a transmission link with (a) post-compensated (b) pre-compensated amplifier spans*

The nonlinear behaviour is different for transmission in in-line pre-compensated amplifier spans and the limiting distortions occur due to intra-channel nonlinear effects arising due to highly dispersed pulses being launched into the nonlinear fibre. Hence, the single and 3-channel transmission is affected in a similar manner with the inter-channel nonlinear effects being negligible compared to that of the intra-channel nonlinearities. This is confirmed by the results shown in *Fig 4.28(b)*, where the limiting signal launch power is almost identical for both single and 3-channel transmission.

The numerically simulated 3-channel WDM transmission in *Fig. 4.24* also shows that the inter-channel XPM increases with distance for WDM transmission in the post-compensated amplifier span. This is confirmed by the increasing difference ΔQ between the single-channel and WDM transmission in *Fig 4.28(a)*. For pre-

compensated amplifier spans however ΔQ is almost constant as the single-channel transmission can be likened to that of 'quasi linear' transmission as the pulses are highly dispersed at the beginning of the amplifier span, thus suppressing the XPM [HAY'97].

The results described for the 3-channel WDM transmission, enabled detailed investigation of the inter-channel nonlinear distortion for the different dispersion maps employing the HOM-DMD for dispersion compensation. Practical systems however, employ a large number of WDM channels over a broad bandwidth, which lead to other design considerations, such as maintaining good OSNR and simultaneous dispersion compensation. These effects are therefore investigated in the experimental analysis of a 10-channel WDM transmission, described in the next section.

4.4.5 10-channel WDM transmission of RZ signals over NZDSF

While the RZ modulation format shows good transmission performance compared to NRZ at 40Gbit/s, the large modulation bandwidth makes it less tolerant to incomplete dispersion compensation, which leads to inter-symbol-interference. This raises a significant challenge in the design of long-haul, wideband, high-speed WDM transmission systems. Owing to the dispersion slope property of the fibre, the total dispersion requiring compensation varies significantly over the WDM bandwidth. One technique, trimming the dispersion on a channel-by-channel basis at the transmitter or receiver is effective, but requires additional components and has the disadvantage that the in-line compensation is not optimised for all WDM channels, leading to pulse broadening during propagation and increase in intra-channel nonlinearities, as the pulse overlap increases at the input of every amplifier span. For these reasons, the use of the second- and third-order dispersion compensating device such as the HOM-DMD fibre compensator is an attractive option, and is therefore investigated for simultaneous dispersion compensation of 10 WDM channels, with 100GHz channel spacing over the wavelength region from 1543.5nm-1551.5nm. The dispersion and dispersion slope of 75km NZDSF and the HOM-DMD are shown, individually and for the combined case in *Fig. 4.29*.

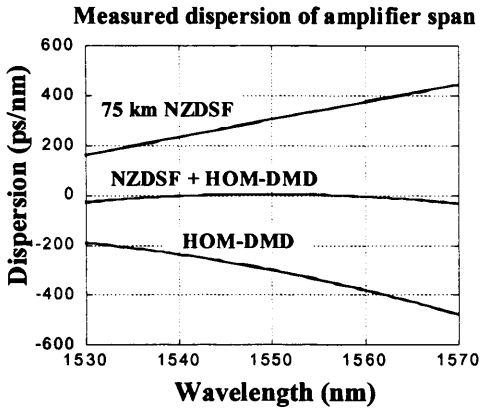

Fig. 4.29 *Dispersion profile for 75km NZDSF and the HOM-DMD. The cascaded link shows residual dispersion close to zero between 1540nm-1560nm indicating good slope compensations*

The experimental set-up for 3-channel WDM transmission shown in *Fig. 4.27* was modified to incorporate 10 WDM channels as shown in *Fig 4.30.* A single modulator was used for data encoding at 10Gbit/s (NRZ), hence, it was necessary to implement pulse shaping by the third EAM after splitting the odd and even channels. This eliminated noise by spectral filtering in the slicer and enabled the individual channel power to be increased by 3dB without damaging the modulator. The OSNR of the signal launched into the recirculating loop was measured to be approximately 20dB, and was significantly less than that obtained in the 3-channel WDM experiment, as the side mode suppression of the DFBs had an extinction ratio in the range of 37-42 dB [MIK'03]. Hence, it was necessary to have a signal launch power of +5dBm to obtain a good OSNR (see section 2.8.1) even though the previous results in section 4.5.3 indicated +3dBm as the optimum channel power. Adjacent WDM channels were orthogonally polarised as described in section 2.7 and in [ZHU'02, FRI'02b].

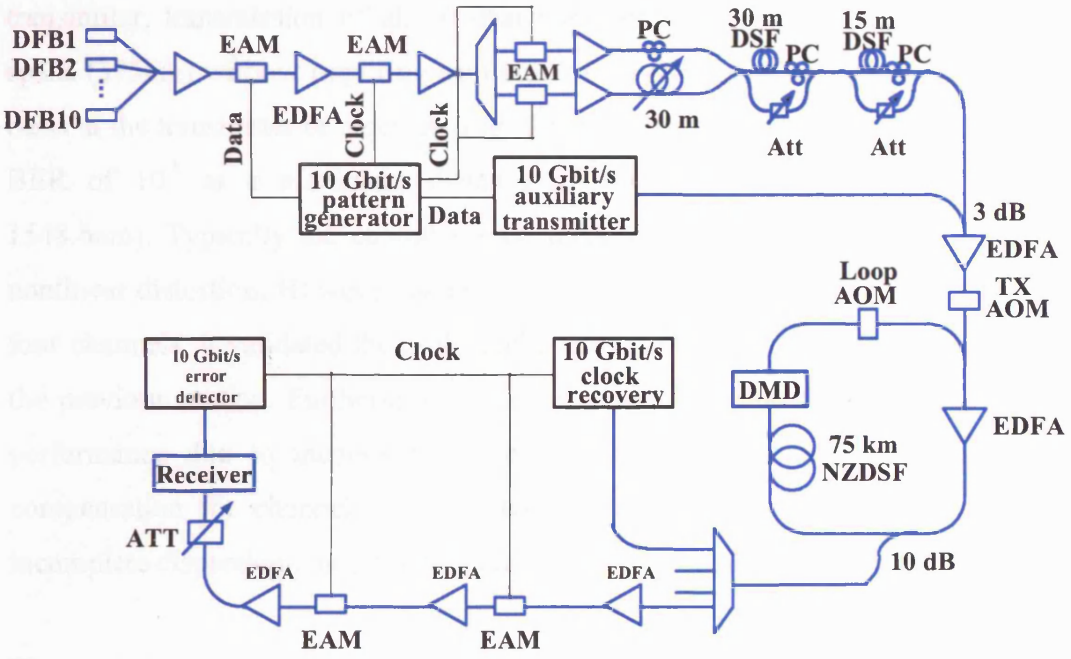

Fig. 4.30 *Simultaneous dispersion slope compensation of HOM-DMD for 10-channel WDM transmission with 100GHz channel spacing*

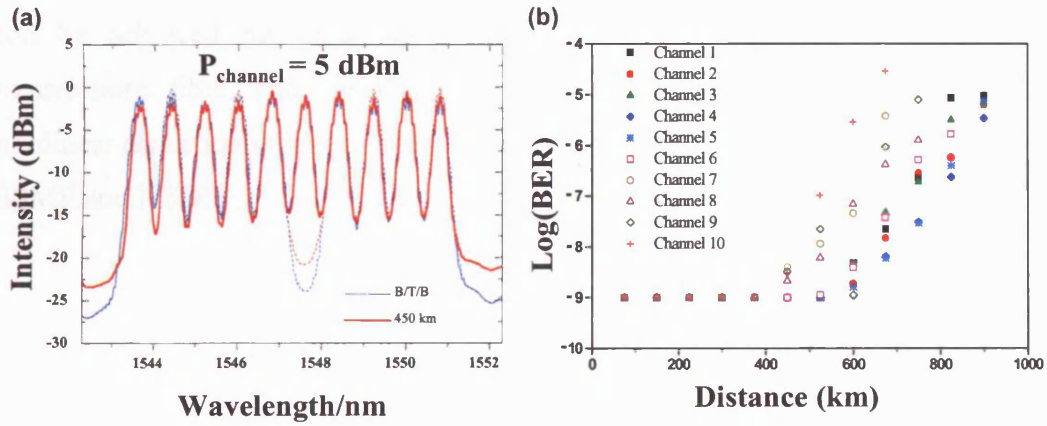

Fig. 4.31 ***(a)*** *Spectrum for back-to-back and 245km transmission showing decrease in OSNR,* ***(b):*** *Transmission distance at BER<10^{-9}* ***Note:*** *The BER at distances less than 375km was in fact much less than 10^{-9} indicated and should not be mistaken for an error floor (Fig. (b))*

The signal spectra measured back-to-back, and after 450 km are plotted in *Fig. 4.31(a)*. Although the WDM transmitter used in the experiment had a low OSNR of 21 dB (measured with a 0.5 nm bandwidth), due to the use of a 1:16 coupler in the

transmitter, transmission of all 10 channels with BER < 10^{-9} was possible over 5 spans (375km) without requiring trimming of the dispersion on a channel-by-channel basis at the transmitter or receiver *(Fig. 4.31(b))*. It was, however, possible to achieve BER of 10^{-9} at a maximum distance of 600km for channels 3-7 (1545.4nm-1548.6nm). Typically the central wavelengths are most susceptible to inter-channel nonlinear distortion. However, as optimum performance was obtained for the central four channels, it validated the 3-channel results for inter-channel nonlinear effects in the previous section. Furthermore, these results also explain the reduction in system performance due to incomplete dispersion compensation due to non-ideal slope compensation for channels at the edge of the WDM bandwidth. The effects of incomplete dispersion compensation are further investigated in chapter 6.

The transmission links investigated thus far consisted of transmission fibre compensated by a dispersion compensation element within each amplifier span. It was shown that intra-channel nonlinear distortion is a dominant source of penalty, particularly for the RZ modulation format, where pulses overlap due to the fibre dispersion. While NZDSF was a good alternative to minimising the pulse overlap, further control of pulse broadening within the nonlinear length of each amplifier span can be achieved by launching pre-dispersed pulses at the transmitter into the transmission fibre. The use of pre-dispersion to minimise the overall intra-channel nonlinear distortion is investigated in the following section for transmission over both SSMF and NZDSF.

4.5 Suppression of intra-channel nonlinear distortion by pre-compensation at the transmitter

The results described in the previous sections showed that optical transmission at 40Gbit/s was limited by intra-channel nonlinear distortion. It was found that minimising the pulse overlap reduces these effects, and NZDSF was investigated as an alternative to SSMF in order to achieve this. This was observed experimentally, and it was shown that the use of in-line pre-compensated amplifier spans, negates the advantage of NZDSF and controlling the pulse spreading was the most effective method of suppressing intra-channel nonlinear distortion. This section therefore investigates dispersion management by adding pre-compensation at the transmitter before the signal is launched into the fibre link. This is an effective technique for controlling the pulse broadening, as it can be optimised independent of the transmission fibre.

Dispersion management in general, can be applied to suppress nonlinear distortion for both NRZ and RZ modulation formats. Indeed, it has been shown that it is possible to reduce the nonlinear distortion in NRZ transmission by approximately 5-10% under-compensating the link in order to off-set the SPM-induced chirp [FUR'01], and also for XPM in WDM systems [SAN'00]. However, in the case of RZ signals, the dominant nonlinear effects, namely IXPM-induced timing jitter and IFWM-induced amplitude jitter and shadow pulses, require suppression for optimum transmission performance, and thus pre-compensation at the transmitter is an effective technique for their mitigation. Previous investigations of this technique are discussed in the literature review of chapter 3. In this work, the analytical rules governing the optimum pre-compensation proposed in [KIL'00] are investigated experimentally, and demonstrated for transmission over SSMF and NZDSF. This study also investigates the effect pre-compensation at the transmitter for varying pulsewidth of RZ signals, while the impact of pre-compensation at the transmitter in the presence of advanced modulation formats is discussed in chapter 5.

Numerical simulations were performed first, in order to investigate the impact of pulsewidth and pulse peak power on optimum pre-compensation at the transmitter. As described in the previous sections, numerical simulations of the system under test calculate the Q-factor as a function of transmission distance. Here, the calculated Q-factor for varying amounts of pre-compensation at the transmitter before transmission over the SSMF fibre link (described in section 4.3) are shown in *Fig. 4.32.*

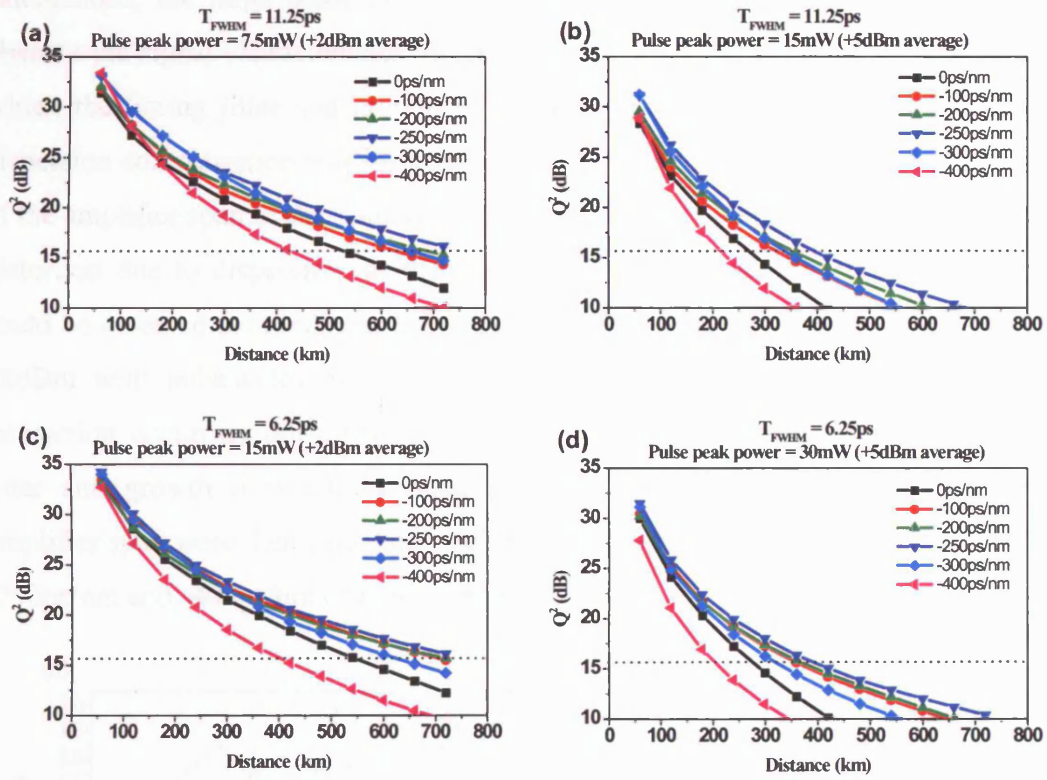

Fig. 4.32 *Calculated Q-factor as a function of transmission distance for varying amounts of pre-compensation*

The results in *Fig. 4.32* show that optimum transmission performance is obtained for a pre-compensation of -250ps/nm at the transmitter. Furthermore, the optimum pre-compensation is independent of signal launch power and pulsewidth. This is significant, as the dispersion-induced pulse broadening increases and therefore pulse peak power decreases with dispersion, when the initial pulsewidth is decreased. The results also indicate that longer transmission distances can be achieved for narrow pulsewidths with similar pulse peak power, but no significant improvement is observed when equal average powers are considered. This can be explained by the

average power differential of the RZ modulation format compared to NRZ for similar pulse peak powers.

In order to separately study the nature and impact of IXPM and IFWM effects within each amplifier span, the corresponding timing jitter and growth of shadow pulses were calculated by numerical simulation. This was carried out by simulating the signal propagation over 0 to 60km (SSMF) in step sizes of 5km. During these calculations, the large pulse broadening due to dispersion makes it impossible to observe the signal characteristics directly. Therefore, at each point along the fibre, at which the timing jitter and growth of shadow pulses were calculated, the relevant dispersion compensation was inserted so that the cumulative dispersion from the start of the amplifier span to the point of calculation was zero. This helped to isolate signal distortion due to dispersion, as the pulses are recompressed and the signal quality could be assessed for nonlinear behaviour. The signal launch power was increased to +8dBm with pulsewidth of 11.25ps (FWHM), in order exaggerate the nonlinear interaction occurring during transmission over a single amplifier span. The timing jitter and growth of shadow pulses as the signal propagates within this single amplifier span were then calculated and the results are shown in *Fig. 4.25* for 0ps/nm, -250ps/nm and -400ps/nm of pre-compensation.

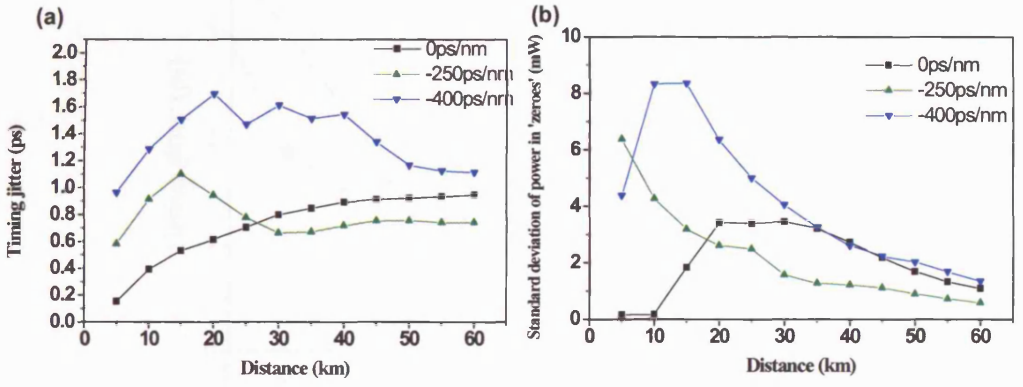

Fig. 4.33 *Evolution of (a) IXPM induced timing jitter (b) Growth of shadow pulses due to IFWM, within a single amplifier span at a launch power of +8dBm and pulsewidth of 11.25ps (FWHM)*

From the results plotted in *Fig. 4.33*, it can be seen that when the pre-compensation is increased to -250ps/nm, the timing jitter is initially larger than that for 0ps/nm pre-

compensation, but it gradually decreases with increasing distance within the amplifier span, and finally falls to values below that when 0ps/nm pre-compensation was used, and measured at the end of the amplifier span. This indicates that the IXPM-induced initially, is reversed during propagation within the amplifier span, and the signal quality improved by -250ps/nm of pre-compensation. For pre-compensation of -400ps/nm, the pulse overlap is still significant at the start of the span when the signal power and fibre nonlinearity are high, thereby leading to an increase in both IXPM and IFWM. The optimum pre-compensation of -250ps/nm however, shows maximum suppression of both IXPM and IFWM at the end of the amplifier span.

The described nonlinear behaviour over a single amplifier span accumulates over every amplifier span in a transmission link. In order to investigate this effect and gain insight of the dominant source of penalty, the IXPM-induced timing jitter and the standard deviation of the growth of shadow pulses due to IFWM was calculated as a function of pre-compensation at the transmitter, at a transmission distance of 600km. The signal launch power was +5dBm, experimentally measured as optimum in the transmission results described in section 4.3, and the results are plotted in *Fig. 4.33.*

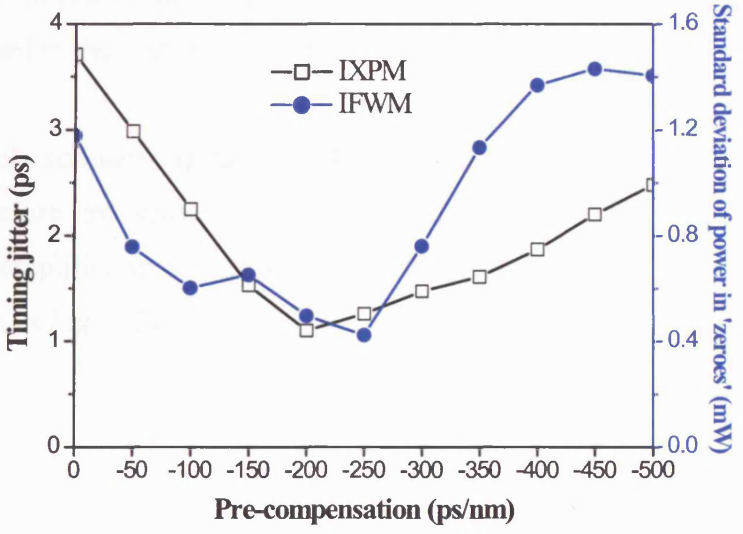

Fig. 4.34 *IXPM-induced timing jitter and IFWM-induced growth of shadow pulses as a function of pre-compensation measured at a transmission distance of 600km, with a signal launch power of +5dBm and pulsewidth of 11.25ps.*

From the results plotted in *Fig. 4.34* it can be seen that at the optimum pre-compensation of -250ps/nm before launching the signal into the fibre link, both the IXPM and IFWM were simultaneously suppressed and resulted in the optimum Q also obtained at this value. These results show that the optimum pre-compensation (D_{opt}) minimises the pulse overlap at point z' within the amplifier span where the power profile is symmetrical. This is described mathematically as:

$$\int_0^{z'} P_{in} e^{-\alpha z} dz = \int_{z'}^{L} P_{in} e^{-\alpha z} dz \qquad (4.1)$$

and $D_{opt} = -D_{fibre} z'$. Thus, the optimum pre-compensation can be obtained from the following expression [KIL'00]:

$$D_{opt} = \frac{-D_{fibre}}{\alpha} \ln\left(\frac{2}{1+e^{-\alpha L}}\right) \qquad (4.2)$$

Equation (4.2) provides the optimum pre-compensation at the transmitter regardless of the fibre used in the transmission link.

The numerically simulated Q-factor with varying amounts of pre-compensation at the transmitter before transmission over the NZDSF fibre link with in span post-compensated amplifier spans optimal for RZ (see section 4.4.3) were then calculated and are shown in *Fig. 4.34*.

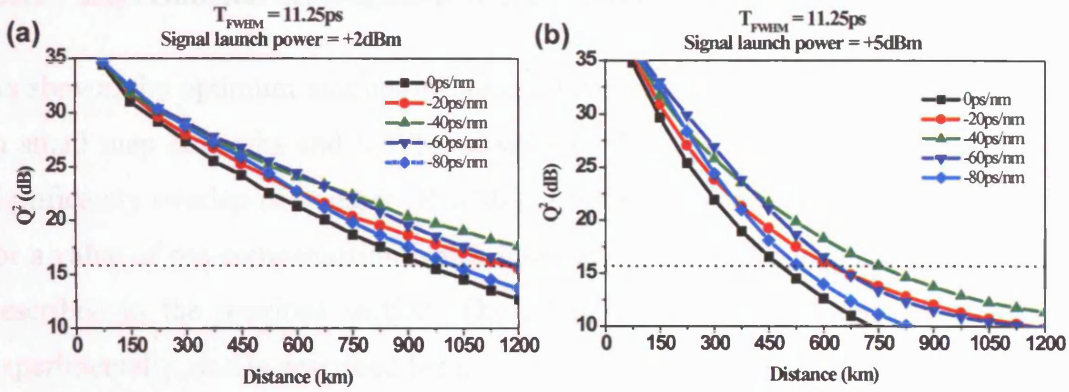

Fig. 4.35 *Simulation of Q-factor as a function of transmission distance for pre-compensation ranging from 0-80ps/nm at signal launch pulse peak power of (a) +2dBm (b) +5dBm average power over NZDSF link with in-line post-compensated amplifier spans*

The results obtained by numerical simulation of transmission over the SSMF link and the NZDSF link with in-line post-compensation are shown in *Fig. 4.32* and *Fig. 4.35* respectively. The optimum pre-compensation at the transmitter was -250ps/nm for transmission over the SSMF link and -40ps/nm for transmission over the NZDSF link. The optimum pre-compensation at the transmitter for the same links calculated using equation (4.2) were $D_{opt} \approx$-230ps/nm and $D_{opt} \approx$-55ps/nm for the SSMF and NZDSF link respectively. These values though not identical are still in agreement with that obtained by numerical simulation, where the pre-compensation was investigated for step increases of 50ps/nm for the SSMF link and 20ps/nm for the NZDSF link. The optimum values of pre-compensation obtained from the simulations were then used in the experimental verification of the use of pre-compensation at the transmitter, for the suppression of intra-channel nonlinear distortion, and is described in the following section.

4.5.1 Experimental investigation of pre-compensation at the transmitter:

As shown, the optimum amount of pre-compensation minimises the IXPM generated in small map strengths and IFWM which arise in large map strengths where pulses significantly overlap each other [HIR'02]. The optimum dispersion map, thus, occurs for a value of pre-compensation which leads to a trade-off between the two effects as described in the previous section. The effectiveness of this technique is explored experimentally, and is described here.

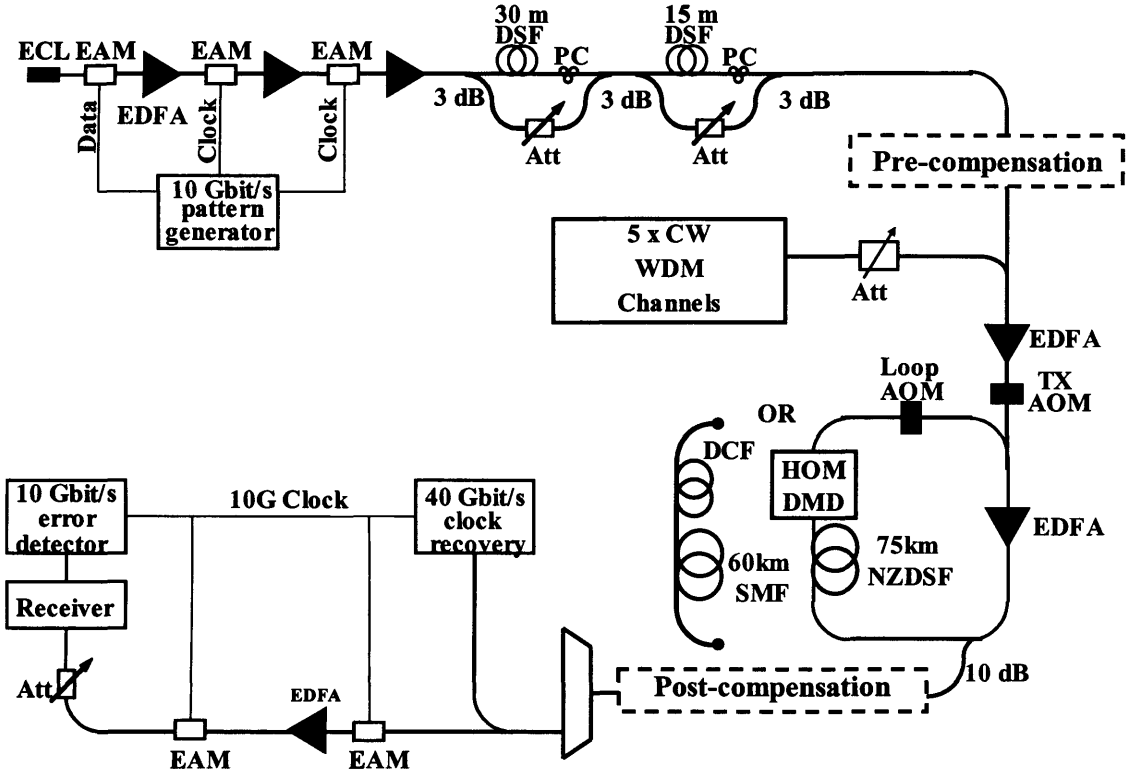

Fig. 4.36 *Experimental set-up for investigation of the suppression of intra-channel nonlinear distortion by dispersion management for transmission over SSMF and NZDSF links*

The experimental set-up for the investigation of pre-compensation at the transmitter is shown in *Fig. 4.36*, and used both the SSMF and NZDSF link. The NZDSF link was investigated with in-line post-compensated amplifier spans, as previous results (described in sections 4.4.3) showed optimum transmission of the RZ format was obtained for this scheme. The optimum pre-compensation of -250ps/nm required at the transmitter for the SSMF link was achieved by cascading a LaserComm Inc

HOM-DMD of -300ps/nm dispersion with 3km of SSMF and the post-compensation consisted of approximately 15km of SSMF. For the NZDSF link the pre-compensation of -40ps/nm was achieved by cascading a LaserComm Inc. HOM-DMD of -80ps/nm dispersion with 10km NZDSF. The post-compensation of +40ps/nm was achieved with a further 10km of NZDSF. The signal power launched into the pre- and post-compensation was approximately 0dBm, ensuring minimum nonlinear distortion. The introduction of pre- and post-compensation added to the loss at the transmitter and receiver. Hence, for accurate comparison with 0ps/nm pre-compensation, the equivalent loss was placed at the transmitter and receiver in order to keep the noise accumulation constant, enabling any improvement in system performance to be attributed solely to the suppression of nonlinear distortion. The losses of both amplifier spans were approximately 20dB.

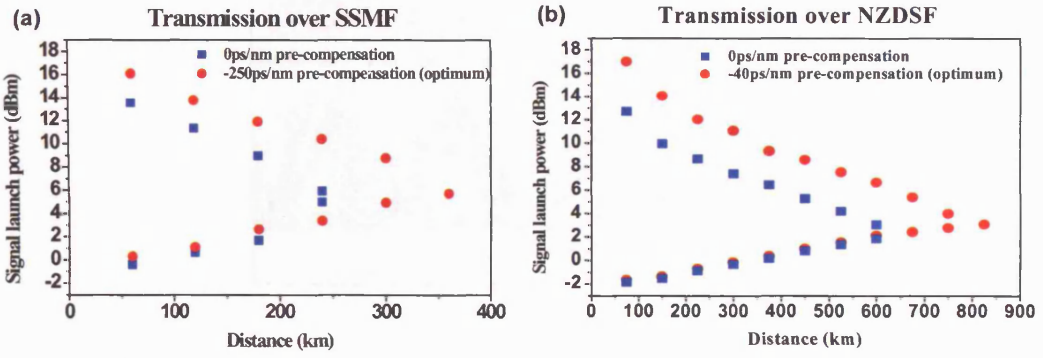

Fig. 4.37 *Experimental results of varying the launch power for BER<10^{-9} for RZ transmission over (a) SSMF (b) NZDSF (squares): 0ps/nm pre-compensation (circles): Optimum pre-compensation obtained by numerical simulation*

The 40Gbit/s experiment was first performed for an amplifier span consisting of 60km SSMF and 12km DCF. The signal input power was varied from -3dBm to +18dBm to investigate the linear and nonlinear power limit for a given distance. *Fig. 4.37* shows the upper and lower launch powers giving BER<10^{-9} as a function of the transmission distance. *Fig 4.37(a)* shows the maximum achievable transmission distance was 240km at an input power of 5.5dBm. The experiment was then repeated with pre-compensation of -250ps/nm, calculated as optimum by numerical simulation and in agreement with equation (4.2). This led to an increase in the maximum achievable

transmission distance by 50% to 360km. The optimum power level at which maximum transmission distance was achieved, was similar to the scheme with 0ps/nm pre-compensation. Furthermore, the nonlinear limit was increased by 4.5dB at 240km, confirming a reduction of the nonlinear interaction between the pulses. This is due to the reduced pulse overlap during transmission caused by the pre-compensation at the transmitter. This can be further confirmed from the eye diagrams measured experimentally and by numerical simulation at a transmission distance of 360km, as shown in *Fig. 4.38 (top)*. It can be seen that the suppression of timing and amplitude jitter is achieved when a pre-compensation of -250ps/nm was used at the transmitter.

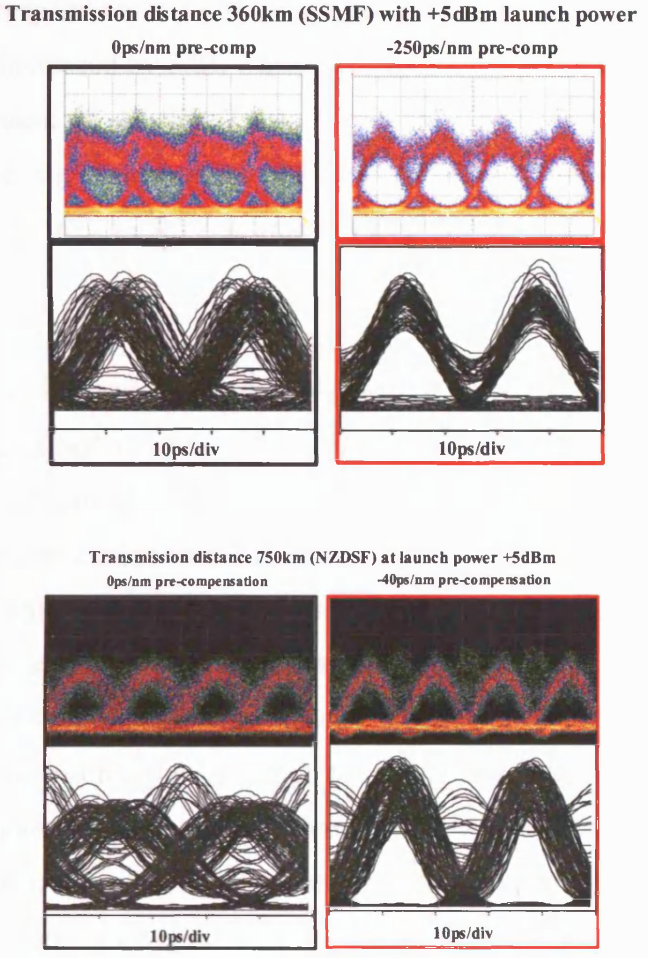

Fig. 4.38 *Comparison of experimental and simulated eye diagrams for transmission over (top): SSMF, (Bottom): NZDSF transmission links*

The SSMF transmission link was then replaced by 75km of NZDSF and the HOM-DMD with post-compensated amplifier spans, and the experiment repeated. For

0ps/nm pre-compensation a maximum transmission distance of 600km was obtained at a signal launch power of +3dBm. This shows a decrease in transmission distance compared to that obtained at a similar signal launch power in the transmission experiments described in section 4.4.3, where a maximum transmission distance of 750km was achieved. This corresponds to a 2dB penalty, and is seen in the noise limited performance. This decrease is a result of the additional loss at the transmitter and receiver, caused by the equivalent loss of the pre and post-compensation respectively. Introducing the optimum pre-compensation of -40ps/nm at the transmitter, a value obtained from the numerical simulations *(Fig. 4.35)*, the maximum transmission distance could be increased to 825km, also at a launch power +3dBm. This corresponds to a 37.5% improvement in the transmission distance. The nonlinear limit is increased by 3dB, which is lower than that obtained for transmission over SSMF (increase of 4.5dB). Thus, it can be concluded that as the nonlinear distortion is more significant in SSMF and the use of pre-compensation at the transmitter is more effective for transmission over SSMF links compared to NZDSF links.

It was recently demonstrated in [BIS'04], that in-line pre-compensated amplifier spans like that described in section 4.4 could be successfully implemented for RZ transmission with improved nonlinear suppression. The technique in [BIS'04] makes use of the nonlinear tolerance of the HOM-DMD, as achieved for NRZ transmission and described in section 4.4.1, with additional pre-compensation at the transmitter. However, the pre-compensation at the transmitter was approximately 120% the dispersion of the DMD compensator placed directly after the EDFA within each amplifier span. This in effect corresponds to a dispersion map of similar likeness to that described here, which uses in-line post-compensation. Hence, while an improvement in the transmission performance maybe obtained, it requires justification against of the large amount of pre-compensation (and post-compensation) required at the transmitter (and receiver) for successful implementation. This may typically comprise fibre lengths of the order of magnitude similar to an extra amplifier span.

To understand the effectiveness of using pre-compensation at the transmitter for the suppression of intra-channel nonlinear distortion in the 'zeroes' and 'ones' separately, the BER was measured against a varying decision level threshold. These

measurements were taken at a transmission distance of 375km for transmission over the NZDSF link at a signal launch power of +3dBm and are shown in *Fig. 4.38*.

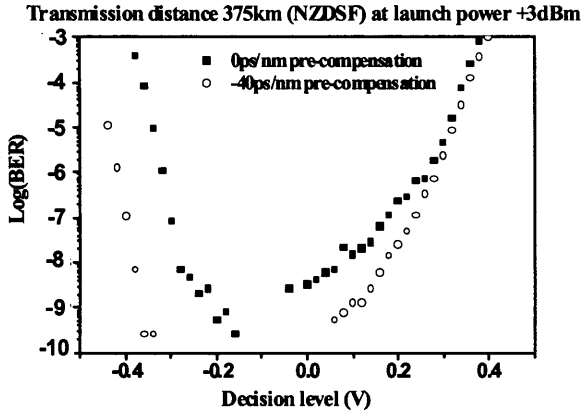

Fig. 4.39 *Experimental measurement of BER vs decision level voltage indicating the suppression errors detected in the 'zeroes' and 'ones' separately for transmission over the NZDSF link. (squares): 0ps/nm pre-compensation (circles): -40ps/nm pre-compensation*

Fig. 4.39 shows that for 0ps/nm pre-compensation, the decision level range over which a BER<10^{-9} is achieved was 100mV. As the ASE noise was the same for both 0ps/nm and -40ps/nm pre-compensation (as can be seen from the lower power limits in Fig 4.36(b)), the increase of errors in the 'zeroes' for transmission with 0ps/nm pre-compensation, is due to IFWM which results in shadow pulses in the 'zero' time slot. Moreover, distortions in the 'one' level are due to a combination of amplitude jitter arising from IFWM, as well as timing jitter from IXPM. Furthermore, the decision level range at which BER<10^{-9}, was increased to over 250mV when the pre-compensation of -40ps/nm was placed at the transmitter, clearly indicating less distortion in both the 'zero' and 'one' levels, and shows the effectiveness of this technique.

4.6 Summary

In this chapter, the impact of signal distortion due to fibre nonlinearity and noise were investigated for transmission at a bit-rate of 40Gbit/s. The transmission of NRZ and RZ modulation formats was studied for the case of SSMF, and found to have limited nonlinear tolerance. The transmission performance was then investigated for transmission over NZDSF, with dispersion compensation achieved with a higher-order-mode dispersion compensator (LaserComm HOM-DMD), enabling improvements in nonlinear tolerance and transmission distance. Further suppression of nonlinear distortion was achieved by dispersion management. Dispersion management was investigated within every amplifier span for NZDSF links exploiting the linear behaviour of the HOM-DMD. Finally, dispersion management using pre-compensation at the transmitter for the suppression of intra-channel nonlinear effects was investigated for improving transmission performance over both SSMF and NZDSF links.

The main results of this chapter are summarised here, providing guidelines for the design of optical systems operating at a bit-rate of 40Gbit/s:

Signal launch power: At low launch powers signal distortion is caused by noise due to ASE in the amplifiers which reduces the OSNR. The noise limitation can be overcome by increasing the signal launch power. However, as the signal launch power increases, the distortion due to nonlinear effects also increases. Hence, it was found that the system margin can be quantified by signal launch power at any transmission distance, where the system is limited by nonlinear distortion at high launch powers and by noise at low launch powers. The optimum signal launch power occurs for a trade-off between noise and nonlinear effects, and ensures maximum transmission distance is achieved.

Modulation format: The noise and nonlinear limitations of NRZ and RZ modulation formats were investigated. It was found that the dominant nonlinear distortion affecting NRZ signals was caused by SPM, while RZ signals were affected by IXPM and IFWM. However, the overall nonlinear and noise tolerance was higher when the

RZ modulation format was used. Experimental transmission using a recirculating fibre loop with a single amplifier span consisting of 60km SSMF compensated by 12km of DCF, enabled a maximum transmission distance of 120km for NRZ signals and 240km for RZ signals.

Alternative transmission fibre and dispersion compensation elements: NZDSF was investigated as an alternative transmission fibre to SSMF, with reduced fibre nonlinearity. The large effective area in NZDSF increased the nonlinear tolerance reducing the SPM in NRZ signals while, the low fibre local dispersion decreased intra-channel nonlinear interaction between overlapping pulses. Dispersion compensation of NZDSF was achieved using a LaserComm HOM-DMD. This was superior to DCF as it consisted of less than 1km of fibre with effective area nearly 4 times that of DCF, resulting in linear behaviour and low loss. This allowed the investigation of in-line pre-compensated links, where the HOM-DMD was placed directly after the EDFA, minimising the signal launch power into the transmission fibre without sacrificing any reduction in OSNR. This increased the maximum achievable transmission distance from 375km with in-line post-compensation to 525km using the NRZ modulation format. However, for RZ signals the maximum transmission distance of 750km was achieved using in-line post-compensation, in-line pre-compensation leads to severely broadened pulses entering the nonlinear transmission fibre and increases the intra-channel nonlinear distortion.

Dispersion management by pre-compensation at the transmitter: Pre-compensation at the transmitter was investigated experimentally for the first time, as a technique for limiting intra-channel nonlinear distortion by ensuring a 30% decrease in pulse overlap in the transmission fibre. This technique was shown to improve the maximum transmission distance by 50% for transmission over SSMF giving a maximum transmission distance of 360km for BER<10^{-9}. While for transmission over the NZDSF link with in-line post-compensation (optimum for RZ), the maximum achievable transmission distance was increased from 600km to 825km for an optimum pre-compensation of -40ps/nm, an improvement of only 36%. It is clear that dispersion management by pre-compensation at the transmitter is more effective for transmission over SSMF where nonlinear distortion is more significant.

WDM transmission: The impairments due to inter-channel nonlinear effects were analysed by comparing single- and 3-channel transmission, and were found to be insignificant compared to the single channel nonlinear distortion. Thus future systems operating at 40Gbit/s should be optimised for single channel transmission. However, the low fibre local dispersion of NZDSF decreases the walk-off between WDM channels and incurs a penalty of 2dB due to XPM. Simultaneous broadband dispersion compensation of 10 WDM channels was demonstrated for a transmission distance of 375km using the HOM-DMD without requiring channel-by-channel dispersion trimming at the receiver. However, it was found that non-central channels in the C-band were susceptible to incomplete dispersion compensation. The XPM penalty was not increased by the increase in WDM channels, but, the transmission performance was limited by a reduction of the OSNR.

Chapter 5 Advanced modulation formats

5.1 Introduction

Chapter 4 described the suppression of intra-channel nonlinear effects by dispersion management, where the pulse overlap is minimised during signal propagation. However, as pulse overlap is inevitable, even for optimum dispersion management, minimising the nonlinear interaction in the presence of pulse overlap is investigated in this chapter through optimisation of the modulation format. This technique is advantageous as it requires changes be made only at the transmitter and receiver, whilst the transmission link and its components remain unchanged.

In general, modulation formats can be separated into two categories based on the optical field component used to encode the data, namely amplitude and phase. However, it is possible for amplitude modulated systems to also include phase modulation, although the phase modulation in such formats would carry no data information. Examples of such formats are carrier-suppressed RZ (CS-RZ) [MIY'98] and alternate-phase RZ (AP-RZ) [OHH'01]. It is also possible for phase modulation formats to be amplitude modulated like that of RZ differential-phase-shift-keying (RZ-DPSK) [YON'96]. The principal difference between systems employing amplitude modulation formats and phase modulation formats, are at the receiver, where phase modulation formats require differential modulation, when the detection process is based on the received optical power (direct detection). In such cases optical delay interferometers are used to convert the relative phase information between bits to intensity modulation. This chapter focuses on amplitude modulation formats with no phase encoded data, but with improved tolerance to intra-channel nonlinear distortion. These formats require simple alterations at the transmitter and use standard IM-DD at the receiver, making them attractive in the implementation of 40Gbit/s transmission over existing systems.

5.2 Alternate-polarisation RZ modulation format

The power margin for a system employing the RZ format over SSMF was investigated for an increasing distance, in a recirculating fibre loop in chapter 4, and it was shown to be superior to the NRZ modulation format at a bit-rate of 40Gbit/s. However, RZ signals were found to be limited by IXPM and IFWM arising from overlapping pulses in the presence of dispersion. As already mentioned, interaction between signals orthogonally polarised were found to be reduced, and was demonstrated in OTDM multiplexing techniques [EVA'92]. In this section, the improvement of the intra-channel nonlinear tolerance achieved by alternating the polarisation between adjacent bits of the RZ format is investigated experimentally. Numerical simulations based on the theory described in chapter 2 (section 2.7) are also carried out and compared with the experimental results.

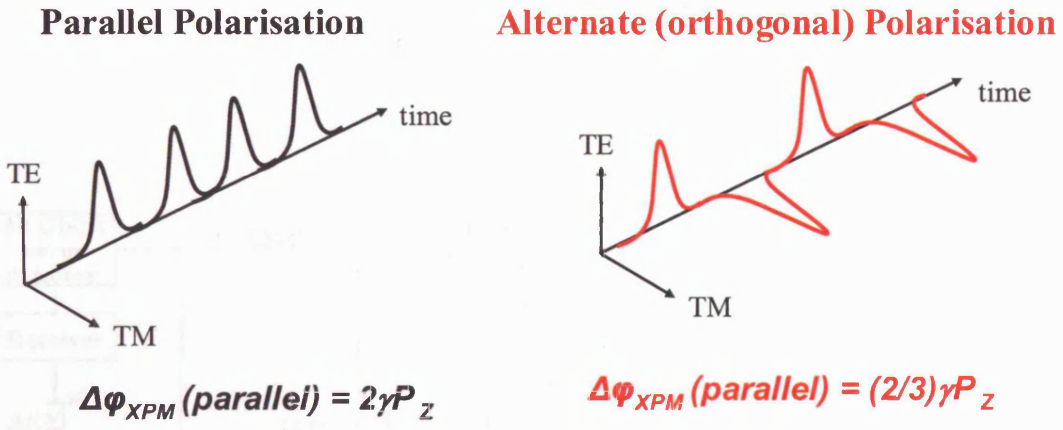

Fig. 5.1 *Schematic diagram indicating the mechanism of the alternate-polarisation modulation format, where adjacent pulses are orthogonally polarised leading to a reduction in the IXPM.*

The experimental set-up for the standard RZ and alternate-polarisation RZ modulation formats are shown in *Fig 5.2*. The decrease in nonlinear interaction due to polarisation division multiplexing where two orthogonally polarised bit streams at 20Gbit/s, were interleaved in the time domain to 40Gbit/s. The use of an OTDM system at the transmitter to generate the 40Gbit/s signal, allowed the adjacent bits of the signal to be orthogonally polarised by use of the polarisation controllers in each stage of the

optical multiplexer. The amplifier span was similar to that described in chapter 4 for transmission over SSMF. The clock was recovered at the receiver, from an auxiliary 10Gbit/s signal transmitted simultaneously with the data signal over the transmission link. It should be noted that the use of the alternate polarisation makes the system less tolerant to polarisation mode dispersion (PMD) [ZHA'98]. However, this experimental set-up consisted of low PMD loop components and fibre, and consequently little or no PMD was observed experimentally (described next). On this basis PMD was neglected in the numerical simulations.

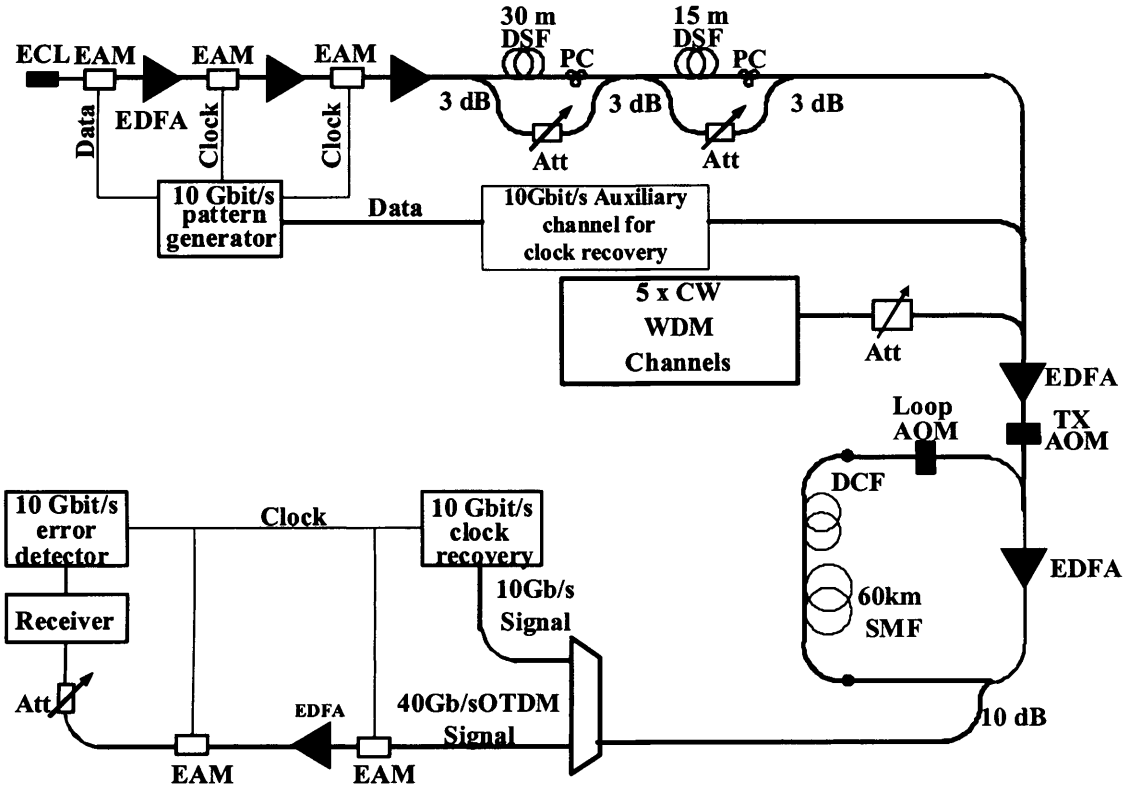

Fig. 5.2 *Experimental investigation of alternate-polarisation RZ using an optical-time-division-multiplexed transmitter for the generation of the 40Gbit/s RZ signal*

As in the previous chapter, the maximum and minimum launch power giving BER<10^{-9} was measured experimentally as a function of the transmission distance for parallel (standard RZ) and orthogonal (alternate-polarisation RZ) polarisation between adjacent pulses, as described previously (section 2.8.5) and the results are shown in

Fig. 5.3(a). Fig. 5.3(b) plots the Q-factor against transmission distance calculated by numerical simulation for comparison with the experimental results. As the results are that of a single channel transmission, the dominant nonlinear effects in this case are IXPM, IFWM and SPM. It was established in chapter 4 that in RZ transmission the distortion due to SPM is minimal. Hence, any improvement in nonlinear limit was attributed to the suppression of intra-channel pulse interactions. The minimum launch power necessary for error free transmission is determined by the SNR degradation due to ASE accumulation.

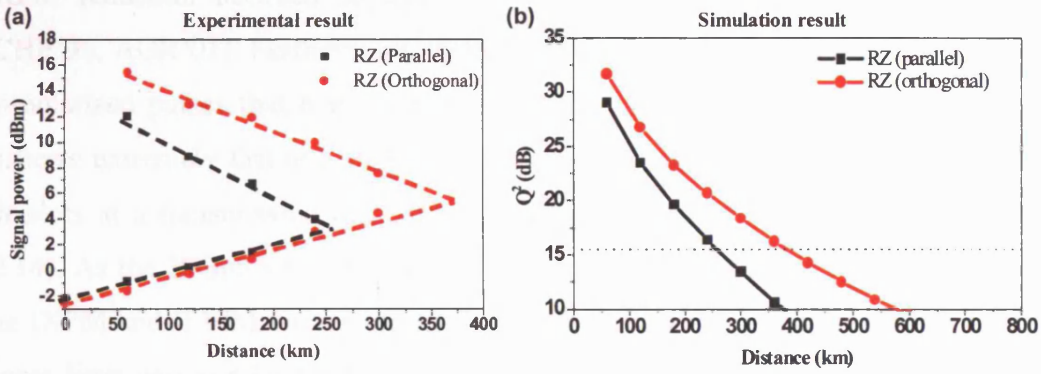

Fig. 5.3 *(a): Launch power range for BER<10^{-9} for 40Gbit/s OTDM transmission in SMF (b): Simulated results of RZ and alternate polarisation RZ over SMF. The dotted line corresponds to error-free transmission*

The experimental results plotted in *Fig. 5.3(a)* show a maximum transmission distance of 240km was achieved with parallel polarisation between adjacent bits. This was consistent with the previous results of standard RZ transmission obtained in chapter 4, where the 40Gbit/s signal was generated with an ETDM transmitter. As such, it can reliably be concluded that no additional penalty was induced by use of the OTDM transmitter, required for implementing the alternate polarisation between adjacent bits in this experiment. Inducing the alternate-polarisation between adjacent bits enabled a maximum transmission distance of 360km to be achieved. This corresponds to a 50% increase in transmission distance, and is achieved as a result of a 4.5dB increase in the nonlinear limit. This quantifies the improvement due to alternate-polarisation RZ modulation format which results in a decrease in IXPM and

IFWM as explained from the theory in section 2.7. The decrease in signal distortion can also be seen in the eye diagrams obtained by numerical simulation at a transmission distance of 360km and launch power of +5dBm, as shown in *Fig. 5.4*. The theory of orthogonal polarisation described in section 2.7 showed that the nonlinear interactions are 2/3 for orthogonally polarised adjacent pulses and not 2 as in the case of parallel polarised pulses. However, this improvement was not observed experimentally, as the birefringence of the transmission fibre is not constant, and causes the polarisation state to evolve randomly. On average this continuous evolution of the polarisation state, can be likened to elliptical polarisation, showing an average IXPM reduction between adjacent pulses by a factor of 2 and consistent with [CHE'96, AGR'01]. Furthermore, the theory does not take into account non-adjacent co-polarised pulses that may overlap each other. It should be noted that the pulses disperse extremely fast in SSMF, and overlap each other over more than 12 adjacent bit slots at a transmission distance of less than 20km, as calculated from equation (2.14). As the 20Gbit/s tributaries have the same polarisation and overlap each other, the IXPM and IFWM were stronger than that expected theoretically [MIK'01b]. The linear limit was similar for both parallel and orthogonally polarised pulses, proving that the linear distortion affected both polarisation states equally. This is a significant result as it proves that the experimental set-up is polarisation insensitive, and the signal is unaffected by PMD and PDL during the recirculating loop transmission.

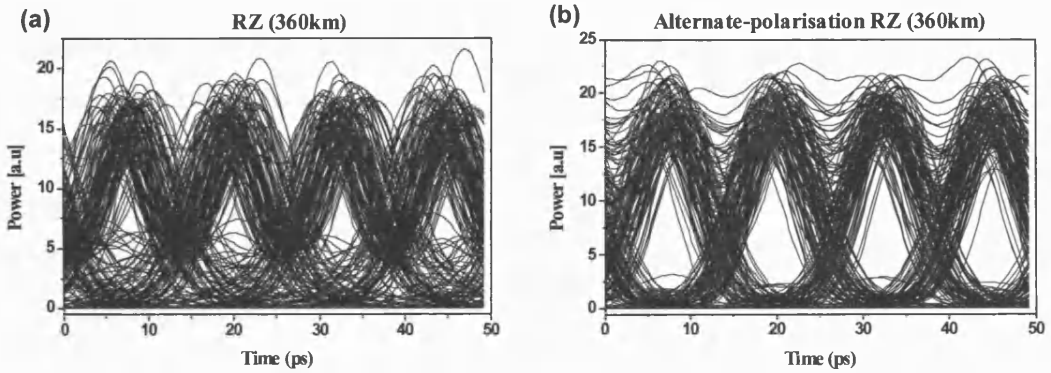

Fig. 5.4 *Simulated eye diagrams for transmission over 360km SSMF at a launch power of +5dBm (a): Standard RZ (parallel polarisation between adjacent bits) (b): Alternate-polarisation RZ (orthogonal polarisation between adjacent bits)*

To study the relative impact of IXPM and IFWM in the overall nonlinear distortion, the timing jitter and standard deviation of power in the 'zero' bit slots were investigated separately as a function of the transmission distance. The IXPM was calculated from the average timing jitter at the full width at half maximum of the jitter in the leading and trailing edges of every pulse, while the standard deviation of the power in the 'zero' bit slots was calculated by recording the power at the mid point of every 'zero' bit to give a measure of the IFWM. These simulated results are shown in *Fig. 5.5.*

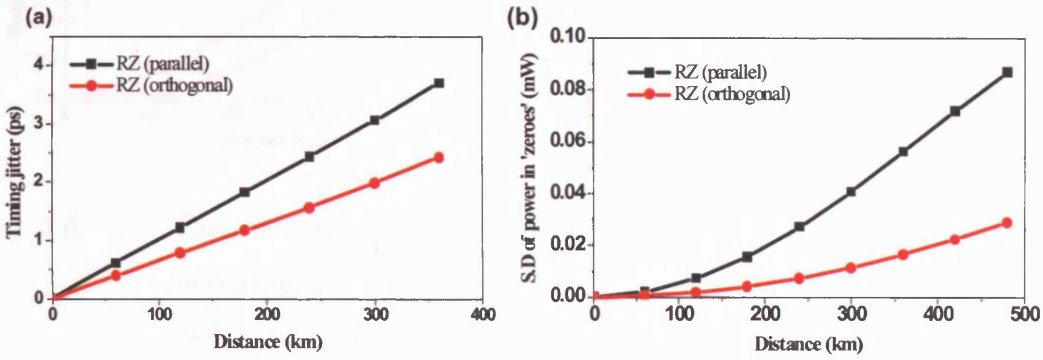

Fig. 5.5 *Simulation results (a): average timing jitter as a function of increasing transmission distance (b): Standard deviation of power in 'zero' bit slots as a function of distance*

The timing jitter calculated from the simulations and plotted in *Fig. 5.5(a)* increases with transmission distance for both parallel and orthogonal polarisation between adjacent bits. It can be seen however, that the use of alternate polarisation decreases the timing jitter from 4ps to 2.5ps at a distance of 360km, indicating suppression of IXPM. As the pulses were linearly polarised throughout the transmission in this simulation, the suppression of the IXPM is approximately a factor of 3, and agrees well with the theory [AGR'01]. In practice the birefringence of the transmission fibre leads to elliptical polarisation and an average IXPM reduction between adjacent pulses by a factor of 2 can be expected [AGR'01]. *Fig. 5.5(b)* shows nearly 70% suppression of IFWM, for alternate polarisation RZ, although total suppression of IFWM as expected from the theory is again not obtained. As described previously, this is explained by the contribution of IFWM which exists due to interaction between

20Gbit/s co-polarised pulses. In addition, as the signal is detected on a polarisation independent photo-detector at the receiver, ISI between adjacent pulses interfere constructively. This effect can be eliminated by the use of polarisation division multiplexing, which eliminates ISI between orthogonally polarised pulses in addition to reducing the OSNR on each polarisation state [SHT'04, MEC'04].

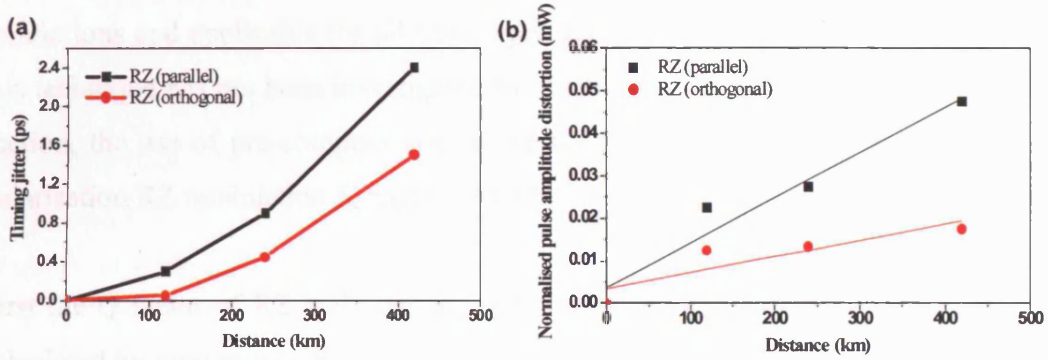

Fig. 5.6 *Experimental results (a):average timing jitter as a function of increasing transmission distance (b): Standard deviation of power in 'zero' bit slots as a function of distance. Note: Experimental measurements were normalised to remove distortion due to ASE*

In order to experimentally measure timing jitter and amplitude distortion, the oscilloscope traces of 128 bit fragments of the transmitted signal were taken at different transmission distances at a signal launch power of +5dBm. The traces were averaged to remove jitter and amplitude distortion associated with ASE accumulation during the transmission. The measured values of the timing jitter σ_t and amplitude distortion σ_a for alternate-polarisation RZ and standard RZ signals are shown in *Fig. 5.6*. The experimentally obtained timing and amplitude jitter are reduced by a factor of approximately 2 compared to those obtained by simulation. This is probably because the simulated results include the signal distortion caused by the ASE of the amplifiers. Taking this effect into consideration, the suppression of the IXPM-induced timing jitter (30%) and IFWM-induced shadow pulses and amplitude distortion (50%), which are in good agreement with the results obtained by simulation and confirms the advantage of employing the alternate-polarisation modulation format for suppressing these intra-channel nonlinear distortions.

5.2.1 Combination of alternate-polarisation RZ and pre-compensation

As described in chapter 4, the intra-channel nonlinearities can be suppressed by pre-compensating the transmission link with an appropriate amount of dispersion compensation fibre. The analytical equation from [KIL'00] shown to be accurate in predicting the optimum pre-compensation without the need for time consuming simulations and applicable for all fibre types and pulsewidths (duty cycle). However, this technique has not been investigated for modulation formats other than RZ. In this section, the use of pre-compensation at the transmitter for the case of the alternate-polarisation RZ modulation format is described.

First the Q-factor of RZ and alternate-polarisation RZ transmission over SSMF was calculated by numerical simulation for increasing transmission distance and plotted in *Fig. 5.7*. The pulsewidth of both modulation formats was 11.25ps (FWHM) at a signal launch power of +5dBm. The amplifier spans were similar to that described in chapter 4, consisting of 60km SSMF perfectly compensated by 12km of DCF.

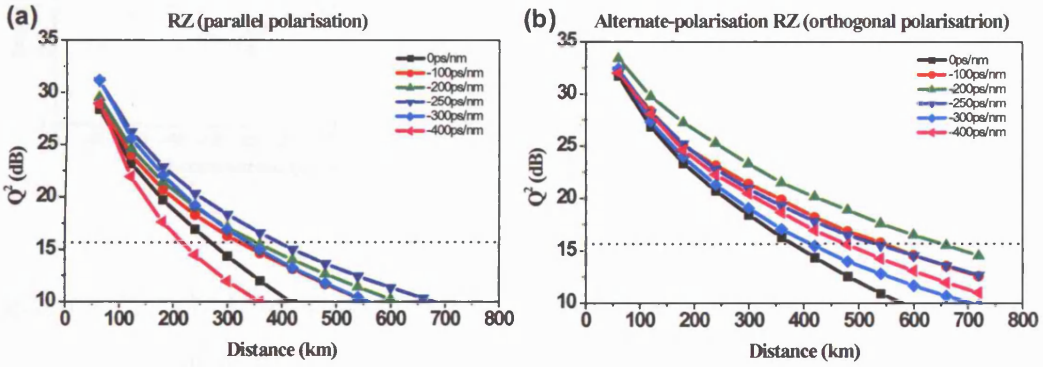

Fig. 5.7 *Simulation of Q-factor as a function of pre-compensation (a): standard RZ modulation format (b): alternate-polarisation RZ modulation format*

It can be seen from *Fig. 5.7(a)* and *Fig. 5.7(b)* that the optimum pre-compensation at the transmitter is -250ps/nm for the standard RZ modulation format and -200ps/nm for the alternate-polarisation RZ, showing that the optimum pre-compensation is

sensitive to the modulation format. This was an unexpected result as the pulse broadening is similar in both RZ and alternate-polarisation RZ and indicates that the optimum pre-compensation calculated according to equation (4.6), may not hold for modulation formats other than RZ. This is because the optimum pre-compensation is based primarily on suppressing the IXPM and IFWM, it is hence reasonable that the optimum pre-compensation varies if the selected modulation format is more effective in suppressing one of these effects compared to the other. Indeed, from the theory of the alternate-polarisation modulation format it was seen that while the IXPM is reduced by a factor of 3, the IFWM averages to zero. Hence, it can be expected that the alternate-polarisation RZ modulation format can tolerate more pulse overlap before signal distortion due to IFWM becomes significant, which explains the reduced amount of required pre-compensation in alternate-polarisation RZ for optimum transmission.

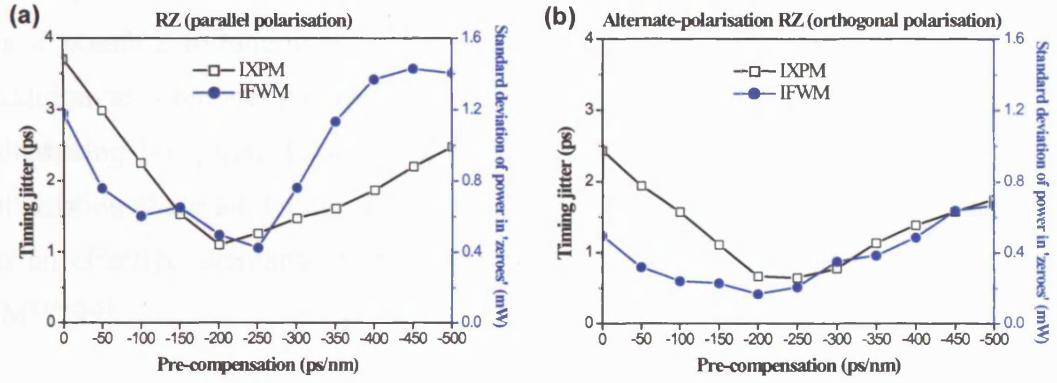

Fig. 5.8 *IXPM-induced timing jitter and IFWM-induced growth of shadow pulses as a function of pre-compensation measured at a transmission distance of 600km, with a signal launch power of +5dBm. (a): Standard RZ (parallel polarisation) modulation format (b): Alternate-polarisation RZ (orthogonal polarisation) modulation format*

In order to analyse the variation of IXPM and IFWM with pre-compensation at the transmitter, which occurs for alternate-polarisation RZ, the timing jitter and standard deviation of power in the 'zero' bit slots were calculated by numerical simulation, at a transmission distance of 600km. The pre-compensation at the transmitter was varied

from 0ps/nm to -500ps/nm and the results are plotted in *Fig. 5.8*. The results show that for a pre-compensation of -200ps/nm the initial IXPM at the start of the amplifier span is reversed. While the IXPM efficiency is reduced by a factor of 3 for alternate-polarisation RZ, it should be noted that the pulse broadening at signal power for inducing IXPM remain constant for both alternate-polarisation RZ and standard RZ, hence the minimal difference in the optimal pre-compensation. The suppression of IFWM however, is nearly 75% stronger for alternate-polarisation RZ (see Fig. 5.4). Therefore, when considering the optimal overall pre-compensation the alternate-polarisation RZ favours -200ps/nm where the pulses are allowed to overlap 20% more than in the -250ps/nm pre-compensation which was optimum for standard RZ.

5.3 Alternate-Phase RZ modulation format

In the previous section, the alternate-polarisation modulation format was investigated as a possible technique for suppression of intra-channel nonlinear distortion. In addition to alternate-polarisation, nonlinear suppression can also be achieved by alternating the phase between adjacent bits [OHH'01]. Modulation formats with alternating phase are known as alternate-phase RZ (AP-RZ) and are investigated here as an effective alternative to both standard RZ and carrier suppressed RZ (CS-RZ) [MIY'99].

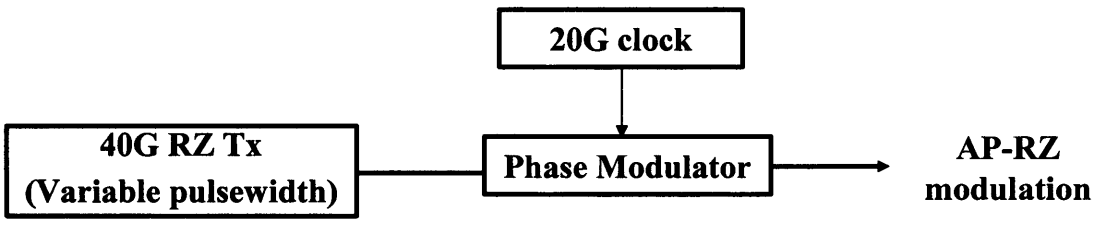

Fig. 5.9 *Schematic diagram for generation of AP-RZ modulation format with variable pulsewidth*

AP-RZ is generated experimentally by imposing a phase modulation onto a conventional RZ signal. This can be achieved by using an additional phase modulator to which a sinusoidal clock signal at half the bit-rate (20 GHz) is applied, as shown schematically in *Fig. 5.9*. A useful feature of this technique is its ability to generate

AP-RZ signals with any desired pulsewidth. In the literature this signal format is also referred to as alternate-chirp RZ (AC-RZ) [OHH'01]. A phase-modulated signal can also be generated using a Mach-Zehnder modulator, as in the CS-RZ format, which is the same as AP-RZ with square phase modulation waveforms and peak-to-peak phase modulation of π rad. However, with the CS-RZ format generated using a Mach-Zehnder modulator the pulsewidth is fixed at 67% of the duty cycle by the modulator transfer function. Although it is impractical to drive a phase modulator with a square wave signal *(Fig. 5.9)*, it is nevertheless investigated in section 5.3.2, as the square-wave phase modulation has been synthesized in optically time-division-multiplexed (OTDM) systems by using a planar lightwave circuit (PLC) as described in [MOR'02].

5.3.1 Suppression of IFWM-induced shadow pulses using AP-RZ signals

It was previously shown how the IFWM leads to signal distortion through emergence of shadow pulses in the 'zero' bit-slots. This effect was investigated by perturbation analysis and compared with numerical split-step-Fourier numerical simulations as described in section 2.6.1. In this section, the suppression of this nonlinear distortion investigated by applying a phase shift of $\Delta\varphi$ between adjacent bits.

For a train of pulses as described by the following equation:

$$A_l = \sum_k A_k(z,t) = \sum_k A(z,t-kT) \qquad (5.1)$$

where T is the bit period and k quantifies the pulse overlap into adjacent bit slots, the expansion of $|A_l|^2 A_l$ (from equation 2.42) gives source terms of the type $A_{T1}A_{T2}A_{T3}^*$, and the linearity of equation (2.42) guarantees that A_p is the sum of the individual contributions from these source terms, as described previously. The contribution from $A_{T1}A_{T2}A_{T3}^*$ falls into bit slot number $T_1+T_2-T_3$. This contribution is due to the IFWM process and manifests itself as amplitude jitter, and shadow pulses depending on whether a signal pulse exists where it occurs.

Analysing the perturbation in bit slot 0 which is non-phase shifted, $A_{T1}A_{T2}A_{T3}^{*}$ and $A_{T1}^{2}A_{T3}^{*}$ give contributions to that bit slot. If all odd bit slots were phase shifted by $\Delta\varphi$, as in the case of alternate-phase modulation, the phase of source term $A_{T1}^{2}A_{T3}^{*}$ is unchanged while that of $A_{T1}A_{T2}A_{T3}^{*}$ is shifted by $2\Delta\varphi$. As these two contributions into the same bit slot now have different phase shifts, tuning the phase modulation can lead to destructive interference between the contributing terms, and suppression of the growth of shadow pulses. Investigation of two-pulse interaction was performed using the perturbation analysis for two pulses A_1 and A_2, and the split-step-Fourier simulations for RZ, and AP-RZ modulation with phase modulation $\Delta\varphi=0$, $\pi/2$ and π radians, showing this effect in *Fig. 5.10*.

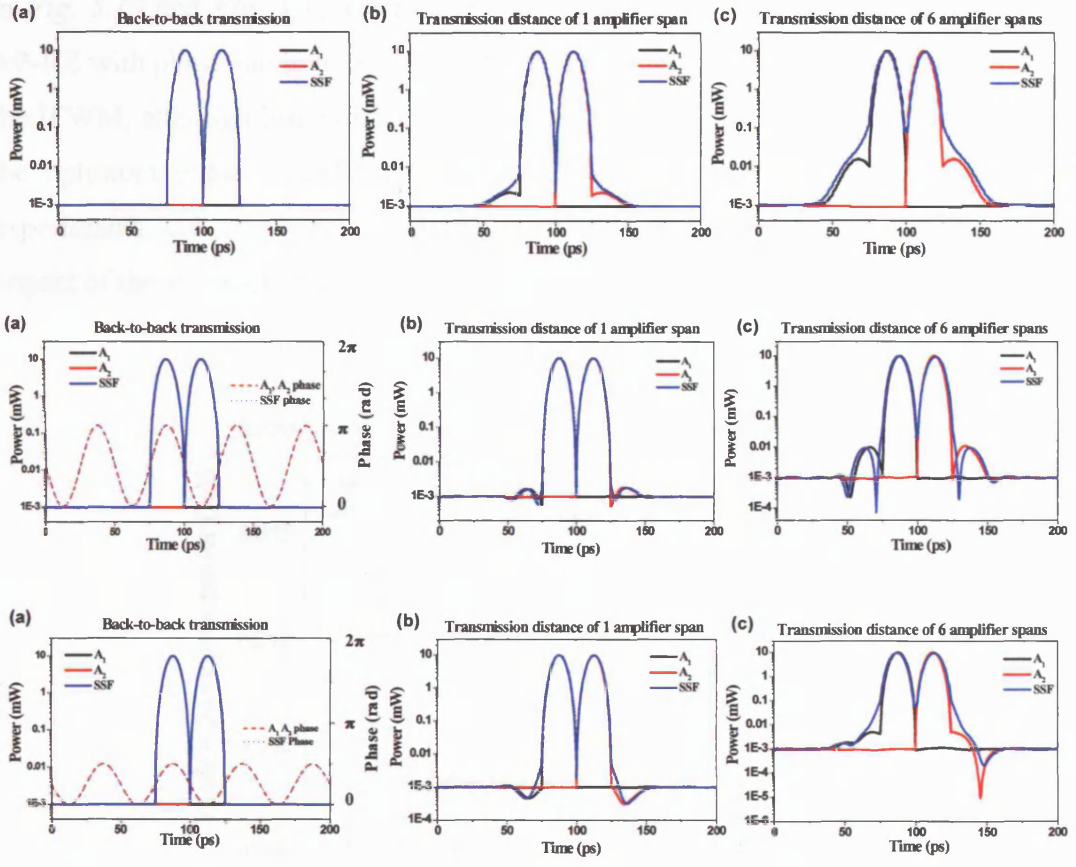

Fig. 5.10 *Signal waveform of two pulses at t = 100ps and 150ps after transmission over (a) back-to-back (b) 60km (c) 360km SSMF with 10mW pulse peak power at output of line amplifiers, showing generated ghost pulses at t = 50ps and 200ps.* ***Top:*** *RZ* ***Middle:*** *π-AP-RZ* ***Bottom:*** *π/2-AP-RZ. Dotted line indicates results obtained by split-step-Fourier numerical simulations*

To investigate the growth of shadow pulses due to IFWM as a function of increasing transmission distance, the standard deviation of power in 'zero' bit-slots are plotted in *Fig. 5.11*. As mentioned previously, higher growth of shadow pulses is obtained using the split-step-Fourier simulations, as this technique incorporates ISI that is not taken into account in the perturbation technique, which treats the two pulses separately and investigates the IFWM nonlinear influence only (therefore eliminating ISI). It can be seen that maximum IFWM is observed for RZ transmission, whilst minimum distortion due to IFWM is seen for AP-RZ transmission with peak-to-peak phase modulation of $\pi/2$ rad, and is in good agreement with the results described in [JOH'02]. However, there is a discrepancy in [JOH'02], where the IFWM efficiency of RZ and AP-RZ with π rad phase modulation should be identical. The results shown in *Fig. 5.10* and *Fig. 5.11* indicate that while maximum suppression is obtained for AP-RZ with phase modulation of $\pi/2$ rad, a phase modulation of π rad also suppresses the IFWM, although less efficiently. It became clear that it is important to investigate the optimum phase modulation for AP-RZ, and verify it further by transmission experiments and numerical simulations. This is work is described next, where the impact of the shape of phase modulation (sinusoidal or square) is also analysed.

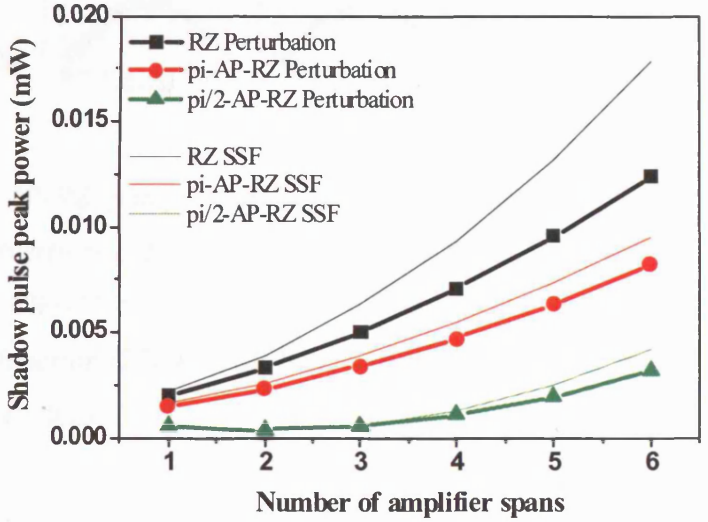

Fig. 5.11 *Calculated shadow pulse peak power for increasing transmission distance for RZ, π-AP-RZ and π/2-APRZ modulation formats, obtained by perturbation analysis and split-step-Fourier (SSF) numerical simulations*

5.3.2 Optimum phase modulation in the AP-RZ modulation format

In this section the characteristics of sinusoidal- and square-wave AP-RZ formats with peak-to-peak values of phase modulation of $\pi/2$ and π rad when transmitted over SSMF are compared. This was done to investigate the effect of chirp from the sinusoidal phase modulation, and also enable comparisons with CS-RZ. In this section however, a similar pulsewidth of 11.25ps (FWHM) was investigated for both shapes of phase modulation, for reasons mentioned at the start of section 5.3. The signal formats and the applied phase modulation are shown schematically, in the time domain, in *Fig. 5.12*.

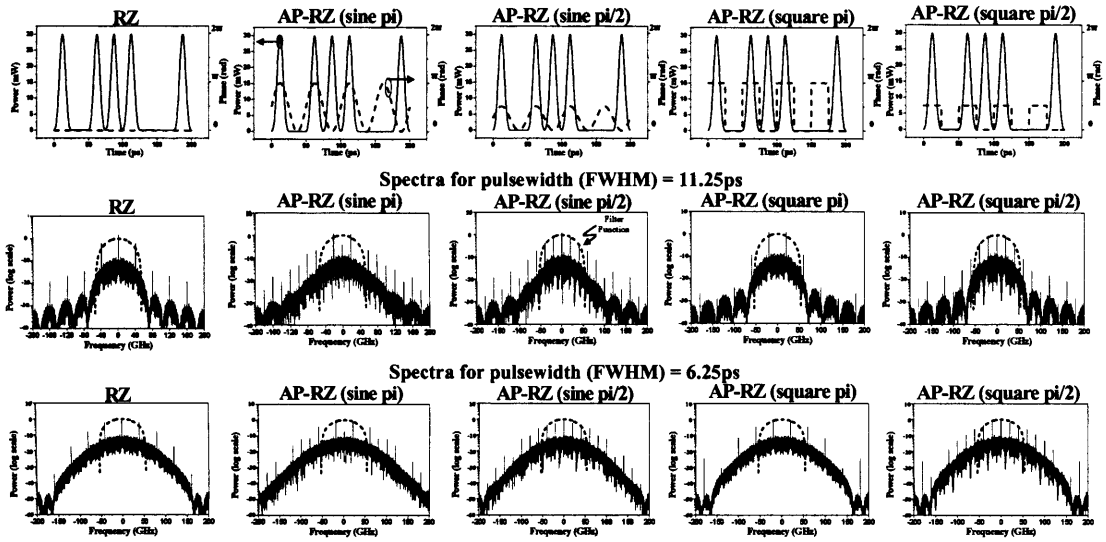

Fig. 5.12 *AP-RZ phase modulation formats (top row) and related spectra (vertical columns) for duty cycles of 45% (FWHM 11.25ps) and 25% (FWHM 6.25ps). The dotted line in the spectra indicates the filter function (75GHz 3dB bandwidth flat-top filter with 100GHz bandwidth at 20dB)*

Section 5.3.1 indicated that the optimum suppression of IFWM occurs for a phase peak-to-peak phase modulation of $\pi/2$ rad [JOH'02]. The optimum value of phase modulation for overall system performance was investigated by calculating the Q-factor as a function of the transmission distance by numerical simulation, particularly when IFWM may not be the limiting distortion. The resultant signal spectra are shown in *Fig. 5.12* for two values of pulsewidths of 6.25ps and 11.25ps, shown for comparison. Variations in transmission performance for different pulsewidths were investigated as the chirping of pulses decreases with the pulsewidth when using fixed sinusoidal phase modulation. It can be seen that the sinusoidal phase modulation results in a broader spectrum compared to square-wave phase modulation owing to the reduction of chirp on the signal. These spectral properties are important if optical pre-filtering of the signals is carried out in order to improve the overall spectral efficiency or if arrayed-waveguide-gratings (AWGs) are used in the multiplexing/de-multiplexing of WDM channels. Throughout section 5.3, the AP-RZ formats with peak-to-peak phase modulation of $\pi/2$ and π rad, are termed as $\pi/2$-AP-RZ and π-AP-RZ, respectively.

As described previously in section 3.3.2, it was necessary to investigate in detail the impact of varying the amount of peak-to-peak phase modulation, comparing $\pi/2$ and π rad, variously explored as optimal [OHH'01, JOH'02, FOR'02]. This requires understanding of the evolution of the differently phase modulated pulses, as determined by the dominant nonlinearity. For each value of peak-to-peak phase modulation the signal is distorted in the presence of IFWM (shadow pulse growth and amplitude distortion) and IXPM (timing jitter) effects, to identify the overall optimum transmission format was investigated by numerical simulation and quantified. In particular, for each AP-RZ format the Q-factor was calculated as a function of the transmission distance and the results are shown in *Fig. 5.13*. The Q-factor takes into account all sources of penalty such as noise, amplitude distortion and timing jitter with a Q factor of 15.56dB corresponding to a BER of 10^{-9}. This level is marked by a dotted line in the graphs shown in *Fig. 5.13*, indicating the maximum transmission distance.

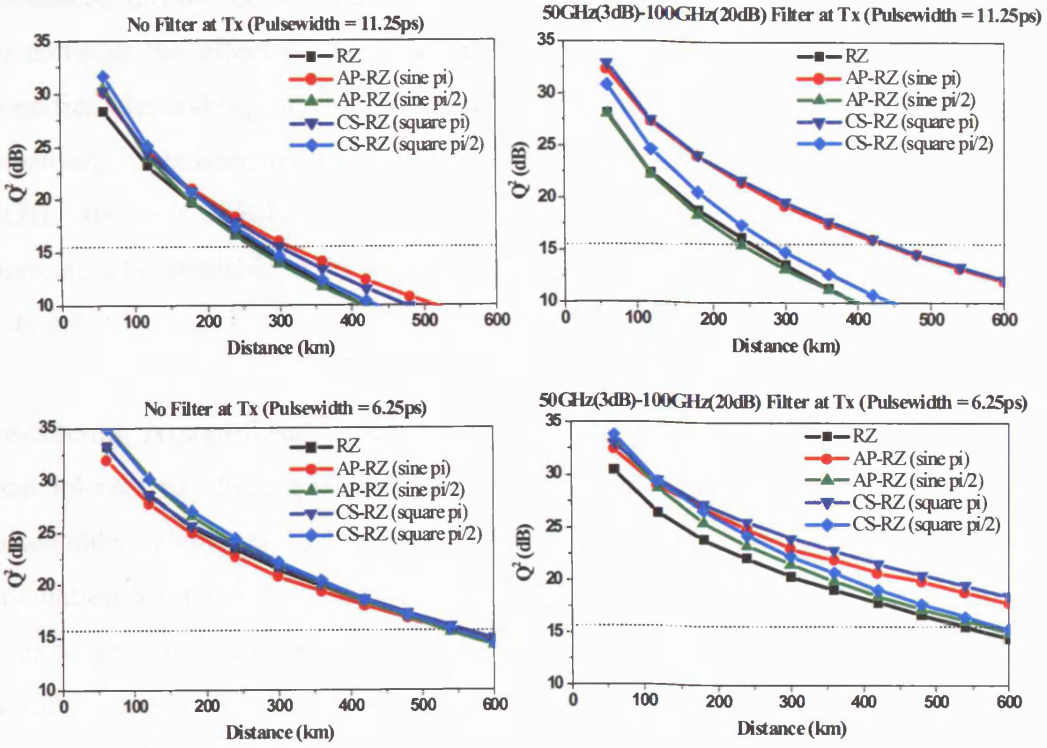

Fig. 5.13 *Results of the achievable Q-factors for increasing transmission distance Left: Non-filtered signals at transmitter, Right: Pre-filtered signals at transmitter, Top: 45% duty cycle (FWHM = 11.25ps), Bottom: 25% duty cycle (FWHM 6.25ps)*

The results in *Fig. 5.13* indicate that transmission performance is significantly improved for the shorter pulses, with a maximum transmission distance of 240km achieved with a pulsewidth of 11.25ps (45% duty cycle) and 540km for a pulsewidth of 6.25ps (25% duty cycle) using the standard RZ modulation format. It is also evident that there is no significant difference between sine and square wave phase modulation at pulsewidths of 6.25ps [MAR'03]. This is because the phase variation is similar in both cases in the middle of the bit slot where the pulse power is at its maximum, and likely to generate the most nonlinear distortion. However, a 1dB improvement is observed for sinusoidal phase modulation compared to square-wave phase modulation in the unfiltered case with pulsewidth of 11.25ps, in good agreement with the results obtained in [OHH'01]. Optically pre-filtering the signal to reduce its bandwidth and allow high spectral efficiency affects the transmission performance. It should be noted that Martensson *et al* investigated the AP-RZ

modulation format for all values of peak-to-peak phase modulation schemes, but did not consider the effect of pre-filtering [MAR'03], which alters the signal spectral properties depending on the value of phase-modulation. *Fig. 5.13* shows the transmission performance of a single channel, pre-filtered by a flat-top filter with 75GHz (0.6nm) 3dB-bandwidth and a 20dB-bandwidth of 100GHz (typical of commercially available AWGs), which would be required in any practical WDM system.

Pre-filtering is significant especially in the π-AP-RZ modulation format, which is most tolerant to filtering where the Q factor is improved by 5dB and 3dB for the pulsewidths of duty cycle 45% and 25% respectively, compared to the standard RZ modulation format at its maximum error-free transmission distance. For a duty cycle of 25%, and no pre-filtering the phase modulation has no significant effect on the overall system Q-factor. It should be noted that the pulse peak power of the pre-filtered signals was lower, leading to reduced nonlinear distortion and hence increased transmission distances with respect to the un-filtered signals. Hence, the results with the pre-filtered signals should not be compared with those of the unfiltered signals. However, the performance within each set of pre-filtered results is still valid for comparing the various modulation formats with similar pulsewidths before filtering.

The results described here show that the overall optimum system Q is achieved with a phase modulation of π rad, rather than $\pi/2$ as asserted in [JOH'02]. Of course, in calculating the Q factors, all sources of penalty giving rise to amplitude distortion and timing jitter were taken into account. However, to understand their relative contribution to the overall penalty, the different sources of impairments must be studied separately and are investigated in the next sections. Given that the behaviour for both sine and square-wave phase modulation is similar (less than 1dB difference), the results for the sinusoidal phase modulated format only are described in the following sections.

IFWM: shadow pulses and amplitude distortion

After transmission over dispersive fibre, while the emergence of shadow pulses can be solely attributed to IFWM, amplitude jitter is a combination of both IFWM and phase-to-intensity conversion of the phase modulation in the AP-RZ signal. The IFWM signal distortion was therefore, analysed separately by calculating the standard deviations of power in the 'zero' and 'one' bit-slots, as functions of transmission distance and the results are shown in *Fig. 5.14* and *Fig. 5.17* respectively.

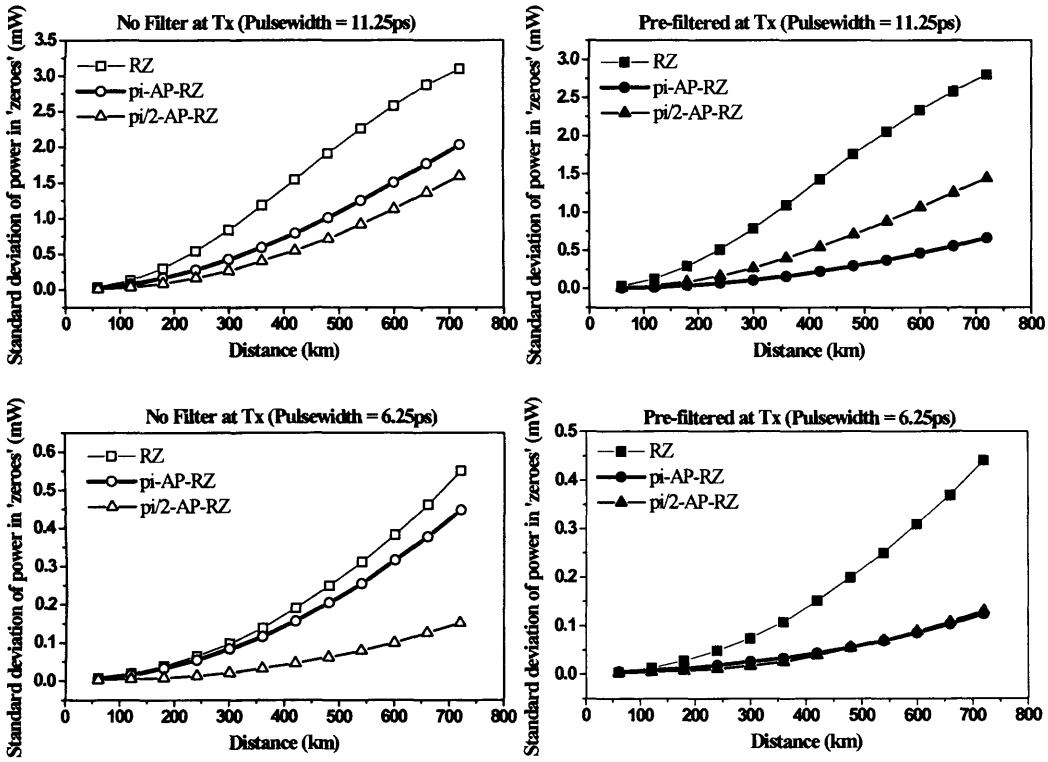

Fig. 5.14 *Calculated growth of shadow pulses calculated as the standard deviation of power in 'zero' bit-slots against transmission distance. Left: Non-filtered signals at transmitter, Right: Pre-filtered signals at transmitter, Top: 45% duty cycle (FWHM = 11.25ps), Bottom: 25% duty cycle (FWHM 6.25ps)*

IFWM-induced shadow pulses are generated by the mixing product resulting from the nonlinear interaction of the overlapping pulses. Changing the phase of one of the participating pulses varies the phase of the resultant mixing product and the IFWM efficiency remains constant [JOH'02]. *Fig. 5.14* shows that the maximum suppression

of the shadow pulses occurs for the π/2-AP-RZ format, due to the destructive interference of the IFWM components generated in the 'zero' bit-slots by the interacting pulses with alternate phase.

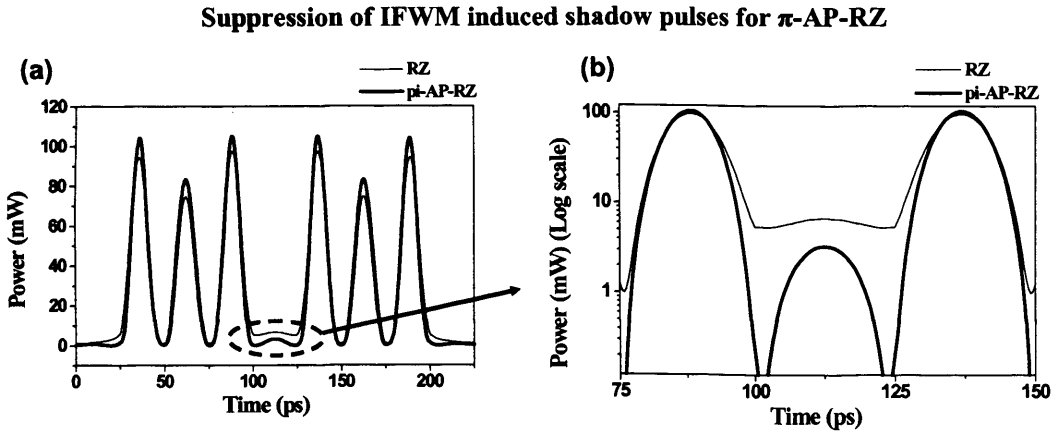

Fig. 5.15 *π-AP-RZ and its suppression of IFWM generated shadow pulses. Signal after 60km transmission at launch peak power of 100mW (a) Linear scale, (b) Log scale*

According to [JOH'02, KAN'03], similar levels of IFWM-induced shadow pulses would be expected for RZ and π-AP-RZ, as shown for two- and three- pulse interactions. However, in a practical system power can exists in a 'zero' bit-slot due the finite modulation extinction ratio, tails from the adjacent 'ones' and pulse broadening. Hence, interference can also take place between this light and the mixing products from IFWM. To illustrate this by way of an example, *Fig 5.15* shows the IFWM-induced shadow pulse in the 'zero' bit-slot of a 1110111 pattern for RZ and π-AP-RZ showing the generation of the observed shadow pulses by numerical simulation. The generated shadow pulse with π-AP-RZ is a factor of 3 lower than that with RZ. This suppression of the IFWM effect can be explained by the destructive interference of the IFWM-induced shadow pulse with the existing light in the zero bit-slot arising from the effects mentioned earlier. Indeed this is confirmed by the non-filtered results in *Fig. 5.14*, which shows that the standard deviation of power in the 'zero' bit slots is lower for the π-AP-RZ modulation format compared to that of the standard RZ transmission. This effect was also confirmed by the perturbation analysis in section 5.3.1

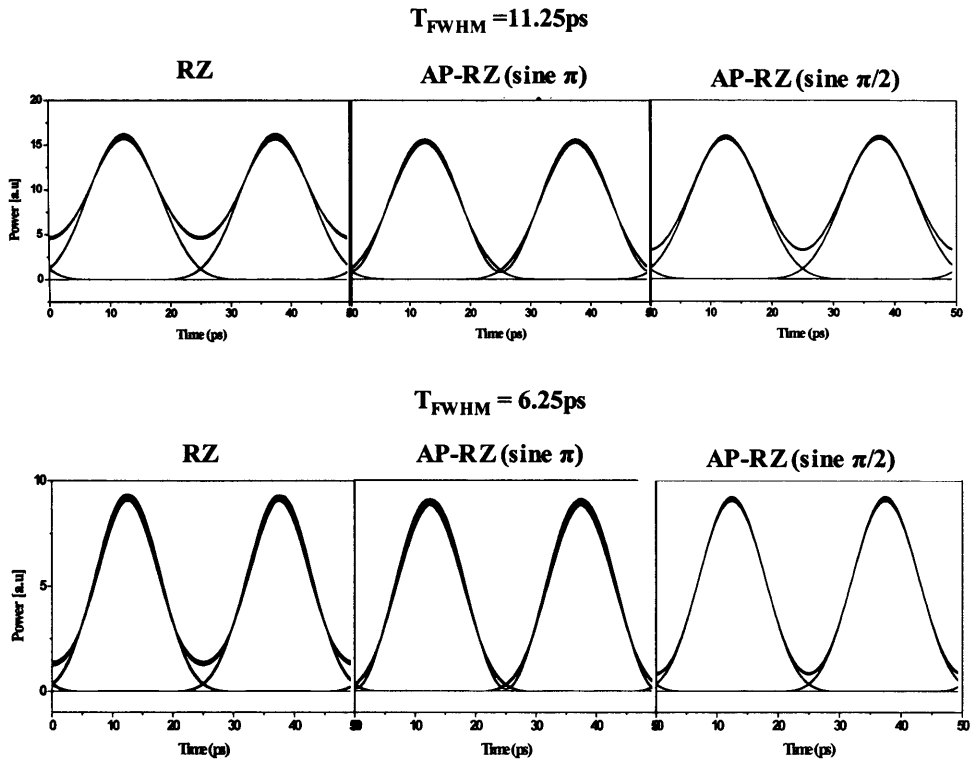

Fig. 5.16 *Phase modulation and its effect on pre-filtering for AP-RZ signals with sinusoidal phase modulation. Filter parameters: 75GHz 3dB bandwidth flat-top filter with 100GHz bandwidth at 20dB*

The pulse broadening induced by pre-filtering of the signal was simulated, and the resultant eye diagrams are plotted in *Fig. 5.16*. It shows that the different modulation formats are affected differently by pre-filtering the signal, and the π-AP-RZ modulation format is least affected by pulse broadening, as shown in [AGA'03]. As the pulsewidth impacts the generation of IFWM-induced shadow pulses, the π-AP-RZ signal leads to maximum suppression of shadow pulses due to IFWM when pre-filtering is employed for the 11.25ps pulse modulation formats. For pre-filtered 6.25ps pulses the pulsewidths are similar for all modulation formats, and the improvement of the suppression of the IFWM-induced shadow pulses in the π-AP-RZ and π/2-AP-RZ modulation formats compared to the standard RZ modulation format are due to the destructive interference on the IFWM product, as discussed earlier. There is no significant change in the IXPM as a result of pre-filtering (see *Fig. 5.18*)

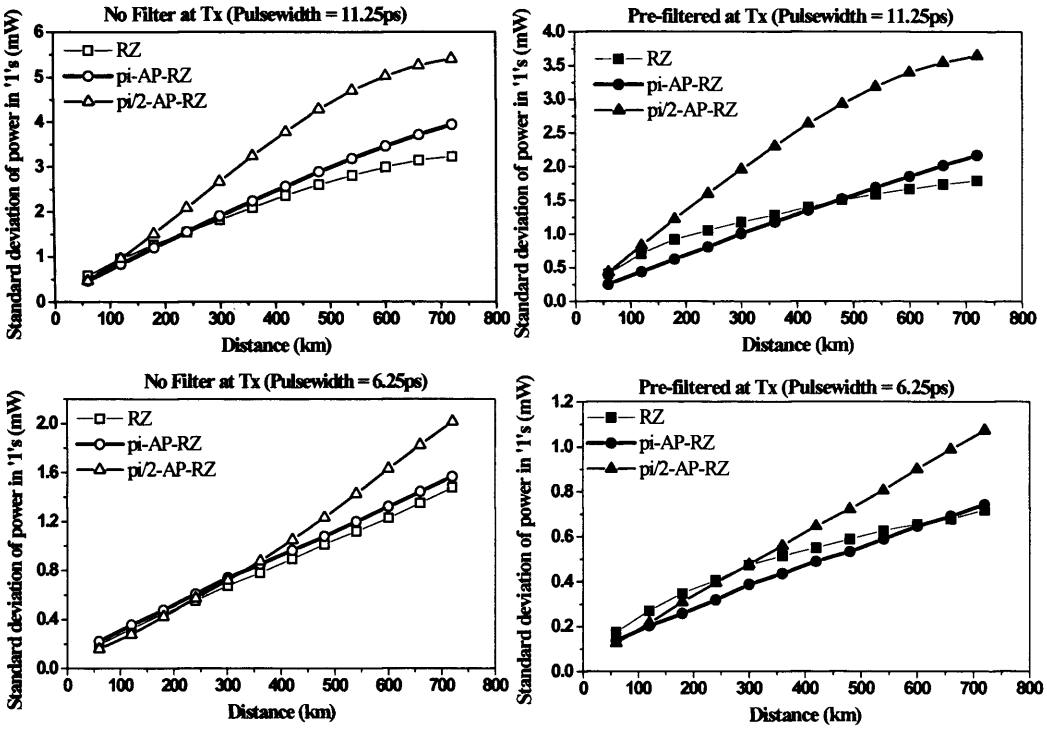

Fig. 5.17 *Calculated growth of amplitude distortion calculated as the standard deviation of power in the 'ones' against transmission distance. Left: Non-filtered signals at transmitter, Right: Pre-filtered signals at transmitter, Top: 45% duty cycle (FWHM = 11.25ps), Bottom: 25% duty cycle (FWHM 6.25ps)*

Fig. 5.17 shows the calculated amplitude distortion for the RZ, π/2-AP-RZ and π-AP-RZ modulation formats. While the π/2-AP-RZ signal gave maximum suppression of the shadow pulses, the amplitude distortion is larger than for the other modulation formats. This is because of the phase-to-intensity conversion generated by the phase modulation, and resulting impact on the SPM distortion which is proportional to the pulse peak power. This effect is emphasized by the fact that the standard RZ signal with no phase modulation is less affected by amplitude jitter compared to the phase modulated formats.

Thus it can be concluded that IFWM-induced shadow pulses in the AP-RZ format can be suppressed, albeit by unequal amounts, either by creating destructive interference of the IFWM components in the 'zero' bit-slots (π/2-AP-RZ) or by the destructive interference of the IFWM component with the tails of adjacent pulses in the 'zero' bit-

slot (π-AP-RZ). Although maximum suppression of IFWM-induced shadow pulses is obtained in the π/2-AP-RZ modulation format, when considering the effect of pre-filtering, and amplitude distortion due to phase-to-intensity conversion, the π-AP-RZ modulation format is optimum.

IXPM: timing jitter effects

Having analysed the penalty due to the growth of shadow pulses and amplitude distortion due to IFWM, the signal distortion due to IXPM was then analysed. To understand the impact of the timing jitter, the simulated eye diagrams were processed within each bit-slot on a normalized time scale. The timing jitter was calculated as the mean standard deviation of the leading and trailing edges at the FWHM of the pulses. This timing jitter was calculated for increasing transmission distance, for each modulation format and is shown in *Fig. 5.18*.

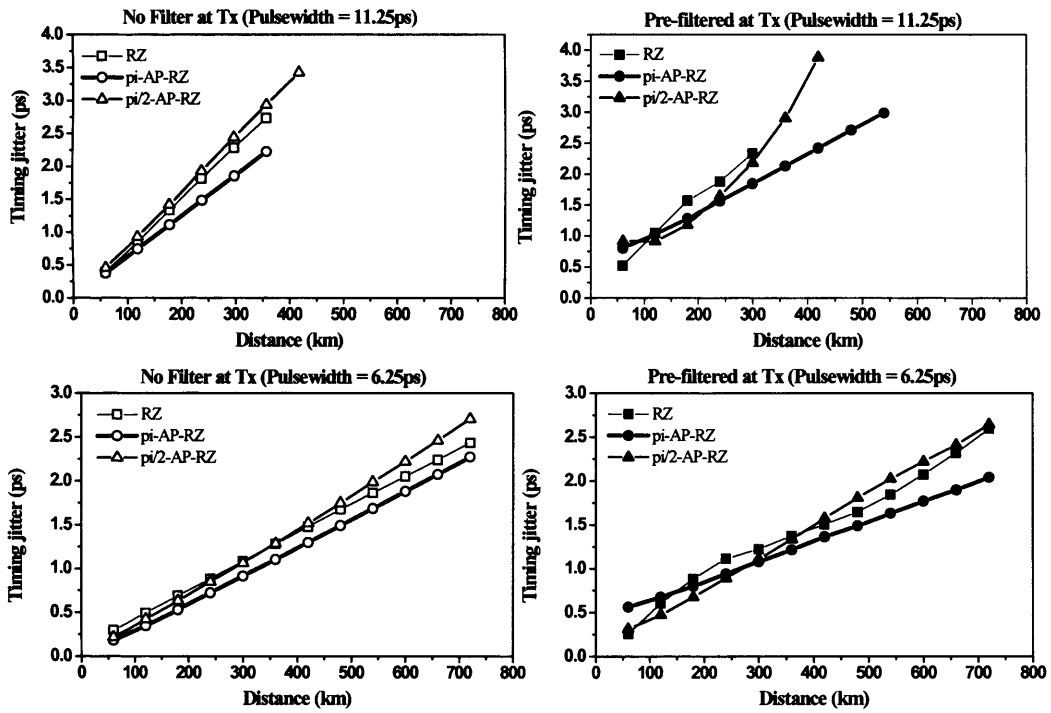

Fig. 5.18 *Calculated timing jitter, defined as average standard deviation of the leading and trailing edges at the FWHM against the transmission distance. Left: Non-filtered signals at transmitter, Right: Pre-filtered signals at transmitter, Top: 45% duty cycle (FWHM = 11.25ps), Bottom: 25% duty cycle (FWHM 6.25ps)*

The IXPM-induced timing jitter is dependent only on the time separation [MEC'01], pulse overlap and rate of change of power of leading and trailing edges, between interacting pulses [MAM'99]. The magnitude of phase modulation does not directly affect the generation of IXPM. Indeed, the results showing the timing jitter as a function of transmission distance in *Fig. 5.12* indicate that the timing jitter variation is within ~1ps for all modulation formats. However, in all cases the $\pi/2$-AP-RZ signal suffers most from timing jitter, while the π-AP-RZ signal suffers the least. It should be noted that it was not possible to calculate the timing jitter when the Q-factor is significantly lower than 15.56dB and the signal distortion is severe, as the leading and trailing edges become indistinguishable due to inter-symbol-interference.

Summary of simulation results: It can be concluded from these simulations that there is no significant difference in varying the phase modulation with a sinusoidal or square waveform. Hence, the AP-RZ format can be employed in both electrical-time-division-multiplexed signals in series with a phase modulator driven by a sinusoidal signal, or in optical-time-division-multiplexed signals where the phase is varied similar to a square wave form by the use of planar lightwave circuits (PLC) [MOR'02]. It was found that for a pulsewidth of 11.25ps (FWHM), the transmission performance is improved by less than 1dB for sinusoidal phase modulation compared to square-wave phase modulation, while at pulsewidths of 6.25ps (FWHM) there is no discernable difference between the two. It can also be concluded that the $\pi/2$ phase modulation is, indeed, optimum for suppressing the growth of shadow pulses due to IFWM, as has been suggested previously [JOH'02]. However, when considering the overall signal distortion induced by effects such as IXPM-induced timing jitter and phase-to-intensity conversion, the π-AP-RZ modulation format is the optimum. The advantages of the π-AP-RZ modulation format are further enhanced when the signals are pre-filtered at the transmitter for optimizing spectral efficiency, as would be required for WDM systems. For narrow pulses with no pre-filtering the timing jitter is the limiting distortion and, hence, employing phase modulation gives no significant benefit.

The results described show an improvement in transmission performance due to alternating phase between adjacent pulses compared to the standard RZ modulation format by suppressing nonlinear distortion. As described in chapter 4, the intra-channel nonlinear distortion can be further suppressed through dispersion management. The following section investigates the combination of pre-compensation at the transmitter and AP-RZ modulation format for optimised transmission performance. Unlike in RZ transmission, as the AP-RZ pulses are chirped (sinusoidal phase modulation), the optimum pre-compensation was expected be different to that obtained for RZ, and requires further justification of the theory governing pre-compensation at the transmitter, described in Chapter 4.

5.3.3 Alternate-phase RZ and pre-compensation

As already described in chapters 3 and 4, pre-compensating the pulses prior to transmission can be used to suppress the intra-channel nonlinear distortions for RZ signals. This implies that transmission performance of AP-RZ with pre-compensation, compared to standard RZ, should also be investigated to exploit the suppression of intra-channel nonlinear distortion obtained both by optimising the modulation format, as well as the corresponding dispersion map. It is necessary to investigate the optimum pre-compensation with the AP-RZ modulation format, as the nonlinear behaviour of the AP-RZ format is different from that of the standard RZ modulation format. It has been show in [FOR'02] that the optimum pre-compensation is determined by the value of phase modulation in the AP-RZ format. Therefore, it is interesting to investigate whether the results showing π-AP-RZ format to give the best performance apply in the general case, when pre-compensation at the transmitter is used.

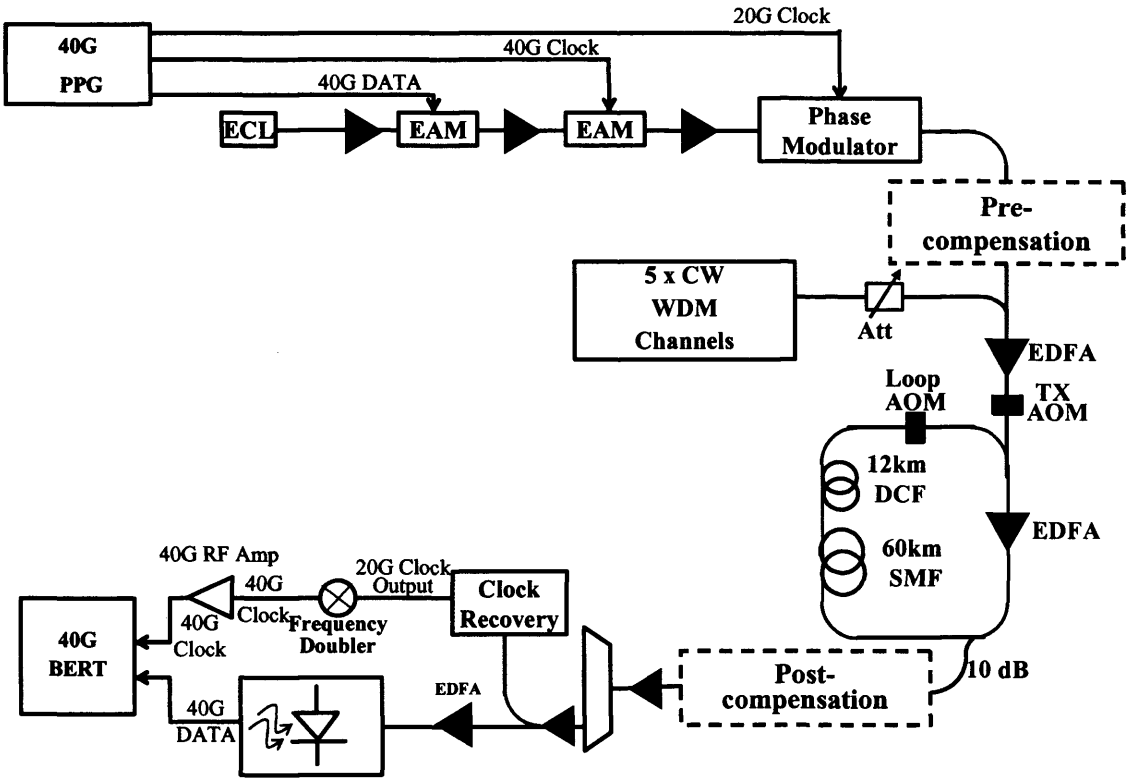

Fig. 5.19 *Experimental recirculating loop set-up with π-AP-RZ and simultaneous pre-compensation*

To explore this, the experimental set-up, shown in *Fig. 5.18*, used the ETDM RZ transmitter for generating a PRBS sequence on 2^{23}-1 with pulsewidth 11.25ps. The RZ signal was then passed through a phase modulator driven by a 20GHz clock signal, inducing a π rad optical phase difference between adjacent pulses, to generate the π-AP-RZ format, without any pre-filtering. The residual dispersion of -8ps/nm, was compensated by a tuneable dispersion compensator (HOM-DMD concatenated with fixed lengths of fibre with known dispersion) as part of the post-compensation before the receiver.

Pre- and post- compensation, with optimum values of dispersion determined in the simulations *(Fig. 5.20)*, were experimentally implemented by cascading appropriate lengths of normal and anomalous dispersion fibre ensuring that the cumulative dispersion over the entire transmission distance was close to zero, as measured on a Agilent chromatic dispersion analyser test-set. The signal power launched into the

pre- and post-compensators was approximately 0dBm, ensuring minimum nonlinear distortion in these fibres.

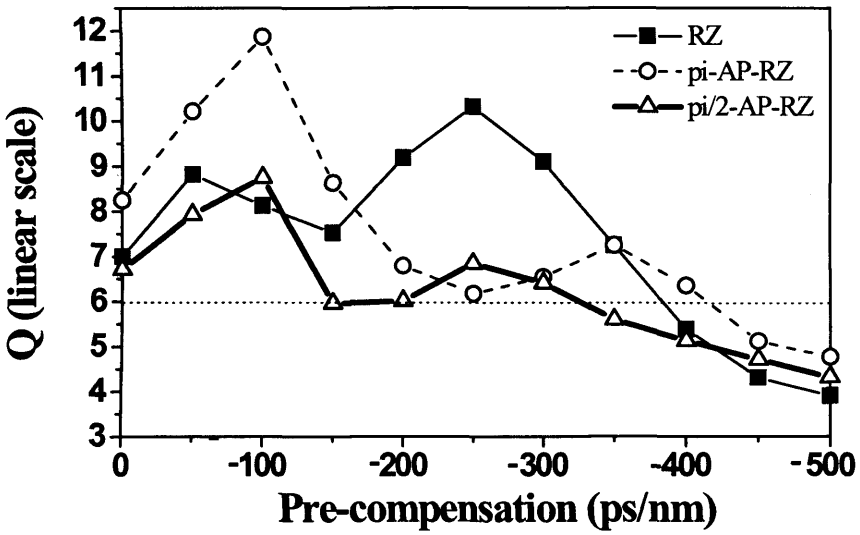

Fig. 5.20 *Calculated linear Q-factors vs pre-compensation for a 240km SMF transmission link*

To select the optimum amount of pre-compensation, the Q-factors were calculated from simulations for a transmission distance of 240km as a function of pre-compensation for RZ, π-AP-RZ and π/2-AP-RZ, and are shown in *Fig. 5.20*. With 0ps/nm, the π-AP-RZ format achieves the highest Q factor, and continues to give the better performance as the value of pre-compensation is increased up to -160ps/nm, with an optimum Q-factor of 12 at -100ps/nm. However, with pre-compensation values greater than -160ps/nm, the RZ format gives the higher Q-factor, with a peak value of 10.4 at -250ps/nm.

For the π/2-AP-RZ modulation format, the optimum Q-factor of 8.7 was also obtained at a pre-compensation of -100ps/nm. This was considerably lower than that obtained for both the RZ (20%) and π-AP-RZ (33%) modulation formats. This result is consistent with that presented in [FOR'02, Fig. 4], even though the values of the link length and pulsewidth investigated were different to those considered in this work. Overall these results indicate that a peak-to-peak phase modulation of π rad (π-AP-RZ) is the optimum value for AP-RZ transmission, and the experiments were focused

on the investigation of the π-AP-RZ format to understand its performance in combination with pre-compensation to further suppress the intra-channel nonlinear distortion. The values of pre-compensation selected for the experiments were 0ps/nm, -100ps/nm and -250ps/nm. The pulse broadening factor described in section 2.3 is calculated for propagation in the SSMF amplifier span used in these experiments 0ps/nm and -250ps/nm pre-compensation, shown in *Fig. 5.21*.

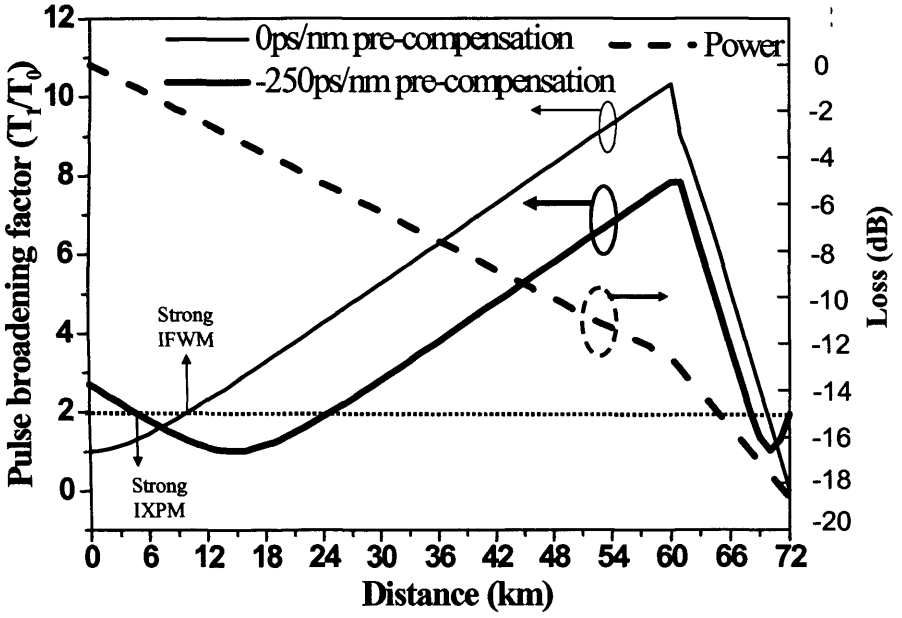

Fig. 5.21 *Dispersion-induced pulse broadening within an amplifier span and the effect of pre-compensation (Standard RZ modulation format)*

For RZ transmission with no pre-compensation, IXPM is strongest at the beginning of the link when there is partial overlap of the pulses. However, as the pulses start to broaden, as a result of dispersion, the IFWM becomes the dominant effect. The optimum pre-compensation ensures that pulsewidth is optimised at the start of the amplifier spans when power is at its highest, for simultaneous suppression of IXPM and IFWM. Furthermore, with pre-compensation the pulses are first compressed and then broadened, as the net dispersion varies from negative to positive. This results in partial cancellation of the IXPM-induced distortion at the beginning of each span, while IFWM is minimized as the pulse overlap is still 25% lower when compared to the case of 0ps/nm pre-compensation (see *Fig. 5.21*). In the case of the π-AP-RZ format the optimum pre-compensation of -100ps/nm was less than the -250ps/nm

required for the standard RZ format, as the π-AP-RZ results in two different amounts of pulse broadening due to the opposite chirp in adjacent pulses. This effect is described in section 2.3.1 and in more detail in chapter 6 *(Fig. 6.6)*. Furthermore, as AP-RZ is more tolerant to IFWM effects, the signals can tolerate an increase in pulse overlap compared to standard RZ resulting in the decrease in the value of pre-compensation required at the transmitter.

Like in previous experiments, the nonlinear and linear limits measured for maximum and minimum launch powers at which a BER<10^{-9} was achieved was measured. These measurements were performed for the 40Gbit/s RZ transmission with 0ps/nm and -250ps/nm pre-compensation at the transmitter and also for π-AP-RZ transmission with 0ps/nm, -100ps/nm and -250ps/nm pre-compensation at the transmitter as shown in *Fig. 5.22*.

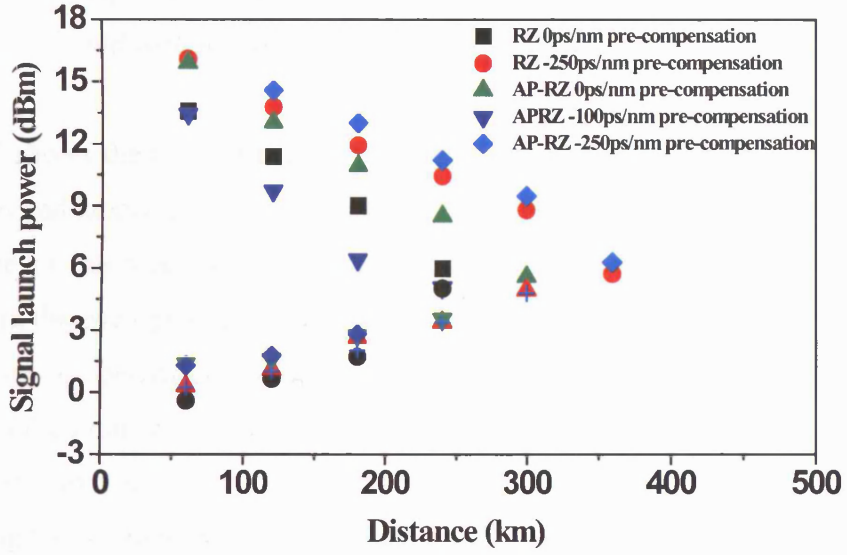

Fig. 5.22 *Launch power range for BER<10^{-9} for RZ and AP-RZ transmission for 0ps/nm and optimised pre-compensation at the transmitter*

From *Fig. 5.22*, it can be seen that with 0ps/nm pre-compensation, the alternate-phase of the AP-RZ signal results in a 2.6dB increase in the nonlinearity-limited launch power after 240km compared to that of the RZ. With pre-compensation of -250ps/nm the nonlinear limit for the RZ format is increased by 4.5dB for the same distance

compared to transmission with 0ps/nm pre-compensation. For the same pre-compensation of -250ps/nm, the π-AP-RZ is the least tolerant to nonlinear effects, as predicted by the simulations *(Fig. 5.20)*. The highest nonlinear limit was obtained with π-AP-RZ format, with the lower value of pre-compensation of -100ps/nm. In this case, the maximum launch power was 0.5 dB higher than the optimum values with RZ for a distance of 240km. The 2dB variation in the linear limit between the different modulation formats and compensation schemes is caused by the decrease in OSNR due to loss in pre-compensation fibre.

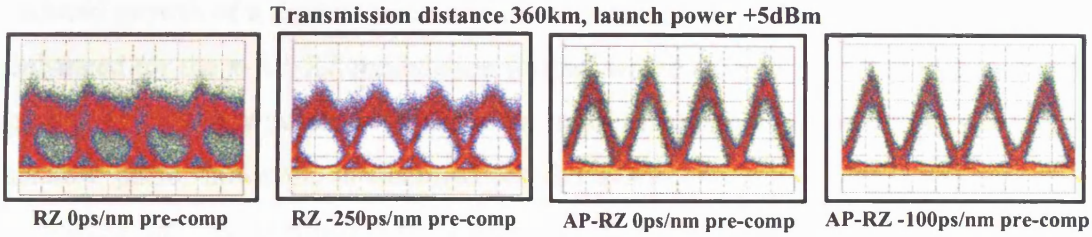

Fig. 5.23 *Improved eye-opening for comparison between RZ and AP-RZ with and without optimum pre-compensation*

Fig. 5.23 shows the experimentally measured eye diagrams at a transmission distance of 360km and launch power +5dBm, the optimum power in all cases. There is a clear advantage of the π-AP-RZ modulation format, with respect to standard RZ, when comparing the eye opening of RZ with 0ps/nm pre-compensation with π-AP-RZ with 0ps/nm pre-compensation. As the dispersion profile of the link is identical in both cases, and the improvement can be solely attributed to the alternate-phase modulation. The suppression of nonlinear distortion due to pre-compensation is evident when comparing the RZ modulation format with 0ps/nm and -250ps/nm pre-compensation.

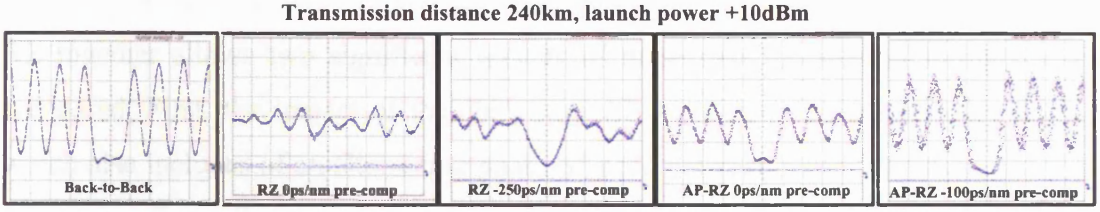

Fig. 5.24 *Experimentally measured shadow pulses and its suppression by AP-RZ and pre-compensation*

Fig. 5.24 shows a comparison of an identical segment of the PRBS consisting of a '111110111111' pattern, where the growth of the shadow pulse is most clearly visible, owing to the many IFWM contribution from the interacting 'ones' appearing in the single 'zero' bit slot. The transmission distance was fixed at 240km and the launch power increased to +10dBm in order to maximize the IFWM effect. For the RZ modulation format with 0ps/nm pre-compensation, the 'zero' bit slot is completely masked by the growth of the shadow pulse and SPM-induced pulse broadening. However with pre-compensation of -250ps/nm the 'zero' bit slot is maintained with reduced growth of a shadow pulse and inter-symbol-interference. This effect is further enhanced for the π-AP-RZ modulation format, where at 0ps/nm pre-compensation the growth of a shadow pulse is visible in the 'zero' bit slot. Maximum suppression of the shadow pulse, however, is obtained for the π-AP-RZ format with -100ps/nm pre-compensation, as predicted by simulation and observed in the experimentally measured nonlinear-limited launch power graph in *Fig. 5.22*.

When considering the use of pre-compensation to improve the suppression of intra-channel nonlinear distortion it is important to consider the two cases of phase modulation, because unlike in square-wave phase modulation (eg. CS-RZ), the sinusoidal phase modulation chirps the pulses. Hence, the dispersion properties for the two cases are different and the optimum pre-compensation could be expected to be different.

5.3.4 Comparison of AP-RZ with CS-RZ in the presence of pre-compensation

As mentioned in the literature review in chapter 3, AP-RZ was proposed as an alternative to CS-RZ with improved nonlinear tolerance. Analysing AP-RZ and CS-RZ together allows two significant aspects of these two modulation formats to be compared. First, the impact of the chirp in π-AP-RZ can be compared with CS-RZ which also includes of an alternating phase of π rad between adjacent pulses, but with zero chirp. Secondly, the advantage of the reduced duty cycle, which is tuneable in the case of AP-RZ and fixed at 67% for CS-RZ, can be compared. The optimum pre-compensation was shown to be independent of pulsewidth in chapter 4, and is

therefore valid in the comparison of π-AP-RZ with pulsewidth of 11.25ps (FWHM) and CS-RZ with pulsewidth of 16.5ps (FWHM), consistent with Mach-Zehnder generation of CS-RZ in experimental systems. In order to investigate these effects, the Q-factor was calculated as a function of transmission distance for both π-AP-RZ and CS-RZ modulation formats by numerical simulation at a launch power of +5dBm, and the results plotted in *Fig. 5.25*.

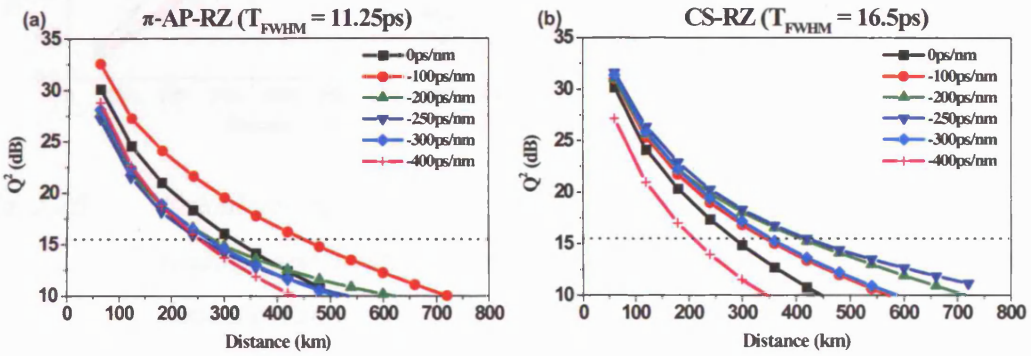

Fig. 5.25 *Simulation of Q-factor as a function of pre-compensation (a): π-AP-RZ modulation format (b): CS-RZ modulation format for transmission over SSMF*

The results shown in *Fig. 5.25* indicate that the optimum phase modulation for sine-wave (π-AP-RZ) and square-wave phase (CS-RZ) modulation was -100ps/nm and -250ps/nm respectively. The difference in the optimum pre-compensation can indeed be explained by the chirp of the signal in the sinusoidal phase modulated case. As the square wave phase modulation induces no chirp on the signal, the optimum phase modulation is identical to that obtained for standard RZ (chapter 4). Furthermore, a 2dB improvement in transmission performance is obtained using the π-AP-RZ modulation format compared to CS-RZ and is consistent with the literature [OHH'01].

Having investigated the overall transmission performance, the IXPM and IFWM distortion was then analysed separately in the presence of pre-compensation. *Fig. 5.26* plots the calculated timing jitter, defined as the average standard deviation of the leading and trailing edges at the full-width-half-maximum (FWHM) as a function of the transmission distance. While *Fig. 5.27* shows the standard deviation of power in

the 'zero' bit slots, which corresponds to the growth of IFWM-induced shadow pulses.

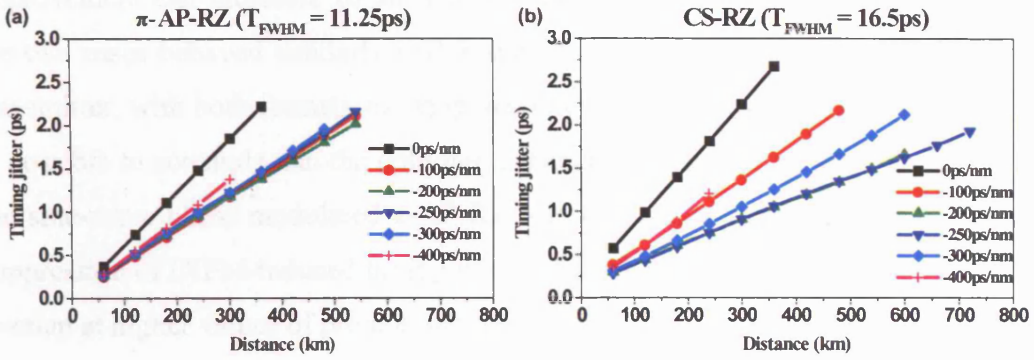

Fig. 5.26 *Calculated timing jitter, defined as average standard deviation of the leading and trailing edges at the FWHM against the transmission distance. (a): π-AP-RZ (b): CS-RZ*

Fig 5.26 shows that the timing jitter is at its maximum for 0ps/nm pre-compensation in both modulation formats. Maximum suppression of IXPM-induced timing jitter is achieved for pre-compensation in the region of -100ps/nm to -200ps/nm for the π-AP-RZ modulation format. For CS-RZ signals however, maximum suppression of IXPM is achieved for a pre-compensation of -250ps/nm, as expected for signals with zero chirp. Further increase in pre-compensation does not improve the timing jitter in either format.

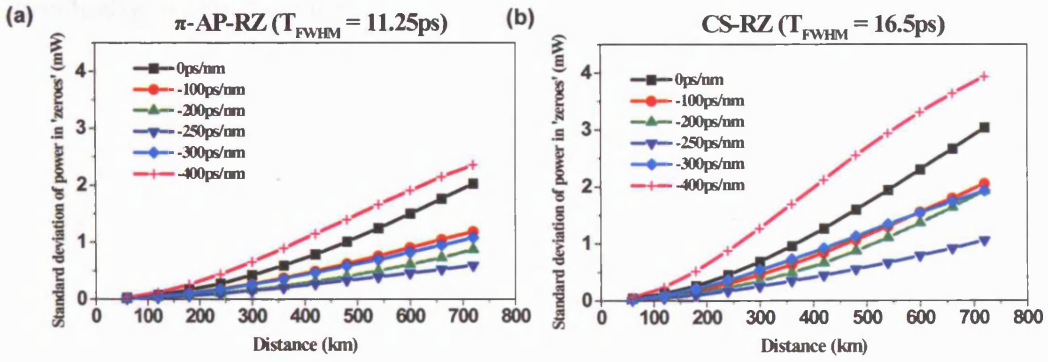

Fig. 5.27 *Calculated growth of shadow pulses calculated as the standard deviation of power in 'zero' bit-slots against transmission distance. (a): π-AP-RZ (b): CS-RZ*

In the case of IFWM-induced shadow pulses the π-AP-RZ modulation format was less affected compared to the CS-RZ modulation format *(Fig. 5.27)*, and this improvement can therefore be attributed to the chirp present in π-AP-RZ. However, the two cases behaved similarly with respect to the value of pre-compensation at the transmitter, with both formats showing maximum suppression at -250ps/nm. Hence, it is possible to conclude that the optimum pre-compensation of -100ps/nm obtained for the sine-wave phase modulated π-AP-RZ was lower than that for CS-RZ due to the suppression of IXPM-induced timing jitter, where the chirp decreases the partial pulse overlap at higher values of pre-compensation.

It can be seen that the combination of advanced modulation formats and pre-compensation achieves over 5dB greater suppression of intra-channel nonlinear distortion compared to using each scheme individually. The use of pre-compensation lends itself to all modulation formats, although the optimum pre-compensation has been shown to vary with the modulation format used. It is, therefore, desirable to have a modulation format which suppresses the nonlinear distortion by a similar amount without requiring any pre-compensation at the transmitter. In this work, alternate-polarisation, and AP-RZ have been demonstrated individually to achieve this. However, their improvement in nonlinear tolerance may not be considered to be cost efficient in some commercial systems. As such, an enhanced modulation format combining both alternate-polarisation and alternate-phase was investigated to explore its effectiveness in achieving nonlinear suppression greater than that of each format individually, without the use of pre-compensation at the transmitter.

5.4 Combination of alternate-polarisation RZ and alternate-phase RZ modulation formats

So far this chapter has described the application of alternate-polarisation RZ and alternate-phase RZ modulation formats for the suppression of intra-channel nonlinear distortion. It was also shown that these two modulation formats could be employed with an optimum pre-compensation to give further improvement in transmission performance. This section investigates a simple simultaneous implementation of alternate-polarisation RZ with AP-RZ to investigate if this yields a modulation format capable of doubling the nonlinear suppression.

In 40Gbit/s OTDM transmission the use of alternating polarisation has been shown to be effective in reducing intra-channel nonlinear interactions between adjacent pulses, as described in section 5.2. However, as nonlinear distortion still occurs due to interactions between pulses in each 20Gbit/s tributary channel, which have the same polarisation, the technique proposed here would suppresses this nonlinear interaction by alternating the phase between such co-polarised pulses. This is shown schematically in *Fig. 5.28*.

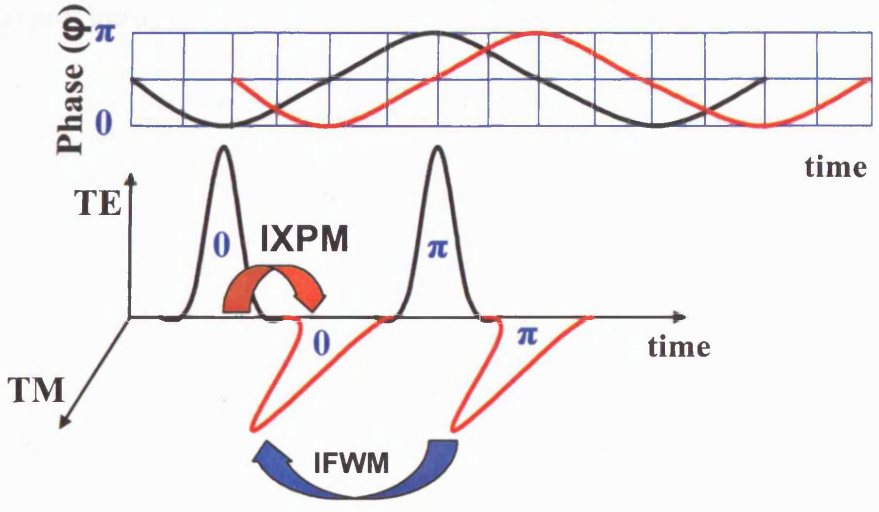

Fig. 5.28 *Alternate -polarisation and -phase combined RZ modulation format*

To investigate the effectiveness of this combined suppression technique the experimental set-up shown in *Fig. 5.29* was used. Two cascaded OKI electro-absorption modulators driven by a 20Gbit/s data signal (2^{23}-1 PRBS) with 50% duty cycle and 40GHz clock signal, respectively, were used to generate a 20Gbit/s RZ signal with FWHM pulsewidth of 11.25ps. The 20Gbit/s data signal was generated by two 10Gbit/s PRBS streams which were fed into the 1st and 3rd ports of an electrical 4:1 multiplexer operating at 40Gbit/s with the 2nd and 4th ports terminated giving the same pulsewidth as in previous experiments. The resultant 20Gbit/s optical signal was modulated using a phase modulator driven by a 10GHz clock signal, generating a 20Gbit/s AP-RZ signal. This was divided and delayed by a single stage passive time-division-multiplexer stage, enabling the polarisation in one arm to be adjusted to give orthogonal polarisation between adjacent bits (alternate-polarisation) of the multiplexed 40Gbit/s signal. The 40Gbit/s signal was pre-amplified and launched into a recirculating loop with SSMF amplifier spans as used in previous experiments described in this thesis. As before, the loop span residual dispersion of -8ps/nm, was compensated by a tuneable dispersion compensator before the receiver. The polarisation of the signal entering the loop was adjusted to give the minimum bit-error-rate for all measurements. Investigation of the signal degradation due to intra-channel nonlinear distortion was carried out by varying the signal launch power as described previously.

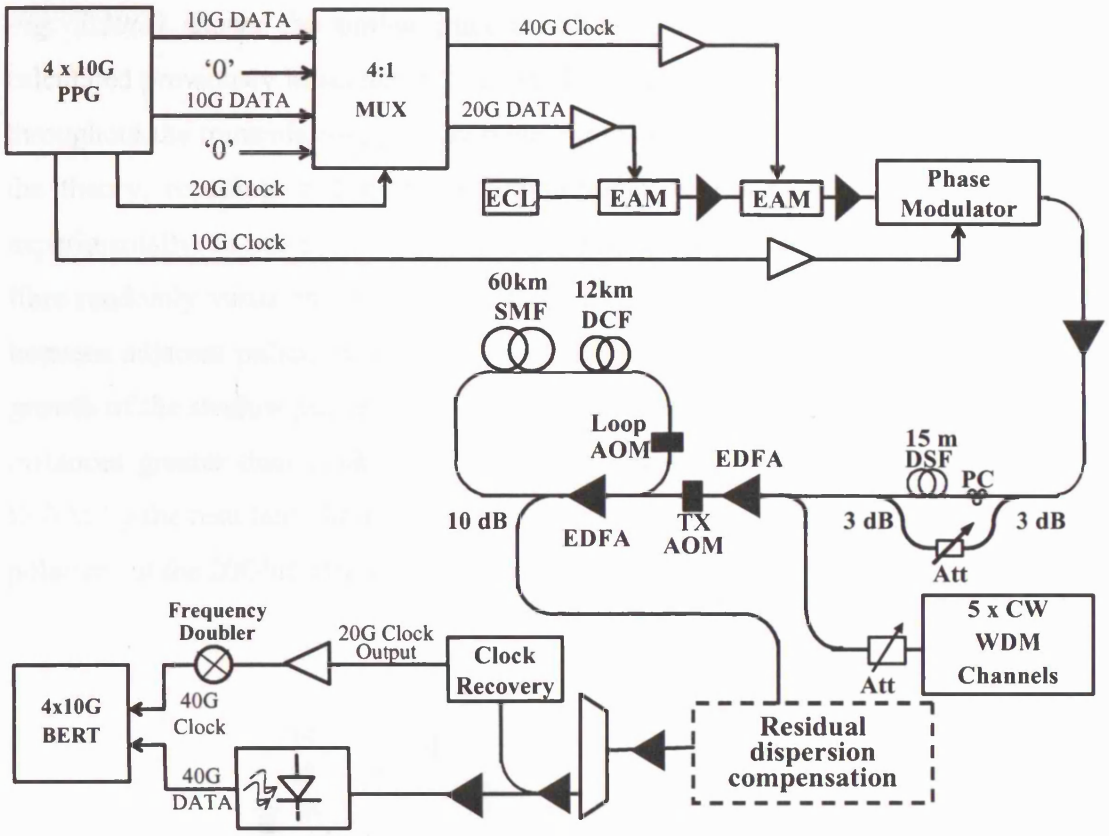

Fig 5.29 *Alternate -polarisation and alternate-phase combined RZ modulation format transmitter and recirculating loop experimental set-up*

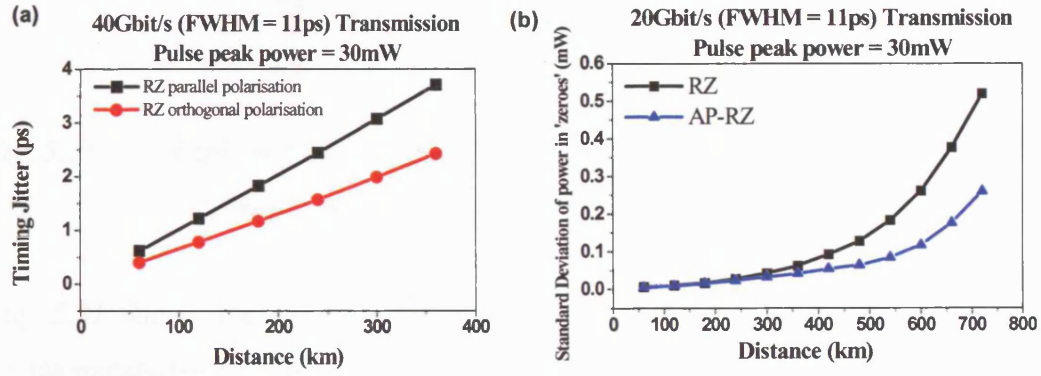

Fig. 5.30 *Simulations: (a) Timing jitter with increasing distance for 40Gbit/s standard RZ transmission with parallel and alternate polarisation (b) Increase in growth of shadow pulses for 20Gbit/s RZ transmission with and without alternate-phase with peak-to-peak value of π radians*

Fig. 5.30(a) shows the timing jitter at 40Gbit/s due to alternate-polarisation, as calculated previously in section 5.2. The pulses were assumed to be linearly polarised throughout the transmission, thereby reducing the IXPM by a factor of 3 according to the theory, resulting in longer transmission distances compared to that expected experimentally. In practice, as explained earlier, the birefringence of the transmission fibre randomly varies the polarisation state, resulting in an average IXPM reduction between adjacent pulses by a factor of 2 [CHE'96, AGR'01]. *Fig. 5.30(b)* shows the growth of the shadow pulses with increasing distance, which are nearly 50% lower at distances greater than 360km for the AP-RZ signal due to the suppression of the IFWM by the resultant phase mismatch between the overlapping pulses which are co-polarised at the 20Gbit/s tributary channel rate.

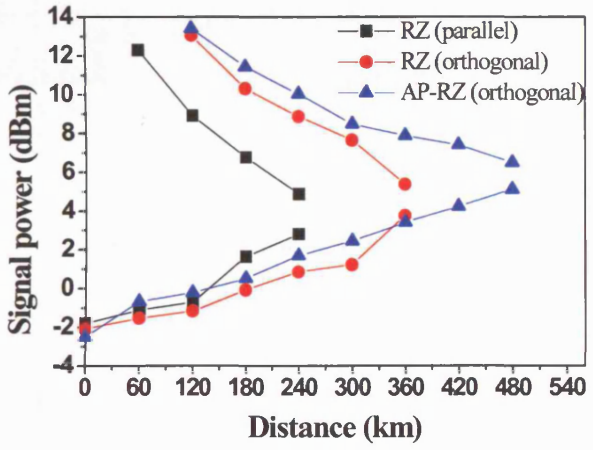

Fig. 5.31 *Experimental results: Maximum and minimum launch powers for 40Gbit/s transmission over SSMF giving BER<10^{-9}*

Fig. 5.31 shows the experimentally measured nonlinear limit (high power limit) versus transmission distance. For standard RZ transmission, with parallel polarisation between the adjacent bits, the maximum achievable transmission distance was 240km, at a launch power of +5dBm (as in previous experiments). For the alternate-polarisation only scheme, the maximum transmission distance was increased by 120km (50% improvement) to 360km, at an optimum launch power similar to that of the standard RZ case. However, at the transmission distance of 240km the results show a 4dB increase in the nonlinear limit, indicating the reduced nonlinear

interaction between the adjacent bits, as a result of the alternate-polarisation. The results of the combined AP-RZ and alternate-polarisation scheme in *Fig. 5.31* show that the nonlinear limit was increased by 5.1dB at 240km. Furthermore, it enabled a transmission distance of 480km, twice the maximum transmission distance achieved for standard RZ transmission. The experimentally measured eye diagrams are shown in *Fig. 5.32* for transmission over 360km at a signal launch power of +8.5dBm. The experimental results show that the transmission performance can be optimised by employing a combination of alternate-phase modulation and alternate-polarisation for suppressing the intra-channel nonlinear distortions for transmission at 40Gbit/s.

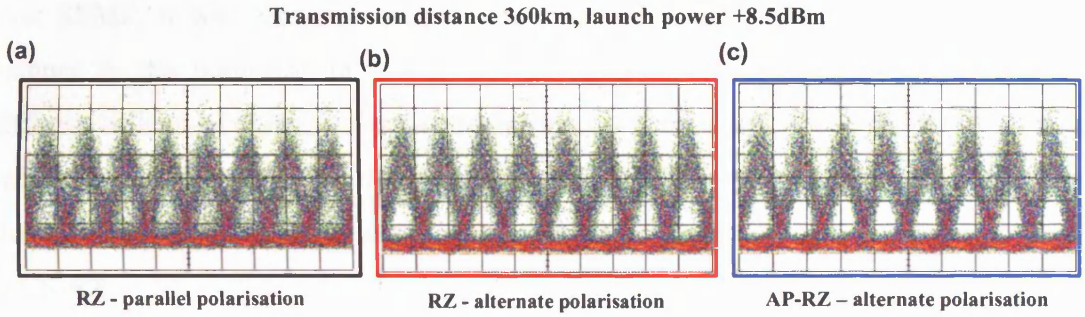

Fig. 5.32 *Improved eye-opening for comparison between (a) RZ (b) alternate-polarisation RZ and (c) alternate-polarisation and alternate-phase combined RZ at a transmission distance of 360km and launch power +8.5dBm*

5.5 Summary

In this chapter, the suppression of intra-channel nonlinear distortion was demonstrated by use of the alternate-polarisation modulation format. Alternate-polarisation reduces the IXPM-induced timing jitter by 50% and the IFWM-induced amplitude jitter and shadow pulses by 30%. The high local dispersion of the SSMF leads to nonlinear interaction between the co-polarised pulses at 20Gbit/s, while the polarisation changes from linear to elliptical during transmission leading to a higher signal distortion compared to that of the theory.

It was found by simulation that the π-AP-RZ modulation format was the optimum for all cases, with and without pre-compensation. The technique of combining pre-compensation with the π-AP-RZ modulation format for maximum suppression of the intra-channel nonlinear distortions was investigated experimentally for the first time. The pre-compensation of -250ps/nm for standard RZ modulation gave a 4.5dB improvement in the nonlinear limit. The π-AP-RZ resulted in a 2dB improvement for 0ps/nm pre-compensation and 5dB improvement for the optimum -100ps/nm pre-compensation compared to the standard RZ transmission. These results yielded the optimum value for the phase modulation and pre-compensation to allow increased transmission distances in the highly dispersed pulse propagation regime at 40Gbit/s over SSMF. It was also shown that while AP-RZ and CS-RZ behave in a similar manner in the nonlinear investigation, the chirping caused by AP-RZ results in different values of optimum pre-compensation, where CS-RZ behaves in a similar fashion to the standard RZ modulation format. However, for suppression of intra-channel nonlinear distortion a 2dB improvement is observed for π-AP-RZ compared to CS-RZ.

The novel technique of combining the alternate-phase RZ with alternate-polarisation to suppress the dominant intra-channel nonlinear distortion at 40Gbit/s over SSMF was proposed and described. The results showed that it is possible to double the maximum transmission distance to 480km by using this scheme compared to a maximum distance of 240km achieved with a standard RZ transmission. The results also show a 5.1dB increase in the nonlinearity-limited launch power at a distance of 240km for this signal format compared to the standard RZ scheme.

Chapter 6 Dispersion tolerances of 40Gbit/s signals

A major constraint of optical transmission at channel bit rates of 40Gbit/s and higher is that they suffer from significantly reduced tolerances towards dispersion and nonlinear effects. The advanced modulation formats described thus far, showed the ability to improve nonlinear tolerances compared to the standard RZ modulation format. The experiments described, however, investigated the nonlinear tolerance for transmission in the presence of 100% dispersion compensation, although commercially deployed fibre links often suffer from incomplete dispersion compensation owing to the variable lengths between repeater stations and the fixed step sizes of the dispersion compensation modules. The impact of in-line residual dispersion *(see Fig 2.5),* due to incomplete dispersion compensation in each amplifier span, on the transmission performance for different modulation formats becomes key in the design of the next generation transmission systems, and the tolerance of any format to incomplete dispersion compensation is of utmost importance. This chapter investigates the dispersion tolerance of the AP-RZ modulation format (π-AP-RZ) which was highly tolerant to nonlinear distortion, and is compared against the RZ and CS-RZ modulation formats. This investigation was studied for linear and nonlinear signal propagation of these formats using an amplifier span with variable residual dispersion, in a recirculating loop test-bed. This helped to understand the optimum trade-off which exists between nonlinear and dispersion tolerance of the different modulation formats.

6.1 Experimental technique for investigating in-line residual dispersion

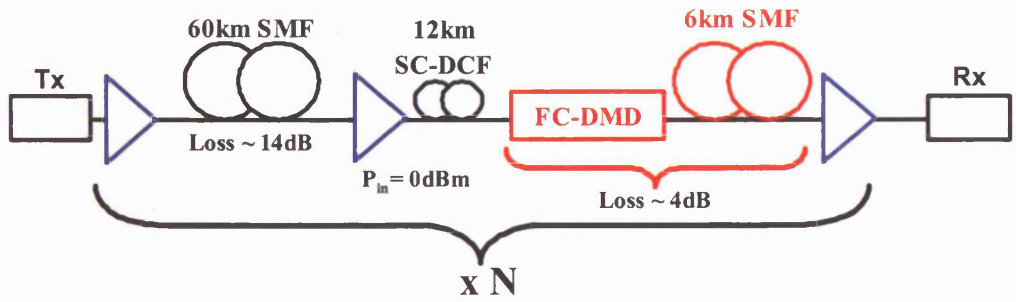

Fig. 6.1 *Schematic diagram of the amplifier span used for investigating the impact of in-line residual dispersion during transmission in a single span recirculating fibre loop test-bed.*

The amplifier span shown in *Fig. 6.1* consisted of 60km SSMF compensated by 12km of slope compensated DCF (SC-DCF), the same basic transmission span used in all the experimental investigation over SSMF in chapters 4 and 5. The dispersion profile of these two fibre types is shown in *Fig. 4.5*, and was used in the experiments described thus far with dispersion compensation at the receiver when a large number of recirculations were investigated. For the purpose of varying the in-line residual dispersion compensation, a further 6km of SSMF was placed along with a field configurable HOM-DMD. The field configurable DMD had a non-zero dispersion slope and consisted of 4 possible dispersion settings (step size of 10ps/nm), a similar device to that described in [RAM'02b]. The dispersion profile of the complete amplifier span in *Fig. 6.1* is shown in *Fig. 6.2*. It shows the increase in dispersion slope due to the additional fibre elements. The amount of in-line residual dispersion per span could, therefore, be continuously varied and accurately set to ±0.5ps/nm by changing the transmitter wavelength. The residual dispersion in the amplifier span is variable in the range +32ps/nm to -48ps/nm, over the range of transmitter wavelengths from 1540-1560nm, using the 4 settings on the HOM-DMD. For the purpose of this work, however, the range of residual dispersion of ±15ps/nm was investigated in the amplifier span and is indicated by the shaded region in *Fig. 6.2*. This technique for investigating different dispersion maps is simpler and more flexible compared to varying the length of the transmission fibre or using different fibre sets. In addition, as the dispersion elements are entirely fibre based, there are no filtering elements present, avoiding the cascading penalty caused by non-ideal continuously tuneable dispersion compensators inside the loop [KUZ'99, KUZ'00, ROU'02].

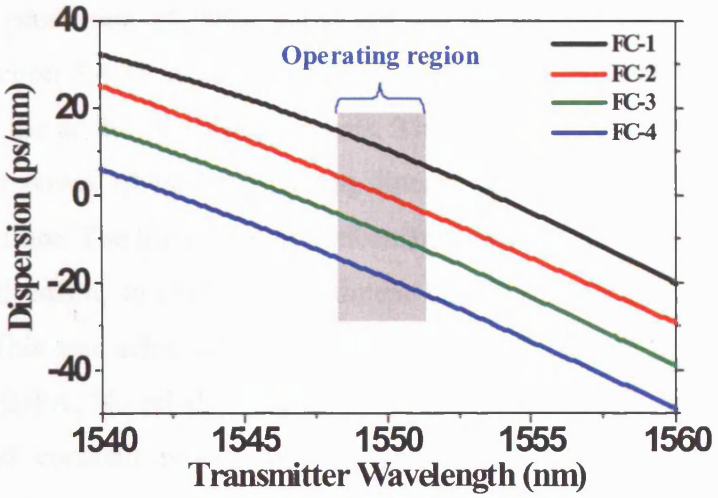

Fig. 6.2 *Measured dispersion of amplifier span consisting of 60km SSMF compensated by 12km of SC-DCF, with further HOM-DMD and 6km of SSMF, enabling dispersion variation by wavelength tuning*

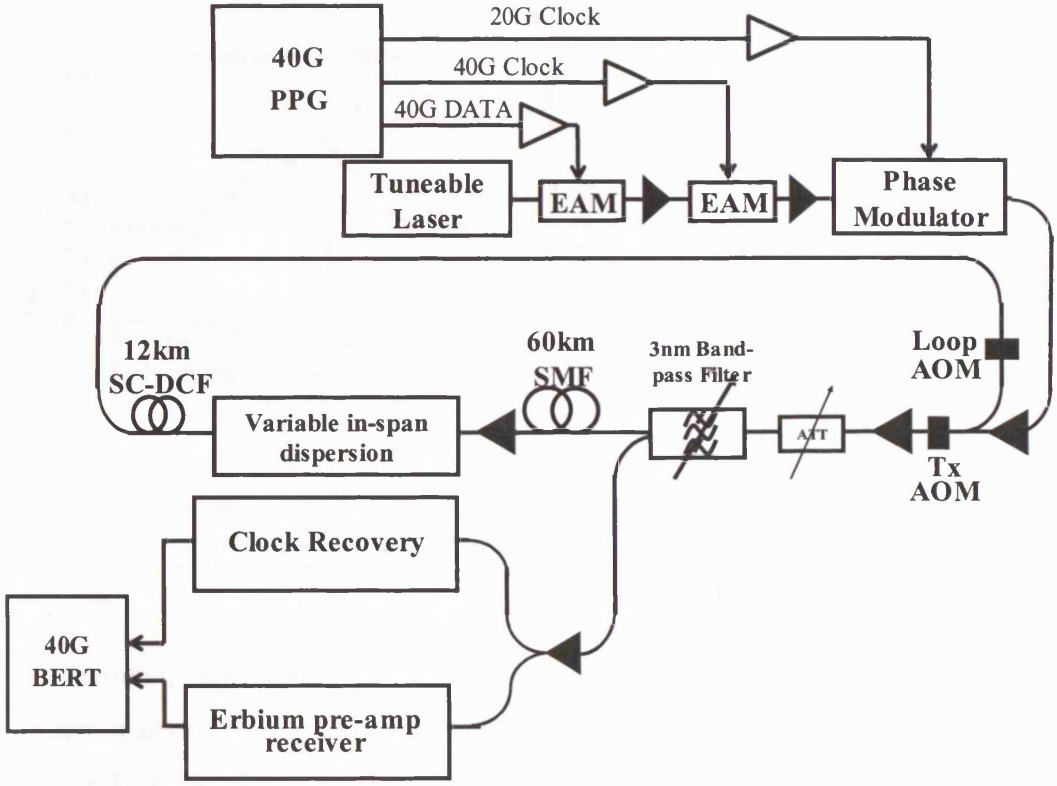

Fig. 6.3 *Experimental set-up for investigation of in-line residual dispersion tolerance for the RZ and AP-RZ modulation format*

The experimental set-up used for the investigation of dispersion tolerance is shown in *Fig. 6.3*. The generation of the RZ and AP-RZ modulation format is as described previously (section 5.4.3). A second loop amplifier was required to compensate the 5dB loss from the additional fibre elements. The second loop amplifier was operated with an output power of 0dBm, ensuring linear transmission within the dispersion compensating fibre. The transmission performance was investigated at launch powers of +5dBm and 0dBm, to study the nonlinear and linear transmission performance, respectively. This was achieved by using a variable optical attenuator in front of the transmission EDFA. No rebalancing of the loop was necessary, as the second loop EDFA ensured constant power into the transmission EDFA. This differs from previous experiments described in this thesis, where the signal launch power was varied by varying the coupling ratio between the signal channel and 5 CW WDM channels into the amplifier, without the need for a second loop EDFA. Furthermore, this set-up with the dispersion compensation placed between two EDFAs improves the OSNR in the recirculating loop by over 5dB, as described in section 2.8.1.

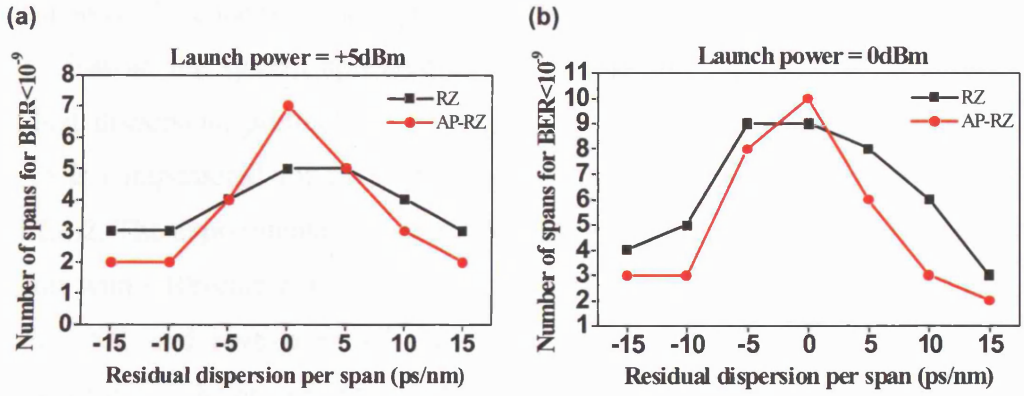

Fig. 6.4 *Experimental results of maximum transmission distance as a function of the residual dispersion per span at signal launch power of (a) +5dBm (b) 0dBm*

The maximum achievable transmission distance was measured for a link with amplifier spans with ±15ps/nm in-line residual dispersion. These measurements were taken for both the RZ and AP-RZ modulation formats. In order to investigate the impact of linear and nonlinear transmission, signal launch powers of +5dBm and 0dBm, were used. *Fig. 6.4* shows the maximum transmission distance (BER<10^{-9}) as

a function of the residual dispersion per span. From these results it can be seen that for transmission over amplifier spans with 0ps/nm residual dispersion, at a launch power of +5dBm the AP-RZ modulation format resulted in a maximum achievable transmission distance of 420km, compared to 300km achieved with the RZ format. This corresponds to a 40% increase in transmission distance, due to the enhanced suppression of the intra-channel nonlinear distortion in the AP-RZ format, as described previously in section 5.3. Reducing the launch power to 0dBm reduced this improvement to 11%, where maximum transmission distances of 600km and 540km were achieved for AP-RZ and RZ, respectively. This confirmed suppression of nonlinear distortion as the cause of the improvement in performance with AP-RZ. The maximum achieved transmission distance of 540km for RZ and 600km for AP-RZ is longer than those achieved previously (section 5.3). This was due to the improved OSNR in the recirculating loop, as the dispersion compensating fibre was placed between two EDFAs, as described in section 2.8.1.

It can also be seen from the results in *Fig. 6.4* that the maximum achievable transmission distance is not symmetrical either side of the 0ps/nm residual dispersion point, instead the system appeared to favour slightly positive (under-compensated) residual dispersion, particularly for RZ signals. This behaviour is typical of SPM, which is compensated for by slight positive dispersion, as described in sections 2.3 and 2.4.2. The experimental and simulated eye diagrams at a transmission distance of 240km with +10ps/nm residual dispersion per span of the RZ transmission is shown in *Fig. 6.9,* and reveals raised cross over point between adjacent bits, which is characteristic of the presence of SPM, and therefore confirming this effect.

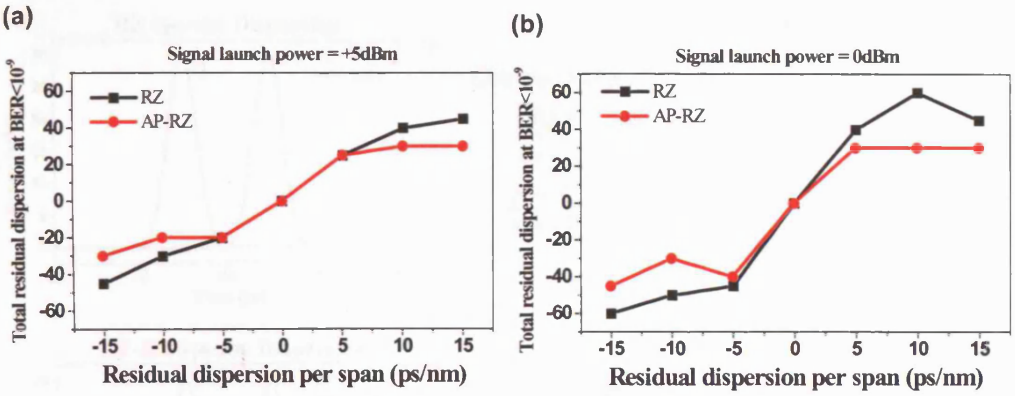

Fig. 6.5 *Experimental results of total residual dispersion at which BER<10^{-9} is achieved (a) +5dBm (b) 0dBm*

To obtain the maximum tolerable residual dispersion, the residual dispersion per span is multiplied with the maximum number of spans at which a BER<10^{-9} is achieved, as obtained from *Fig. 6.4*, and is plotted in *Fig. 6.5*. It can be seen that for transmission at +5dBm launch power the dispersion tolerances for the RZ and AP-RZ modulation formats are ±45ps/nm and ±30ps/nm, respectively. These tolerances are increased when the nonlinear distortion is decreased (0dBm launch power) and are ±60ps/nm for RZ and -45→+30ps/nm for AP-RZ. In the absence of nonlinear distortion, the maximum transmission distance is limited by the accumulation of ASE noise with increasing number of amplifier spans. However, it should be noted that the maximum tolerable residual dispersion at the receiver of each modulation format is independent of the in-line residual dispersion in each amplifier. This is shown in *Fig. 6.4(b)* where the variation in total residual dispersion is less than 15ps/nm for all cases of in-line residual dispersion, despite the significant difference in transmission distance.

In order to understand the effect of chirp (present in AP-RZ) in the presence of uncompensated dispersion, two consecutive pulses of the RZ and AP-RZ modulation format were simulated for propagation in the presence of 0ps/nm and +10ps/nm dispersion. The back-to-back pulses and the pulses after propagation in the presence of +10ps/nm dispersion are shown in *Fig. 6.6*.

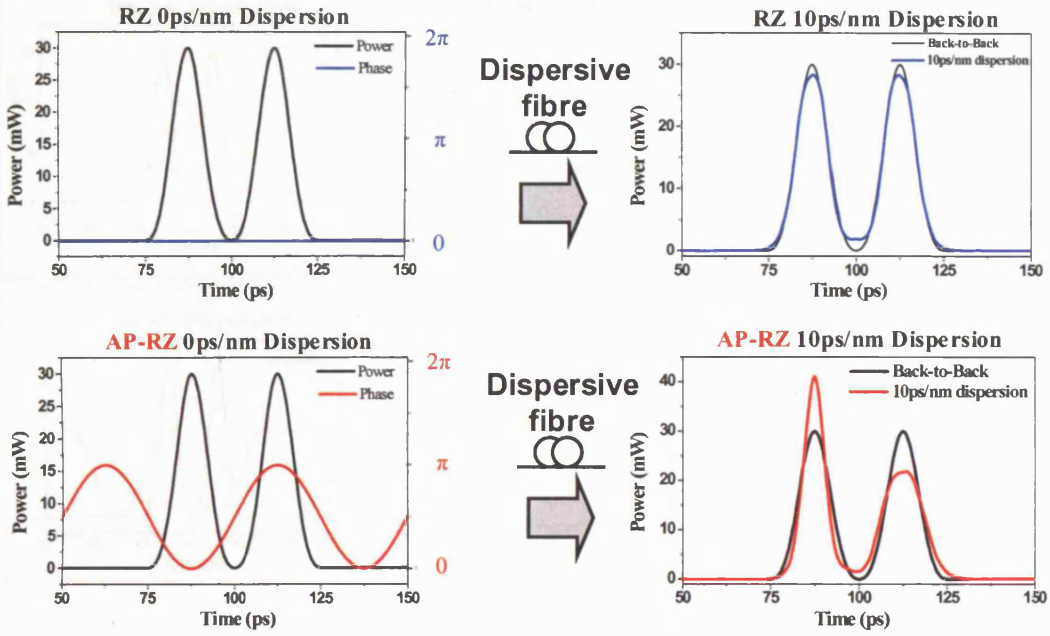

Fig. 6.6 *Signal distortion in the AP-RZ modulation format due to phase-to-intensity modulation (PM-IM) in the presence of uncompensated dispersion*

Fig. 6.6 can be analysed to study the dispersion properties and explain the tolerance results of the RZ and AP-RZ modulation format. In the presence of +10ps/nm dispersion the RZ pulses shows 0.005% pulse broadening and reduction in the pulse peak power. The sinusoidal phase modulation of the AP-RZ format results in adjacent pulses being oppositely chirped. Thus, in the presence of positive dispersion the negatively chirped pulse undergoes 32% pulse compression and increase in peak power, while the positively chirped pulse undergoes pulse broadening and decrease in peak power by a similar amount. This behaviour is characteristic of phase-to-intensity modulation (PM-IM) conversion, and is detected as amplitude jitter at the receiver, which distorts the signal, and reduces the overall dispersion tolerance of AP-RZ, compared to RZ.

While PM-IM is significant in AP-RZ the opposite phase between adjacent pulses decreases the ISI. Hence, this effect was investigated for propagation over higher values of dispersion, such as +50ps/nm and +100ps/nm, for the same two consecutive pulses described previously, and the results are plotted in *Fig. 6.7*.

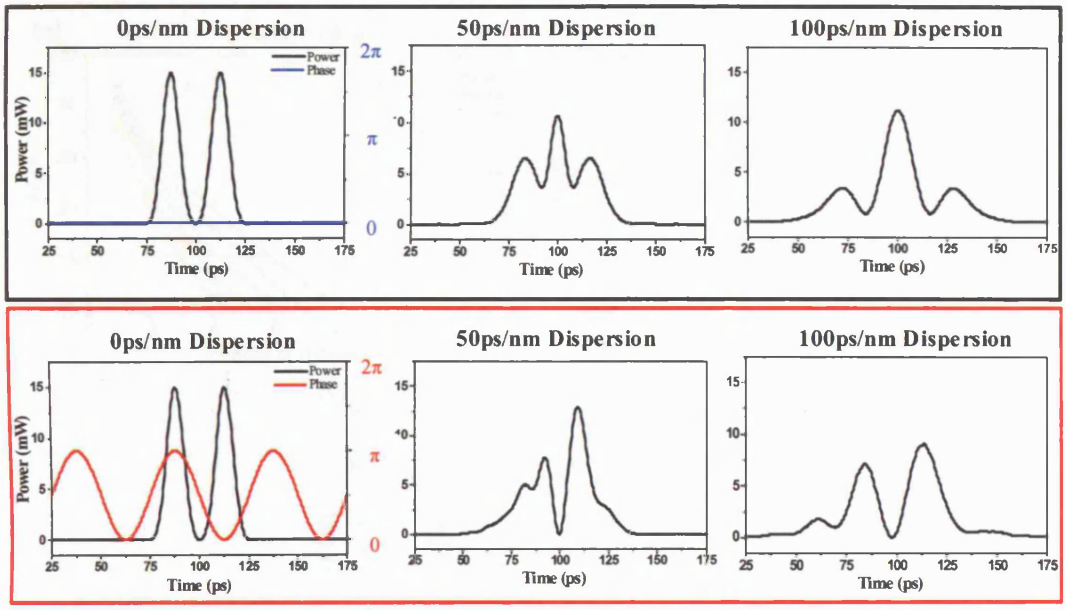

Fig. 6.7 *Signal distortion in the RZ modulation format due to inter-symbol-interference (ISI) in the presence of large amount of uncompensated dispersion for RZ and AP-RZ*

It can be seen from *Fig. 6.7*, that the ISI between the RZ pulses grows steadily with increasing dispersion, as expected. For AP-RZ, while ISI between the two pulses are decreased, the pulse shape is significantly affected, giving no significant benefit due to the alternating phase.

6.2 Dispersion tolerance comparison of RZ and AP-RZ with the CS-RZ modulation format

The dispersion tolerance of the RZ and AP-RZ modulation format was further investigated by numerical simulation and compared with CS-RZ transmission. The Q factor was calculated against increasing transmission distance as a function of the in-line residual dispersion, varying between ±15ps/nm, and the results are shown in *Fig. 6.8* and *Fig. 6.10.*

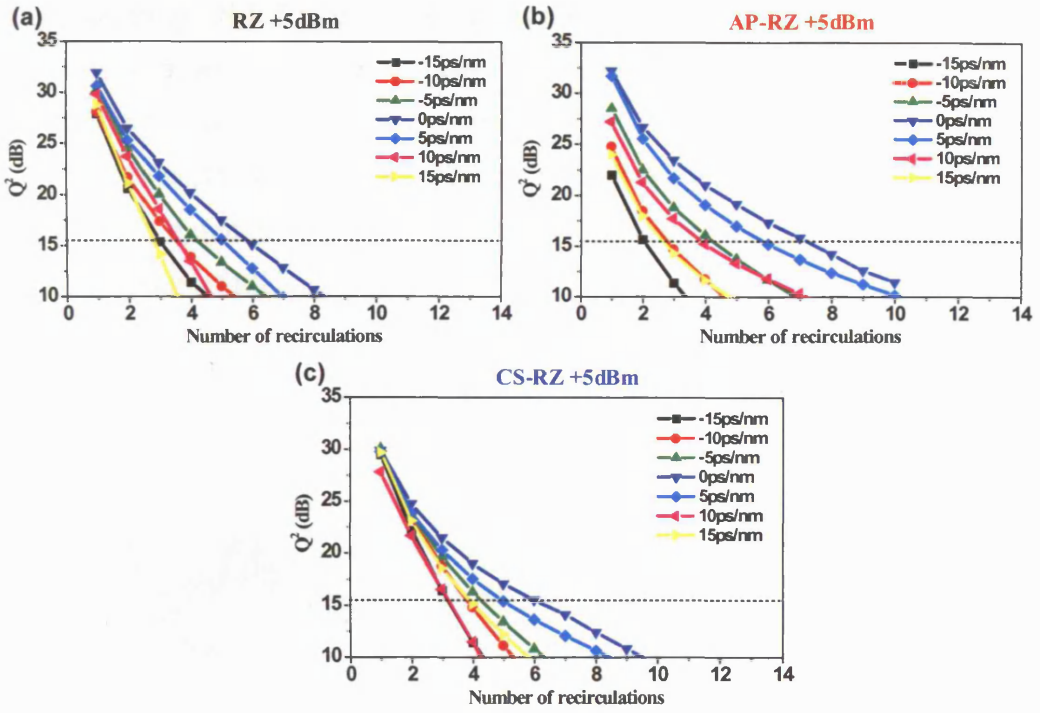

Fig. 6.8 *Numerically calculated Q-factor against transmission distance at a signal launch power of +5dBm, for ±15ps/nm in-line residual dispersion (a) RZ (T_{FWHM}=11.25ps) (b) AP-RZ (T_{FWHM}=11.25ps) (c) CS-RZ (T_{FWHM}=16.5ps). Note: Dotted line indicates Q-factor of 15.56dB which corresponds to a BER=10^{-9}*

As with experimental results, maximum transmission distance is achieved using the AP-RZ format for the case of fully compensated amplifier spans at a signal launch power of +5dBm. However, this advantage is lost in the presence of residual dispersion per span, and longer transmission distances are achieved using RZ modulation. The CS-RZ transmission shown in *Fig. 6.8(c),* yields a maximum transmission distance of 6 recirculations (360km) which is less than that for AP-RZ (7 recirculations, 420km) and longer than that obtained for RZ (5 recirculations, 300km). This is consistent with previous results [OHH'01, SEK'03]. However, in the presence of residual dispersion, the maximum transmission distance is obtained for CS-RZ transmission. This is because unlike in the case of AP-RZ, no PM-IM conversion takes place in the presence of dispersion, as the pulses are not chirped, despite the alternating phase. However, the alternating phase does give the maximum suppression

of ISI, indicating CS-RZ to be the most dispersion tolerant format. The eye diagrams in *Fig. 6.9,* obtained both experimentally and by numerical simulation, show that the RZ format is limited by ISI, which is confirmed by the raised cross point between the pulses, while the AP-RZ modulation format is limited by amplitude jitter due to PM-IM. However, optimum eye opening penalty is obtained for CS-RZ, which shows good suppression of ISI and no PM-IM.

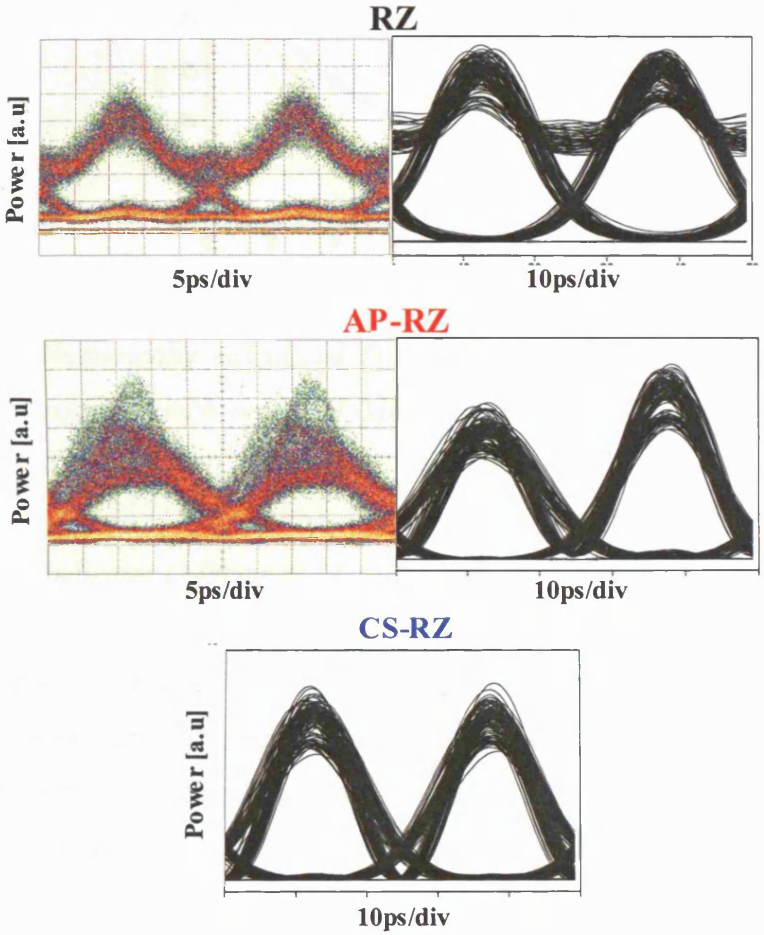

Fig. 6.9 *Comparison of eye diagrams measured experimentally and by numerical simulation at a launch power of +5dBm after 4 recirculations with +10ps/nm residual dispersion per amplifier span (+40ps/nm total residual dispersion) for RZ, AP-RZ and CS-RZ modulation formats*

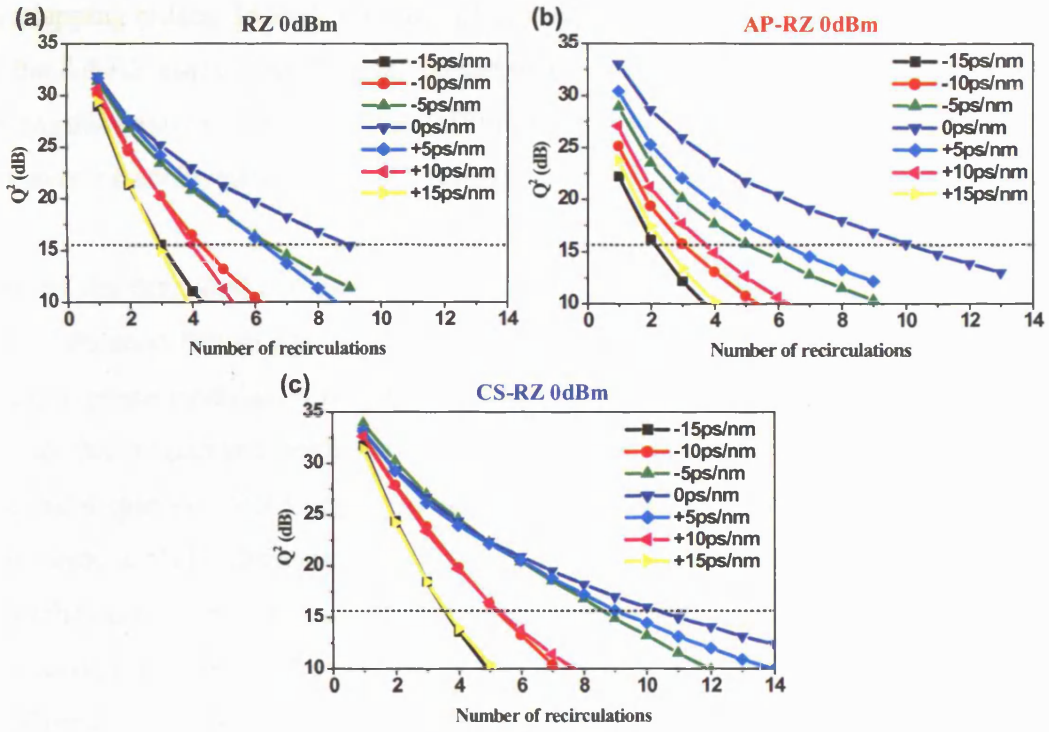

Fig. 6.10 *Numerically calculated Q-factor against transmission distance at a signal launch power of 0dBm (linear propagation), for ±15ps/nm in-line residual dispersion (a) RZ (T_{FWHM}=11.25ps) (b) AP-RZ (T_{FWHM}=11.25ps) (c) CS-RZ (T_{FWHM}=16.5ps). Note: Dotted line indicates Q-factor of 15.56dB which corresponds to a BER=10^{-9}*

The results shown in *Fig. 6.10* correspond to the numerically calculated Q-factor for transmission over amplifier spans with in-line residual dispersion varying between ±15ps/nm at a signal launch power of 0dBm and nonlinear distortions are suppressed. Unlike for transmission at +5dBm, both AP-RZ and CS-RZ show a maximum transmission distance of 10 recirculations (600km) in the presence of 0ps/nm residual dispersion, as nonlinear distortions are not present thereby eliminating the advantage of AP-RZ. Furthermore, in the presence of residual dispersion, longer transmission distances are achieved with CS-RZ, showing a maximum dispersion tolerance of ±50ps/nm. As explained previously, the phase modulation in AP-RZ chirps the pulses leading to the conversion of PM-IM in the presence of dispersion even for linear signal propagation, thereby reducing the overall dispersion tolerance. Conversely, the alternate-phase present in CS-RZ does not chirp the pulses and further improves dispersion tolerance by minimising ISI through destructive interference between

overlapping pulses. Indeed, the PM-IM conversion which takes place in the presence of the AP-RZ modulation format and dispersion distorts the signal such that for linear propagation (signal launch power 0dBm or less) superior transmission performance can even be achieved using the RZ format.

The results described compare the dispersion and nonlinear tolerance of the standard RZ modulation format against the alternate phase RZ (AP-RZ) modulation with peak-to-peak phase modulation of π rad, and also CS-RZ, at 40Gbit/s over SSMF. It was found that maximum nonlinear tolerance can be achieved with AP-RZ but with limited dispersion tolerance. Maximum, dispersion tolerance is achieved with CS-RZ, but with a 2dB decrease in nonlinear tolerance. In general, while advanced modulation formats can significantly improve these tolerances, and ultimately lead to less complex fibre link design than for standard formats [MIK'04], they require additional components at the transmitter. Consequently, the RZ format may in some cases be considered to be advantageous despite being non-optimal in both nonlinear and dispersion tolerance.

6.3 Summary

A novel experimental technique for evaluating transmission performance in the presence of in-line residual dispersion was described in this chapter. The dispersion and nonlinear tolerance of the standard RZ and AP-RZ modulation formats were investigated experimentally and compared with that of the CS-RZ modulation format studied by numerical simulation. It was found that for fully compensated spans the AP-RZ modulation format is the most effective in suppressing the intra-channel nonlinear effects. However, in the presence of incomplete dispersion compensation the AP-RZ shows phase-to-amplitude modulation and is, hence, less tolerant to residual dispersion compared to the standard RZ format. The most dispersion tolerant modulation format appeared to be CS-RZ, where the alternate-phase and zero chirp ensures minimal ISI due to destructive interference between adjacent pulses.

Chapter 7 Summary and conclusions

The work described in this thesis, focused on the study of the fundamental limitations of optical transmission at a channel bit-rate of 40Gbit/s. The work centred primarily on the investigation of intra-channel nonlinear distortion such as intra-channel four-wave-mixing (IFWM) and intra-channel cross-phase-modulation (IXPM), and the importance of dispersion-induced pulse overlap necessary for these physical processes to take place. Such understanding is key in identifying the dominant nonlinear distortion in a given system configuration and is useful for optimising the overall system performance. This thesis also discusses issues related dispersion tolerance and its optimisation through careful selection of modulation format.

The most common modulation formats such as NRZ and RZ were examined and the dominant nonlinearities such as SPM, IXPM and IFWM were described. It was found that NRZ transmission was limited by SPM, while RZ transmission was limited by timing jitter due to IXPM and amplitude jitter and the growth of shadow pulses due to IFWM. Moreover, the maximum transmission distance of 240km over SSMF was achieved for RZ transmission. It was also concluded that the high local dispersion in SSMF is key to the emergence of intra-channel nonlinear effects, as the RZ pulses overlap and interact with each other through fibre nonlinearity. Therefore, a technique for minimising this distortion was considered by reducing the pulse overlap, and NZDSF with fibre local dispersion approximately one quarter that of SSMF was selected for transmission.

Transmission over NZDSF: Dispersion compensation of NZDSF was achieved using a HOM-DMD with very high nonlinear tolerance. Hence, amplifier spans with the HOM-DMD placed at the output of the EDFA were investigated, enabling the investigation of in-line pre-compensated amplifier spans. This technique reduced the signal power at the input of the NZDSF transmission fibre reducing the nonlinear distortion. The results showed that the maximum transmission distance for NRZ modulation format could be increased to 525km with this novel dispersion management scheme. However, optimum dispersion management for RZ transmission was achieved with the standard in-line post-compensated amplifier spans with NZDSF, yielding a maximum transmission distance of 750km.

Pre-compensation at the transmitter: It was found that pre-compensated amplifier spans created significant pulse overlap, which interacts through fibre nonlinearity in the NZDSF giving rise to significant IFWM distortion, thereby limiting the transmission performance. However, the overall system performance was found to be improved for transmission over NZDSF compared to SSMF for both NRZ and RZ modulation formats. Based on these results it was found that overall nonlinear distortion could be suppressed by accurate control of pulse overlap through dispersion management. Numerical and analytical study of potential suppression of intra-channel nonlinear distortion by pre-compensating the signal at the transmitter had been proposed, but no experimental verification of this technique existed. In this work, this technique was demonstrated experimentally for the first time giving good agreement with results obtained by numerical simulation and analytically. Furthermore, pre-compensation at the transmitter was found to be effective for transmission over both SSMF and NZDSF with maximum transmission distances of 360km and 825km achieved respectively. However, as intra-channel nonlinear distortion is higher in SSMF owing the larger pulse overlap, the improvement in system performance through dispersion management was found to be 14% higher than that of transmission over NZDSF.

WDM transmission: This work also investigated degradation in system performance for WDM transmission. It was found that inter-channel nonlinear distortion was not significant at 40Gbit/s owing to the high walk-off rate (even in NZDSF), and transmission performance is limited by the single channel effects. Simultaneous broadband dispersion compensation was also demonstrated using the HOM-DMD, and a maximum transmission distance of 375km was achieved for 10 WDM channels with 100GHz (0.8nm) channel spacing.

Alternate-polarisation RZ: The thesis describes the techniques for the suppression of intra-channel nonlinear distortion using advanced modulation formats, based on the RZ format. A detailed investigation of alternate-polarisation RZ, where adjacent pulses were orthogonally polarised is described. It was found that the alternate polarisation RZ can reduce the impact of IXPM by 50% and IFWM by 30%, compared to the standard RZ modulation format. Although, higher suppression of

these effects were theoretically predicted, it was found that owing to the large local dispersion in SSMF, nonlinear interactions take place between overlapping pulses with the same polarisation, reducing the theoretically achievable suppression. Numerical simulations of combining pre-compensation at the transmitter with alternate-polarisation RZ showed that the maximum transmission distance of 360km (achieved experimentally), could be increased to 600km.

Alternate-phase RZ: Alternating the phase between adjacent pulses was also investigated for suppressing intra-channel nonlinear distortion. The results showed good agreement with previously published theoretical work, where optimum suppression of IFWM was achieved for a peak-to-peak phase modulation of $\pi/2$ rad. However, the results of this work showed that optimum performance of the AP-RZ format was achieved for a phase modulation of π rad, where the combined reduction of ISI and IFWM is achieved at a maximum transmission distance of 300km.

The work has also shown that advanced modulation formats can be combined with pre-compensation at the transmitter to improve the suppression of the intra-channel nonlinear distortions by 5dB. An important feature of this work showed that the optimum pre-compensation was dependent on the modulation format. The work also proposed a new modulation format, with the simultaneous implementation of alternate-polarisation and AP-RZ capable of maximum suppression of intra-channel nonlinear distortion without the need for dispersion management. This format utilises the nonlinear tolerance of orthogonal polarisation between adjacent pulses, while further suppressing nonlinear interaction between overlapping pulses of the same polarisation through alternate-phase, leading to a maximum achievable transmission distance of 480km.

Dispersion tolerance: As 40Gbit/s systems are extremely sensitive to dispersion, the work investigated the in-line residual dispersion tolerance of the RZ and AP-RZ modulation format. This work was carried out for propagation in both the nonlinear and linear regime. The results showed that for amplifier spans with 0ps/nm residual dispersion, optimum performance is obtained for the AP-RZ modulation in the presence of fibre nonlinearities. This was also true for linear transmission although the improvement was significantly less than that obtained in the nonlinear regime. As

the residual dispersion of each amplifier span was increased, the RZ transmission format was found to be limited by ISI, while AP-RZ was limited by PM-IM due to the alternately chirped pulses. In fact, maximum dispersion tolerance was observed for RZ (-60ps/nm - +60ps/nm) compared to AP-RZ (-45ps/nm - +30ps/nm). The dispersion tolerance of CS-RZ modulation format was also investigated by numerical simulation and was found to give a maximum dispersion tolerance of ±50ps/nm in the nonlinear regime. A novel experimental technique for investigation of dispersion tolerance was proposed and demonstrated. This technique was based on varying the residual dispersion in a single-span recirculating loop by tuning of the transmitter wavelength according to the dispersion slope of the fibre.

Modulation format / **Dispersion management**	**NRZ**	**RZ**	**Alternate-polarisation RZ**	**Alternate-phase RZ**	**Alternate-polarisation + alternate-phase RZ**	**CS-RZ**
SSMF	120(exp)	240 (exp)	360 (exp)	300 (exp)	480 (exp)	240 (sim)
NZDSF in-line pre-compensation	525(exp)	375 (exp)	-	-	-	-
NZDSF in-line post-compensation	375(exp)	750 (exp)	-	-	-	-
SSMF+pre-compensation at the transmitter	-	360 (exp)	600 (sim)	360 (exp) 420 (sim)	-	360 (sim)
NZDSF in-line post-compensation+pre-compensation at the transmitter	-	825 (exp)	-	-	-	-
SSMF with DCF placed between 2 EDFAs to reduce the span loss	-	540(0dbm) 300(+5dBm) (exp)	-	600(0dBm) 420(+5dBm) (exp)	-	600(0dBm) 300(0dBm) (sim)

Table 7.1 *Summary of maximum transmission distances (km) achieved for varying dispersion management and modulation format. Note: (exp) and (sim) indicate distances achieved experimentally and by numerical simulation respectively.*

Table 7.1 lists the maximum achievable transmission distances, for the different combinations of modulation format and dispersion management schemes, as carried out in this work. It should be noted, however, that the main focus of this work was to compare different techniques for transmission over basic amplifier spans with zero residual dispersion. Hence, the experiments were carried out using the same basic spans in order to compare the relative impact of nonlinearities and identify the dominant effects, rather than optimise achievable transmission length in each particular case. Possible techniques for this are pre-compensation at the transmitter and advanced modulation formats.

The longest transmission distance of 825km is achieved for transmission over NZDSF, with pre-compensation at the transmitter, using the RZ modulation format. Furthermore, it shows that the NRZ modulation format can be used in 40Gbit/s transmission with an achievable transmission distance of 525km, also using NZDSF, but with in-line pre-compensated amplifier spans. Transmission over SSMF showed similar behaviour where longer transmission distances were achieved with the RZ format (360km) compared to NRZ (120km), although these distances are both shorter than those achieved with NZDSF. However, it was found that by using advanced modulation formats (more complex compared to NRZ/RZ) it was possible to achieve a transmission distance of 600km over SSMF using the AP-RZ modulation format. While, this distance is still shorter than the maximum achieved with NZDSF, it amounts to a decrease of only 27%. Therefore, taking into account the costs associated with deploying NZDSF when SSMF readily available, the performance benefit gained by using NZDSF is off-set against the cost of using SSMF. While advanced modulation formats were not investigated for transmission over NZDSF, it can be concluded that while the maximum transmission distance may increase, the percentage of improvement will not be as high as that seen when advanced modulation formats were used for transmission over SSMF. This is because the intra-channel nonlinear effects, which the advanced modulation formats are designed to suppress, are significantly lower in NZDSF, making the use of advanced modulation formats over NZDSF less efficient. This behaviour was seen when pre-compensation at the transmitter was used for the RZ format, where an improvement of 50% was obtained for the SSMF link, but only 36% for the NZDSF link.

In future work, a detailed investigation on the suppression of intra-channel nonlinear distortion by optical regeneration is required. The work described on the AP-RZ, and CS-RZ modulation formats indicate that an improved performance due to regeneration can be expected due to the suppression of ISI. To date, as all regeneration investigation has been based on RZ transmission, a logical continuation of this work would study the performance of advanced modulation formats in the presence of optical regeneration. In particular, the PM-IM of AP-RZ in the presence of uncompensated dispersion can be treated as amplitude jitter and compensated using a regenerator, and can be used instead of dispersion trimming at the receiver. The benefit of this will be two-fold: it achieves dispersion compensation, and also improves the receiver sensitivity. Finally, dispersion management techniques and their impact as investigated in chapter 4 can be extended for the investigation at bit-rates of 80Gbit/s and 160Gbit/s. As the pulse broadening increases significantly, transmission in the 'quasi-linear' regime could prove to be an effective alternative. However, more stringent requirements on the dispersion compensation will be necessary as the dispersion tolerance will be in the region of 0ps/nm, and increasing this tolerance will require further investigation. These studies will contribute to the overall understanding of the fundamental limitations to optical transmission.

Chapter 8 Appendices

8.1 Appendix 1: Symbols, common values and units

Symbol	Parameter	Typical values	Units
D	Dispersion parameter	17 (SSMF), 4 (NZDSF), 85 (DCF)	ps/(nm.km)
β_2	Group velocity dispersion	21.7 (SSMF), 5.6 (NZDSF), 108.5 (DCF)	ps/(nm^2.km)
c	Speed of light	$3x10^8$	m/s
h	Planck's constant	$6.626x10^{-34}$	J.s
ε_0	Vacuum permitivity	$8.852x10^{-12}$	F/m
α	Attenuation coefficient	0.21 (SSMF, NZDSF), 0.5 (DCF)	dB.km
γ	Nonlinear coefficient	1.52 (SSMF), 1.20 (NZDSF), 4.86 (DCF)	1/(W.km)
A_{eff}	Effective area	55 (SSMF), 70 (NZDSF), 20 (DCF)	μm^2
L_D	Dispersion length	SSMF: 10.4 (40Gbit/s)	km
T_{FWHM}	Pulsewidth	11.25ps (40Gbit/s)	ps
Q	Q-factor	15.56 for BER<10^{-9}	dB
$\sigma_{1,0}$	Standard deviation of power in 'zeroes' and 'ones'	-	-
Δf	Bandwidth	-	Hz
$\Delta\lambda$	Channel spacing	0.8 (40Gbit/s)	nm

8.2 Appendix 2: Glossary

AM	Amplitude Modulation
AOM	Acousto-Optic-Modulator
ASE	Amplifier Spontaneous Emission
ATT	Attenuator
AP-RZ	Alternate-Phase Return-to-Zero
APol	Alternate-Polarisation
AWG	Arrayed Waveguide Grating
BER	Bit-Error-Rate
BERT	Bit-Error-Rate Test-set
CW	Continuous Wave
DCF	Dispersion Compensating Fibre
DFB	Distributed Feedback Laser
DSF	Dispersion Shifter Fibre
EAM	Electro-Absorption-Modulator
ECL	External Cavity Laser
EDFA	Erbium Doped Fibre Amplifier
EOP	Eye Opening Penalty
ETDM	Electrical Time-Division-Multiplexer
FBG	Fibre Bragg Grating
FEC	Forward Error Correction
FFT	Fast Fourier Transform
FWHM	Full Width Half Maximum
FWM	Four-Wave-Mixing
GVD	Group Velocity Dispersion
IFWM	Intra-channel Four-Wave-Mixing
IM-DD	Intensity Modulation Direct Detection
ISI	Inter-Symbol-Interference
IXPM	Intra-channel Cross-Phase-Modulation
LP	Linear Polarisation
MUX	Multiplexer
MZ	Mach-Zehnder
NF	Noise Figure

NLSE	Nonlinear Schrödinger Equation
NRZ	Non-Return-to-Zero
NZDSF	Non-Zero Dispersion Shifted Fibre
OSA	Optical Spectrum Analyser
OTDM	Optical Time-Division-Multiplexer
OSNR	Optical Signal-to-Noise Ratio
PC	Polarisation Controller
PDL	Polarisation Dependent Loss
PLL	Phase Locked Loop
PM	Phase Modulation
PMD	Polarisation Mode Dispersion
PPG	Pulse Pattern Generator
PRBS	Pseudo Random Bit Sequence
RX	Receiver
SSF	Split-Step Fourier
SNR	Signal-to-Noise Ratio
SPM	Self Phase Modulation
SSMF	Standard Single Mode Fibre
SBS	Stimulated Brillouin Scattering
SRS	Stimulated Raman Scattering
TE	Transverse Electric
TM	Transverse Magnetic
TX	Transmitter
WDM	Wavelength Division Multiplexing
XPM	Cross Phase Modulation

Chapter 9 References

[ABL'00]: M. J. Ablowitz, T. Hirooka, "Resonant nonlinear intrachannel interactions in strongly dispersion-managed transmission systems", Optics. Lett., Vol. 25, No. 24, pp 1750-1752, 2000.

[AGA'03]: A. Agarwal, S. Banerjee, D. F. Grosz, A. P. Kung, D. N. Maywar, A. Gurevich and T. H. Wood, "Ultra-high-capacity long-haul 40-Gb/s WDM transmission with 0.8-b/s/Hz spectral efficiency by means of strong optical filtering", IEEE Photon. Technol. Lett., Vol. 15, No.3, pp 470-472, 2003.

[AGR'01]: Agrawal G.P, Nonlinear Fibre Optics, 3rd Edition Academic Press Inc, 2001.

[AGR'97]: Agrawal G.P, Fiber-optic communication systems, 2nd Edition John Wiley & Sons, Inc. 1997.

[ALI'02]: N. Alic and Y. Fainman "Data dependent phase coding for mitigation of intrachannel four wave mixing", in Proc. Lasers and Electro Optics Society Conference (LEOS 2002), Glasgow, Scotland, Paper ThI2, 2002.

[ALL'99]: S. B. Alleston, P. Harper, I.S. Penketh, I. Bennion, N. J. Doran, and A. D. Ellis, "1000km transmission of 40Gbit/s single channel RZ data over dispersion managed standard (non-dispersion shifted) fibre", Electron. Lett. Vol. 35, No. 10, pp 823-824, 1999.

[APP'03]: S. Appathurai, V. Mikhailov, R. I. Killey and P. Bayvel, "Suppression of intra-channel nonlinear distortion in 40Gbit/s transmission over standard single mode fibre using alternate-phase RZ and optimised pre-compensation", in Proc. 29th European Conf. on Optical Commun. (ECOC 2003), Rimini, Italy, Tu3.6.5, 2003.

[APP'04]: S. Appathurai, V. Mikhailov, R. I. Killey and P. Bayvel, "Suppression of intra-channel nonlinear distortion in 40Gbit/s transmission using alternate-phase RZ and alternate-polarisation", in Proc. Optical Fiber Commun. Conf. (OFC 2004), Los Angeles, CA, ThE5, 2004.

[APP'04b]: S. Appathurai, V. Mikhailov, R. I. Killey and P. Bayvel, "Investigation of the optimum alternate-phase RZ modulation format and its effectiveness in the suppression of intra-channel nonlinear distortion in

40Gbit/s transmission over standard single mode fiber", IEEE Journal of Selected Topics in Quantum Electronics, Vol. 10, No. 2, pp 239-249, 2004

[APP'04c]: S. Appathurai, V. Mikhailov, R. I. Killey and P. Bayvel, "Investigation of nonlinear and in-line residual dispersion tolerance of RZ/AP-RZ modulation formats at 40Gbit/s", in Proc. 30th European Conf. on Optical Commun. (ECOC 2004), Stockholm, Sweden, Mo4.5.4, 2004.

[BEC'99]: P. C. Becker, "Erbium-doped fibre amplifiers and technology", Academic Press, 1999

[BER'93]: N. S Bergano, K. W Kerfoot and C. R Davidson, "Margin measurements in optical amplifier systems", IEEE Photon. Technol. Lett., Vol. 5, No.3, pp 304-306, 1993.

[BER'96]: N. S. Bergano, C. R. Davidson and F. Heismann, "Bit-synchronous polarisation and phase modulation scheme for improving the performance of optical amplifier transmission systems", Electron. Lett., Vol. 32, No. 1, pp 52-54, 1996.

[BER'96b]: N. S. Bergano and C. R. Davidson, "Wavelength division multiplexing in long-haul transmission systems" , J. Lightwave Technol, Vol. 14, No.6, pp 1299-1308, 1996.

[BER'99]: A. Bertaina, S. Bigo, C. Francia, S. Gauchard, J. –P. Hermaide and M. W. Chbat "Experimental investigation of dispersion management for 8x10-Gb/s WDM transmission system over nonzero dispersion shifted fiber", IEEE Photon. Technol. Lett., Vol. 11, No.8, pp 1045-1047, 1999.

[BIG'04]: S. Bigo, G. Charlet, E. Corbel, "What has hybrid phase/intensity encoding brought to 40Gbit/s ultralong-haul systems?", in Proc. 30th European Conf. on Optical Commun. (ECOC 2004), Stockholm, Sweden, Th2.5.1, 2004.

[BIG'99]: S. Bigo, and A. Bertaina, "WDM transmission experiments at 32 x 10Gb/s over nonzero dispersion-shifted fibre and standard single-mode fibre", IEEE Photon. Technol. Lett., Vol. 11, No.10, pp 1316-1318, 1999.

[BIS'03]: H. Bissessur, G. Charlet, E. Gohin, S. Simmonneau, L. Pierre and W. Idler, "1.6Tbit/s (40 x 40Gbit/s) DPSK transmission over 3 x 100km of

TeraLight fibre with direct detection", Electron. Lett. Vol. 39, No. 2, pp 192-193, 2003.

[BIS'04]: H. Bissesur, A. Hugbart, C. Bastide, S. Gauchard and S. Ruggeri, "Transmission of 32x43Gb/s over 27x100km of TeraLight fiber with low-cost EDFA amplification", in Proc. Optical Fiber Commun. Conf. (OFC 2004), Los Angeles, CA, ThE3, 2004.

[BOS'95]: A. Boskovic, S. V. Chernikov, J. R. Taylor, L. G. Nielsen, and O. A. Levring, "Measurement of n_2 of various types of fibres used for ultra-high bit rate transmission", High Speed and Long Distance Optical Transmission, IEE Colloquium, pp 15/1-15/5, 1995.

[BOS'96]: A. Boskovic, S. V. Chernikov, J. R. Taylor, L. G. Nielsen, and O. A. Levring, "Direct measurement of nonlinear coefficient of various types of telecommunications optical fibers", in Proc. Conf. on Lasers and Electro-Optics Society, (CLEO 1996), Anaheim, CA, CMA7, pp 6-7, 1996.

[BRE'96]: D. Breuer, K. Ennser and K. Petermann, "Comparison of NRZ and RZ modulation format for 40Gbit/s TDM standard-fibre systems", in Proc. 22nd European Conf. on Optical Commun. (ECOC 1996), Oslo, Norway, TuD3.3, pp 199-202, 1996.

[BRE'97]: D. Breuer and K. Petermann, "Comparison of NRZ- and RZ-modulation format for 40-Gb/s TDM standard fibre systems", IEEE Photon. Technol. Lett., Vol. 9, No.3, pp 398-400, 1997.

[BRE'97b]: D. Breuer, F. Kuppers, A. Mattheus, E. G. Shapiro, I. Gabitov, and S. K. Turitsyn, "Symmetrical dispersion compensation for standard monomode-fiber-based communication systems with large amplifier spacing", Optics. Lett., Vol. 22, No.13, pp 982-984, 1997.

[BRE'98]: D. Breuer, H. J. Ehreke, F. Kuppers, R. Ludwig, K. Petermann, H. G. Weber and K. Weich, "Unrepeatered 40-Gb/s RZ single-channel transmission at 1.55μm using various fiber types", IEEE Photon. Technol. Lett., Vol. 10, No.6, pp 822-824, 1998.

[CAI'02]: J.-X. Cai, C. R. Davidson, Y. Cai, A. N. Pilipetskii, H. Li, A. Mills, R. -M Mu, U. Feiste, L. Xu, A. J. Lucero, D. G. Foursa and N. S. Bergano, "Transmission of thirty eight 40Gb/s channels (1.5>Tb/s)

over transoceanic distance", in Proc. Optical Fiber Commun. Conf. (OFC 2002), Anaheim, California, Post-deadline FC4, 2002.

[CAI'03]: J. X. Cai, D. G. Foursa, C. R. Davidson, Y. Cai, G. Domagala, H. Li, L. Liu, W. W. Patterson, A. N. Pilipetskii, M. Nissov and N. S. Bergano, "A DWDM demonstration of 3.73Tb/s over 11,000km using 373 RZ-DPSK channels at 10Gb/s", in Proc. Optical Fiber Commun. Conf. (OFC 2003), Post deadline, Atlanta, GA, PD22, 2003.

[CAR'97]: G. M. Carter, J. M. Jacob, C. R. Menyuk, E. A. Golovchenko and A. N. Pilipetskii, "Timing jitter reduction for a dispersion managed soliton system: Experimental evidence", Optics. Lett., Vol. 22, No.8, pp 513-515, 1997.

[CAU'03]: A. Cauvin, Y. Frignac and S. Bigo, "Single-channel nonlinear impairments at various bit-rates in dispersion managed systems", in Proc. 29th European Conf. on Optical Commun. (ECOC 2003), Rimini, Italy, Mo.4.2.4, 2003.

[CHA'02]: G. Charlet, J.-C Antona, S. Lanne, P. Tran, W. Idler, M. Gorlier, S. Borne, A. Klekamp, C. Simmonneau, L. Pierre, Y. Frignac, M. Molina, F. Beaumont, J.-P. Hamaide, and S. Bigo, "6.4Tb/s (159x42.7Gb/s) capacity over 21x100km using bandwidth-limited phase-shaped binary transmission", in Proc. 28th European Conf. on Optical Commun. (ECOC 2002), Copenhagen, Denmark, Post-deadline PD4.1, 2002.

[CHA'04]: G. Charlet, E. Corbel, J. Lazaro, A. Klekamp, R. Dischler, P. Tran, W. Idler, H. Mardoyan, A. Konczykowska, F. Jorge and S. Bigo, "WDM transmission at 6Tbit/s capacity over transatlantic distance, using 42.7Gb/s differential phase-shift keying without pulse carver", in Proc. Optical Fiber Commun. Conf. (OFC 2004), Post deadline, Los Angeles, CA, PDP36, 2004.

[CHE'02]: K. S. Cheng and J. Conradi, "Reduction of pulse-to-pulse interaction using alternative RZ formats in 40-Gb/s systems", IEEE Photon. Technol. Lett., Vol. 14, No.1, pp 98-100, 2002.

[CHE'96]: S. V. Chernikov and J. R. Taylor, "Measurements of n_2 and normalization factor for random polarization in optical fibers", in Proc. Optical Fiber Commun. Conf. (OFC 1996), San Jose, CA, ThS5, 1996.

[CHE'98]: S. V. Chernikov, F. Koch, J. R. Taylor and L. Gruner-Nielsen, "Measurements of the effect of bending on dispersion in dispersion-compensating fibers", in Proc. Optical Fiber Commun. Conf. (OFC 1998), San Jose, CA, TuD4, 1998.

[CHO'01]: S. Choudhary and T. Hoshida, "Influence of extinction ratio of clock modulator on dispersion tolerance of carrier suppressed return to zero signals", in Proc. Lasers and Electro Optics Society Conference, (LEOS 2000), San Deigo, CA, Paper ThC5, 2001.

[CHR'93]: A. R. Chraplyvy, A. H. Gnauck, R. W. Tkach and R. M. Derosier, "8x10Gb/s transmission through 280km of dispersion-managed fiber", IEEE Photon. Technol. Lett., Vol. 5, No.10, pp 1233-1235, 1993.

[DeA'96]: C. De Angelis and S. Wabnitz, "Interactions of orthogonally polarised solitons in optical fibers", Opt. Commun., Vol. 125, pp 186-196, 1996.

[DES'94]: E. Desurviere, "Erbium-doped fibre amplifiers", John Wiley & Sons; 1994

[DIA'02]: E. M. Dianov, "Advances in Raman fibers", J. Lightwave Technol., Vol. 20, No. 8, pp 1457-1462, 2002.

[ELL'97]: A. D. Ellis "All optical networking beyond 10Gbit/s; OTDM networks based on electro-optic modulators and fibre ring lasers", PhD thesis, University of Aston in Birmingham, April 1997

[ELR'91]: A. F. Elrefaie and R. E. Wagner, "Chromatic dispersion limitations for FSK and DPSK systems with direct detection receivers", IEEE Photon. Technol. Lett., Vol. 3, No.1, pp 71-73, 1991.

[ESS'99]: R. J Essiambre, B. Mikkelsen, and G. Raybon, "Intra-channel cross phase modulation and four wave mixing in high-speed TDM systems", Electron. Lett., 35, 18, pp 1576-1578, 1999.

[EVA'92]: S. G. Evangelides Jr., L. F. Mollenauer, J. P. Gordon and N. S. Bergano, "Polarization multiplexing with solitons", J. Lightwave Technol, Vol. 10, No.1, pp 28-35, 1992.

[FLU'01]: C. R. S. Fludger and R. J. Mears, "Electrical measurements of multipath interference in distributed Raman amplifiers", J. Lightwave Technol, Vol. 19, No.4, pp 536-545, 2001.

[FOR'02]: M. Forzati, J. Martensson, J. Li, A. Bernston, A. Djupsjobacka and P. Johannisson, "Reduction of intrachannel four-wave mixing using the

alternate-phase RZ modulation format", IEEE Photon. Technol. Lett., Vol. 14, No.9, pp 1285-1287, 2002.

[FOR'94]: F. Forghieri, R. W. Tkach and A. R. Chraplyvy, "Reduction of four-wave-mixing crosstalk in WDM systems using unequally spaced channels", IEEE Photon. Technol. Lett., Vol. 6, No.6, pp 754-756, 1994.

[FOR'97]: F. Forghieri, P. R. Prucnal, R. W. Tkach and A. R. Chraplyvy, "RZ versus NRZ in nonlinear WDM systems", IEEE Photon. Technol. Lett., Vol. 9, No.7, pp 1035-1037, 1997.

[FOU'02]: D. G. Foursa, C. R. Davidson, M. Nissov, M. A. Mills, L. Xu, J. X. Cai, A. N. Pilipetskii, Y. Cai, C. Breverman, R. R. Cordell, T. J. Carvelli, P. C. Corbett, H. D. Kidorf, and N. Bergano, "2.56 Tb/s (256x10Gb/s) transmission over 11,000km using hybrid Raman/EDFAs with 80nm of continuous bandwidth", in Proc. Optical Fiber Commun. Conf. (OFC 2002), Anaheim, California, Post-deadline FC3, 2002.

[FRA'99]: C. Francia, "Constant step-size analysis in numerical simulation for correct four-wave-mixing power evaluation in optical fiber transmission systems", IEEE Photon. Technol. Lett., Vol. 11, No.1, pp 69-71, 1999.

[FRI'00]: Y. Frignac and S. Bigo, "Numerical optimization of residual dispersion in dispersion-managed systems at 40Gbit/s", in Proc. Optical Fiber Commun. Conf. (OFC 2000), Baltimore, MD, TuD3, 2000.

[FRI'02]: Y. Frignac J. –C. Anotona, S. Bigo and J. –P. Hamaide, "Numerical optimization of pre and in-line dispersion compensation in dispersion-managed systems at 40Gbit/s", in Proc. Optical Fiber Commun. Conf. (OFC 2002), Anaheim, CA, ThFF5, 2002.

[FRI'02b]: Y. Frignac, G. Charlet, W. Idler, R. Dischler, P. Tran, S. Lanne, S. Borne, C. Martinelli, G. Veith, A. Jourdan, J. -P. Hamaide and S. Bigo, "Transmission of 256 wavelength-division and polarization-division-multiplexed channels at 42.7Gb/s (10.2Tb/s capacity) over 3x100km of TeraLight^{TM} fiber", in Proc. Optical Fiber Commun. Conf. (OFC 2002), Anaheim, California, Post-deadline FC5, 2002.

[FUJ'03]: M. Fujiwara, M. Teshima and K. Iwatsuki, "Narrow bandwidth polarisation scrambler using delay-coupled binary phase pulse for super-dense WDM networks", Electron. Lett., Vol. 39, No. 5, pp 452-453, 2003.

[FUK'01]: K. Fukuchi, T. Kasamatsu, M. Morie, R. Ohhira, T. Ito, K. Sekiya, D. Ogasahara, and T. Ono, "10.92-Tb/s (273x40-Gb/s) triple-band/ultra-dense WDM optical-repeatered transmission experiment", in Proc. Optical Fiber Commun. Conf. (OFC 2001), Post deadline, Anaheim, CA, PD24, 2001.

[FUK'02]: K. Fukuchi, "Wideband and ultra-dense WDM transmission technologies toward over 10-Tb/s capacity", in Proc. Optical Fiber Commun. Conf. (OFC 2002), Los Angeles, CA, ThX5, 2002.

[FUR'01]: C. Furst, C. Sheerer, G. Mohs, J.-P. Elbers and C. Glingener, "Influence of the dispersion map on limitations due to cross-phase modulation in WDM multi-span transmission systems", in Proc. Optical Fiber Commun. Conf. (OFC 2001), Anaheim, California, MF4, 2001.

[GIL'03]: D. M. Gill, X. Liu, S. Banerjee and Y. Su, "$\pi/2$ Alternate-phase ON-OFF keyed 40-Gb/s transmission on standard single mode fiber", IEEE Photon. Technol. Lett., Vol. 15, No.12, pp 1776-1778, 2003.

[GNA'00]: A. H. Gnauck, L. D. Garrett, Y. Danziger, U. Levy and M. Tur, "Dispersion and dispersion slope compensation in NZDSF for 40-Gb/s operation over the entire C band", in Proc. Optical Fiber Commun. Conf. (OFC 2000), Baltimore, Maryland, WL2, 2000.

[GNA'02]: A. H. Gnauck, G. Raybon, S. Chandrasekhar, J. Lethold, C. Doerr, L. Stulz, A. Agrawal, S. Banerjee, D. Grosz, S. Hunsche, A. Kung, A. Marhelyuk, D. Maywar, M. Movassaghi, X. Liu and C. Xu, "2.5Tb/s (64x42.7Gb/s) Transmission over 40x100km NZDSF using RZ-DPSK format and all-Raman-amplified spans", in Proc. Optical Fiber Commun. Conf. (OFC 2002), Anaheim, California, Post-deadline FC2, 2002.

[GNA'04]: A. H. Gnauck, J. Leuthold, C. Xie, I. Kang, S. Chandrasekhar, P. Bernasconi, C. Doerr, L. Buhl, J. D. Bull, N. A. F. Jaeger, H. Kato and A. Guest, "6x42.7-Gb/s transmission over ten 200-km EDFA-

amplified SSMF spans using alternate-polarization RZ-DPSK", in Proc. Optical Fiber Commun. Conf. (OFC 2004), Post deadline, Los Angeles, CA, PDP35, 2004.

[GNA'04b]: A. H. Gnauck, X. Liu, X. Wei, D. M. Gill and E. C. Burrows, "Comparison of modulation formats for 42.7Gb/s single-channel transmission through 1980km of SSMF", IEEE Photon. Technol. Lett., Vol. 16, No.3, pp 909-911, 2004.

[GNA'85]: A. H. Gnauck, B. L. Kasper, R. A. Linke, R. W. Dawson, T. L. Koch, T. J. Bridges, E. G. Burkhardt, R. T. Yen, D. P. Wilt, J. C. Campbell, K. Ciemiecki Nelson and L. G. Cohen, "4-Gbit/s Transmission over 103km of optical fiber using a novel electronic multiplexer/demultiplexer", J. Lightwave Technol, Vol. 3, No.5, pp 1032-1035, 1985.

[GOV'98]: D. S. Govan, W. Forysiak and N. J. Doran, "Long-distance 40Gbit/s soliton transmission over standard fiber by use of dispersion management", Optics. Lett., Vol. 23, No.19, pp 1523-1525, 1998.

[GOW'93]: S. Gowar, "Optical communication systems", Prentice Hall: New York, 1993

[GRO'02]: D. F. Grosz, A. Agrawal, S. Banerjee, A. P. Kung, D. N. Maywar, A. Gurevich, T. H. Wood, C. R. Lima, B. Faer, J. Black, and C. Hwu, "5.12Tb/s (128x42.7Gb/s) transmission in 0.8bit/Hz spectral efficiency over 1280km of standard single-mode fibre using all-Raman amplification and strong signal filtering", in Proc. 28th European Conf. on Optical Commun. (ECOC 2002), Copenhagen, Denmark, Post-deadline PD4.3, 2002.

[GRU'96]: L. Gruner-Nielsen, A. Boskovic, S. V. Chernikov, and J. R. Taylor, "Measurement of nonlinear refractive index n_2 of dispersion compensating fibre", in Proc. 22nd European Conf. on Optical Commun. (ECOC 1996), Oslo, Norway, TuP.08, pp 249-251, 1996.

[GUY'96]: M. J. Guy, S. V. Chernikov, J. R. Taylor and D. G. Moodie, "Demonstration of the feasibility of dual frequency operation of an electroabsorption modulator for demultiplexing in a 16 channel 40Gbit/s OTDM system", Electron. Lett., Vol. 32, No. 12, pp 1138-1139, 1996.

[HAD'96]: A. Hadjifotiou, G. Pettitt, D. Garthe and W. S. Lee, "Forty Gbit/s optical TDM system for transmission over 560km of commercial single-mode fibre", Global Telecommunicatios conference, Globecom '96, "Communications: The key to global prosperity", Vol. 3, pp 18-22, 1996

[HAG'98]: K. Hagimoto, Y. Miyamoto and Y. Yamabayashi, "40Gbit/s transmission systems", in Proc. Optical Fiber Commun. Conf. (OFC 1998), San Jose, CA, WC3, 1998.

[HAR'73]: R. H Hardin and F. D. Tappert, "Applications of the split-step Fourier methodto the numerical solution of nonlinear and variable coefficient wave equations", SIAM Review Chronicle, 15:423, 1973

[HAR'99]: P. Harper, S.B Alleston, I. Bennion and N.J Doran, "40Gbit/s dispersion managed soliton transmsission over 1160km in Standard fibre with 75km span length", Electron. Lett., Vol. 35, No. 24, pp2128-2130, 1999.

[HAS'73]: A. Hasegawa and F. Tappert, "Transmission of stationary nonlinear optical pulses in dispersive dielectric fibers", Appl. Phys. Lett., vol. 23, pp 142-144, 1973.

[HAY'01]: M. I. Hayee, M. C. Cardakli, A. B. Sahin and A. E. Willner, "Doubling of bandwidth utilization using two orthogonal polarizations and power unbalancing in a polarization-division-multiplexing scheme", IEEE Photon. Technol. Lett., Vol. 13, No.8, pp 881-883, 2001.

[HAY'97]: M. I. Hayee and A. E. Willner, "Pre- and post-compensation of dispersion and nonlinearities in 10-Gb/s WDM systems", IEEE Photon. Tech. Lett., Vol. 9, No.9, pp 1271-1273, 1997.

[HAY'99]: M. I. Hayee and A. E. Willner, "NRZ versus RZ in 10-40-Gb/s dispersion-managed WDM transmission systems", IEEE Photon. Tech. Lett., Vol. 11, No.8, pp 991-993, 1999.

[HIN'01]: S. Hinz, D. Sandel, F. Wust, R. Noe, "Polarization multiplexed 2 x 20Gb/s RZ using interference detection", in Proc. Optical Fiber Commun. Conf. (OFC 2001), Anaheim, California, WM4, 2001.

[HIR'02]: T. Hirooka and M. J. Ablowitz, "Analysis of timing and amplitude jitter due to intrachannel dispersion-managed pulse interactions", IEEE Photon. Tech. Lett., Vol. 14, No.5, pp 633-635, 2002.

[HIR'03]: A. Hirano, Y. Miyamoto and S. Kuwahara, "Performance of CSRZ-DPSK and RZ-DPSK in 43-Gbit/s/ch DWDM G.652 single mode fiber transmission", in Proc. Optical Fiber Commun. Conf. (OFC 2003), Atlanta, GA, ThE4, 2003.

[HOD'02]: A. Hodzic, B. Konrad and K. Petermann, "Prechirp in NRZ-based 40Gb/s single-channel and WDM transmission systems", IEEE Photon. Technol. Lett., Vol. 14, No.2, pp 152-154, 2002.

[HOD'02b]: A. Hodzic, B. Konrad and K. Petermann, "Alternative modulation formats in N x 40Gb/s WDM standard fibre RZ-transmission systems", J. Lightwave Technol, Vol. 20, No.4, pp 598-607, 2002.

[HOD'03]: A. Hodzic, B. Konrad and K. Petermann, "Improvement of system performance in N x 40-Gb/s WDM transmission using alternate polarizations", IEEE Photon. Technol. Lett., Vol. 15, No.1, pp 153-155, 2003.

[HOL'02]: R. Holzlohmer, H. N. Ereifej, V. S. Grigoryan, G. M. Carter and C. R. Menyuk, "Experimental and theoretical characterisation of a 40Gb/s long-haul single-channel transmission system", J. Lightwave Technol, Vol. 20, No.7, pp 1124-1131, 2002.

[HUI'04]: R Hui, S. Zhang, B. Zhu, R. Huang, C. Allen, and D. Demarest, "Advanced optical modulation formats and their comparison in fiber-optic systems", Technical report, Information & telecommunication technology centre, University of Kansas, 2004.

[HUM'91]: P. A. Humblet, and M. Azizoglu, "On the bit error rate of lightwave systems with optical amplifiers", J. Lightwave Technol, Vol. 9, No.11, pp 1576-1582, 1991.

[INO'00]: T. Inoue, and A. Maruta "Pre-spread RZ pulse transmission for reducing intra-channel nonlinear interactions", in Proc. Lasers and Electro Optics Society Conference, (LEOS 2000), Puerto Rico, Paper MJ3, 2000.

[ISL'02]: M. N. Islam, "Raman amplifiers for telecommunications", IEEE Journal of Selected Topics in Quantum Electronics, Vol. 8, No. 3, pp 548-558, 2002

[IZA'92]: H. Izadpanah, C. Lin, J. L Gimlett, A. J. Antos, D. W. Hall and D. K. Smith, "Dispersion compensation in 1310nm optimised fibre, EDFAs

and 1310/1550nm WDM", Electron. Lett. Vol. 22, No. 15, pp 1469-1470, 1992.

[JAC'92]: M. K. Jackson, G. R. Boyer, J. Paye, M. A. Franco, and A. Mysyrowicz, "Temporal diffraction by nonlinear interaction in optical fibres", Optics. Lett., Vol. 17, No.24, pp 1770-1772, 1992.

[JOH'01]: P. Johannisson, D. Anderson, A. Bernston and J. Martensson, "Generation and dynamics of ghost pulses in strongly dispersion-managed fiber-optic communication systems", Optics. Lett., Vol. 26, No.16, pp1227-1229, 2001.

[JOH'02]: P. Johannisson, D. Anderson, M. Marklund, A. Bernston, M. Forzati and J. Martensson, "Suppression of nonlinear effects by phase alternation in strongly dispersion-managed optical transmission", Optics. Lett., Vol. 27, No.12, pp 1073-1075, 2002.

[JOH'02b]: P. Johnanisson, "Nonlinear impairment in strongly dispersion-managed optical communication systems", Licentiate of Engineering Thesis, Chalmers University of Technology, Sweden, 2002.

[KAD'02]: S. Kado, Y. Emori and S. Namiki, "Gain and noise tilt control in multi-wavelength bi-directionally pumped Raman amplifier", in Proc. Optical Fiber Commun. Conf. (OFC 2002), Anaheim, CA, TuJ4, 2002.

[KAM'02]: Ivan Kaminow and Tingye Li, "Optical Fiber Telecommunications IV B Systems and Impairments", Academic Press, 2002.

[KAN'03]: A. V. Kanaev, G. G. Luther, V. Kovanis, S. R. Bickham and J. Conradi "Ghost pulse generation suppression in phase-modulated 40-Gb/s RZ transmission", J. Lightwave Technol., Vol. 21, no. 6, pp 1486-1489, 2003.

[KAN'04]: I. Kang, C. Xie, C. Dorrer and A. Gnauck, "Implementations of alternate-polarisation differential-phase-shift-keying transmission", Electron. Lett. Vol. 40, No. 5, pp 333-335, 2004.

[KAW'99]: S. Kawanishi, H. Takara, K. Uchiyama, I. Shake and K. Mori, "3Tbit/s (160Gbit/s x 19ch) OTDM/WDM transmission experiment", in Proc. Optical Fiber Commun. Conf. (OFC 1999), Post deadline, San Diego, CA, PD1, 1999.

[KAZ'96]: L. Kazovsky, S. Benedetto and A. Willner, "Optical fiber communication systems", Artech: Boston, MA 1996

[KEI'99]: G. E. Keiser, "A review of WDM technology and applications", Optical Fiber Technol., Vol. 5, No.1, pp 3-39, 1999.

[KIL'00]: R. I. Killey, H. J. Thiele, V. Mikhailov and P. Bayvel, "Reduction of intrachannel nonlinear distortion in 40-Gb/s-based WDM transmission over standard fiber", IEEE Photon. Technol. Lett., Vol. 12, No.12, pp 633-635, 2000.

[KIL'02]: R. I. Killey, V. Mikhailov, S. Appathurai and P. Bayvel, "Investigation of nonlinear distortion in 40-Gb/s transmission with higher order mode fiber dispersion compensators", J. Lightwave Technol., Vol. 20, no. 12, pp 2282-2289, 2002.

[KNU'02]: S. N. Knudsen, "Design and manufacture of dispersion compensating fibers and their performance in systems", in Proc. Optical Fiber Commun. Conf. (OFC 2002), Anaheim, California, Wu3, 2002.

[KOG'00]: H. Kogelnik, "High-capacity optica communicatios: Personal recollections", IEEE Trans. Select. Areas Quantum Electron., Vol. 6, No.6, pp 1279-1286, 2000.

[KON'01]: B. Konrad and K. Petermann, "Optimum fiber dispersion in high-speed TDM systems", IEEE Photon. Technol. Lett., Vol. 13, No.4, pp 299-301, 2001.

[KUM'01]: S. Kumar, "Intrachannel four-wave mixing in dispersion managed RZ systems", IEEE Photon. Tech. Lett., Vol. 13, No.8, pp 800-802, 2001.

[KUZ'00]: M. Kuznetsov, N. M. Forberg, S. R Henion, C. Reinke and C. Fennely, "Dispersion-induced power penalty in fiber-Bragg-grating WDM filter cascades using optically preamplified and nonpreamplified receivers", IEEE Photon. Tech. Lett., Vol. 12, No.10, pp 1406-1408, 2000.

[KUZ'99]: M. Kuznetsov, N. M. Forberg, S. R Henion and K. A Rauschenbach, "Power penalty for optical signals due to dispersion slope in WDM filter cascades", IEEE Photon. Tech. Lett., Vol. 11, No.11, pp 1411-1413, 1999.

[LEE'01]: S. Lee, Q. Yu, Y. Xie, O. H. Adamczyk and A. E. Willner, "A short recirculating fiber loop testbed with accurate reproduction of Maxwellian PMD statistics", in Proc. Optical Fiber Commun. Conf. (OFC 2001), Anaheim, California, WT2, 2001.

[LEE'96]: W. S. Lee, D. Garthe and A. Hadjifotiou, "Modelling and experimental comparison of a 40Gbit/s OTDM system over a transmission distance of 560km", in Proc. Optical Fiber Commun. Conf. (OFC 1996), San Jose, CA, TuD1, 1996.

[LIU'02]: X. Liu, X. Wei, A. H. Gnauck, C. Xu and L. K. Wickham, "Suppression of intrachannel four-wave-mixing-induced ghost pulses in high-speed transmissions by phase inversion between adjacent marker blocks", Optics. Lett., Vol. 27, No.13, pp 1177-1179, 2002.

[LIU'95]: Y. Liu, 10th Int. Conf. on Integrated Optics and Optical Fibre Communication (IOOC'95), Hong Kong, PDP-19, 1995.

[LUD'99]: R. Ludwig, U. Feiste, E. Dietrich, H. G. Weber, D. Breure, M. Martin and F. Kuppers, "Experimental comparison of 40Gbit/s RZ and NRZ transmission over standard single mode fibre", Electron. Lett., 35, 25, pp 2216-2218, 1999.

[MAM'99]: P. V Mamyshev and N. A Mamysheva, "Pulse-overlapped dispersion-managed data transmission and intra-channel four-wave-mixing", Optics Lett., Vol. 24, No.21, pp1454-1456, 1999.

[MAR'01]: J. Martensson, A. Bernston, M. Westlund, A. Danielsson, P. Johnanisson, D. Anderson and M. Lisak, "Timing jitter owing to intrachannel pulse interactions in dispersion-managed transmission systems", Optics. Lett., Vol. 26, No.2, pp 55-57, 2001.

[MAR'02]: J. Martensson, J. Li, A. Bernston, A. Djupsjobacka and M. Forzati, "Suppression of intra-channel four-wave mixing by phase modulation at one quarter of bit rate", Electron. Lett. Vol. 38, No. 23, pp 1463-1465, 2002.

[MAR'03]: J. Martensson, J. Li, A. Bernston, A. Djupsjobacka M. Forzati and J. Li, "Phase modulation schemes for improving intra-channel nonlinear tolerance in 40Gbit/s transmission", in Proc. Optical Fiber Commun. Conf. (OFC 2003), Atlanta, GA, FE5, 2003.

[MAR'04]: V. Marembert, C. Schubert, S. Ferber, K. Schulze, C. Schmidt-Langhorst, C. Boerner, M. Kroh, R. Ludwig, S. Watanabe, F. Futami, R. Okabe and H. G. Weber, "Single-channel 640Gbit/s DPSK Transmission over 160km fibre link", in Proc. 30th European Conf. on

Optical Commun. (ECOC 2004), Post deadline, Stockholm, Sweden, Th4.4.2, 2004.

[MAR'91]: D. Marcuse, "Single-channel operation in very long nonlinear fibers with optical amplifiers at zero dispersion" , J. Lightwave Technol, Vol. 9, No.3, pp 356-361, 1991.

[MAR'94]: D. Marcuse, A. R. Chraplyvy, R. W. Tkach "Dependence of cross-phase modulation on channel number in fiber WDM systems" , J. Lightwave Technol, Vol. 12, No.5, pp 885=890, 1994.

[MAT'99]: F. Matera, M. Settembre, M. Tamburrini, F. Favre, D. Le Guen, T. Georges, M. Henry, G. Michaud, P. Franco, A. Schiffini, M. Romagnoli, M. Guglielmucci, and S. Cascelli, "Field demonstrations of 40Gb/s soliton transmission with alternate polarisations", J. Lightwave Technol, Vol. 17, No.11, pp 2225-2234, 1999.

[MEC'00]: A. Mecozzi, C. B. Clausen, and M. Shtaif, "Analysis of intrachannel nonlinear effects in highly dispersed optical pulse transmission", IEEE Photon. Technol. Lett. Vol. 12, No. 4, pp 392-394, 2000.

[MEC'00b]: A. Mecozzi, C. B. Clausen, and M. Shtaif, "System impact of intra-channel nonlinear effects in highly dispersed optical pulse transmission", IEEE Photon. Technol. Lett. Vol. 12, No. 12, pp 1633-1635, 2000.

[MEC'01]: A. Mecozzi, C. B. Clausen, M. Shtaif, S. -G. Park and A. H. Gnauck, "Cancellation of timing and amplitude jitter in symmetric links using highly dispersed pulses", IEEE Photon. Technol. Lett., Vol. 13, No.5, pp 445-447, 2001.

[MEC'04]: A. Mecozzi, and M. Shtaif, "Signal-to-noise-ratio degradation caused by polarization-dependent loss and the effect of dynamic gain equalisation", J. Lightwave Technol, Vol. 22, No.8, pp 1856-1871, 2004.

[MIK'01]: B. Mikkelsen, G. Raybon, R. J. Essiambre, P. G. Bernasconi, K. Dreyer, L. W. Stulz, S. N. Knudsen, "High spectral efficiency (0.53bit/s/Hz) WDM transmission of 160Gb/s per wavelength over 400km of fibre", in Proc. Optical Fiber Commun. Conf. (OFC 2001), Baltimore, Maryland, Post-deadline PD29-1, 2001.

[MIK'01b]: V. Mikhailov, R.I. Killey, S. Appathurai and P. Bayvel, "Investigation of intra-channel nonlinear distortion in 40Gbit/s transmission over standard fibre", in Proc. 27th European Conf. on Optical Commun. (ECOC 2001), Amsterdam, Netherlands, Mo.L.3.4, pp 92-93, 2001.

[MIK'02]: V. Mikhailov, R.I. Killey, S. Appathurai and P. Bayvel, "Investigation of intra-channel nonlinear distortion in 40Gbit/s transmission over non-zero dispersion shifted fibre", in Proc. 28th European Conf. on Optical Commun. (ECOC 2001), Copenhagen, Denmark, paper 8.1.6, 2002.

[MIK'02b]: V. Mikhailov, R.I. Killey, S. Appathurai and P. Bayvel, "Wideband 40Gbit/s WDM transmission under higher-order-mode fibre dispersion management", in Proc. Lasers and Electro Optics Society Conf. (LEOS 2002), Glasgow, United Kingdom, paper MI4, 2002.

[MIK'04]: B. Mikkelsen, C. Rasmussen, P. Mamyshev, F. Liu, S. Dey and F. Rosca, "Deployment of 40Gb/s systems: Technical and cost issues", in Proc. Optical Fiber Commun. Conf. (OFC 2004), Los Angeles, California, ThE6, 2004.

[MIK'99]: B. Mikkelsen, G. Raybon, R. –J. Essiambre, K. Dreyer, Y. Su, L. E. Nelson, J. E. Johnson, G. Shtengel, A. Bond, D. G. Moodie and A. D. Ellis, "160Gbit/s single channel transmission over 300km non-zero dispersion shifted fibre with semiconductor based transmitter and demultiplexer", in Proc. 25th European Conf. on Optical Commun. (ECOC 1999), Nice, France, Post-deadline, PD2, 1999.

[MIY'00]: T. Miyano, M. Fukutoku, K. Hattori and H. Ono, "Suppression of degradation induced by SPM/XPM+GVD in WDM transmission using a bit-synchronous intensity modulated DPSK signal", in Proc. Optoelectronics and Commun. Conf. (OECC 2000), Chiba, Japan, paper 14D3-3, 00.

[MIY'98]: Y. Miyamoto, K. Yonenaga, and S. Kuwahara, "Dispersion tolerant RZ signal using baseband differential code and carrier suppressed modulation", in Proc. 24th European Conf. on Optical Commun. (ECOC 1998), Madrid, Spain, pp 351-352, 1998.

[MIY'99]: Y. Miyamoto, A. Hirano, K. Yonenaga, A. Sano, H. Toba, K. Murata and O. Mitomi, "320Gbit/s (8x40Gbit/s) WDM transmission over

367km with 120km repeater spacing using carrier-suppressed return-to-zero format", Electron. Lett. Vol. 35, No. 23, pp 2041-2042, 1999.

[MOL'02]: L. Moller, Y. Su, G. Raybon, S. Chandrasekhar and L. L. Buhl, "Penalty interference of nonlinear intra-channel effects and PMD in ultra high-speed TDM systems", Electron. Lett., Vol. 38, No. 6, pp 281-283, 2002.

[MOL'03]: L. F. Mollenauer, A. Grant, X. Liu, X. Wei, C. Xie, I. Kang and C. Doerr, "Demonstration of 109x10G dense WDM over more than 18,000km using nivel, oeriodic-group-delay-complemented dispersion compensation and dispersion managed solitons", in Proc. 29th European Conf. on Optical Commun. (ECOC 2003), Post deadline, Rimini, Italy, Th4.3.4, 2003.

[MOL'96]: L. F. Mollenauer, P. V. Mamyshev and M. J. Neubelt, "Polarisation-channel-interleaved CS-RZ transmission at 40Gbit/s with 0.8bit/s/Hz spectral efficiency", Electron. Lett. Vol. 32, No. 5, pp 471-473, 1996.

[MOO'95]: D. G. Moodie, A. D. Ellis, A. R. Thurlow, M. J. Harlow, I. F. Lealmen, S. D. Perrin, L. J. Rivers and M. J. Robertson, "Multiquantum well electroabsorption modulators for 80Gbit/s OTDM systems", Electron. Lett. Vol. 25, No. 10, pp 1370-1371, 1995.

[MOR'00]: I. Morita, K. Tanaka, N. Edagawa and M. Suzuki, "40Gbit/s single-channel transmission over standard single mode fibre using distributed Raman amplification", Electron. Lett. Vol. 25, No. 10, pp 1370-1371, 1995.

[MOR'02]: I. Morita and N. Edagawa, "Study on optimum OTDM signals for long-distance 40Gbit/s transmission", in Proc. Optical Fiber Commun. Conf. (OFC 2002), Anaheim, CA, TuA4, 2002.

[MOR'02b]:I. Morita, T. Tsuritani, N. Yoshikane, A. Agata, K. Imai and N. Edagawa, "100% spectral-efficient 25 x 42.7Gbit/s transmission using asymmetrically filtered CS-RZ signal and a novel crosstalk suppressor", in Proc. 28th European Conf. on Optical Commun. (ECOC 2002), Copenhagen, Denmark, Post-deadline PD4.7, 2002.

[MOR'99]: I. Morita, N. Edagawa, and M. Suzuki, "40Gb/s single-channel soliton transmission over transoceanic distances by reducing Gordon-Haus

timing jitter and soliton-soliton interaction", J. Lightwave Technol, Vol. 17, No.12, pp 2506-2511, 1999.

[MUR'00]: M. Murakami, T. Matsuda, H. Maeda and T. Amai, "Long-haul WDM transmission using higher-order fiber dispersion management", J. Lightwave Technol, Vol. 18, No.9, pp 1197-1204, 2000.

[MUR'00b]: H. Murai, H. T. Yamada, A. R. Pratt and Y. Ozeki, "8x40Gbit/s transmission over 640km of large-effective-area nonzero-dispersion shifted fibre", Electron. Lett., Vol. 36, No. 17, pp 1479-1480, 2000.

[NAK'00]: M. Nakazawa, T. Yamamoto, and K. R. Tamura, "1.28Tbit/s-70km OTDM transmission using third- and fourth-order simultaneous dispersion compensation with a phase modulator", Electron. Lett. Vol. 36, No. 24, pp 2027-2029, 2000.

[OHH'01]: R. Ohhira, D. Ogasahara and T. Ono, "Novel RZ format with alternate-chirp for suppression of nonlinear degradation in 40Gb/s based WDM", in Proc. Optical Fiber Commun. Conf. (OFC 2001), Anaheim, CA, WM2, 2001.

[OTA'01]: T. Otani, and M. Suzuki, "80Gbit/s 15 WDM OTDM RZ signal transmission over 295km NZDSF", in Proc. 27th European Conf. on Optical Commun. (ECOC 2001), Amsterdam, Netherlands, TuL2.5, 2001.

[PEC'03]: P. Pecci, S. Lanne, Y. Frignac, J. –C. Antona, G. Charlet and S. Bigo, "Tolerance to dispersion compensation parameters of six modulation formats in systems operating at 43Gbit/s", Electron. Lett. Vol. 39, No. 25, pp 1844-1846, 2003.

[PEN'97]: D. Penninckx, M. Chbat, L. Pierre and J. –P. Thiery, "The phase-shaped binary transmission (PSBT): A new technique to transmit far beyond the chromatic dispersion limit", IEEE Photon. Technol. Lett., Vol. 9, No.2, pp 259-261, 1997.

[PER'73]: S. D. Personick, "Receiver design for digital fiber optic communication systems", Bell Syst. Technol. J., Vol. 52, pp 843-844, 1973.

[PIN'04]: E. Pincemin, D. Grot, C. Borsier, J. D. Ania-Castanon and S. K. Turitsyn, "Impact of the fibre type and dispersion management on the

performance of an NRZ 16x40Gb/s DWDM transmission systesm", IEEE Photon. Technol. Lett., Vol. 16, No.10, pp 2362-2365, 2004.

[POO'88]: S. B. Poole, D. N. Payne, R. J. Mears, M. E. Fermann, and R. I. Laming, "Fabrication and characterisation of low-loss optical fibres containing rare-earth ions", J. Lightwave Technol., Vol. 4, no. 7, pp 870-876, 1988.

[POO'94]: C. D. Poole and J. M. Wiesenfield, "Optical fibre-based dispersion compensation using higher order modes near cutoff", J. Lightwave Technol, Vol. 12, No.10, pp 1746-1758, 1994.

[RAL'04]: J. D. Ralston, J. M. Kahn and K. –P. Ho, "Advanced modulation and signal processing techniques for 40Gb/s optical transmission systems", Proc. SPIE Vol. 4872 : Optical transmission systems and equipment for WDM networking, Editor(s): Benjamin B. Dingel, Brewster R. Hemenway, Achyut K. Dutta, Ken-Ichi Sato, July 2002, paper 4872-04, 2004.

[RAM'00]: C. J. Rasmussen, "Simple and fast method for step size determination in computations of signal propagation through nonlinear fibres", in Proc. Optical Fiber Commun. Conf. (OFC 2001), Anaheim, CA, WDD-29, 2001.

[RAM'01]: S. Ramachandran, G. Raybon, B. Mikkelsen, M. Yan, L. Cowsar and R. –J. Essiambre, "1700-km transmission at 40Gbit/s with 100km amplifier-spacing enabled by higher-order-mode dispersion compensation", in Proc. 27th European Conf. on Optical Commun. (ECOC 2001), Amsterdam, Netherlands, We.F.2.2, 2001.

[RAM'02]: S. Ramachandran, "Higher-order-mode dispersion compensation for broadband dispersion and non-linearity management in transmission systems", in Proc. Optical Fiber Commun. Conf. (OFC 2002), Anaheim, CA, WU5, 2002.

[RAM'02b]: S. Ramachandran, S. Ghalmi, S. Chandrasekhar, I. Ryazansky, M. Yan, F. Dimarcello, W. Reed and P. Wisk, "Wavelength continuous broadband adjustable dispersion compensator using higher-order-mode fibers and switchable fiber-gratings", in Proc. 28th European Conf. on Optical Commun. (ECOC 2002), Copenhagen, Denmark, Post-deadline PD4.4, 2002.

[RAS'03]: C. Rasmussen, T. Fjelde, J. Bennike, F. Liu, S. Dey, B. Mikkelsen, P. Mamyshev, P. Serbe, P. Van Der Vagt, Y. Akasaka, D. Harris, D. Gapontsev, V. Ivshin, and P. Reeves-Hall, "DWDM 40G transmission over trans-pacific distance (10,000km) using CSRZ-DPSK, enhanced FEC and all-Raman amplified 100km UltraWave^{TM} fiber spans", in Proc. Optical Fiber Commun. Conf. (OFC 2003), Post deadline, Atlanta, GA, PD18, 2003.

[RAY'00]: G. Raybon, B. Mikkelsen, R. –J. Essiabre, A. J. Stentz, T. N. Nielsen, D. W. Peckham, L. Hsu, L. Gruner-Nielsen, K. Dreyer, and J. E. Johnson, "320Gbit/s single-channel pseudo-linear transmission over 200km of nonzero-dispersion fiber", in Proc. Optical Fiber Commun. Conf. (OFC 2000), Post deadline, Baltimore, MA, PD29, 2000.

[RHE'00]: J. –K. Rhee, D. Chowdhury, K. S. Cheng and U. Gliese, "DPSK 32x10Gb/s transmission modelling on 5x90km terrestrial system", IEEE Photon. Technol. Lett., Vol. 12, No.12, pp 1627-1629, 2000.

[RHO'00]: M. Rhode, C. Caspar, N. Heimes, M. Konitzer, E. –J. Bachus, N. Hanik, "Robustness of DPSK direct detection transmission format in standard fibre WDM systems", Electron. Lett., Vol. 36, No. 17, pp 1483-1484, 2000.

[ROU'02]: I. Roudas, N. Antoniades, T. Otani, T. E. Stern, R. E. Wagner, D. Q. Chowdhury, "Accurate modelling of optical multiplexer/demultiplexer concatenation in transparent multi-wavelength optical networks" , J. Lightwave Technol, Vol. 20, No.6, pp 921-936, 2002.

[SAN'00]: A. Sano, Y. Miyamoto, S. Kuwahara and H. Toba, "A 40-Gb/s/ch WDM transmission with SPM/XPM suppression through prechirping and dispersion management", J. Lightwave Technol., Vol. 18, no. 11, pp 1519-1527, 2000.

[SEK'03]: K. Sekiya, T. Ito, H. Sugahara, K. Fukuchi, R. Ohhira and T. Ono, "Flexible 40Gbit/sWDM transmission beyond 1000km enabled by 195μm^2 A_{eff} PSCF and AC-RZ signal format", Electron. Lett. Vol. 39, No. 4, pp 386-388, 2003.

[SHA'01]: E. G. Shapiro, M. P. Fedoruk, and S. K. Turistsyn, "Numerical estimate of BER in optical systems with strong patterning effects", Electron. Lett., Vol. 37, No. 19, pp 1179-1181, 2001.

[SHA'03]: E. G. Shapiro, M. P. Federuk, S. K. Turitsyn and A. Shafarenko, "Reduction of nonlinear intrachannel effects by channel asymmetry in transmission lines with strong bit overlapping", IEEE Photon. Technol. Lett., Vol. 15, No.10, pp 1473-1475, 2003.

[SHA'04]: E. G. Shapiro, M. P. Fedoruk, and S. K. Turistsyn, "Direct modelling of error statistics at 40Gbit/s rate in SMF/DCF link with strong bit overlapping", Electron. Lett., Vol. 40, No. 22, pp 1436-1437, 2004.

[SHA'98]: I Shake, H. Takara, K. Mori, S. Kawanishi, and Y. Yamabayashi, "Influence of inter-bit four-wave-mixing in optical TDM transmission", Electron. Lett., Vol. 34, No. 16, pp 1600-1601, 1998.

[SHT'04]: M. Shtaif, and A. Mecozzi, "Polarization dependent loss and its effect on the signal-to-noise-ratio in fibre-optic systems", IEEE Photon. Technol. Lett., Vol. 16, No.2, pp 671-673, 2004.

[SIN'03]: O. V. Sinkin, R. Holzlohner, J. Zweck and C. R. Menyuk, "Optimisation of the split-step Fourier method in modelling optical-fiber communication systems", J. Lightwave Technol, Vol. 21, No.1, pp 61-68, 2003.

[SMI'97]: N. J. Smith, N. J. Doran, W. Forysiak and F. M. Knox, "Soliton transmission using periodic dispersion compensation", J. Lightwave Technol, Vol. 15, No.10, pp 1808-1822, 1997.

[SU'02]: Y. Su, G. Raybon, L. K. Wickham, R. –J. Essiambre, S. Chandrasekhar and S. Radic, "40Gb/s transmission over 2000km of nonzero dispersion shifted fiber using 100km amplifier spacing", in Proc. Optical Fiber Commun. Conf. (OFC 2002), Anaheim, California, ThFF3 pp. 609-610, 2002.

[SUZ'95]: M. Suzuki, I. Morita, N. Edagawa, S. Yamamoto, H. Taga and S. Akiba, "Reduction of Gordon-Haus timing jitter by periodic dispersion compensation in soliton transmission", Electron. Lett. Vol. 31, No. 23, pp 2027-2029, 1995.

[SUZ'98]: K. –I. Suzuki, N. Ohkawa, M. Murakami and K. Aida, "Unrepeatered 40Gbit/s RZ signal transmission over 240km conventional singlemode fibre", Electron. Lett. Vol. 34, No. 8, pp 799-800, 1998.

[TAN'02]: T. Tanaka, K. Torii, M. Yuki, H. Nakamoto, T. Naito and I. Yokota, "200-nm Bandwidth WDM transmission around 1.55μm using

distributed Raman amplifier", in Proc. 28th European Conf. on Optical Commun. (ECOC 2002), Post deadline, Copenhagen, Denmark, PD4.6, 2002.

[THI'00]: H. J. Thiele, "Investigation of high-speed optical transmission in the presence of fibre nonlinearities", PhD thesis, University of London, July 2000.

[TKA'95]: R. W. Tkach, A. R. Chraplyvy, F. Forghieri, A. M. Gnauck and R. M. Derosier, "Four-photon mixing in high-speed WDM systems", J. Lightwave Technol, Vol. 13, No.5, pp 841-849, 1995.

[TSU'00]: S. Tsuda and V. L. da Silva, "Transmission of 80 x 10 Gbit/s WDM channels with 50GHz spacing over 500km of LEAF® fiber", in Proc. Optical Fiber Commun. Conf. (OFC 2000), Baltimore, Maryland, MF4-1, pp 149-151, 2000.

[TUR'01]: M. Tur, E. Herman and Y. Danziger, "Nonlinear properties of dispersion management modules employing high-order mode fibers", in Proc. Optical Fiber Commun. Conf. (OFC 2001), California, TuS5, 2001.

[TUR'03]: S. K. Turitsyn, M. P. Federouk, V. K. Mezentsev and E. G. Turitsyna "Theory of optimal power budget in quasi-linear dispersion managed fibre links", Electron. Lett. Vol. 39, No. 1, pp 29-30, 2003.

[TUR'99]: S. K. Turitsyn, M. P. Federouk and A. Gornakova, "Reduced-power optical solitons in fiber lines with short-scale dispersion management", Optics. Lett., Vol. 24, No.13, pp 869-871, 1999.

[TUR'99b]: S. K. Turitsyn, T. Schaefer and V. K. Mezentsev, "Generalized momentum method to describe high-frequency solitary wave propagation in systems with varying dispersion", Physical Review Vol. E58 No. 5 R5264-R5267 (1998).

[VEN'94]: A. M. Vengsarkar, A. E. Millner, M. Haner, A. H. Gnauck, W. A. Reed, and K. L. Walker, "Fundamental-mode dispersion-compensating-fibres: Design considerations and experiments", in Proc. Optical Fiber Commun. Conf. (OFC 1994), ThK2 pp. 225-227, 1994.

[WAL'91]: G. R. Walker, D. M. Spirit, D. L. Williams and S. T. Davey, "Noise performance of distributed fibre amplifiers", Electron. Lett., Vol. 27, No. 15, pp 1390-1391, 1991. [WAN'01]: B. C. Wang, L. Xu, V.

Baby, D. Y. Zhou, R. J. Runser, I. Glesk and P. R. Prucnal, "Experimental study on the regeneration capability of the terahertz optical asymmetric demultiplexer", Optics. Commun., Vol. 189, No.1-4, pp 83-88, 2001.

[WEI'03]: X. Wei, A. H. Gnauck, X. Liu and J. Leuthold, "Nonlinearity tolerance of RZ-AMI format in 42.7Gbit/s long-haul transmission over standard SMF spans", Electron. Lett. Vol. 39, No. 20, pp 1459-1461, 2003.

[WIN'02]: P. J. Winzer, A. H. Gnauck, G. Raybon, S. Chandrasekhar, Y. Su and J. Leuthold, "40-Gb/s Return-to-zero alternate-mark-inversion (RZ-AMI) transmission over 2000km", IEEE Photon. Technol. Lett., Vol. 15, No.5, pp 766-768, 2003.

[WIN'03]: P. J. Winzer and R. –J. Essiambre, "Advanced optical modulation formats", in Proc. 29th European Conf. on Optical Commun. (ECOC 2003), Rimini, Italy, Th2.6.1, 2003.

[XIE'00]: Y. Xie, S. Lee, Z. Pan, J.-X. Cai, A. E. Willner, V. Grubsky, D. S. Starodubov, E. Salik and J. Feinberg, "Tunable compensation of the dispersion slope mismatch in dispersion-managed systems using a sampled nonlinearly chirped FBG", IEEE Photon. Technol. Lett., Vol. 12, No.10, pp 1417-1419, 2000.

[XIE'04]: C. Xie, I. Kang, A. H. Gnauck, L. Moller, L. F. Mollenauer and A. R. Grant "Suppression of intra-channel nonlinear effects with alternate-polarization formats", J. Lightwave Technol., Vol. 22, no. 3, pp 806-812, 2004.

[YAN'01]: M. Yan, J. Chen, W. Jiang, J. Li, J. Chen and X. Li, "Pump depletion induced noise and crosstalk in distributed optical fiber Raman amplifiers", IEEE Photon. Technol. Lett., Vol. 13, No.7, pp 403-405, 2001.

[YON'96]: K. Yonenaga, S. Aisawa, N. Takachio, K. Iwashita, "Reduction of four-wave mixing induced penalty in unequally spaced WDM systems using optical DPSK", Electron. Lett., Vol. 32, No. 23, pp 2118-2119, 1996.

[ZHA'02]: Q. Zhang, J. Maloney, C. Menyuk, K. Hall, A. Liang, J. Jacob, M. Lagasse, B. Brewington, E. Thoen, S. Vergheses and F. Sun, "Performance comparison of dispersion managed 40 Gbps

transmission CSRZ vs. RZ", in Proc. Conf. Of Lasers and Electro-Optics (CLEO 2002), Long Beach, CA, Paper CThO37, 2002.

[ZHA'98]: X. Zhang, M. Karlsson, P. A. Andrekson, and E. Kollveit, "Polarization-division multiplexed solitons in optical fibers with polarisation mode dispersion", IEEE Photon. Technol. Lett., Vol. 10, No.8, pp 1742-1744, 1998.

[ZHU'02]: Y. Zhu, W.S. Lee, P. Lobb, C. Ward, D. Watley, S. Savory, C. R. S. Fludger, B. Shaw and A. Hadjifotiou, "Polarisation-channel-interleaved CS-RZ transmission at 40Gbit/s with 0.8bit/s/Hz spectral efficiency", Electron. Lett., Vol. 38, No. 8, pp 381-382, 2002.